NOVEL GONADOTROPIN-RELEASING HORMONE, TACHYKININ AND NEUROMEDIN U NEUROPEPTIDE SIGNALING SYSTEMS IN *CAENORHABDITIS ELEGANS*

Lotte FROONINCKX

Supervisor:
Prof. L. Schoofs

Co-supervisor:
Dr. I Beets

Members of the Examination Committee:
Prof. L. Moons *(KU Leuven)*
Prof. W. Luyten *(KU Leuven)*
Prof. A. Aertsen *(KU Leuven)*
Prof. Rob Jelier *(KU Leuven)*
Dr. O. Mirabeau *(Institut Curie)*

Dissertation presented in
partial fulfillment of the
requirements for the degree of
Doctor in Science

April 2015

Dankwoord

Vijf jaar geleden kwam ik bij professor Schoofs ‘solliciteren’ als een enthousiaste thesisstudent van de bio-ingenieurs die graag wat meer wou leren over dat kleine wormpje ‘*C. elegans’.* Het wormpje heeft mij niet teleurgesteld ☺. Ik ben nog steeds blij dat ik tijdens mijn doctoraat onderzoek heb gedaan naar ‘neuropeptide signaalsystemen in *C. elegans’* en ben heel wat mensen dankbaar die mij de voorbije jaren hebben geholpen bij het realiseren van dit doctoraat.

Mijn promotor Prof. Liliane Schoofs dank ik om mij gedurende 4 jaar op te vangen in haar onderzoeksgroep. Mijn co-promotor Dr. Isabel Beets wil ik danken voor al haar advies, hulp en steun, zowel in het labo als bij het schrijven van papers en mijn doctoraatsthesis! Een welgemeende dikke merci!

I would also like to thank the members of my examination committee: Prof. Lieve Moons, Prof. Abram Aertsen, Prof. Rob Jelier, Prof. Walter Luyten and especially Dr. Olivier Mirabeau for their constructive comments and advice.

Ook op (Prof.) Dr. Liesbet Temmerman kon ik steeds rekenen. Haar niet aflatende enthousiasme, gaf mij steeds de moed om te blijven geloven in het onderzoek.

De laatste maanden van mijn doctoraat heb ik heel wat hulp gekregen van Jan Watteyne. Dankjewel om het tachykinine verhaal verder te zetten!

Dankjewel aan de studenten die ik begeleidde. Vooral Jorge Palaci en Elien Van Sinay, jullie waren ‘voorbeeldstudenten’ en het was een eer om jullie te begeleiden.

Dankjewel Luc, Nick, Esra, Maria, Els, Johny en Marijke voor de technische en administratieve hulp.

Mijn doctoraatsjaargenootjes: Wouter, Liesbeth, Lise, Jelle, Sven, Senne en Rik. Het was fijn om samen met jullie die 4 jaar te doorlopen, samen up en downs te beleven, steeds iemand te hebben waar je met (niet-) werkgerelateerde kwesties terecht kon.

Merci aan al de HSV-ers die ervoor zorgden dat het elke dag fijn was om naar het labo te komen! Getrakteerd worden met een stukje kriekentaart als je op zaterdag gaat werken, Kinder Bueno's delen of paaseitjes-vasten… Het zijn maar een paar voorbeelden van al die geweldige herinnering die ik aan mijn collega's heb!

Mijn huisgenootjes van de voorbije 4 jaar: Annelies, Daan, Marijke, Sarah, Céline, Lien, Jelle, Valérie, Jan en Sven! Bedankt dat ik nooit alleen moe(s)t thuiskomen!

De meisjes van de scouts: Lien, Veerle, Evelien en Nele. Ik hoop dat we die verjaardagen voor altijd samen blijven vieren! Het ware heel fijne activiteiten, waar ik steeds naar uitkijk!

De meisjes van de lagere school: Sarah, Eline, Dorien, Hannah-Laura, Judith, Sanne, Annelies en Sigrid. Fijn dat we elkaar weer wat vaker zien. Bedankt voor de fijne momenten samen!

De bio-ingenieurs: Valerie, Tom, Bernd, Kristien, Joaquin, Wim, Pieter, Pieter-Jan, Wanda, Sander, Kristine, Daan en Annelies. We zien elkaar niet zo vaak meer, maar het is toch altijd een beetje thuiskomen als we samen op stap gaan!

(Chiro) Hulsen, Britt, Christine en Vic, dankjewel om mij steeds met open armen te ontvangen.

Mama en papa, zonder jullie onvoorwaardelijke steun had ik het nooit gehaald! Jullie hebben mij geleerd om in mezelf te geloven en mijn dromen waar te maken! Ook als die droom inhoudt om tijdens mijn doctoraat op mijn eentje een huis te kopen en verbouwen, stonden jullie voor mij klaar! Een welgemeende dankjewel! Het was werkelijk niet gelukt zonder jullie!

Broer/chef Pieter-Jan, bedankt om mij 'terug' kennis te laten maken met een niet-academische wereld. Ik ben ontzettend trots op mijn kleine broer! Ik weet niet of je beseft hoeveel jij en je onderneming de laatste maanden voor mij betekenden, dankjewel!

Sven, misschien wel het beste wat mij tijdens mijn doctoraat is overkomen! Jij was doorheen mijn doctoraat de rots in de branding! Bedankt voor al je liefde, geduld, steun en goede zorgen.

Table of contents

List of abbreviations

5-HT	serotonin
7TM	seven transmembrane
ACh	acetylcholine
AKH	adipokinetic hormone
BLAST	Basic Local Alignment Search Tool
cAMP	cyclic adenosine monophosphate
CCK	cholecystokinin
cDNA	complementary deoxyribonucleic acid
cGMP	cyclic guanosine monophosphate
CHO	Chinese hamster ovary
CREB	cAMP response-element binding protein
DA	Dopamine
DAG	diacylgycerol
DiI	1,1′-Dioctadecyl-3,3,3′,3′-tetramethylindocarbocyanine perchlorate
EC_{50}	half maximal effective concentration
EEG	electroencephalogram
EGF	epidermal growth factor
FaRP	FMRFamide-related peptide
FLP	FMRFamide-like peptide
GABA	γ-aminobutyric acid
GFP	Green fluorescent protein
GnRH	gonadotropin-releasing hormone
GNRR	gonadotropin-releasing hormone receptor related
GPCR	G protein-coupled receptor
HEK	human embryonic kidney
HPLC	high performance liquid chromatography
INS	insulin-like peptide
IP3	inositol-1,4,5-trisphosphate
LN	local interneuron
MAST	motif alignment and Search tool
MEME	multiple expectation maximization for motif elicitation
ML	maximum likelihood
mRNA	messenger ribonucleic acid

NKA	neurokinin A
NKB	neurokinin B
NLP	neuropeptide-like peptide
NMJ	neuromuscular junction
NMU	neuromedin U
NMUR	neuromedin U receptor
NPR	neuropeptide receptor
NPY	neuropeptide Y
NTC	nematocin
NTR	nematocin receptor
OA	octopamine
OSN	olfactory receptor neuron
PCR	polymerase chain reaction
PDF	pigment dispersing factor
PIP2	phosphatidylinositol 4,5-bisphosphate
PK	pyrokinin
PKA	protein kinase A
PKC	protein kinase C
PKG	protein kinase G
PLCβ	phospholipase Cβ
PN	projection neuron
RNAi	ribonucleic acid interference
SP	substance P
TA	tyramine
TGF-α	transforming growth factor α
TKR	tachykinin receptor
TTL	transcriptional-translational feedback loop
VP/OT	vasopressin/oxytocin

Summary

To survive organisms need to be capable to sense environmental cues and respond properly in order to maintain internal homeostasis. The nervous and endocrine systems ensure that the coordination and integration of internal and external stimuli works properly. Neuropeptides are small signaling molecules that play an important role as neurotransmitters, neurohormones or neuromodulators in these processes. Neuropeptides generally signal through G protein-coupled receptors (GPCRs). The identification of their corresponding GPCRs is an important step in elucidating the function of neuropeptides. In this study, we aim to investigate neuropeptidergic signaling in the roundworm *Caenorhabditis elegans.* This transparent model organism is amenable to genetic manipulation and has a relatively simple and defined nervous system, allowing us to investigate how neuropeptides guide behavior and physiological processes by analyzing the neural circuits they act on.

In the first place we performed an *in silico* prediction of the repertoire of neuropeptide GPCRs encoded in the genome of *C. elegans* using the MEME/MAST tool. Here, the common motif sequences of previously deorphanized neuropeptide GPCRs were used to scan the entire *C. elegans* genome for the presence of these motifs. Doing so, 129 hypothetical *C. elegans* neuropeptide GPCRs were manually annotated. From this list three groups of orphan receptors related to gonadotropin-releasing hormone/adipokinetic hormone (GnRH/AKH), tachykinin or neuromedin U/pyrokinin (NMU/PK) signaling systems were chosen for ligand identification using a combined *in silico* and library-based reverse pharmacology approach. A total of four receptors (GNRR-3, TKR-1, TKR-2 and NMUR-1) were coupled to their activating ligands in an *in vitro* assay. For the functional analysis we focused on the GnRH/AKH and tachykinin signaling systems.

NLP-22, one of the neuropeptides that activated the GnRH/AKH-like receptor GNRR-3 in our *in vitro* assay, was recently shown to induce sleep-like behavior in *C. elegans.* Like sleep in vertebrates, this behavior is actively regulated by neural circuits and engages multiple neurochemical systems, including neuropeptides. Genetic overexpression of *gnrr-3*

indicates that this receptor also modulates sleep-like behavior. However, in contrast to NLP-22, this receptor seems to inhibit sleep. Besides NLP-22, GNRR-3 was also activated by NLP-2 peptides in our *in vitro* assay. Like *gnrr-3,* overexpression of *nlp-2* inhibits sleep. This effect is abolished when *nlp-2* is overexpressed in *gnrr-3* deletion mutants, indicating that NLP-2 peptides interact with GNRR-3 *in vivo* as well. Sleep is generally characterized by a decline in locomotion and feeding, and reduced responsiveness to arousing stimuli. NLP-2/GNRR-3 signaling seems to specifically inhibit the reduction of locomotion during sleep, whereas the remaining sleep characteristics are unperturbed. *nlp-2* transcript levels are cyclic and in phase with the transcription of *lin-42,* which encodes the PERIOD homolog that regulates the timing of sleep-like behavior in *C. elegans. In vivo* localization of *nlp-2* shows that this neuropeptide is expressed in the sensory AWA neurons, suggesting that *nlp-2* could inhibit sleep in response to specific cues which are sensed by AWA.

Tachykinins are a multifunctional family of neuropeptides that occur in both vertebrates and invertebrates. In this study we demonstrate that tachykinins are conserved in nematodes as well. The genome of *C. elegans* encodes two tachykinin receptors, TKR-1 and TKR-2. Both receptors are activated *in vitro* by the *in silico* predicted *C. elegans* tachykinin neuropeptides. *In vivo* localization of the tachykinin receptors and the tachykinin peptides shows that they are expressed in the nervous system. Based on the identified expression pattern, their role in navigation, chemotaxis, nociception and adaptation were investigated. However, we did not observe an effect of impaired tachykinin signaling on the performed assays.

In summary, four novel *C. elegans* neuropeptide signaling systems were identified. Our results indicate that the NLP-2/GNRR-3 system modulates sleep behavior and the neuronal expression pattern of the tachykinin system suggests a modulatory role in nociception. The powerful genetic tools and high-throughput phenotyping assays endow this model organism with unique advantages to investigate the cellular and molecular function of the identified signaling systems.

Samenvatting

Om te overleven is het essentieel dat een organisme veranderingen in zijn omgeving kan waarnemen en hier gepast op kan reageren zodat de interne homeostase behouden blijft. Het zenuw- en endocrien stelsel zorgen ervoor dat de coördinatie en integratie van zowel interne als externe prikkels correct verlopen. Neuropeptiden zijn kleine signaalmoleculen die hierbij een belangrijke rol spelen als neurotransmitters, neurohormonen of neuromodulators. Neuropeptiden signaleren doorgaans via de activatie van G-proteïne gekoppelde receptoren (GPCRs). Een belangrijke stap in het ontrafelen van de functie van neuropeptiden is de identificatie van hun receptoren. De doelstelling van dit doctoraat is de neuropeptiderge signalering bij de rondworm *Caenorhabditis elegans*, te onderzoeken. Dit modelorganisme heeft een relatief eenvoudig en gedefinieerd zenuwstelsel, is makkelijk genetisch manipuleerbaar en is transparant. Deze eigenschappen scheppen tal van mogelijkheden om te onderzoeken hoe neuropeptiden een rol spelen bij de modulatie van zowel gedrag als fysiologische processen.

In eerste instantie hebben we de genen die coderen voor neuropeptide GPCRs *in silico* voorspeld. Bij deze voorspelling maakten we gebruik van de MEME/MAST applicatie. Hierbij zochten we eerst naar geconserveerde sequentie-motieven in gekende neuropeptide GPCR coderende genen. Vervolgens werd het volledige genoom van *C. elegans* gescand op het voorkomen van deze motieven. Zo werden in totaal 129 hypothetische *C. elegans* neuropeptide GPCRs manueel geannoteerd. Hieruit werden drie groepen van GPCRs geselecteerd die gelijkend zijn op zoogdier en insect gonadotropine-releasing hormoon/adipokinetisch hormoon (GnRH/AKH), tachykinine of neuromedine U/pyrokinine (NMU/PK) receptoren. Gebruik makende van *in silico* voorspelling van de liganden en omgekeerde farmacologie werden in totaal 4 receptoren (GNRR-3, TKR-1, TKR-2 en NMUR-1) gekoppeld aan hun activerende liganden in een *in vitro* assay. Voor de functionele analyse werd er gefocust op de GnRH/AKH en tachykinine signaalsystemen.

Onze resultaten tonen aan dat één van de GnRH/AKH-achtige weesreceptoren (GNRR-3) *in vitro* geactiveerd wordt door NLP-22, een nematode-specifiek neuropeptide, dat bij *C.*

elegans slaapgedrag induceert. Net zoals bij vertebraten wordt slaap bij *C. elegans* gereguleerd door neuronale circuits. Neuropeptiden vervullen hierbij een belangrijke rol. Genetische overexpressie van *gnrr-3* toont aan dat deze receptor ook een rol speelt bij slaap, maar in tegenstelling tot NLP-22, lijkt deze receptor slaap te inhiberen. Naast NLP-22 werd GNRR-3 *in vitro* eveneens geactiveerd door NLP-2 neuropeptiden. We tonen aan dat overexpressie van *nlp-2* net als *gnrr-3* slaap inhibeert. Dit effect wordt teniet gedaan bij overexpressie van *nlp-2* in *gnnr-3* deletiemutanten, wat suggereert dat deze peptiden ook *in vivo* interageren met GNRR-3. Slaap wordt in het algemeen gekenmerkt door een afname van beweging en voedselopname, en door een toename in de tijd die nodig is om te reageren op externe stimuli. Het NLP-2/GNRR-3 signaalsysteem verhindert specifiek de afname van beweging tijdens het slapen, terwijl de andere slaapkenmerken niet beïnvloed worden. Analyse van de transcriptie van *nlp-2* toont aan dat deze cyclisch is en in fase met de transciptie van *lin-42*, dat codeert voor het PERIOD homoloog en de timing van slaap bij *C. elegans* reguleert. *nlp-2* komt tot expressie in de sensorische AWA neuronen, wat erop wijst dat *nlp-2* slaap zou kunnen inhiberen als gevolg van specifieke stimuli die waargenomen worden door AWA.

Tachykinines zijn een multifunctionele familie van neuropeptiden die zowel bij vertebraten en invertebraten voorkomen. In deze studie tonen we aan dat tachykinines ook geconserveerd zijn bij nematoden. Het genoom van *C. elegans* codeert voor twee tachykinine receptoren, TKR-1 en TKR-2. Beide receptoren worden *in vitro* geactiveerd door de *in silico* voorspelde *C. elegans* tachykinine neuropeptiden. Zowel de tachykinine receptoren als de tachykinine neuropeptiden zijn gelokaliseerd in het zenuwstelsel. Op basis van het geïdentificeerde cellulair expressiepatroon van de tachykinine systemen werd hun rol in navigatie, chemotaxis, nociceptie en adaptatie onderzocht. Er werd echter geen effect geobserveerd in deze assays.

De resultaten van dit doctoraat tonen aan dat het ontrafelen van neuropeptiderge signaalsystemen bij *C. elegans* nog veel potentieel biedt. In deze studie werden vier neuropeptiderge signaalsystemen geïdentificeerd. We konden hierbij een rol voor het NLP-2/GNRR-3 signaalsysteem in slaap aantonen en het neuronale expressiepatroon van het *C.*

elegans tachykinine signaalsysteem doet vermoeden dat deze een modulatorische functie heeft bij pijnperceptie. De vele genetische technieken en ‘high-throughput’ fenotypering analyses die mogelijk zijn bij dit modelorganisme laten toe om de cellulaire en moleculaire functie van de geïdentificeerde signaalsystemen verder te onderzoeken

Chapter 1. Introduction

This chapter has partially been published in:

Frooninckx L, Van Rompay L, Temmerman L, Van Sinay E, Beets I, Janssen T, Husson SJ, Schoofs L (2012). Neuropeptide GPCRs in *C. elegans*. *Frontiers in endocrinology* 3: Article 167.

Our nervous system allows us to quickly detect, communicate and coordinate information about the external and internal environment, thereby helping us to adapt our behavior and physiology in a constantly changing environment. Improper functioning of the nervous system results in neurological disorders such as addictions, dementia, epilepsy and multiple sclerosis. Neurological disorders make up 11 % of the world's disease burden and are estimated to affect up to one billion people worldwide (Collins *et al.*, 2011). These numbers emphasize the importance of understanding the organization and functioning of the brain. Although much progress has been made in the field of neuroscience using vertebrate models, unraveling the functioning of the nervous system is obviously hampered by its complexity (Alivisatos *et al.*, 2012; Sporns, 2014).

The nematode *Caenorhabditis elegans* has a simple and compact nervous system consisting of only 302 neurons. The determination of the entire structure and connectivity of its neurons was already accomplished almost 30 years ago. Today this nematode is still the only animal for which the entire nervous system has been mapped (White *et al.*, 1986). Despite its simplicity, many of the genetic pathways and neural signaling mechanisms used in *C. elegans* are similar to those of mammals (Bargmann, 1998).

Neuropeptides are small signaling proteins that play a key role in the functioning of the nervous system. Neuropeptides can act as neurotransmitters, neurohormones or neuromodulators and are involved in the majority of physiological processes such as reproduction, development, learning, sleep, and nociception among others. Despite their crucial role in the regulation of behavioral and physiological processes, for most neuropeptide systems the precise mode of action and the evolution thereof remains uncharacterized.

The *C. elegans* genome encodes over 100 predicted neuropeptide precursors of which several are already shown to be evolutionarily conserved (Janssen *et al.*, 2008a; Janssen *et al.*, 2008b; Lindemans *et al.*, 2009b; Lindemans *et al.*, 2009a; Beets *et al.*, 2012). Its simple and defined neuronal network combined with powerful genetic tools endows *C. elegans* with unique advantages making it a suitable model to investigate neuropeptidergic signaling. In this project we aim to identify novel *C. elegans* neuropeptide systems and provide insight into their functions and evolution. Therefore this introduction starts with a

short overview of the advantages the model organism *C. elegans* offers, and provides a general description of its neurobiology focusing on neuropeptidergic signaling.

1.1 The model organism Caenorhabditis elegans

When Sydney Brenner wanted to investigate how genes control the development of complex structures like nervous systems, he decided he needed an experimental organism which was suitable for genetic analysis and in which the structure of the nervous system could be determined. He chose to use the nematode *C. elegans* as a model organism to study developmental neurobiology (Brenner, 1974). In 2002, Sydney Brenner, John Sulston and Robert Horvitz received the Nobel Prize for their discoveries concerning the genetic regulation of organ development and programmed cell death using this nematode as an experimental model system. Today, this tiny nematode is used in many research areas as a model system to study basic principles of animal biology ranging from cell structure and functioning to neuronal circuits and behavior.

C. elegans is a free-living nematode (roundworm) that is naturally found in microbe-rich habitats such as rotting plant matter (Félix and Braendle, 2010). In the lab, *C. elegans* is maintained on agar plates that are seeded with *Escherichia coli* OP50. The life cycle of *C. elegans* is comprised of the embryonic stage, four larval stages termed L1 to L4, and adulthood (figure 1.1). The end of each larval stage is marked with a molt, which is preceded by a sleep-like state called lethargus (Sing and Sulston, 1978).

Under optimal laboratory conditions and dependent on the cultivation temperature, this life cycle only takes three to four days and adult worms can have a total lifespan of about two to three weeks. During unfavorable conditions, such as limited food and high population density, L2 larvae can develop into dauer larvae, which can survive for several months. During this dauer stage, feeding is arrested and locomotion reduces. When conditions improve, the dauer stage ends and the animal develops into a reproductive adult (Cassada and Russell, 1975; Byerly *et al.*, 1976).

C. elegans has hermaphrodite and male sexes. The majority of a population consists of hermaphrodites, which normally reproduce by self-fertilization. This reproductive mode produces about 300 progeny, of which only 0.05% are males that arise from a meiotic non-

disjunction of the X chromosome. When hermaphrodites reproduce by cross-fertilization with males, the number of progeny can exceed 1000 of which 50% are males (Ward and Carrel, 1979; Altun and Hall, 2009).

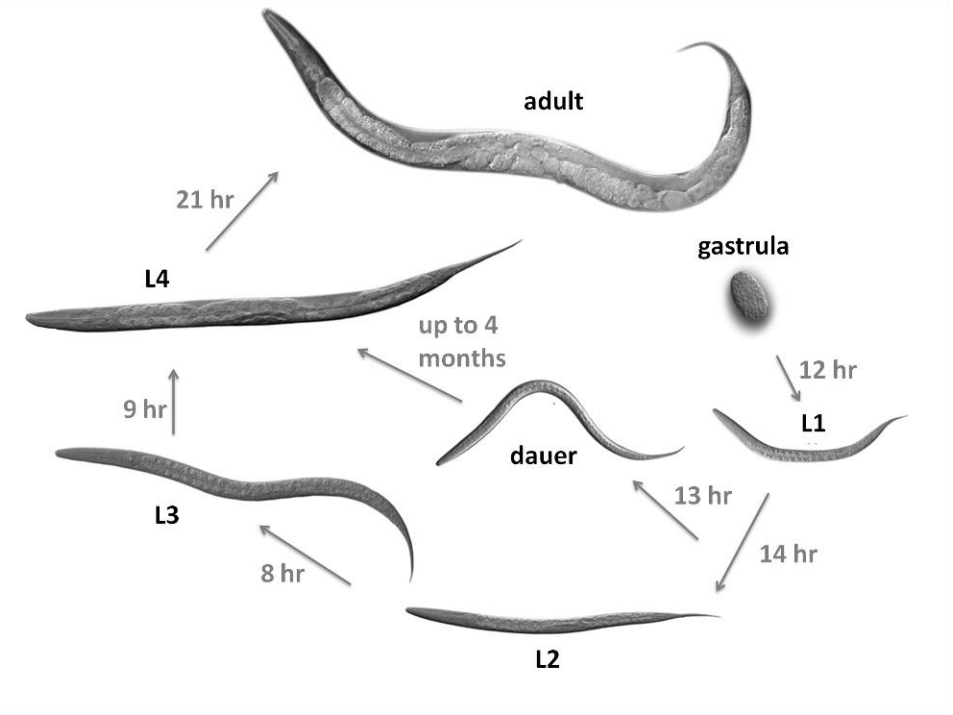

Figure 1.1. Life cycle of *C. elegans* at 20°C. Under favorable conditions, *C. elegans* develops from egg to adult through four larval stages (L1-L4). During unfavorable conditions, the worm enters a dauer stage which can survive for several months (adapted from Altun & Hall, 2009).

A fundamentally attractive feature of *C. elegans* is the ease of generating mutations. Random mutations are easily generated by chemical or radiation mutagenesis, while transposon- and enzyme-based techniques allow site-specific mutagenesis (Brenner, 1974; Friedland *et al.*, 2013; Kutscher and Shaham, 2014). Self-fertilization of hermaphrodites allows the maintenance of mutations in homozygous populations, while male mating is used to isolate and transfer mutations between strains (Kutscher and Shaham, 2014). Moreover, these strains can be stored as frozen stocks indefinitely in liquid nitrogen. Strains are generally collected and stored by the *National Bioresource Project* or the *Caenorhabditis Genetic Center*, making these strains readily available to researchers.

In 1998, Craig Mello and Andrew fire discovered the mechanism of RNA interference (RNAi) in *C. elegans*, which can be accomplished by feeding worms bacteria expressing

dsRNA (Fire *et al.*, 1998). The availability of bacterial RNAi libraries, which cover 94% of protein coding genes, allows the study of gene function in high-throughput and genome wide screens (Kamath and Ahringer, 2003).

C. elegans was the first multicellular organism whose genome was completely sequenced (The *C. elegans* Sequencing Consortium, 1998). The 97-megabase genomic sequence contains approximately 20,000 protein coding genes, of which over 40% are similar to those in other organisms. The annotated genome is readily accessible at WormBase (www.wormbase.org). In addition to the annotated gene sequence, WormBase provides information such as corresponding protein sequences, availability of mutant alleles, phenotypic descriptions, and expression patterns (Harris *et al.*, 2009a).

C. elegans has a relatively simple and well-defined anatomy. The anatomical architecture of the whole animal has been determined by serial section electron microscopy and its complete cell lineage, which is invariant between animals, has been established (Sulston *et al.*, 1983; Altun and Hall, 2009). Adult worms measure about one millimeter in length and they are transparent throughout their entire life, which allows easy visualization of cellular processes in living worms. In 1994, the lab of Martin Chalfie was the first to express green fluorescence protein (GFP) in *C. elegans* and demonstrated that it can be used as an expression marker to study gene expression patterns (Chalfie, 1995). Today GFP is one of the most important tools to visualize cellular processes, for which Osamu Shimomura, Martin Chalfie, and Roger Tsien were awarded the Nobel Prize in Chemistry in 2008.

A simple and defined anatomy, short life cycle, ease of cultivation and sequenced genome, along with the availability of powerful molecular and genetic tools, made *C. elegans* one of the most popular model organisms of the 21st century.

1.2 The neurobiology of C. elegans

C. elegans has a relatively simple and well-defined nervous system. The nervous system of adult hermaphrodites consists of 302 neurons, whereas adult males have 383 neurons. Most of the additional male-specific cells are involved in male mating behavior and are located in the posterior body (Jarrell *et al.*, 2012). The majority of the *C. elegans* neurons have their cell bodies clustered in ganglia in the head, the tail, or the ventral and dorsal nerve cords. The largest neuropile is located in the circumpharyngeal nerve ring in the head, to which over half of the neurons send axons. Based on their function, *C. elegans* neurons are classified into four categories: (1) motor neurons, (2) sensory neurons, (3) interneurons, and (4) polymodal neurons (White *et al.*, 1986; Altun and Hall, 2011).

C. elegans can detect various environmental cues including mechanical stimuli, temperature, chemicals, osmolarity, oxygen levels, pH, and light (Bargmann, 2006; Ward *et al.*, 2008). The perception of these environmental stimuli is accomplished through the sensory neurons. Sensory neurons generally belong to bilaterally symmetric pairs in which the left and right members of each class are structurally similar and arranged into sensory organs, called sensilla. However, some sensory functions including oxygen sensation are performed by nonsensillar neurons as well. Two large sensilla, the amphids, are located laterally at the tip of the head and harbor the sensory endings of 12 sensory neuron pairs (figure 1.2). In the tail, a pair of analogous sensilla, the phasmids, harbor only 2 neuron pairs. The amphid and phasmid sensilla are the main chemosensory organs of the worm. The other sensilla in the head are mainly involved in mechanosensation and arranged into two concentric rings around the mouth. The inner ring includes six inner labial sensilla that each harbors 2 sensory endings. The outer ring is composed of six outer labial sensilla and four cephalic sensilla, each containing a single sensory neuron ending. Two other sensilla, the anterior and posterior deirid, are involved in mechanosensation and harbor the ciliated endings of the ADE and PDE sensory neurons respectively. The anterior deirid is located bilaterally at the posterior part of the head, positioned within the alae, whereas the posterior deirid is positioned dorsal to the alae, located halfway between the vulva and tail (White *et al.*, 1986; Altun and Hall, 2011).

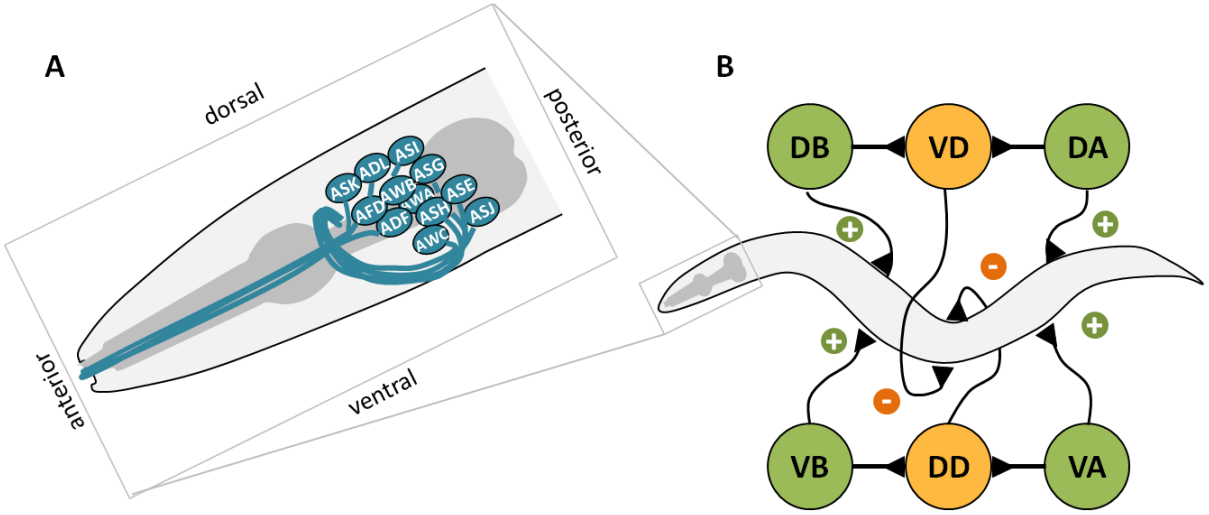

Figure 1.2 Schematic structure of the *C. elegans* (A) amphid neurons and (B) motor neurons regulating locomotion. (A) The primary chemosensory organs of *C. elegans* are the amphid sensilla. They contain the ciliated nerve endings of 12 pairs of sensory neurons whose cell bodies are located in the anterior region of the second pharyngeal bulb and possess axons that associate with the nerve ring. (B) *C. elegans* sinusoidal locomotion is propagated by alternatively contracting and relaxing opposing ventral and dorsal body wall muscles which are regulated by cholinergic (indicated in green; DB and VB for forward locomotion, and DA and VA for backward locomotion) and GABAergic (indicated in orange; VD and DD) motor neurons **(**figures adapted from Altun and Hall, 2011; and Donnelly *et al.*, 2013).

The worm can adapt its behavior upon the perception of environmental cues. The main behavioral output of these responses is manifested as alterations in locomotion (de Bono and Maricq, 2005; Yemini *et al.*, 2013). Due to the anatomy of the body wall muscles and their synaptic inputs, *C. elegans* locomotion is restricted to dorsal and ventral turns of the body. The body wall muscles are organized into two dorsal rows and two ventral rows, which are controlled by distinct classes of motor neurons connected to the muscles by neuromuscular junctions (NMJs). In total, 113 of the 302 *C. elegans* neurons are motor neurons. The neurons involved in body locomotion are subdivided in 6 classes (DA, DB, DD, VA, VB, and VD). A- and B-type neurons (VA, VB, DA, DB) are stimulatory cholinergic motor neurons, whereas D-type neurons (VD, DD) are inhibitory GABAergic motor neurons and strictly post-synaptic to other motor neurons. VA, VB, and VD neurons innervate ventral muscles, whereas DA, DB, and DD neurons innervate the dorsal muscles (figure 1.2). The connectivity of these neurons ensures that upon the contraction of the

ventral muscles following the excitation of cholinergic motor neurons (*e.g.* VA or VB), the opposing dorsal muscles relax because of inhibition by GABAergic motor neurons (*e.g.* DD), resulting in the typical sinusoidal locomotion pattern of *C. elegans.* One set of excitatory and inhibitory dorsal (DB and DD, respectively) and ventral (VB and VD, respectively) neurons controls forward movement, and a second set (DA, DD, VA, and VD) controls backward movement (White *et al.*, 1986; Kaplan and Driscoll, 1997; de Bono and Maricq, 2005). Turning is propagated by hypercontraction of the dorsal or ventral muscles, which is under control of the DD or VD neurons respectively (Donnelly *et al.*, 2013).

For simple behaviors, sensory neurons sometimes communicate directly with motor neurons, but in more complex behavioral circuits, several layers of interneurons integrate sensory information and relay it to motor neurons. Interneurons comprise the largest group of neurons in the nematode. They compare and process sensory inputs in individual neuronal circuits and modulate the decision to execute a given motor program. They also function as circuit couplers where information from two or more circuits converge to establish circuit hierarchies (Macosko *et al.*, 2009; Altun and Hall, 2011).

C. elegans is the only animal for which a detailed neural connectivity map of the entire nervous system has been constructed. In adult hermaphrodites, the connectome of the somatic nervous system consist of 282 neurons and approximately 6000 chemical synapses, 1500 neuromuscular junctions, and 900 gap junctions (White *et al.*, 1986; Varshney *et al.*, 2011). These connections are stereotypical from animal to animal with more than 75% reproducibility (White *et al.*, 1986). Interactive visualizations of this connectivity map are easily accessible on several online tools such as WormAtlas (www.wormatlas.org) and OpenWorm (www.openworm.org).

Chemical signaling in the *C. elegans* nervous system occurs through classical neurotransmitters including acetylcholine (ACh), γ-aminobutyric acid (GABA), glutamate, nitric oxide, serotonin, and other monoamines (Brownlee and Fairweather, 1999). These small-molecule neurotransmitters are packed into synaptic vesicles and subsequently released by exocytosis (Gasnier, 2000; Weimer and Jorgensen, 2003; Scalettar, 2006). In addition to classical neurotransmitters, cell-to-cell communication via chemical signaling in *C. elegans* also occurs through a wide plethora of neuropeptides.

Despite its compact and relatively simple nervous system, *C. elegans* is capable of several complex behaviors. For instance, worms can discriminate and approach or avoid chemicals, odorants, temperatures, and food sources. Moreover, the worm can learn to move towards or away from these stimuli and can store memories (de Bono and Maricq, 2005). It is becoming clear that knowledge of the neuronal connectivity diagram alone may not be sufficient to explain how the nervous system generates these complex behaviors (Bargmann, 2012; Marder, 2012). The anatomical connectivity diagram encodes the potential for multiple neuronal circuits which may generate multiple behaviors, but only a subset of those circuits are accessible at any given time and are shaped by context and internal states. At the molecular level, context and internal states are often represented by neuromodulators: small molecules that change the composition of a neuronal circuit, recruiting new neurons, or excluding previous participants by modifying neuronal dynamics, excitability, or synaptic efficiency (Bargmann, 2012; Marder, 2012).

A recent study on neuromodulatory circuits that generates roaming and dwelling states in *C. elegans* demonstrates the power of using *C. elegans* to investigate the molecular and circuit mechanisms underlying complex behavioral states. Feeding *C. elegans* spontaneously switch between two foraging states called roaming and dwelling. Both states include common locomotion patterns such as forward locomotion, reversals and turns. Roaming animals move quickly across a bacterial lawn and turn infrequently to explore the bacterial lawn. Dwelling animals move slowly and turn more frequently remaining in a small area (Fujiwara *et al.*, 2002; Ben Arous *et al.*, 2010). Combining high resolution locomotion assays with cell-specific knockdown and rescue, optogenetic stimulation, and calcium imaging, Flavell and coworkers showed that serotonergic signaling initiates and extends dwelling states, whereas neuropeptidergic signaling by pigment dispersing factor (PDF) initiates and extends roaming states (Flavell *et al.*, 2013). Serotonin released from the serotonergic NSM and HSN neurons inhibits the AIY, RIF, and ASI neurons that promote roaming through the activation of the serotonin-gated chloride channel MOD-1. On the other hand, PDF signaling from the PVP, AVB, and SIAV neurons promotes roaming through cAMP dependent activation of its receptor PDFR-1 on the AIY, RIM, and RIA neurons. As depicted on the wiring diagram (figure 1.3), these neuromodulatory connections do not follow the classical sensory to motor neuron hierarchy and do not overlap with the

anatomical connectivity of the associated neurons, indicating that these modulatory circuits are orthogonal to the synaptic wiring diagram (Flavell *et al.*, 2013).

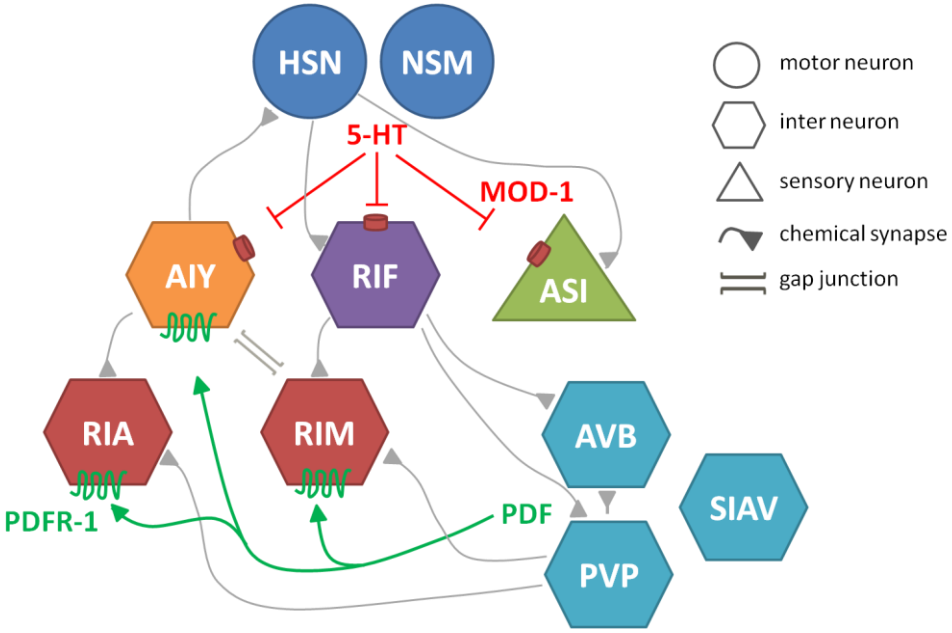

Figure 1.3 Serotonin and PDF initiate and extend opposing behavioral states in *C. elegans*. Serotonin (5-HT) released from NSM and HSN neurons inhibits the AIY, RIF, and ASI neurons that promote roaming through the activation of the serotonin-gated chloride channel MOD-1. Whereas PDF signaling from the PVP, AVB, and SIAV neurons promotes roaming through the activation of its receptor PDFR-1 on the AIY, RIM, and RIA neurons (figure adapted from Flavell *et al.*, 2013).

1.3 Neuropeptidergic signaling in the nematode C. elegans

C. elegans neuropeptides are implicated in the modulation of essentially all behaviors including locomotion, reproduction, social behavior, mechano- and chemosensation, learning and memory (Li and Kim, 2008; Frooninckx *et al.*, 2012; Peymen *et al.*, 2014). It is assumed that possibly all *C. elegans* neurons synthesize and secrete neuropeptides (Holden-Dye and Walker, 2012). Combined biochemical and bioinformatic approaches showed that the *C. elegans* genome encodes over 100 neuropeptide precursors, of which more than 250 potential peptides can be derived (Nelson *et al.*, 1998; Pierce *et al.*, 2001; Nathoo *et al.*, 2001; Husson *et al.*, 2005; Husson *et al.*, 2007b; Husson *et al.*, 2014). These neuropeptides are subdivided into three major families based on sequence and structural similarities: (1) the FMRFamide (Phe-Met-Arg-Phe-amide)-like peptides (FLP), the insulin-like peptides

(INS), and the neuropeptide-like family (NLP), which consists of peptides that bear no resemblance to FMRFamide- or insulin-like peptides (Husson *et al.*, 2007b; Li and Kim, 2008).

1.3.1 Biosynthesis of *C. elegans* neuropeptides

As in mammals, *C. elegans* neuropeptides are derived from peptide precursors or preproproteins that encode a single or multiple neuropeptides. Typically, mature neuropeptides are derived from their preproproteins by several posttranslational modifications, for which the processing pathway in *C. elegans* is shown to be conserved (Husson *et al.*, 2006; Husson *et al.*, 2007a). Preproproteins have an aminoterminal signal peptide, which drives translocation of the precursor into the secretory pathway. This signal peptide is cleaved off by a signal peptidase in the endoplasmatic reticulum. The remaining proprotein is transported to the Golgi-complex, where the proprotein convertase KPC-2 (or EGL-3) cleaves the remaining proprotein at specific dibasic cleavage sites like lysine-arginine (KR), arginine-arginine (RR), or arginine-Xn-arginine (RXnR) where n is 2, 4, 6 or 8 amino acids. Next, the carboxypeptidase EGL-21 removes the basic amino acids that are still attached at the carboxyterminus. Some peptides go through more posttranslational modifications such as carboxyterminal amidation or aminoterminal pyroglutamation, which protects them from degradation. When the peptides are mature they are packed into dense core vesicles in which they are transported to their destination sites (Husson *et al.*, 2014).

1.3.2 G protein-coupled receptor signaling

Neuropeptides usually act through the activation of G protein-coupled receptors (GPCRs). GPCRs are defined as seven transmembrane receptors that generally signal through G proteins (Pierce *et al.*, 2002). GPCRs make up about 7% of all predicted protein-coding genes in *C. elegans* (Bargmann, 1998; Fredriksson and Schiöth, 2005). Most of them (~1300) encode nematode-specific chemoreceptors, which are thought to compensate for the absence of visual and auditory systems in *C. elegans* (Thomas and Robertson, 2008). The remaining GPCRs can be classified according to the GRAFS classification system and comprise the Glutamate, Rhodopsin, Adhesion, Frizzled and Secretin families (Schiöth and Fredriksson, 2005). Neuropeptides usually bind to GPCRs which belong to the Rhodopsin and Secretin families (Schiöth and Fredriksson, 2005).

G protein-coupled signaling pathways are highly conserved among *C. elegans* and mammals. Typically the inactive receptor is bound to a heterotrimeric Gαβγ protein. Upon binding of an activating ligand, the receptor changes its confirmation and acts as a guanine nucleotide exchange factor by catalyzing the release of GDP and binding of GTP by the Gα subunit. The activated heterotrimeric Gαβγ protein dissociates from the receptor and splits into a Gα-GTP and a Gβγ subunit. Gα-GTP can regulate different effectors depending on the Gα subtype ($G\alpha_s$, $G\alpha_{i/o}$, $G\alpha_q$ and $G\alpha_{12/13}$; figure 1.4). $G\alpha_q$ is known for its activation of phospholipase Cβ (PLCβ), which splits phosphatidylinositol 4,5-bisphosphate (PIP2) into diacylglycerol (DAG) and inositol-1,4,5-trisphosphate (IP3). Binding of IP3 to IP3 dependent calcium channels leads to an increase in calcium, and DAG will bind and activate protein kinase C (PKC). $G\alpha_s$ and $G\alpha_{i/o}$ act through adenylyl cyclase by stimulating ($G\alpha_s$) or inhibiting ($G\alpha_{i/o}$) its activity and thereby regulating the concentration of cyclic adenosine monophosphate (cAMP), which activates protein kinase A (PKA). $G\alpha_{12/13}$ activates Rho dependent pathways. The Gβγ subunit also regulates certain downstream effectors such as ion channels and PLCβ. G protein signaling is terminated by internalization of the GPCR, which is initiated by phosphorylation through GPCR kinases (GRKs) (Ritter and Hall, 2009).

C. elegans has homologs for most of the above described G proteins and downstream second messengers. The worm has 21 Gα, 2 Gβ (GPB-1 and GPB-2), and 2 Gγ (GPC-1 and GPC-2) proteins. GPB-1 and GPC-2 seem to be mediators in the classical G protein signaling as the homologs of Gβ and Gγ, respectively. For each of the four mammalian Gα subtypes, there is a homologous Gα protein in *C. elegans* (GSA-1 ($G\alpha_s$), GOA-1 ($G\alpha_{i/o}$), EGL-30 ($G\alpha_q$) and GPA-12 ($G\alpha_{12/13}$)). The remaining *C. elegans* Gα subtypes are believed to be specific for chemosensory GPCRs (Bastiani and Mendel, 2006; Jansen *et al.*, 1999). EGL-30 and GSA-1 are the only Gα proteins for which the conservation of their downstream targets has been demonstrated. The classical role of the EGL-30 $G\alpha_q$ protein is intensively studied in neuromuscular junctions where it stimulates the release of the neurotransmitter ACh. EGL-30 binds and activates EGL-8, the PLCβ homolog, which splits PIP2 into IP3 and DAG. In neuromuscular junctions, DAG binds to UNC-13 which regulates synaptic vesicle release of ACh through syntaxin (Lackner *et al.*, 1999). IP3 on the other hand can bind to the IP3 dependent calcium channel ITR-1 which leads to a calcium

response (Bastiani *et al.*, 2003; Baylis and Vázquez-Manrique, 2012). The $G\alpha_s$ protein homolog GSA-1 seems to function through the adenylate cyclase ACY-1. GSA-1 is an essential protein but constitutive activation of GSA-1 in the presence of ACY-1 causes neurodegeneration (Berger *et al.*, 1998; Korswagen *et al.*, 1997). Constitutive expression of rat $G\alpha_s$ correspondingly causes the same neurodegenerative phenotype.

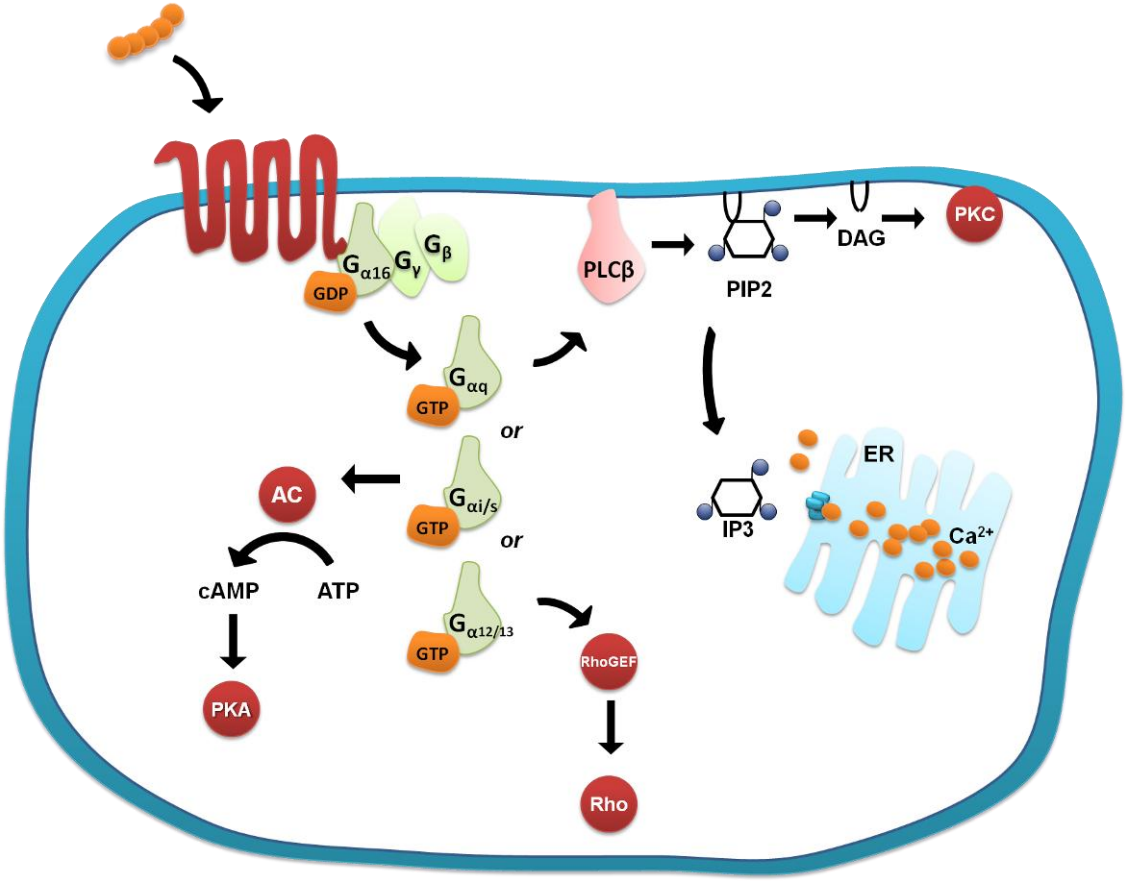

Figure 1.4 The classical G protein signaling pathways. (L, ligand; CM, cell membrane; GDP, guanosine diphosphate; GTP, guanosine triphosphate; AC, adenylate cyclase; cAMP, cyclic adenosine monophosphate; ATP, adenosine triphosphate; PKA, protein kinase A; PLCβ, phospholipase Cβ; PIP2, phosphatidylinositol 4,5-bisphosphate; DAG, diacylglycerol; IP3, inositol-1,4,5-trisphosphate; ER, endoplasmatic reticulum; PKC, protein kinase C; GEF, guanine nucleotide exchange factor).

1.3.3 Finding neuropeptide ligands for orphan GPCRs

A crucial step in the characterization of a predicted neuropeptide GPCR is the identification of its natural ligand(s), termed ‘deorphanization’. For this purpose, a reverse pharmacology approach can be applied (Mertens *et al.*, 2004b; Beets *et al.*, 2011). In this strategy, the

orphan GPCR is expressed in a heterologous expression system. Often Chinese hamster ovary (CHO) or human embryonic kidney (HEK) cells are the recombinant system of choice because of their ease of use and proven history of functional GPCR expression (Szekeres, 2002). Subsequently, receptor expressing cells are challenged with a library of compounds and activation of the GPCR of interest is measured. The compound library is usually compiled based on bioinformatic predictions and peptidomic analyses of reversed phase high performance liquid chromatography (RP-HPLC) fractions of a tissue extract (Beets *et al.*, 2011).

In the past few years, several successful strategies have been developed for receptor deorphanization (Mertens *et al.*, 2004b; Beets *et al.*, 2011). One of the most frequently used methods is probably the calcium mobilization assay based on the detection of intracellular calcium that is released from storage sites upon receptor activation. This method is often combined with the co-expression of a promiscuous Gα protein, such as the $G\alpha_{16}$ subunit, which can direct the intracellular signaling cascade of most GPCRs through a calcium flux, regardless of their endogenous G protein coupling (Kostenis, 2001). Alternatively, chimeric G proteins can be used to lead the signal cascade to a pathway of choice (Coward *et al.*, 1999). The resulting calcium flux can then be detected by bioluminescent proteins such as aequorin, or by fluorescent calcium indicators (*e.g.* Fluo-4). In the bioluminescent assay, cells expressing the apo-aequorin protein are charged prior to the assay with the cofactor coelenterazine to form a calcium-sensitive aequorin complex. When calcium binds to aequorin, the complex is oxidized and blue light is omitted. Similar to the luminescence assay, receptor expressing cells can be loaded with a fluorophore, of which the fluorescence increases upon binding of calcium (Mertens *et al.*, 2004). Thanks to the development of automated systems for simultaneous compound addition and signal detection in various well-plate formats, calcium mobilization methods can be used in high-throughput screening assays. Once the activating ligand(s) of a receptor are found, the potential endogenous signaling pathway is investigated by omitting the promiscuous $G\alpha_{16}$ protein. Coupling of a receptor with $G\alpha_{q,}$ $G\alpha_{s}$, or $G\alpha_{i}$ can be visualized by respectively measuring the calcium increase or cAMP in-/decrease.

1.3.4 Characterized neuropeptide systems in *C. elegans*: state of the art

While over a 100 neuropeptide GPCRs have been predicted in *C. elegans* (Janssen *et al.*, 2010; Frooninckx *et al.*, 2012), only 31 have been successfully deorphanized (table 1.1). The neuropeptide systems that have been functionally characterized so far will be discussed in more detail here.

Table 1.1 List of deorphanized neuropeptide GPCRs in *C. elegans*. Underlined neuropeptides are the most potent ligands.

Protein	WormBase ID	Ligand	Reference
NPR-1	WP:CE06941	FLP-18-1, FLP-18-2, FLP-18-3, FLP-18-4, FLP-18-5, FLP-18-6, FLP-21	(Kubiak *et al.*, 2003a; Rogers *et al.*, 2003)
NPR-2a	WP:CE32924	FLP-21	(Beets, 2013)
NPR-2b	WP:CE32925	FLP-21	(Beets, 2013)
NPR-3	WP:CE08056	FLP-15-1, FLP-15-2	(Kubiak *et al.*, 2003b)
NPR-4	WP:CE37317	FLP-1-6, FLP-4-2, FLP-18-1, FLP-18-2, FLP-18-3, FLP-18-4, FLP-18-5, FLP-18-6	(Lowery *et al.*, 2003)
NPR-5a	WP:CE33345	FLP-1-2, FLP-3-1, FLP-3-3, FLP-3-6, FLP-3-8, FLP-18-1, FLP-18-2, FLP-18-3, FLP-18-4, FLP-18-5, FLP-18-6, FLP-21	(Kubiak *et al.*, 2008)
NPR-5b	WP:CE36962	FLP-1-2, FLP-3-1, FLP-3-3, FLP-3-6, FLP-3-8, FLP-4-2, FLP-18-1, FLP-18-2, FLP-18-3, FLP-18-4, FLP-18-5, FLP-18-6, FLP-21	(Kubiak *et al.*, 2008)
NPR-6	WP:CE31509	FLP-18-3, FLP-18-6, FLP-21	(Lowery *et al.*, 2003)
NPR-10a	WP:CE19767	FLP-3-1, FLP-3-3, FLP-3-5, FLP-3-6, FLP-3-7, FLP-3-8, FLP-18-1, FLP-18-3, FLP-18-4, FLP-18-5, FLP-18-6	(Lowery *et al.*, 2003)
NPR-10b	WP:CE36989	FLP-3-1, FLP-3-3, FLP-3-5, FLP-3-6, FLP-3-7, FLP-3-8,	(Lowery *et al.*, 2003)

Protein	WormBase ID	Ligand	Reference
		FLP-18-1, FLP-18-3, FLP-18-4, FLP-18-5, FLP-18-6	
NPR-11	WP:CE47199	FLP-1-6, FLP-5-2, FLP-14, FLP-18-3, FLP-21, NLP-1a	(Lowery *et al.*, 2003; Chalasani *et al.*, 2010)
FRPR-3	WP:CE06880	FLP-7-1, FLP-7-2, FLP-7-3, FLP-11-1	(Mertens *et al.*, 2004a)
FRPR-18a	WP:CE29348	FLP-2-1, FLP-2-2	(Mertens *et al.*, 2005)
FRPR-18b	WP:CE29349	FLP-2-1, FLP-2-2	(Mertens *et al.*, 2005)
TKR-1	WP:CE44282	TK-1, TK-2a, TK-2b	this thesis
TKR-2	WP:CE16937	TK-1, TK-2a, TK-2b	this thesis
NPR-22a		FLP-1-6, FLP-7-1, FLP-7-2, FLP-7-3, FLP-7-4, FLP-9, FLP-11-1, FLP-11-2, FLP-11-3, FLP-13-4, FLP-22	(Mertens *et al.*, 2006)
CKR-2e	WP:CE48226	FLP-1-1, NLP-12-1, NLP-12-2, NLP-13-3, NLP-14-1	(Janssen *et al.*, 2008b)
CKR-2f	WP:CE48324	FLP-1-1, NLP-12-1, NLP-122, NLP-13-3, NLP-1-1a	(Janssen *et al.*, 2009b)
GNRR-1a	WP:CE17102	NLP-47	(Lindemans *et al.*, 2009b)
GNRR-3	WP:CE40886	NLP-2-1, NLP-2-2, NLP-2-3, NLP-22, NLP-23-2	this thesis
NTR-1	WP:CE13377	NTC-1	(Beets *et al.*, 2012)
NMUR-1	WP:CE45664	NLP-44-1, NLP-44-3	this thesis
NMUR-2	WP:CE38395	NLP-44-3	(Lindemans *et al.*, 2009a)
EGL-6a	WP:CE04219	FLP-10, FLP-17-1, FLP-17-2	(Ringstad and Horvitz, 2008)
EGL-6b	WP:CE43400	FLP-10, FLP-17-1, FLP-17-2	(Ringstad and Horvitz, 2008)

Protein	WormBase ID	Ligand	Reference
SPRR-1	WP:CE43810	NLP-42-1, NLP-42-2	(Beets, 2013)
AEX-2	WP:CE31607	NLP-40-3	(Wang *et al.*, 2013)
PDFR-1a	WP:CE30860	PDF-1a, PDF-1b, PDF-2	(Janssen *et al.*, 2008a)
PDFR-1b	WP:CE37087	PDF-1a, PDF-1b, PDF-2	(Janssen *et al.*, 2008a)
PDFR-1c	WP:CE37088	PDF-1a, PDF-1b, PDF-2	(Janssen *et al.*, 2008a)

1.3.4.1 NPR-1 signaling: inhibition of food-dependent aggregation and aerotaxis

The neuropeptide receptor 1 (NPR-1) was the first neuropeptide GPCR to be deorphanized in *C. elegans* (Kubiak *et al.,* 2003; Rogers *et al.,* 2003). This receptor shows homology to the vertebrate neuropeptide Y (NPY) receptor family that is implicated in a variety of physiological processes such as food intake and stress (Heilig, 2004; Arora and Anubhuti, 2006). In the nematode *C. elegans*, NPR-1 is involved in a multitude of functions such as food-dependent behaviors, thermal avoidance, ethanol tolerance, sex-specific pheromone responses, molting-associated quiescence, and innate immunity (de Bono and Bargmann, 1998; Davies *et al.*, 2004; Gray *et al.*, 2004; Cheung *et al.*, 2005; Rogers *et al.*, 2006; Styer *et al.*, 2008; Reddy *et al.*, 2009; Milward *et al.*, 2011; Glauser *et al.*, 2011; Jang *et al.*, 2012; Choi *et al.*, 2013).

The most explicit function of NPR-1 was elucidated with the observation of aggregating and solitary feeders in wild type isolates of *C. elegans* (de Bono and Bargmann, 1998). This behavioral difference could be attributed to a single amino acid difference. Aggregating isolates carry an *npr-1* Phe-215 allele, whereas solitary feeders possess an *npr-1* Val-215 allele. Since a functional null mutation of *npr-1* converts the solitary wild type N2 lab strain into an aggregating one, NPR-1 activity is suggested to suppress aggregating behavior. The RMG inter/motor neuron seems to be the cellular hub of this NPR-1 mediated feeding behavior, as demonstrated by the full rescue of the solitary behavior through RMG specific expression of NPR-1 in an *npr-1* knockout mutant (Macosko *et al.,* 2009). The RMG neuron

is the hub of a gap junction network that connects five sensory neurons, which are known to trigger aggregation, while NPR-1 inhibits this gap junction driven activation of RMG (figure 1.5). The RMG neural network can be considered a multifunctional sensory circuit that uses neuropeptide GPCR signaling amongst others to coordinate behavioral output. In addition to its effects on aggregation behavior, deletion of the NPR-1 receptor increases the threshold for heat avoidance, and cell-specific rescue of *npr-1* demonstrates the role of the RMG interneuron in the regulation of heat avoidance behavior (Glauser *et al.*, 2011). Similarly, RMG-specific rescue of *npr-1* restores pheromone avoidance defects in the *npr-1* mutant background (Jang *et al.*, 2012).

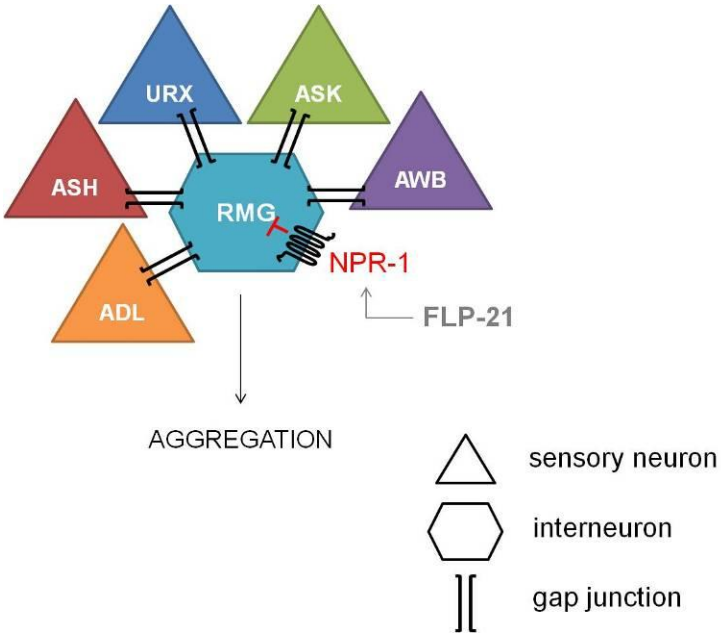

Figure 1.5 Inhibition of the RMG inter/motor neuron by NPR-1. The RMG neuron is the hub of a gap junction network connecting the ADL, ASH, URX, ASK, and AWB sensory neurons, which are known to trigger aggregation. Activation of NPR-1 by the neuropeptide FLP-21 inhibits this gap junction driven activation of RMG and the resulting food-dependent aggregation behavior (figure adapted from Macosko *et al.*, 2009).

In insects and mollusks, FMRFamide-related peptides (FaRPs) are reported as ligands for NPY-like receptors (Tensen *et al.*, 1998; Feng *et al.*, 2003). In 2003, two independent groups were able to deorphanize the NPR-1 receptor by screening *C. elegans* and other invertebrate FaRPs as potent compounds. Both FLP-21 and FLP-18 peptides activated the

solitary Val-215 receptor (Table 1.1). The social Phe-215 receptor variant could only be activated by FLP-21. NPR-1 signaling occurs through a $G\alpha_{i/o}$ type of G protein (Kubiak *et al.*, 2003; Rogers *et al.*, 2003).

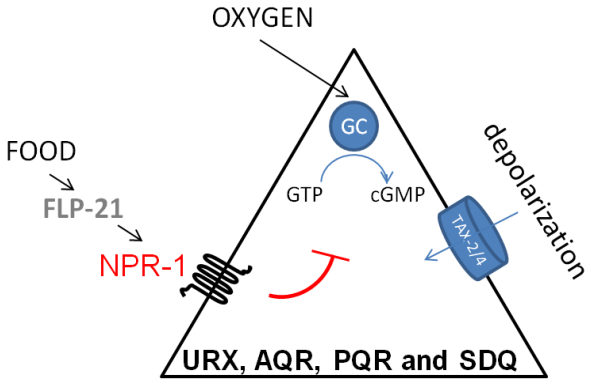

Figure 1.6 Regulation of aerotaxis by NPR-1. *C. elegans* detects oxygen through the URX, PQR, AQR, and SDQ neurons. Oxygen sensing in these neurons is mediated by soluble guanylate cyclase homologs (sGC-35 and sGC-36). When ambient oxygen levels decrease, cGMP levels rise and the cGMP gated TAX-2/TAX-4 ion channel opens, which leads to the depolarization of the neurons. Activation of NPR-1 by the FLP-21 peptide in the presence of food inhibits this activation (Chang *et al.*, 2006; Cheung *et al.*, 2005).

Besides its role in feeding behavior, NPR-1 also regulates aerotaxis (figure 1.6). *C. elegans* exhibits a strong behavioral preference for 5-12% oxygen, avoiding higher and lower oxygen levels. Oxygen levels are primarily sensed by the URX, PQR, AQR, and SDQ neurons (Gray *et al.*, 2004). Oxygen sensing in these neurons is mediated by soluble guanylate cyclase homologs (GCY-35 and GCY-36). When ambient oxygen levels increase, cyclic guanosine monophosphate (cGMP) levels rise and the cGMP-gated TAX-2/TAX-4 ion channels open, leading to the depolarization of the neurons (Couto *et al.*, 2013). Activation of NPR-1 in the presence of food inhibits the activation of these neurons (Cheung *et al.*, 2005; Rogers *et al.*, 2006; Chang *et al.*, 2006; Milward *et al.*, 2011). Oxygen binding globins such as GLB-5 further tune the behavioral responses to varying oxygen concentrations, and this effect is again modified by NPR-1 (Persson *et al.*, 2009).

1.3.4.2 FLP-18 signaling through NPR-4 and NPR-5 controls foraging and metabolism

Both a reverse pharmacology study expressing orphan receptors in CHO cells and an independent *Xenopus laevis* oocyte assay demonstrated that the *flp-18*-encoded peptides are the most potent ligands of NPR-5a and NPR-5b, the splice variants of *npr-5* (Table 1.1; Cohen *et al.,* 2009; Kubiak *et al.,* 2008). The latter study also showed that another member of the GPCR rhodopsin family, NPR-4, is activated by FLP-18 peptides (Table 1.1; Cohen *et al.,* 2009), which in addition to their activation of NPR-1 (Kubiak *et al.,* 2003) indicates these are widely deployed ligands of GPCRs. NPR-5a and NPR-5b seem to transduce the FLP-18 signal mainly through a $G\alpha_q$ type of G protein, while NPR-4 might use a different cellular signaling machinery.

flp-18(db99) loss-of-function mutants display defects in chemosensation, dauer formation, and foraging, and accumulate excess intestinal fat and exhibit reduced aerobic metabolism. Distinct subsets of these phenotypes are phenocopied by *npr-4* and *npr-5* deletion mutants. Each one of the FLP-18 receptors regulates fat metabolism in response to the release of FLP-18 peptides from AIY and RIG interneurons in the head, some of the multiple expression sites of *flp-18*. NPR-4 mediated regulation of intestinal fat occurs at the level of the gut, while NPR-5 modulates the activity of a number of amphid sensory neurons. FLP-18 neurohormones released from AIY interneurons act on NPR-4 in AVA and RIV interneurons and appear to be implicated in odor responses and foraging behavior. The chemosensory ASJ neurons regulate dauer formation through activation of NPR-5. All of these observations led to the proposition of a model (figure 1.7) in which sensory detection of nutritional availability is coupled to adequate responses such as foraging behavior and metabolic alterations via RFamide-like receptor signaling (Cohen *et al.,* 2009).

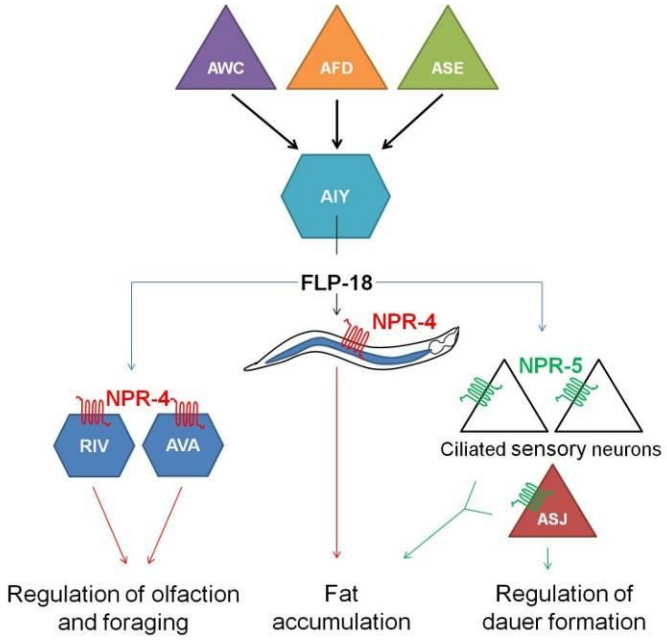

Figure 1.7 Regulation of *C. elegans* foraging and metabolism by FLP-18 neuropeptide signaling through the RFamide-like receptors NPR-4 and NPR-5. The detection of nutrition by *C. elegans* sensory neurons (AWC, AFD, and ASE) is likely coupled to the release of FLP-18 neuropeptides from AIY interneurons and subsequent signaling through the RFamide-like receptors NPR-4 and NPR-5. By acting on NPR-4 in the intestine and NPR-5 in ciliated neurons, FLP-18 neuropeptides control fat storage. Signaling through NPR-4 in RIV and AVA neurons also modulates responses to odor and foraging behavior. Another food-dependent decision, dauer formation, is regulated by FLP-18 action on NPR-5 in the ASJ neurons (figure adapted from Cohen *et al.*, 2009).

1.3.4.3 Off-food search behavior: feedback signaling through NPR-11

Characterization of the neuropeptide GPCR NPR-11 is a good example of how the knowledge of the entire neuronal wiring diagram makes *C. elegans* a powerful model organism. When worms are removed from a food source, they display a local search behavior characterized by increased turning rates during the first 15 minutes. This behavior is known to depend on the activity of the AWC olfactory neurons, which release both glutamate and the neuropeptide NLP-1. Glutamate is necessary for increased turning rates during the off-food search behavior of the worm, a behavioral change that is also observed in knockout mutants of *nlp-1*. No increase is noticed in glutamate-depleted mutants, suggesting that NLP-1 acts as a co-transmitter for glutamate by decreasing its effect (Chalasani *et al.*, 2010).

To identify the receptor through which NLP-1 is signaling, Chalasani *et al.* looked for orphan GPCRs expressed in neurons that are connected to the AWC sensory neurons (Chalasani *et al.*, 2010). A knockout mutation of the NPY/NPF-like receptor NPR-11, resulted in a similar phenotype as displayed by the *nlp-1* mutant. A calcium-based assay confirmed the NLP-1/NPR-11 interaction.

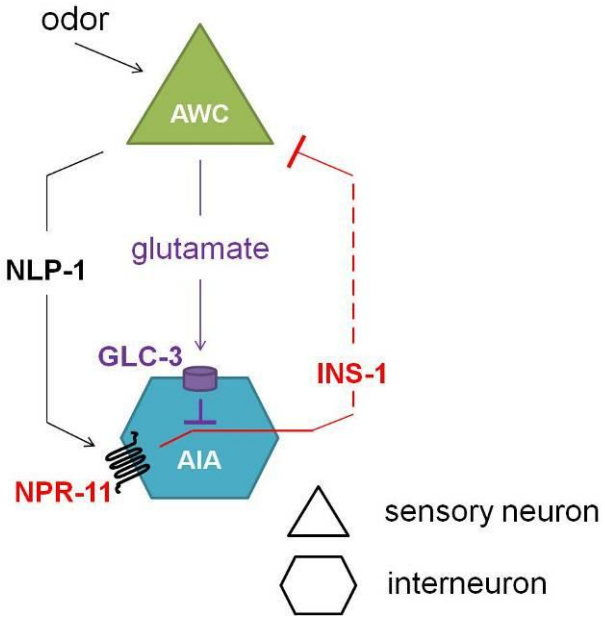

Figure 1.8 Neuropeptidergic feedback regulation of the AWC sensory neurons. The AIA interneurons are inhibited via the glutamate-gated chloride channel GLC-3 upon release of the neurotransmitter glutamate from the AWC neurons. Alternatively, when odor is sensed, the AWC neurons release NLP-1, which in turn activates NPR-11 on the AIA interneurons. Upon activation of NPR-11, INS-1 is released, inhibiting AWC activity and thereby reducing its inhibition on AIA (adapted from Chalasani *et al.*, 2010).

Comparison of the calcium response of AWC neurons during the local search behavior upon food removal suggested that NPR-11 activation by NLP-1 evokes a negative feedback loop, which dampens AWC activity (figure 1.8). NPR-1 is expressed in the AIA interneurons, which also express the insulin-like peptide INS-1. Indeed, an *ins-1* mutant shows the same increase in turning rates upon food removal as the *nlp-1* and *npr-11* mutants. Calcium imaging of the AWC neurons could confirm the role of INS-1 as a suppressor of AWC activity (Chalasani *et al.*, 2010).

1.3.4.4 Conservation of AKH/GnRH signaling through the C. elegans receptor GNRR-1

Gonadotropin releasing hormone (GnRH) is mainly known for its role in reproduction in vertebrates (Kah *et al.*, 2007). The GnRH receptor and its ligand are highly conserved in vertebrates and homologs of the receptor are predicted in a variety of invertebrates (Roch *et al.,* 2011). Remarkably, insect GnRH receptor orthologs are activated by adipokinetic hormone (AKH), corazonin, and AKH/corazonin-related peptide, which are known to be involved in energy metabolism, pigmentation and cardiac regulation (Lindemans *et al.*, 2011; Roch *et al.*, 2011). The genome of *C. elegans* is predicted to encode for a family of eight GnRH-related receptor genes (*gnrr-1* to *gnrr-8*). At the start of this study, only one of these receptors (GNRR-1, isoform a) had been deorphanized (Lindemans *et al.,* 2009a). Since *Drosophila melanogaster* AKH (*Dm*-AKH) was capable of activating this receptor, an *in silico* search was performed for an AKH/GnRH-like peptide in *C. elegans.* This way, Lindemans *et al.* were able to identify the decapeptide NLP-47 (pQMTFTDQWT) as the endogenous ligand for GNRR-1a (Lindemans *et al.*, 2009a). AKH is known to regulate lipid mobilization during flight in insects (Gäde and Auerswald, 2003). In *C. elegans*, fat contents were therefore examined by performing an RNAi knockdown of *gnrr-1* and/or *nlp-47*. No significant differences between knockdowns and wild type worms were observed (Lindemans *et al.,* 2009a). Nevertheless, injection of synthetic *Ce*-AKH/GnRH into the cockroach *Periplaneta americana* resulted in a significant increase in the levels of haemolymph carbohydrates. In contrast to an invariant fat content, RNAi knockdown of *gnrr-1* or *nlp-47* did induce a delay in egg-laying in *C. elegans* (Lindemans, *et al.,* 2009a). The identification of an AKH/GNRH-like signaling system involved in *C. elegans* reproduction is an interesting finding and could be a key to the interplay between reproduction and energy metabolism.

Since no clear ortholog for GnRH was found in insects and nematodes, it was proposed that GnRH has been preserved in lophotrochozoans, but lost in the ecdysozoans (Tsai and Zhang, 2008). Nevertheless, phylogenetic analysis of the ligands of the ecdysozoan GnRH receptors suggests that AKH and corazonin share a common ancestor with GnRH (Lindemans *et al.*, 2011; Roch *et al.*, 2011).

1.3.4.5 The NMU-like signaling pathway regulates food-dependent longevity

In vertebrates, neuromedin U (NMU) is a highly conserved neuropeptide that plays a fundamental role in key physiological processes such as smooth muscle contraction, regulation of blood pressure, feeding and energy homeostasis, stress responses, and immune regulation (Brighton *et al.,* 2004). All NMU peptides that have been isolated from vertebrates have an identical C-terminal pentapeptide (FRPRNamide) (Brighton *et al.*, 2004). The presence of an NMU-like receptor in invertebrates was first reported for the fruit fly *D. melanogaster*. The fruit fly genome encodes four NMU receptor homologs. These receptors are activated by pyrokinin neuropeptides (PRXamide) and are involved in many functions such as feeding behavior and visceral muscle contraction (Melcher and Pankratz, 2005; Park *et al.,* 2002; Schoofs *et al*., 1993).

The *C. elegans* genome encodes four NMU receptor homologs. To date, only NMUR-1 has an assigned phenotype. Wild type *C. elegans* display an altered lifespan depending on the type of food source they live on. NMUR-1 was demonstrated to be involved in this food source dependent regulation of lifespan (Maier *et al.,* 2010). At the start of this project the activating ligand of NMUR-1 was not yet identified. In contrast, though still a receptor of unknown function, NMUR-2 has been deorphanized based on an *in silico* search for *C. elegans* homologs of the *Drosophila* pyrokinin peptides. This revealed three putative PRXamide peptides, all encoded by the same peptide precursor gene *nlp-44*. Only one of these peptides, NLP-44-3, could activate NMUR-2 (Lindemans *et al.,* 2009b).

1.3.4.6 PDF-like signaling: locomotion and reproduction

In *C. elegans*, the pigment dispersing factor receptors (PDFRs) of the secretin receptor family PDFR-1a, b, c, d and e represent five splice isoforms of *pdfr-1* (Janssen *et al.*, 2008a; Barrios *et al.*, 2012). Their endogenous neuropeptide ligands are orthologs of the *Drosophila* pigment dispersing factor (PDF) neuropeptide including PDF-1a, PDF-1b, and PDF-2 that are encoded by the *pdf-1* and *pdf-2* genes. All three PDF peptides are able to activate three PDFR-1 (a,b and c) isoforms though with significant differences in their affinity (Janssen *et al.*, 2008a). PDFR-1a and PDFR-1b signaling occurs via a $G\alpha_s$ type of G protein, while PDFR-1c signaling occurs through a $G\alpha_{i/o}$ type of G protein . PDFR-1d and PDFR-1e were only recently recovered from cDNA (Barrios *et al.*, 2012), and have not yet

been pharmacologically characterized in detail. The PDF-like neuropeptide pathway is highly conserved in nematodes, and PDF neuropeptides are also found in insects and crustaceans. In the latter, they were initially discovered and named pigment dispersing hormones Furthermore, all three *C. elegans* PDF receptors are closely related to insect orthologs, such as the *D. melanogaster* PDF receptor (Janssen *et al.,* 2008a). In *C. elegans*, the *pdfr-1* gene is expressed in each body wall muscle cell and, like *pdf-1* and *pdf-2*, in neuronal cells that are involved in the sensing and integration of environmental stimuli and the control of locomotion (Janssen *et al.*, 2008a; Janssen *et al.,* 2009a).

Functional characterization reveals that the PDF signaling system of *C. elegans* is involved in both locomotion and egg-laying, which stresses the pleiotropic nature of its biological functions. Similar to insects, PDF signaling promotes arousal in *C. elegans* (Choi *et al.*, 2013; Flavell *et al.*, 2013). The PDF system is also implicated in reproduction, as the timing of egg-laying appears to be delayed in *C. elegans pdf-1(tm1996), pdf-2(tm4393)* and *pdf-2(tm4780)* deletion mutants (Meelkop *et al.,* 2012). The PDFR-1b and PDFR-1d isoforms could rescue a male-specific defect in mate-searching behavior. This defect is mediated through PDF-1 peptides, but not PDF-2; and seems to be needed in gender-shared neurons for the regulation of this sex-specific behavior (Barrios *et al.,* 2012). Functions for PDF signaling in locomotion and reproduction have been demonstrated in other invertebrate species as well (Helfrich-Förster *et al.,* 2000; Renn *et al.,* 1999; Hamanaka *et al.,* 2005). Recently, proteomic analysis proposed the involvement of PDF signaling in lipid metabolism and stress resistance (Temmerman *et al.*, 2012).

1.3.4.7 The CCK/gastrin-like signaling system regulates feeding and metabolism

Cholecystokinin (CCK) and gastrin are well-characterized peptide hormones in vertebrates. By acting on two conserved GPCRs, CCK1R and CCK2R; they are implicated in a variety of digestive functions including the stimulation of digestive enzyme production, intestinal motility, and the promotion of satiety in order to regulate food intake (Dufresne *et al.*, 2006; Konturek *et al.,* 2003; Clerc *et al.,* 2007). In arthropods, the sulfakinin (SK) family of neuropeptides is both structurally and functionally related to the well-conserved vertebrate CCK and gastrin peptides (Schoofs and Nachman, 2006). A Basic Local Alignment Search Tool (BLAST) analysis of the *C. elegans* genome revealed *ckr-1* and *ckr-2* as the

homologous genes of the vertebrate CCK/gastrin receptors and their SK counterparts in insects (Kubiak *et al.,* 2002; Meeusen *et al.,* 2003; McKay *et al.,* 2007). The *ckr-2* gene is predicted to encode six splice isoform receptors of which two, CKR-2e and CKR-2f[1], have been cloned and characterized. By use of a reverse pharmacology approach, the endogenous *C. elegans* NLP-12-1 and NLP-12-2 neuropeptides - encoded by the *nlp-12* gene - were appointed the CCK/gastrin-like ligands of CKR-2e and CKR-2f (Janssen *et al.,* 2008b). Signaling of the CCK receptors occurs through a $G\alpha_q$. The *nlp-12* gene is expressed in a single tail neuron, identified as DVA, while *ckr-2* is expressed in cholinergic and GABAergic motor neurons (Janssen *et al.,* 2008b; Hu *et al.,* 2011).

The *C. elegans ckr-2* deletion mutant displays decreased intestinal amylase activity/secretion relative to wild type worms, suggesting the involvement of CKR-2 signaling in the stimulation of digestive enzyme secretion. The CCK/gastrin signaling system also appears to be involved in the control of fat storage since *ckr-2* as well as *nlp-12* deletion mutants show an increased fat content compared to wild type animals (Janssen *et al.,* 2008b). Both observations are in accordance with the functions attributed to the CCK/gastrin signaling system in vertebrates and the SK signaling system in arthropods.

[1] As the predicted isoforms of *ckr-2* WormBase (release WS135) did not match with the cloned isoforms at the time of publication, the authors designated the cloned isoforms CKR-2a and CKR-2b (Janssen *et al.,* 2008b). In the current WormBase release (WS245) CKR-2a and CKR-2b are annotated as CKR-2e and CKR-2f.

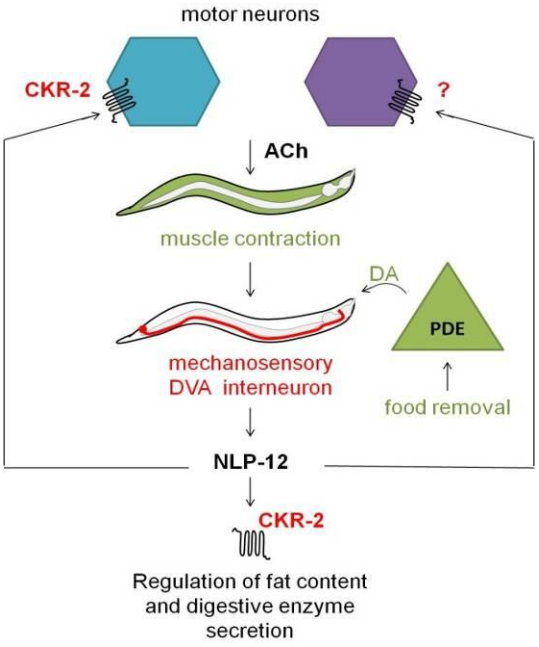

Figure 1.9 CKR-2 signaling in *C. elegans*. DVA integrates both proprioceptive information from muscle contraction and sensory information from PDE. Upon muscle contraction, NLP-12 neuropeptides are released by a single tail neuron, DVA. Subsequent activation of the NLP-12 receptor, CKR-2, potentiates transmission at cholinergic neuromuscular junctions, thereby providing a mechanism for proprioceptive control of locomotion (Hu *et al.*, 2011). Upon food removal, dopaminergic signaling from the mechanosensory PDE neuron stimulates NLP-12 signaling by DVA, which stimulates acetylcholine release from cholinergic motor neurons (Bhattacharya *et al.*, 2014). NLP-12 signaling through CKR-2 also appears to be involved in the regulation of fat storage and digestive enzyme production (Janssen *et al.*, 2008b).

Recently Bhattacharya and colleagues showed that NLP-12 signaling regulates local search behavior in response to changes in food availability (Bhattacharya *et al.*, 2014). Following removal from food, *C. elegans* increases its turning frequency which is mediated by the mechanosensory neuron PDE. Upon removal from food, dopamine signaling from PDE stimulates the release of NLP-12 neuropeptides from the DVA neuron which enhances the release of acetylcholine from cholinergic motor neurons stimulating turning frequency and amplitude and thereby local search behavior (figure 1.9). However, this effect seems to be independent of the CKR-2 receptor, indicating that NLP-12 peptides may signal through another, yet to be identified, receptor.

Besides processing sensory information from PDE neurons, the stretch sensitive sensory neuron DVA is also involved in a mechanosensory feedback loop (figure 1.9) for proprioceptive control of normal locomotion, whereby muscle contraction aids the secretion of NLP-12 by the stretch-activated DVA neuron (Hu *et al.*, 2011). Hu and colleagues showed that muscle contraction-induced signaling of NLP-12 through CKR-2 enhances presynaptic ACh release to potentiate transmission at neuromuscular junctions and as such adjust the pattern of locomotion (Hu *et al.*, 2011; Hu *et al.*, 2015).

1.3.4.8 An FaRP signaling pathway involved in egg-laying behavior

The *egl-6* gene encodes two GPCR isoforms that are both involved in the inhibition of egg-laying. In comparison with wild type, *egl-6* gain-of-function *(n592)* and *egl-6* overexpression mutants display slower egg-laying rates and longer retention of embryos (Ringstad and Horvitz, 2008). Ligands for EGL-6 were first suggested by looking at neuropeptides displaying the defective egg-laying phenotype of *egl-6* overexpression when they are overexpressed in wild-type worms but not in *egl-6* deletion mutants. This way, *flp-10* and *flp-17* turned out to encode for the ligands of EGL-6. In addition, a *Xenopus laevis* oocyte assay demonstrated that FLP-10, FLP-17-1, and FLP-17-2 were able to unambiguously activate the EGL-6 GPCR at nanomolar concentration (Ringstad and Horvitz, 2008).

These FaRPs signal from multiple cell types via EGL-6 in a $G\alpha_{i/o}$-dependent manner to inhibit egg-laying (figure 1.9). In response to environmental cues, FLP-17 neurohormones are principally expressed in BAG sensory neurons and thought to modulate egg-laying behavior by acting on EGL-6 in HSN motor neurons. The latter neurons are known to stimulate the action of vulval muscles and are involved in egg-laying (Trent *et al.*, 1983; White *et al.*, 1986). The non-neuronal expression of FLP-10 peptides in parts of the hermaphrodite's reproductive system also inhibits egg-laying (Ringstad and Horvitz, 2008; Kim and Li, 2004). Upon unfavorable conditions, signaling through ACh also inhibits egg-laying in parallel to the aforementioned peptidergic inhibition (Ringstad and Horvitz, 2008).

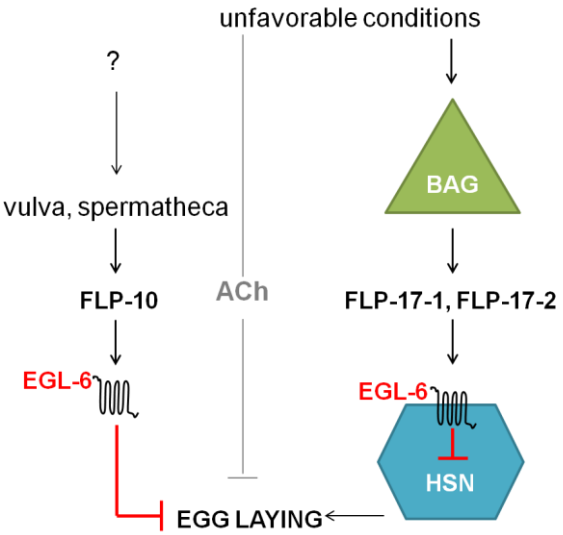

Figure 1.9. Unfavorable conditions cause the release of FLP-17 neuropeptides from BAG neurons to inhibit *C. elegans* egg-laying. These neurohormones activate EGL-6 in HSN neurons in order to inhibit egg-laying. Release of FLP-10 by the vulva and spermatheca along with subsequent signaling via EGL-6 also inhibits egg-laying. How parts of the hermaphrodite's reproductive system might inhibit egg-laying is not yet fully understood. In parallel to peptidergic inhibition, cholinergic signals inhibit egg-laying upon unfavorable conditions (Ringstad and Horvitz, 2008).

1.3.4.9 VP/OT signaling has a conserved role in associative learning and reproduction

Recently, a vasopressin/oxytocin (VP/OT)-related signaling system has been identified in *C. elegans*. In mammals, this system is involved in a plethora of peripheral hormonal functions including water homeostasis, reproduction, and stress responses (van Kesteren *et al.*, 1995; Aikins *et al.*, 2008). Both vasopressin and oxytocin neuropeptides also function as neuromodulators in the central nervous system influencing social cognition and behavior, memory and learning (de Wied *et al.*, 1993; Young and Wang, 2004; Meyer-Lindenberg *et al.*, 2011). In the roundworm, a single VP/OT-like peptide, named nematocin (NTC-1), and two nematocin receptors (NTR-1 and NTR-2) have been identified. The NTR-1 receptor is activated by the nematocin peptide in a dose-dependent way. On the other hand, the NTR-2 receptor is not directly activated by NTC-1 but co-expression of NTR-1 and NTR-2 is suggested to affect the intracellular levels of cAMP upon nematocin binding (Garrison *et al.*, 2012; Beets *et al.*, 2012).

In hermaphrodites, the *ntc-1* gene is mainly expressed in the DVA and AVK neurons amongst others. Since *ntr-1* is expressed in the left ASE (ASEL) gustatory neuron, and the ASH and ADF chemosensory neurons that function in chemotaxis toward water-soluble cues, Beets *et al.* (2012) studied the salt chemotaxis behavior of *ntc-1* and *ntr-1* mutants. Similar to wild type worms, *ntc-1* and *ntr-1* mutants are attracted to low NaCl concentrations. When pre-exposed to these low NaCl concentrations in the absence of food, wild type worms show avoidance of NaCl, a behavioral switch termed gustatory plasticity that represents a type of associative learning (Hukema *et al.*, 2008). However, the aversive response of pre-exposed worms is reduced in *ntc-1* and *ntr-1* mutants. These results indicate that nematocin signaling is implicated in gustatory associative learning, similar to the effects of vasopressin and oxytocin on mammalian cognition. Moreover, AVK-specific expression of *ntc-1* and ASEL-specific expression of *ntr-1* in the *ntc-1* and *ntr-1* mutant background, respectively, partially restored gustatory plasticity. Genetic analysis and supplementation studies indicated that the TRPV channel protein OSM-9, the Gγ-subunit GPC-1 and serotonin and dopamine signaling interact with the nematocin pathway in regulating gustatory plasticity (Beets *et al.*, 2012).

In addition to the function of nematocin signaling in learning behavior, *ntc-1*, *ntr-1* and *ntr-2* are expressed in sexually dimorphic patterns and have been shown to function in male mating behavior. Males that fail to functionally express any of these genes perform poorly in several steps of their mating behavior compared with wild type worms. Mutations in the receptors NTR-1 and NTR-2 cause partly overlapping defects in the mating response. Remarkably, cell-specific knockout of nematocin in the mechanosensory DVA neuron, which is not male-specific, seems to be responsible for most of the male mating defects. These findings indicate that nematocin signaling is necessary to coordinate male mating behaviors (Garrison *et al.*, 2012).

1.3.4.10 NLP-40 regulates rhythmic behavior through AEX-2

Rhythmic behaviors are driven by endogenous biological clocks in pacemakers which must reliable transmit timing information to target tissues that exert rhythmic output. In *C. elegans* the defecation motor program is driven by calcium oscillators in the intestine. Recently, Wang and coworkers identified the neuropeptide NLP-40 as the timing signal

which is released by the intestine and triggers the cyclical activation of the motor neurons enervating the enteric muscles resulting in defecation (Wang *et al.*, 2013). A previous study observed that, similar to *nlp-40* mutants, cyclical enteric muscle contraction is absent in mutants for the neuropeptide receptor AEX-2, which is expressed in the motor neurons on which NLP-40 acts. Corroborating AEX-2 as the target for NLP-40, two peptides encoded by the *nlp-40* gene, NLP-40-3-1 and NLP-40-3-2, could activate the receptor in a calcium bioluminescence assay (Wang *et al.*, 2013).

1.4 Conclusions and aims of the project

Neuropeptides are the most abundant group of signaling molecules of the nervous system. However, for most of them, their function, mode of action and evolution remains elusive. The nematode *C. elegans* offers a lot of advantages, which make it a suitable organism to investigate neuropeptidergic signaling. The sequenced genome allows researchers to browse through it and predict novel neuropeptide GPCRs based on sequence similarities to known neuropeptide GPCRs.. Its simple and defined anatomy, combined with powerful molecular and genetic tools, offer the possibility to investigate the function of these systems at the cellular level. In this study we aimed to identify novel neuropeptide systems in *C. elegans* and to provide more insight into the function and evolution of these systems.

Chapter 3 describes the *in silico* identification of putative neuropeptide GPCRs encoded in the genome of *C. elegans.* From this prediction a dozen of receptors related to mammalian and insect neuromedin, tachykinin and GnRH/AKH signaling systems were selected for further characterization using reverse pharmacology approach. Using this strategy we were able to couple four orphan receptors to their cognate ligands and investigated their phylogeny.

In **chapter 4** we investigated the functional implication of the identified GnRH/AKH-like systems in reproduction and fat storage. For the characterized GnRH/AKH-like receptor GNRR-3 one of its identified ligands, NLP-22, was previously identified as a somnogenic peptide. Hence, we investigated whether GNRR-3 and its activating RPamide ligands play a role in the regulation of lethargus, a sleep-like state in *C. elegans*.

In order to gain more insight into the function of the deorphanized *C. elegans* tachykinin-like systems, the expression patterns of both the tachykinin neuropeptides and the receptors were investigated using fluorescent reporters (**Chapter 5**). Both neuropeptide and receptor reporters were localized to neurons shown to be involved in locomotion, chemotaxis, learning and nociception. Based on this expression pattern a possible role of the identified tachykinin-like systems in these behaviors was explored (**Chapter 5**).

Chapter 6 summarizes the results of this doctoral research and discusses the data in view of the current literature and future prospects.

Most of the research on the function of neuropeptide signalling in this study focuses on two behaviors: sleep (**chapter 4**) and nociception (**chapter 5**). Therefore we will first provide a detailed review of the current knowledge of the neuronal and molecular pathways underlying these behaviors in *C. elegans* (**chapter 2**).

Chapter 2. An introduction to sleep and nociception in *C. elegans*

This chapter has partially been published in:

Frooninckx, L., Mirabeau, O., Nelson, M. D., Wouters, A., Temmerman, L., Raizen, D. M., Schoofs, L., Beets, L. Discovery of a wake-promoting neuropeptide pathway in *C. elegans*. Submitted for publication in *eLife*

2.1 Sleep in the nematode C. elegans

Although we spend one-third of our lives sleeping, we still don't fully understand the underlying principles of this behavior. In contrast to the initial assumptions, sleep is not simply the passive absence of wakefulness, but it is an actively regulated process that requires the coordinated activity of neuronal circuits. Sleep has mainly been investigated in mammals, however, the appreciation that sleep could be conserved throughout the animal kingdom allows scientists to investigate the molecular mechanisms underlying the regulation of sleep using model organisms with a simple and well defined anatomy and powerful genetic tools (Zimmerman *et al.*, 2008).

2.1.1 Defining sleep

In mammals the close relationship between electroencephalogram (EEG) recordings and the behavioral observation of sleep allows to use electrophysiological criteria to define sleep (Fuller *et al.*, 2006; Brown *et al.*, 2013). However, non-mammalian species with significant differences in their (neuro)anatomy do not produce the same electrophysiological recordings as mammals and behavioral criteria are required to characterize sleep in these species. Henri Piéron, who was among the first scientists to study sleep from a physiological perspective, defined sleep as a periodic biological necessity that has its own internally produced rhythm and is characterized by an absence of awareness and sensory functioning. These characteristics provided the basis for the first behavioral definition of sleep (Piéron, 1913). In 1984, Campbell and Tobler reviewed almost 200 studies concerning sleep duration in invertebrates, fish, amphibians, reptiles, birds and mammals. They included studies that used both electrophysiological criteria as well as behavioral criteria to define sleep and reviewed both methodologies. Faced with the absence of a common definition of sleep, the authors emphasized the importance of using universal criteria when investigating sleep in (non-)mammalian species and suggested to use a behavioral definition of sleep which consisted of four criteria: (1) the assumption of a specific posture, (2) behavioral quiescence, (3) an elevated arousal treshold, and (4) state reversibility with stimulation (Campbell and Tobler, 1984). Homeostasis (5) and the association of sleep with a molecular clock (6) have recently been added to these criteria as well (Hendricks *et al.*, 2000b; Zimmerman *et al.*, 2008).

2.1.2 Lethargus, a sleep-like state in *C. elegans*

C. elegans has a sleep-like state during a developmental timing termed lethargus. The worm develops through four larval stages, L1-L4, and undergoes a corresponding molt at the end of each stage. Prior to each molt, the worm goes through a 2-3 hour period of behavioral quiescence named L1-L4 lethargus (figure 2.1) (Sing and Sulston, 1978). This sleep-like state meets the general behavioral criteria of sleep as it is associated with a biological clock and is characterized by cessation of locomotion and feeding, a specific posture, an elevated arousal threshold, reversibility and homeostasis (Raizen *et al.*, 2008; Nelson and Raizen, 2013).

2.1.2.1 Behavioral quiescence and specific posture

The comparison between lethargus quiescence and sleep was first made by Raizen and colleagues (Raizen *et al.*, 2008). The most obvious behavioral features of lethargus are quiescence of locomotion and feeding. At the onset of lethargus animals gradually stop feeding and moving over a period of 15 minutes (Sing and Sulston, 1978). Under normal conditions when feeding on *E. coli* OP50, adult worms feed at a pumping rate of approximately 250 pumps per minute. During lethargus this rate drops to almost zero (Raizen et al., 2012).

During locomotion, *C. elegans* typically assumes a sinusoidal posture, whereas during lethargus, *C. elegans* assumes a relaxed posture which is characterized by a reduced curvature and muscle activity (Schwarz *et al.*, 2012; Iwanir *et al.*, 2013). This reduction in curvature is specific to lethargus quiescence and not simply a function of reduced locomotion, as during bouts of reduced locomotion outside of lethargus animals do not assume this posture. A detailed study of the locomotion quiescence during lethargus revealed that the microarchitecture of this behavioral state is composed of individual bouts of quiescence and motion (Iwanir *et al.*, 2013).

It has been suggested that quiescence during lethargus may be a consequence of mechanical constriction during molting. However, this hypothesis is inconsistent with the reversibility of lethargus quiescence and with the existence of bouts of motion throughout lethargus (Raizen *et al.*, 2008; Iwanir *et al.*, 2013).

2.1.2.2 Reduced responsiveness and reversibility

A key feature of sleep is reduced sensory responsiveness. During lethargus, responses to mechanical and olfactory cues are delayed in *C. elegans* (Raizen *et al.*, 2008). This is due to both anatomical and physiological mechanisms of sensory gating. During lethargus, an extracellular material forms a plug at the opening of the buccal cavity, which prevents food and other material from entering the pharynx and thus minimizes sensory stimulation of pharyngeal neurons (Sing and Sulston, 1978). Like mammalian sleep, sensory gating during lethargus is controlled at the neuronal level as well. During lethargus, overall spontaneous neuronal activity is reduced. Moreover, sensory neurons including the mechanosensory ALM neurons and the polymodal ASH neurons display reduced sensitivity to stimuli during lethargus (Schwarz *et al.*, 2011; Cho and Sternberg, 2014). Recently, Cho and colleagues investigated the regulation of the ASH-mediated avoidance circuit during lethargus and showed that during lethargus the activity of the interneurons AVA and AVD, which are downstream to ASH in the avoidance circuit, become asynchronous. When compared to the input ASH neuron, AVD and AVA interneurons receive and exhibit simultaneous activity when awake. During lethargus AVD calcium transients exhibit a lag, whereas AVA transients do not. So far, it has not been determined how this asynchrony of the command interneurons is regulated.

A remarkable feature of sleep is its reversibility. During lethargus worms respond to arousal promoting stimuli, however with a delay. As mentioned above, at the neuronal level this delay is caused by both reduced calcium transients in the sensory neurons and downstream asynchronization of the AVA and AVD interneurons. However, upon a second stimulation lethargus worms respond immediately similar to non-lethargus worms (Raizen *et al.*, 2008). Cho and colleagues showed that restoration of the synchrony of the interneurons is sufficient to remove the delay in sensory responsiveness: upon direct depolarization of the reverse command interneurons, animals both in and out of lethargus respond immediately, indicating that the lack of a rapid response upon ASH depolarization is due to a delayed transmission of excitatory information from the sensory to the interneurons during lethargus (Cho and Sternberg, 2014).

2.1.2.3 Homeostatic regulation of lethargus

Like sleep, lethargus is under homeostatic regulation. The increased propensity for sleep during wakefulness and the prolonged sleep time and depth of sleep following sleep deprivation is defined as sleep homeostasis. The existence of a homeostatic sleep rebound after deprivation demonstrates that sleep is not simply a period of reduced activity, but that it serves a fundamental function that cannot be bypassed (Cirelli and Tononi, 2008). Moreover, prolonged sleep deprivation has shown to be lethal in rats and in *Drosophila* (Rechtschaffen *et al.*, 1989; Shaw *et al.*, 2002; Kang and Avery, 2009). In *C. elegans* the arousal threshold, the peak quiescence, and the mean quiescence bout duration are all increased after one hour of enforced locomotion during lethargus. However, timing of the end of the quiescent period is unaltered by quiescence deprivation, indicating a temporal constraint on the timing of lethargus (Raizen *et al.*, 2008). Similarly, Iwanir and coworkers showed that during lethargus the duration of quiescence bouts declines, which may be the signature of a decreasing need for consolidated intervals of behavioral quiescence towards the end of lethargus. Moreover, the duration of bouts of quiescence positively correlates with the duration of the preceding bouts of motion (Iwanir *et al.*, 2013).

Furthermore, forced locomotion for 30 minutes during L4 lethargus is shown to be lethal for 11% of the worms. Microscopic inspection of the arrested animals showed that they were unable to shed their L4 cuticle (Driver *et al.*, 2013). Recently, Driver and coworkers showed that deprivation of lethargus quiescence causes translocation of the FOXO transcription factor DAF-16 to the nucleus, which depends on the dafachronic acid nuclear receptor DAF-12. In contrast to wild type worms *daf-16* mutants do not show an increased response latency upon quiescence deprivation during L4 lethargus and approximately 42% of the *daf-16* mutants do not survive 30 minutes quiescence deprivation. This phenotype could be rescued by expressing *daf-16* in the intestine, indicating that sleep is not exlusively regulated by the nervous system (Driver *et al.*, 2013).

2.1.2.4 The PERIOD homolog LIN-42 regulates timing of lethargus

In contrast to most animals, the lethargus sleep-like state is not associated with a circadian clock, but instead is associated with a developmental clock mechanism that controls the timing of larval transition stages during development. In *C. elegans*, the timing of these

larval transition stages is regulated by the heterochronic gene *lin-42*. Remarkably, *lin-42* is homologous to the *period* gene, a clock gene that has a circadian expression pattern and regulates sleep timing in both *Drosophila* and mammals (Jeon *et al.*, 1999).

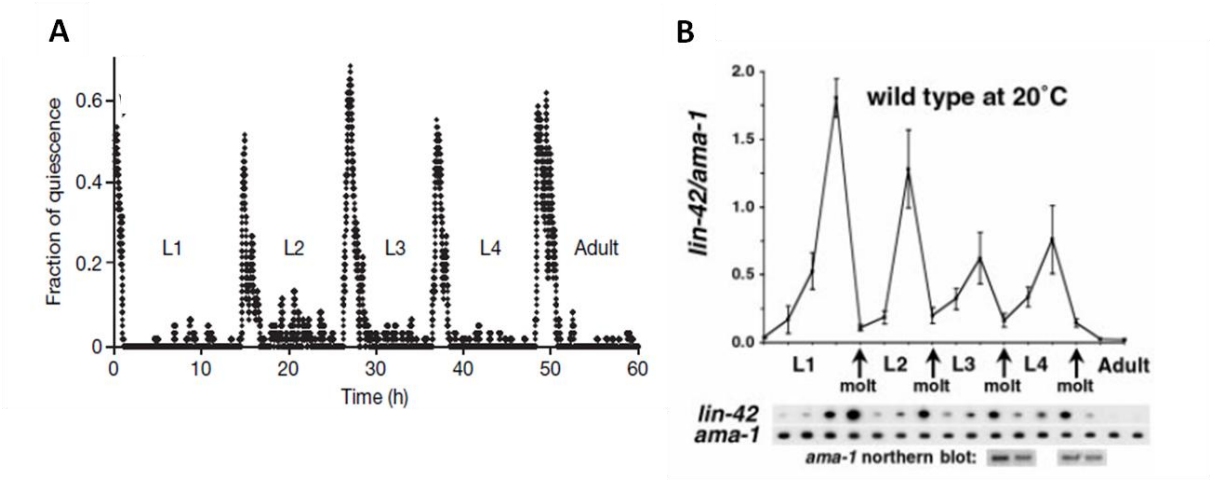

Figure 2.1 *C. elegans* sleep-like behavior is associated with lethargus, which is regulated by the PERIOD homologue LIN-42. (A) Fraction of quiescence during embryonic development of wild type *C. elegans* at 20°C (from Raizen *et al.*, 2008). (B) mRNA levels of *lin-42* cycle with the larval molts during *C. elegans* development (from Jeon *et al.*, 1999).

In mammals the timing of sleep and wakefulness coincide with the daily cycles of daylight and darkness that result from the spin of the earth. This circadian rhythm of sleep and wakefulness is regulated by an endogenous biological clock and therefore continues even when the organism is isolated from environmental time cues. However, when organisms remain isolated their biological clock becomes free running and starts deviating from the 24-hour cycle. Therefore the biological clock has to be entrained with environmental cues in order to keep its rhythm coordinated with the circadian rhythm of the environment.

The molecular mechanisms of this biological clock seem to be conserved among animals and to rely on the rhythmic expression of clock genes, which is generated by transcriptional-translational feedback loops (TTLs). These TTLs were first discovered in the fruit fly *D. melanogaster* where the biological clock is shown to consists of two interlocked TTLs (Ozkaya and Rosato, 2012). In the first loop, heterodimers of the transcription factors CLOCK and CYCLE activate the transcription of *period(per)* and *timeless(tim).* Their protein products PER and TIM associate in the cytoplasm and enter the nucleus where they inhibit their own transcription through the inhibition of their transcription factors

CLOCK/CYCLE. This feedback loop of activation and inhibition of transcription takes about 24 hours and is stabilized by a second loop that regulates the expression of the CLOCK transcription factor. In this second loop the transcription factors CLOCK/CYCLE activate the transcription of *vrille* and *Pdp1ε (Par domain protein 1ε), which* encode transcription factors that inhibit and activate transcription of the *clock* gene. Proper timing and stability of these loops are regulated by several posttranslational modifications of clock proteins. Several kinases, phosphatases and E3-ubiquitin ligases have been identified as regulators of the stability and activity of the clock proteins. The first discovered and best-characterized posttranslational modifications is the phosphorylation of PER by the DOUBLE-TIME (DBT) kinase. Phosphorylation of PER by DBT regulates the accumulation and nuclear transportation of PER by promoting its degradation (Yu and Hardin, 2006; Ozkaya and Rosato, 2012).

In the nematode *C. elegans* the heterochronic gene *lin-42,* which is homologous to mammalian and *Drosophila period*, has a rhythmic expression as well. In contrast to the circadian rhythm of *per* mRNA levels in mammals and *Drosophila*, *lin-42* mRNA oscillates in synchrony with the four larval molts during postembryonic development (figure 2.1) (Jeon *et al.,* 1999). *lin-42* mutants exhibit arhythmic timing of the molting cycles and seam cell development (Abrahante *et al.*, 1998; Jeon *et al.*, 1999; Monsalve *et al.,* 2011). Forced expression of *lin-42* results in anachronistic molts and quiescence, indicating that *lin-42* acts as a molecular developmental clock that is required for the timing of the larval transition stages (Monsalve *et al.*, 2011). In addition to *lin-42*, the *C. elegans* genome also contains homologues of *Drosophila* and mammalian *timeless, tim-1, doubletime, kin-2,* and *clock/cycle, aha-1,*as well (Romanowski *et al.*, 2014). Similar to *lin-42,* RNAi of *tim-1* and *kin-2* indicates their involvement in the proper timing of seam cell development (Banerjee *et al.*, 2005). However, *lin-42* mRNA still has a cyclical expression pattern in the absence of a functional LIN-42 protein and *tim-1* mRNA has no cyclical expression pattern (Jeon *et al.*, 1999). These differences between *C. elegans* and other animals suggest that the molecular mechanisms by which *lin-42* controls larval developmental timing do not involve a transcription-translation loop with negative feed-back regulation.

2.1.3 Genetic regulation of behavioral quiescence during lethargus

Several signaling pathways involved in the regulation of mammalian and *Drosophila* sleep have shown to be involved in the regulation of lethargus as well. In *Drosophila*, increased protein kinase G (PKG) activity is associated with increased sleep time (Donlea *et al.*, 2012). Also in mice PKG is implicated in the regulation of the timing and quality of sleep as well as in the regulation of wakefulness. cGMP-dependent protein kinase type I mutant mice show strikingly altered distribution of sleep and wakefulness and reduction in sleep duration (Langmesser *et al.*, 2009). EGL-4, a cGMP dependent PKG promotes both locomotion and feeding quiescence in *C. elegans.* A gain-of-function mutant of *egl-4* shows behavioral quiescence associated with lethargus during its adult stage and shows increased quiescence during lethargus and longer latency responses to stimuli. Accordingly, loss-of-function *egl-4* mutants show reduced quiescence during lethargus (Raizen *et al.*, 2008). cAMP signaling is shown to inhibit sleep in both *D. melanogaster* and *C. elegans.* Loss-of-function mutations of the cAMP phosphodiesterase gene, *pde-4*, and gain-of-function mutation of the adenylate cyclase gene, *acy-1*, both increasing cAMP levels, result in decreased response latency in *C. elegans* (Raizen *et al.*, 2008). In *Drosophila*, reduced levels of cAMP in the adenylate cyclase mutant *rutabaga* are associated with increased sleep, while increased cAMP levels in the cAMP phosphodiesterase *dunce* mutants are associated with reduced sleep (Hendricks *et al.*, 2001). Moreover, blocking cAMP response-element binding protein (CREB) activity results in an increased sleep rebound in fruit flies. In mice, reduced CREB activity is shown to be associated with an increase of time spent sleeping as well (Graves *et al.*, 2003). However, a recent study reports that cAMP signaling and CREB activity are increased during REM sleep, and may contribute to hippocampus-dependent memory consolidation (Luo *et al.*, 2013).

Both in rodents and *Drosophila*, neuronal epidermal growth factor (EGF) signaling have been associated with sleep. In rodents, transforming growth factor α (TGF-α) has a rhythmic transcription and secretion in the suprachiasmatic nucleus (Kramer *et al.*, 2001). In line with this expression pattern, infusion of TGF-α into the brains of hamsters decreases locomotion and shifts the timing of sleep-wake transitions. In *Drosophila*, activation of EGF receptor (EGFR) signaling increases sleep (Foltenyi *et al.*, 2007). This effect is dependent on a functional EGFR and correlates with increased phosphorylation of ERK, suggesting

activation of the Ras-MAPK pathway by EGFR signaling. Furthermore, pan-neuronal knockdown of *Rho,* was shown to decrease sleep with more than 50%. Although the duration of sleep bouts was shorter, this was accompanied by an increase in the number of times flies started to sleep compared to control flies, indicating that flies with reduced EGFR signaling did have a sleep need, but were unable to maintain the sleep state. In *C. elegans*, *lin-3* and *let-23,* encode the sole EGF-like and EGFR homologs. Van Buskirk and Sternberg showed that LIN-3/LET-23 signaling plays a sleep-promoting role in the nematode as well (Van Buskirk and Sternberg, 2007). Forced expression of *lin-3* induces feeding and locomotion quiescence. This effect of LIN-3 is abolished in mutants of *let-23(sy12)* or *plc-3(sy698),* which encodes for PLC-γ, but not in mutants with impairments in the Ras-MAPK or PI(3)K pathways, indicating that LIN-3/LET-23 signaling induces quiescence by activating the PLC-γ pathway and not the Ras-MAPK or PI(3)K pathways (Van Buskirk and Sternberg, 2007). The effect of LIN-3 on feeding and locomotion quiescence requires expression of its receptor LET-23 in the ALA neurons, as expression of *let-23* in ALA rescues the *lin-23* overexpression phenotype. The effect of LIN-3/LET-23 signaling seems to play an important role in the regulation of feeding and locomotion quiescence during the sleep-like state lethargus, as feeding and locomotion are less repressed during lethargus in *let-23* and *plc-3* mutants (Van Buskirk and Sternberg, 2007).

Notch signaling is a highly conserved signaling pathway with a role in development and cell fate. In *C. elegans*, decreased Notch signaling reduces arousal thresholds during lethargus. Moreover, induced expression of its co-ligand OSM-11 is sufficient to induce anachronistic quiescence, which is shown to depend on the EGL-4 (PKG) and on the LIN-3/LET-23 EGF pathway (Singh *et al.*, 2011). In *Drosophila* the transcription factor *bunched,* which regulates Notch activity, is upregulated after sleep deprivation. Here, Notch signaling seems to be involved in regulating sensitivity to sleep loss, as enhanced Notch signaling reduces sleep homeostasis and prevents learning impairments induced by sleep deprivation (Seugnet *et al.*, 2011).

Recently, Turek and colleagues identified the RIS interneuron as a quiescence-inducing neuron in *C. elegans*. Upon ablation or optogenetic activation of RIS worms do not longer show quiescent behavior during lethargus or become quiescent respectively (Turek *et al.*,

2013). The sleep inducing effect seems to be dependent on expression of the AP2 transcription factor in RIS and neuropeptidergic signaling (Turek *et al.*, 2013).

Sleep, wakefulness and the transition between these stable behavioral states are regulated by the coordinated interplay of neuronal circuits. Classical neurotransmitters and neuropeptides play a pivotal role herein (Richter *et al.*, 2014). Recently, a role for dopamine and serotonin signaling in the regulation of lethargus has been described. Loss of the serotonin receptor *ser-4* results in decreased total lethargus quiescence compared to wild type worms (Singh *et al.*, 2014). This is similar to the sleep-promoting effect of serotonin signaling in *Drosophila* (Yuan *et al.*, 2006). In *Drosophila* dopamine signaling has a wake promoting effect. Although the site of action of the D1 receptor as well as the neuronal circuitry of dopamine signaling in *Drosophila* sleep have been identified, little is known about the signaling cascade acting downstream of the D1 receptor in sleep (Ueno *et al.*, 2012). *C. elegans* mutants for the dopamine receptor gene *dop-1* and the dopamine transporter gene *dat-1,* have an increased total quiescence during L4 lethargus (Singh *et al.*, 2014). Gαs, adenylate cyclase and protein kinase A are identified as downstream regulators of DOP-1 signaling in lethargus quiescence inhibition in *C. elegans*.

To date only a few neuropeptides have been found to regulate lethargus in *C. elegans.* The neuropeptide receptor NPR-1 and its ligands FLP-18 and FLP-21 regulate the cessation of locomotion and reduced responsiveness during lethargus (Choi *et al.*, 2013). This seems to be mediated through inhibition of secretion of PDF-1, an arousal promoting peptide. Using a yellow fluorescent protein (YFP)-tagged proPDF-1 with the *pdf-1* promoter, Choi *et al.* (2013) were able to assess the level of PDF-1 secretion. Both L4 larvae and adult worms showed high levels of YFP fluorescence in the coelomocytes, which are specialized scavenger cells that internalize proteins secreted into the body cavity, whereas lower coelomocyte fluorescence was observed during the L4 to adult lethargus. PDH and PDF neuropeptides are highly conserved in crustaceans, insects and nematodes. Their receptors display sequence homologies with the deuterostomian VIP/PACAP secretin GPCR receptor family, suggesting that these peptide systems could be evolutionary related (Janssen *et al.*, 2008a; Mirabeau and Joly, 2013; Jékely, 2013). In *Drosophila,* the neuropeptide PDF is a crucial component of the biological clock, promoting circadian locomotor activity (Meelkop *et al.*, 2011).

Recently, Nelson and colleagues identified NLP-22 as somnogenic neuropeptide in *C. elegans.* mRNA of the neuropeptide NLP-22 shows cyclical expression in synchrony with lethargus and is regulated by the PERIOD homolog LIN-42. Induced overexpression of *nlp-22* induces quiescence that resembles all behavioral aspects of lethargus quiescence, indicating that NLP-22 plays a profound role in lethargus. (Nelson *et al.*, 2013). Since *nlp-22* is expressed in the RIA neurons, it was hypothesized that these neurons may be sleep-promoting. To test this hypothesis, the authors used genetic ablation of the RIA neurons, and noticed reduced quiescence behavior supporting the hypothesis. However, optogenetic activation of the RIA neurons promoted locomotion during lethargus, whereas no effect was seen in L4 larvae. These results suggest that the RIA neurons are complex regulators of lethargus quiescence with both locomotion and quiescence promoting roles (Nelson *et al.*, 2013).

Gene expression studies of *C. elegans* development by microarray study or mRNA sequencing have identified a plethora of new genes that oscillate in phase with the molting cycles, revealing novel putative genetic regulators of molting and/or lethargus behavior (Turek and Bringmann, 2014; Hendriks *et al.*, 2014).

2.1.4 Non-lethargus associated quiescence

C. elegans also shows quiescent behavior outside of lethargus. However, these quiescent states are associated with special conditions. Satiety induces feeding and locomotion quiescence in *C. elegans* (You *et al.*, 2008). Similar to lethargus, satiety-induced quiescence is dependent on PKG signaling. You and colleagues showed that satiety-induced quiescence is dependent on neuropeptidergic signaling as well, since mutants with impaired neuropeptide processing do not show quiescence upon refeeding after starvation (You *et al.*, 2008).

Besides satiety, several stress-related factors such as heat (Hill *et al.*, 2014; Nelson *et al.*, 2014), exposure to chemical toxicants (Jones and Candido, 1999) or infection (Los *et al.*, 2013) have shown to induce quiescence in *C. elegans*. So far heat-induced quiescence has been most intensively studied. Short exposure (< 1 min) to noxious heat (> 30°C) evokes an avoidance or escape behavior (Baumeister and Wittenburg, 1999; Schild and Glauser, 2013). Prolonged exposure to high temperatures (30 min, 35°C) causes a quiescence

response in which the worms stop locomotion and feeding up to one hour after exposure (Hill *et al.*, 2014; Nelson *et al.*, 2014). If perturbed during this stress-induced quiescence, worms are impaired for survival and show elevated expression of cellular stress reporter genes, indicating that this stress-induced quiescence helps to restore cellular homeostasis upon exposure to stress. Therefore this stress-induced quiescence is referred to as recovery quiescence (Hill *et al.*, 2014). Like lethargus, recovery quiescence upon prolonged heat exposure is associated with reduced responsiveness to aversive stimuli, is reversible upon strong mechanical stimulation and seems to be dependent on LIN-3/EGF-signaling to the quiescence-inducing ALA interneuron (Hill *et al.*, 2014; Nelson *et al.*, 2014). ALA induces quiescence through the release of the *flp-13* peptides. So far the receptor through which *flp-13* peptides signal to induce quiescence remains elusive (Nelson *et al.*, 2014). Besides heat-induced recovery quiescence, cold, hyperosmotic stress, ethanol and tissue damage-induced recovery quiescence seem to be dependent on the ALA neuron as well (Hill *et al.*, 2014).

Recently, Cho and colleagues showed that the response latency during satiety and LIN-3/EGF-induced quiescence is caused by interneuron asynchronization, similar to lethargus quiescence (Cho and Sternberg, 2014). This indicates that these quiescent sates are regulated by similar mechanisms as lethargus.

2.2 The neural circuits underlying avoidance behavior in C. elegans

The ability to detect and avoid noxious stimuli in the environment is critical to an organism's survival. The nematode *C. elegans* avoids several noxious stimuli such a nose touch (Kaplan and Horvitz, 1993), high osmotic strength (Culotti and Russell, 1978), water-soluble and volatile chemical repellents (Ward, 1973; Dusenbery, 1974; Troemel *et al.*, 1997; Sambongi *et al.*, 1999; Sambongi *et al.*, 2000; Hilliard *et al.*, 2002; Hilliard *et al.*, 2004; Bargmann, 2006) and heat (Baumeister and Wittenburg, 1999). Upon encountering a noxious cue forward moving worms stop moving, withdraw (reversal) and change direction. The neural pathways underlying this behavior are becoming elucidated piece by piece. In this section we provide a chronological overview of the identification of the major neuronal and molecular pathways mediating nociception in *C. elegans.*

2.2.1 Unraveling the neuronal circuit for avoidance behavior in *C. elegans*

Taking advantage of the well-defined and simple anatomy of the *C. elegans* nervous system Martin Chalfie and colleagues were the first to elucidate a neural circuit underlying a behavioral process (Chalfie *et al.*, 1985). Using cell-specific laser ablation they were able to map the sensory, inter- and motor neurons that mediate touch-induced movement in *C. elegans* (figure 2.2). In 1981 Chalfie and Sulston demonstrated that the microtubule neurons, aptly named for the high occurrence of microtubule structures in these cells, are sensory neurons that mediate the withdrawal response to gentle touch in *C. elegans* (Chalfie and Thomson, 1979; Chalfie and Sulston, 1981). The microtubule neurons sensitive to touch could be subdivided in the ALML/R and AVM neurons which mediate touch sensitivity in the head, and the PLML/R neurons which mediate touch sensitivity in the posterior part of the worm. To find out how motor neurons coordinate the forward or backward movement, Chalfie and Sulston ablated DA, DB or DD motor neurons, and subsequently observed that animals could no longer move backward, forward or became uncoordinated, respectively (§1.2, figure 1.2). To determine how sensory signals originating from the microtubule touch neurons are transmitted to the corresponding motor neurons, they investigated the connectivity of sensory and motor neurons. Four pairs of interneurons, AVA, AVB, AVD and PVC, were shown to connect the sensory and motor neurons by chemical synapses and gap junctions (White *et al.*, 1986). Remarkable was the complementary pattern that was seen in this connectivity. The anterior touch neuron AVM connects to the interneuron AVD

by gap junctions and to the PVC interneuron by chemical synapses, whereas the posterior touch neurons PLM connect to PVC by gap junctions and to AVD by chemical synapses (figure 2.2).

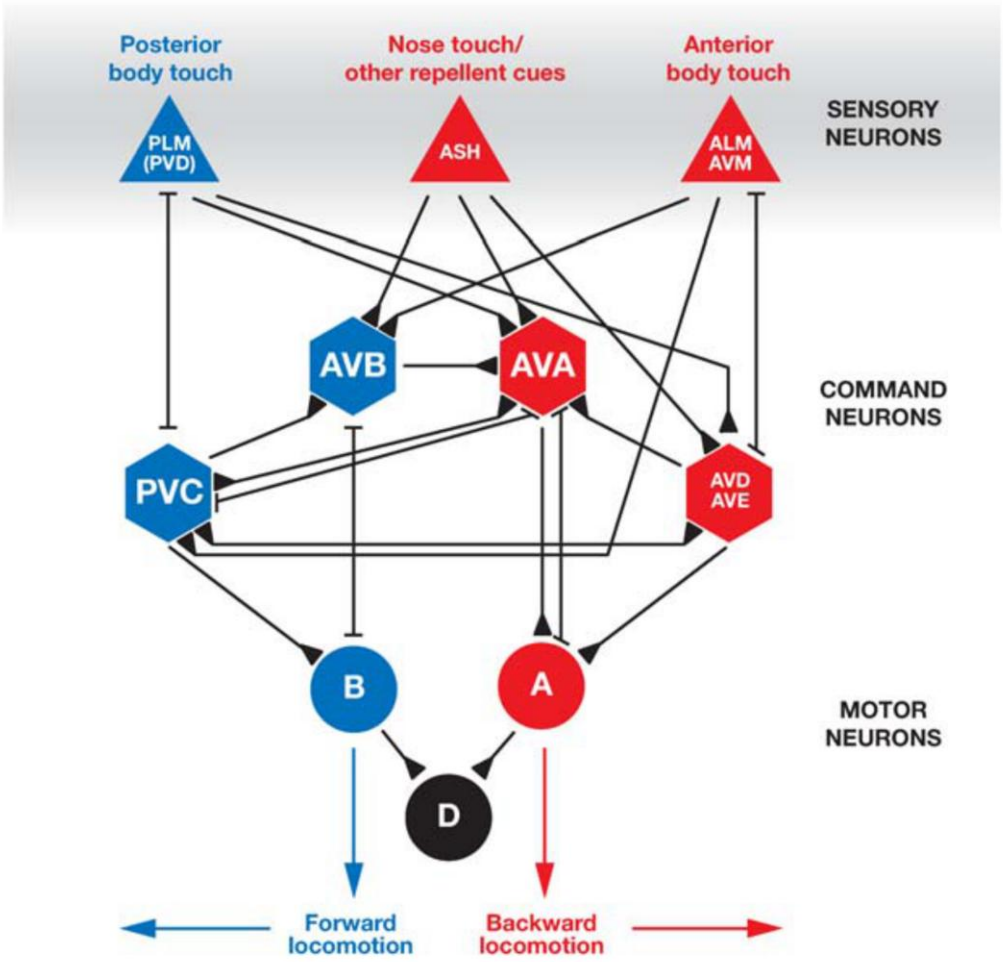

Figure 2.2 The neural circuit mediating touch avoidance. Sensory neurons are depicted as triangles, command interneurons as hexagons and motor neurons as circles. Black lines show the connectivity between these neurons (▲ indicate synapses, ⌶ indicate gap junctions). ASH neurons are required for the response to nose touch, whereas PLM, ALM, and AVM are required for the response to light body touch (from De Bono and Maricq, 2005).

In order to investigate the role of these interneurons in the touch response, each interneuron was ablated and the resulting response to gentle touch was investigated. Ablation of the PVC interneurons resulted in worms that were touch insensitive at their tail but were still touch sensitive at the head. Furthermore, basic locomotion remained unperturbed. After ablation of AVD, young larvae were touch insensitive only in the head but moved normally (Chalfie *et al.*, 1985). These results indicate that the neural circuit for the touch sensitivity

response depends on the fast-acting gap junction connections between the sensory and interneurons (PLM-PVC, ALM/AVM-AVD), rather than on the synaptic connections. Animals remained touch sensitive after ablation of the AVA or AVB cells, but locomotion was drastically affected, with individuals exhibiting irregular movements and a contorted body shape. Combined ablation of AVA and AVD resulted in animals incapable of moving backward, whereas ablation of AVB and PVC together resulted in animals incapable of moving forward. In line with these ablation results, AVA and AVD neurons make connections with the backward-coordinating A-type motor neurons and AVB and PVC neurons connect to the B-type motor neuron, which coordinate forward movement (figure 2.2). Because of their importance to forward and backward movement, AVA, AVB, AVD, and PVC were termed command interneurons (de Bono and Maricq, 2005). Subsequent studies revealed that the command interneurons do not coordinate forward or backward locomotion per se, but rather gate the decision to go forward or backward (Zheng *et al.*, 1999).

Besides withdrawal reflexes to gentle touch, *C. elegans* displays strong avoidance behaviors to noxious and potentially harmful cues as well. The sensory neurons responsible for the perception of these cues have been identified by laser ablation and are listed in table 2.1. The nociceptive cellular circuit involving the primary nociceptor, the ASH sensory neuron, is one of the best characterized neural networks in *C. elegans.* This polymodal sensory neuron detects mechanical stimuli, osmotic strength, heavy metals, detergents, alkaloids and volatile repellants (Bargmann *et al.*, 1990; Troemel *et al.*, 1995; Bargmann and Kaplan, 1998; Sambongi *et al.*, 1999; Sambongi *et al.*, 2000; Hilliard *et al.*, 2002; Hilliard *et al.*, 2004). To understand the nature of polymodal sensory response of ASH at the cellular level, Hilliard and colleagues expressed the calcium indicator protein cameleon in ASH and found that a variety of noxious stimuli including quinine, denatonium, detergents, heavy metals, both hyper- and hypo-osmotic shock and nose touch evoke strong calcium responses in ASH (Hilliard *et al.*, 2005).

Table 2.1 Sensory neurons mediating aversive responses in C. elegans

Nociceptive cue	Sensory neuron	Reference
High osmolarity	ASH	(Bargmann *et al.*, 1990)
Gentle touch	AVM, ALM, PLM, FLP, OLQ, CEP	(Chalfie and Thomson, 1979; Chatzigeorgiou and Schafer, 2011)
Harsh touch	ASH, FLP, ALA, BDU, SDQ, AQR, ADE, , PDE, PVD, PHA, PHB	(Way and Chalfie, 1989; Kaplan and Horvitz, 1993; Li *et al.*, 2011; Sanders *et al.*, 2013)
Odors	ASH, ADL, AWB	(Troemel *et al.*, 1995)
Heavy metals	ASH, ADL, ASE	(Sambongi *et al.*, 1999)
Protons	ASH, ADF, ASE, ASK	(Sambongi *et al.*, 2000)
Alkaloids	ASH, ASK	(Hilliard *et al.*, 2004)
Detergents	ASH, ASK	(Hilliard *et al.*, 2002)
High Carbon dioxide	BAG, AFD	(Hallem and Sternberg, 2008; Bretscher *et al.*, 2011)
Low oxygen	BAG, URX	(Zimmer *et al.*, 2009)
Temperature	AFD, PHC, FLP, PVD	(Chatzigeorgiou *et al.*, 2011; Liu *et al.*, 2012)

Like the touch sensitive microtubule neurons, ASH makes synaptic contacts with the command interneurons (White *et al.*, 1986). In 1995 two independent studies revealed that the ASH mediated avoidance response to harsh touch is dependent on the presence of the AMPA-type ionotropic glutamate receptor encoded by *glr-1* (Maricq *et al.*, 1995; Hart *et al.*, 1995). Expression of *glr-1* is restricted to a subset of motor and interneurons, including the command interneurons, suggesting that ASH mediated nose touch is signaled to the command interneurons through the release of glutamate (Maricq *et al.*, 1995; Hart *et al.*, 1995). Moreover, ASH is known to be glutamatergic, and worms deficient in glutamatergic transmission are severely defective in nose touch avoidance (Mellem *et al.*, 2002). This hypothesis was recently substantiated by Piggott and colleagues (Piggott *et al.*, 2011). Using genetically encoded calcium sensors they showed that the AVA interneurons exhibit a calcium response during both spontaneous and avoidance driven reversals (Ben Arous *et al.*,

2010; Piggott *et al.*, 2011). In *eat-4* mutants, deficient in glutamergic transmission, AVA is no longer activated upon nose touch. Expression of the wild-type *eat-4* allele in ASH restores this defect. Postsynaptical of ASH, AVA was shown to respond to glutamate through GLR-1, as AVA activity upon nose touch is dependent on the presence of the functional *glr-1* gene (Piggott *et al.*, 2011). Interestingly, the osmotic avoidance response mediated by ASH is not altered in *glr-1* mutants. Moreover, ALM, AVM or PLM mediated touch avoidance is not interrupted in *glr-1* mutants either, suggesting that different sensory cues are processed by different signaling pathways even if these sensory cues are detected by the same neuron (Maricq *et al.*, 1995; Hart *et al.*, 1995). Mellem and colleagues showed that this polymodal signaling by the ASH neurons is mediated by the differential activation of the postsynaptic glutamate receptor subtypes: the osmotic avoidance response requires both NMDA (NMR-1) and non-NMDA (GLR-1 and GLR-2) receptors, while the response to mechanical stimuli only requires non-NMDA receptors (Mellem *et al.*, 2002).

Besides moving forward and backward, worms are also able to turn. Turning behavior was first investigated by Wakabayashi and colleagues in 2004 (Wakabayashi *et al.*, 2004; Gray *et al.*, 2005). They investigated which neurons mediate the transition between pivoting and traveling behavior, two behavioral states that occur when well-fed worms are removed from their food source. While feeding on their bacterial lawn (*E. coli* OP50, under lab conditions), *C. elegans* spend most of their time slowly moving and reversing frequently, with only one head swing per reversal, a behavioral pattern called dwelling (Fujiwara *et al.*, 2002; Ben Arous *et al.*, 2009). However, when worms are removed from their food source, they quickly accelerate and initiate an intensive local search behavior in which the pattern of locomotion changes dramatically (Shingai, 2000; Wakabayashi *et al.*, 2004; Gray *et al.*, 2005). Immediately after removal from food, the frequency of short reversals declines and more long reversals and omega turns occur, resulting in larger directional changes, a behavioral state referred to as pivoting (Wakabayashi *et al.*, 2004; Gray *et al.*, 2005). Approximately 30 min after being removed from food, long reversals and omega turns are suppressed and worms move forward for an extended duration, which is referred to as traveling (Wakabayashi *et al.*, 2004). Using laser ablation, Wakabayashi and colleagues identified ASK and AWC as the sensory neurons having the most prominent role in the induction of pivoting (Wakabayashi *et al.*, 2004). To identify the interneurons involved in

local search behavior, they explored the wiring diagram of the *C. elegans* nervous system and identified four interneurons, AIY, AIZ, AIA and AIB, that connected directly to the sensory neurons involved in local search behavior. Laser ablation of AIB or AIZ resulted in worms which moved forward longer without turning, whereas ablation of AIA and AIY had the opposite effect (Wakabayashi *et al.*, 2004).

One year later, Gray *et al.* (2005) continued to investigate the neural circuit underlying pivoting and traveling. Besides AWC and ASK, they identified ASI as sensory neurons being necessary to suppress short reversals immediately after removal from food, and omega turns after prolonged food deprivation. Moreover, they showed that animals lacking the AVA command interneurons, which were previously shown to drive reversals, did not execute long reversals and abnormally few short reversals on food. However, omega turns were present at approximately normal frequencies, suggesting that omega turns and short reversals must be generated by the motor neurons in the head, which comprise a partially independent motor system (Gray *et al.*, 2005). Gray and colleagues investigated how AWC, ASI and ASK connect to the command interneurons and head motor neurons (Gray *et al.*, 2005). Using a digitalized connectivity map of the worm's nervous system, they looked for the shortest and most prominent path between the input and output neurons. Four groups of neurons were identified as major direct and indirect targets of the amphid sensory neurons (figure 2.3). Half of all synaptic output from the AWC and ASK sensory neurons was directed to the interneurons AIA, AIB, AIY, and AIZ (classified as layer 1). These neurons in turn directed a large fraction of their output onto the RIA and RIB interneurons and the head motor neurons RIM and SMB (layer 2). More than half of the synaptic outputs of the layer 2 neurons was directed to layer 3, comprised of additional head interneurons and motor neurons (layer 3a: SAA, RIV, RMD, SMD, SIA, and SIB) and the command interneurons (layer 3b). Using cell-specific laser ablation, the role of the layer 2 interneurons was subsequently investigated (figure 2.3). Similar to animals lacking AIB (layer 1), animals in which RIB (layer 2) interneurons were ablated had fewer long reversals and omega turns during local search (Gray *et al.*, 2005). Likewise, animals in which the RIM (layer 2) motor neurons were ablated showed no suppression of short reversals after removal from their food source, similar to animals lacking AIY (layer 1). As RIM is heavily connected to AVA by gap junctions and synapses, Gray and colleagues suggested that RIM

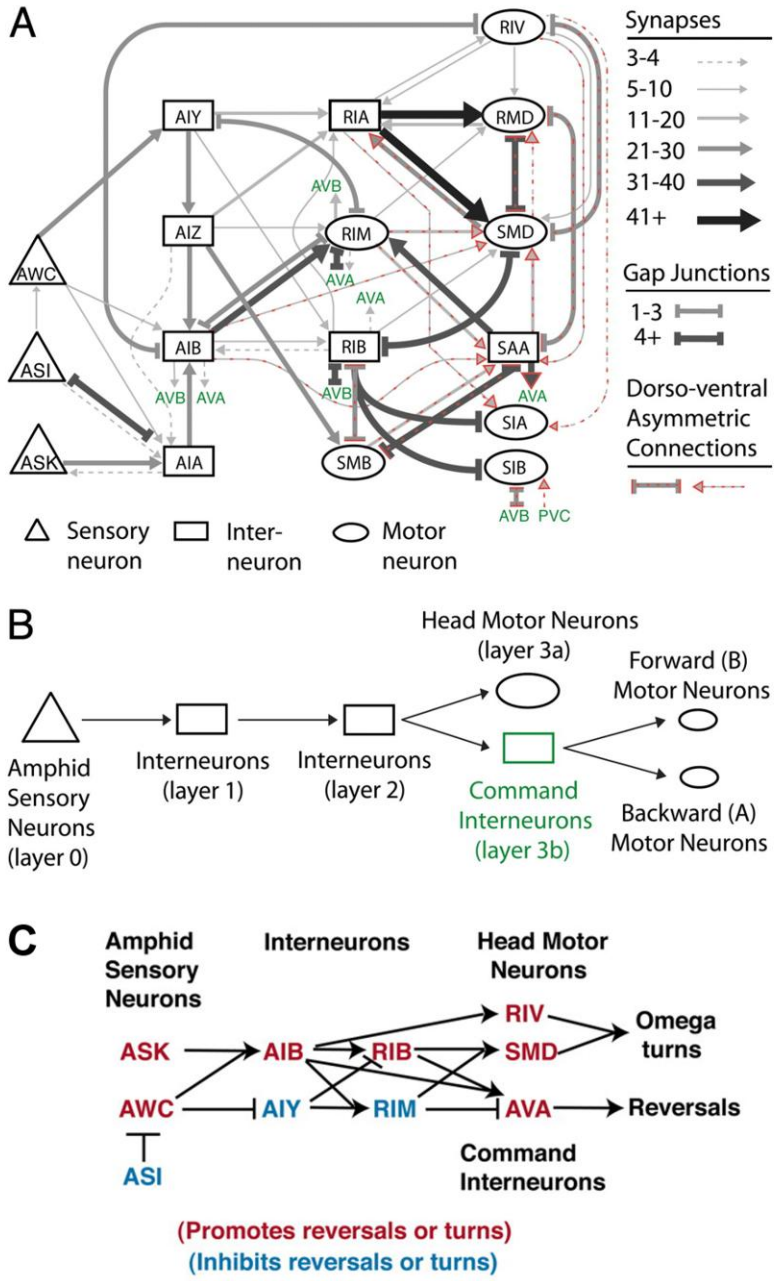

Figure 2.3 Identification of the neuronal pathway mediating food dependent navigation behavior. (A) Connectivity map indicating the shortest and most prominent paths between the input and output neurons mediating food dependent navigation. (B) A schematic representation of the information flow from sensory neurons to motor neurons. (C) Neuronal functions in the navigation circuit from sensory input to motor output. ASI may act partly by inhibiting AWC. ASK and AWC are both believed to stimulate AIB while the latter inhibits AIY. Omega bends are generated by head motor neurons, while the command interneurons evoke reversals.

could inhibit short reversals through these connections. Regarding omega turns, only SMD and RIV motor neurons were shown to mediate this behavior. Neither SMD nor RIV was however essential for reversals/reversal initiation, indicating that the final motor pathways for executing reversals (command interneurons) and omega turns (SMD and RIV) in food dependent navigation behavior are largely distinct (figure 2.3).

Recently, Piggott and colleagues suggested that the neural circuit for spontaneous and ASH induced reversals should be significantly revised. Since killing AVA, AVD an AVE command interneurons results in worms that still initiate spontaneous reversals, albeit at a reduced frequency, they hypothesized there must be another circuit at play, working in parallel to the command neurons to mediate reversals (Piggott *et al.*, 2011). Using laser ablation, optogenetic stimulation and inhibition, and *in vivo* calcium imaging, Piggott and colleagues demonstrated that activation of AIB triggers reversals by inhibiting the RIM interneuron, and this in parallel to the classical command interneuron reversal motor circuit. Having identified the neural pathway mediating spontaneous reversals, Piggott and colleagues investigated if ASH engages both pathways to initiate reversals upon nose touch and hyperosmolarity induced activation. Indeed, they showed that both upon nose touch and osmotic shock, activation of AVA and AIB triggers reversal initiation (Piggott *et al.*, 2011). Similar to the inhibition of RIM by AIB during spontaneous reversals, RIM displayed a considerable drop in neuronal activity upon nose touch as well. However upon osmotic shock, RIM was not inhibited. The behavioral response during osmotic avoidance differs from that to nose touch since osmotic shock represses head movements during reversals. This behavioral strategy is believed to facilitate an efficient escape from hyperosmotic environments, which are considered much more noxious compared to gentle touch (Alkema *et al.*, 2005). Upon osmotic shock activation, AIB still seems to mediate reversal frequency, since ablation of AIB resulted in animals initiating less reversals. RIM activity does however no longer seem to suppress reversal initiation, but instead is recruited to inhibit head oscillations upon osmotic shock (Alkema *et al.*, 2005; Piggott *et al.*, 2011). Remarkably, upon ablation of the AVA, AVD and AVE command interneurons, RIM regained its role in suppressing reversals, suggesting that the excitatory input to RIM upon osmotic shock could be derived from AVA/AVD/AVE which is agreement with the fact that these command interneurons form synaptic connections with RIM (Piggott *et al.*, 2011).

Recently, Pokala and colleagues investigated if the neuronal circuits triggered by hyperosmolarity (glycerol, sensed by ASH) and light anterior touch (stroke with an eyelash at or just posterior to the terminal bulb of the pharynx, sensed by ALM and AVM) engage the same downstream neurons (Pokala *et al.*, 2014). Both ALM, AVM and ASH make synaptic contact with the command interneurons mediating reversals (figure 2.2). But in contrast to ASH, ALM and AVM do not synapse to the AIB interneuron, which is known to mediate turning behavior in freely moving worms (Wakabayashi *et al.*, 2004; Gray *et al.*, 2005). However both osmotic shock and light anterior touch evoke an avoidance response consisting of a reversal followed by turning. Pokala investigated the effect of inactivating neural activity by cell-specific expression of the histamine-gated chloride channel HisCl1. HisCl1 reduces excitability upon administration of histamine, which is not synthesized or used as a neurotransmitter by *C. elegans.* HisCl1-histamine silencing of AVA resulted in worms that did not execute reversals in response to glycerol or anterior touch, but instead paused locomotion and executed an omega turn with a slightly delayed onset (Pokala *et al.*, 2014). In contrast, AIB silencing resulted in worms unable to initiate omega turns in response to glycerol or anterior touch. Since the anterior touch neurons ALM and AVM do not synapse onto AIB, these results suggest that AIB could affect the execution of omega turns without receiving direct sensory input. Remarkably, inactivation of AIB resulted in reduction of reversal length and frequency during glycerol avoidance, but did not affect reversals during touch avoidance, indicating that AIB affects reversal in response to glycerol through the direct synaptic connection with ASH, as previously suggested by Piggott and colleagues (Piggott *et al.*, 2011; Pokala *et al.*, 2014). Postsynaptic of AVA, DA and VA motor neurons mediate reversals although worms are unable to execute omega turns when these motor neurons are silenced (Pokala *et al.*, 2014).

Although the major neural pathways involved in avoidance are starting to become elucidated, we still don't fully understand how these circuits are managed. How is it for example possible that different cues sensed by the same neuron 'activate' different circuits? Clearly, avoidance behavior is not regulated by a simple feed forward circuit, but requires parallel interconnected circuits that are shaped by the context and the nature of the stimuli (Piggott *et al.*, 2011; Pokala *et al.*, 2014). Understanding the relationships between different patterns of neural activity and output will be imperative for modeling neural circuit activity.

For example carbon dioxide (CO_2) avoidance seems to be triggered by both BAG and AFD neurons. However, both neurons display completely different activity patterns upon CO_2 stimulation with AFD neurons responding to increasing CO_2 by a fall and subsequent rise in Ca^{2+}, and exhibiting a Ca^{2+} spike when CO_2 decreases, whereas BAG neurons are activated by CO_2 and remain tonically active while high CO_2 persists (Bretscher *et al.*, 2011). Also the strength of the activating stimulus is shown to influence the activity pattern of the sensory neurons. Whole-cell patch clamp recordings of the ASH neurons showed increased amplitudes of mechanoreceptor currents when more force was applied to the nose tip (Geffeney *et al.*, 2011). Understanding these differential activity patterns may be particularly useful for understanding the role of neuromodulation in behaviors, because neuromodulators usually alter the activity level of their targets rather than completely silencing them (Bargmann, 2012).

2.2.2 Modulation of avoidance behavior in *C. elegans*

C. elegans avoidance behavior from noxious stimuli can be modulated by previous experience, the internal state and external environment of the animal. Repeated application of the soluble repellent copper, which is sensed by the ASH neurons, causes a gradual decrease in the behavioral avoidance response to this noxious stimulus. *In vivo* calcium imaging of ASH neurons shows that repeated chemical stimulation leads to a reversible reduction in the magnitude of the sensory response, indicating that adaptation occurs within the ASH sensory neuron (Hilliard *et al.*, 2005). Adaptation of avoidance is also demonstrated in the neural circuit of touch avoidance. Repeatedly poking the anterior of the worm with a glass probe results in a reduction of the avoidance response, which seems to be mediated by a reduced calcium response in the anterior ALM touch cell (Suzuki *et al.*, 2003).

Feeding state is the paramount environmental factor guiding *C. elegans* behavior, with the presence of food modifying various chemosensory responses including avoidance of damaging agents (Saeki *et al.*, 2001; Chao *et al.*, 2004; Hilliard *et al.*, 2005; Mohri *et al.*, 2005; Harris *et al.*, 2009b; Harris *et al.*, 2010; Ezcurra *et al.*, 2011; Mills *et al.*, 2012). In the presence of food, (*E. coli* OP50) *C. elegans* shows a stronger avoidance response to soluble repellents than in the absence of food. This effect seem to be mediated at the sensory level of the avoidance circuit: *In vivo* calcium imaging shows that in the presence of food, the

ASH neurons respond to soluble repellents with a higher magnitude compared to the absence of food (Ezcurra *et al.*, 2011). Ezcurra and colleagues showed that dopamine (DA) signaling to ASH sensitizes this neuron to soluble repellents upon the acute presence of food.

Besides avoidance to soluble repellents, food also increases avoidance to diluted (30%) 1-octanol. In contrast to soluble repellents, food-dependent increase of diluted 1-octanol avoidance depends on serotonin (5-hydroxytryptamine, 5-HT) signaling (Chao *et al.*, 2004). Moreover, the addition of this monoamine to food-free plates is sufficient to increase avoidance, hereby fully substituting for the presence of food. Increased avoidance to diluted 1-octanol is mediated at different levels throughout the neural avoidance circuit. Three 5-HT receptors, MOD-1, SER-1 and SER-5, are shown to be necessary for the increased avoidance response in the presence of food or exogenous 5-HT (Harris *et al.*, 2009b). However, each receptor mediates sensitivity at a different level of the ASH-mediated circuit: SER-5 in the ASH sensory neurons, MOD-1 in the AIB and AIY interneurons and SER-1 in the RIA interneurons (Harris *et al.*, 2009b). These results suggest that SER-5 increases the responsiveness of ASH to diluted 1-octanol, MOD-1 modulates interneuron signaling to stimulate reversals and turning, and that SER-1 is involved in the control of head oscillations.

Although addition of octopamine (OA) and tyramine (TA), the invertebrate counterparts of norepinephrine and epinephrine (Chase and Koelle, 2007), do not influence avoidance to diluted 1-octanol in the absence of food, these amines do abolish the increased avoidance mediated by food or 5-HT (Wragg *et al.*, 2007). This OA or TA attenuation of 5-HT stimulation of aversive responses to dilute 1-octanol is however abolished in deletion mutants of the *octr-1* or *tyra-3* amine receptors respectively. Expression of wild-type *octr-1* in ASH restores the suppressing effect of OA, indicating that OA suppresses the avoidance response directly at the level of the sensory neuron (Wragg *et al.*, 2007). In addition, *tdc-1* mutant animals defective in the biosynthesis of both TA and OA show an increased avoidance response to diluted 1-octanol compared to wild-type animals. Remarkably, the wild-type response can be restored by exogenous addition of either TA or OA (Wragg *et al.*, 2007).

The effect of OA on the upregulation of avoidance to diluted 1-octanol by serotonin is concentration dependent. Incubation of the animals on plates with 4 mM OA suppresses the effect of 5-HT, but increasing this concentration to 10 mM abolishes this suppressing effect. Mills and colleagues demonstrated that this effect was mediated by the OA receptor SER-3 expressed in the ASH neurons (Mills *et al.*, 2012). Both OCTR-1 and SER-3 exert their effect in ASH. Since SER-3 signaling was shown only to antagonize OCTR-1 at high exogenous OA concentrations Mills and colleagues speculated that OCTR-1 could have a higher affinity for OA than SER-3. However, *in vitro* both SER-3 and OCTR-1 have the same affinity for OA (Mills *et al.*, 2012).

Avoidance to undiluted 1-octanol is also modulated by 5-HT, DA, OA and TA (Chao *et al.*, 2004; Wragg *et al.*, 2007; Baidya *et al.*, 2014). Unlike the avoidance to diluted 1-octanol (30%), serotonin has no effect on the behavioral response to undiluted 1-octanol, but seems to regulate the neural circuit that mediates avoidance depending on the presence of food. On-food the ASH neurons seem to be the main sensory neurons that mediate avoidance to undiluted 1-octanol, whereas off-food AWB and ADL become involved in this process as well. The recruitment of AWB and ADL seems to depend on the presence of serotonin, indicating that this neurotransmitter signals both the presence and absence of food (Chao *et al.*, 2004).

OA and TA decrease the avoidance response to undiluted 1-octanol in the absence of food, however independently of the OCTR-1 or TYRA-3 receptor, which mediate their suppressing effect on avoidance to diluted 1-octanol (Wragg *et al.*, 2007). Instead the suppressing effect of OA was shown to depend on the expression of the amine receptor SER-6 in AWB, ADL and ASI (Mills *et al.*, 2012). However, previous reports and *in vivo* calcium imaging indicate that AWB and ADL do not seem to respond to undiluted 1-octanol in the absence of food (Chao *et al.*, 2004; Mills *et al.*, 2012).

Dopamine deficient c*at-1* mutant animals show an increased response latency to undiluted 1-octanol compared to wild-type animals. This response latency is restored by exogenous administration of DA (Baidya *et al.*, 2014). Remarkably, although the glutamate-gated ion channels GLR-1 and GLR-2 and the NMDA ionotropic glutamate receptor NMR-1 all seem

to take part in the avoidance response to 1-octanol, DA mediated 1-octanol avoidance only depends on NMR-1 (Baidya *et al.*, 2014).

Besides monoamines, neuropeptides have also shown to modulate avoidance behaviors. To our knowledge, so far modulation of avoidance by neuropeptide signaling has only been investigated in light of monoaminergic modulation of avoidance. The involvement of neuropeptides in the modulation of avoidance behaviors can easily be observed in *egl-3* proprotein convertase and *egl-21* carboxypeptidase mutants which lack functional neuropeptide processing enzymes. These animals do not show an increase in diluted 1-octanol avoidance in the presence of 5-HT, indicating that 5-HT stimulation of avoidance responses depends on neuropeptide signaling (Harris *et al.*, 2010). In line with this, Harris and colleagues reported that 1-octanol avoidance is not stimulated by food or serotonin in *nlp-3* mutant animals. However, serotonin stimulation was fully rescued in *nlp-3* mutant animals by the ASH-specific expression of *nlp-3*. Moreover ASH-specific RNAi knockdown of *nlp-3* abolished food or 5-HT stimulation of 1-octanol avoidance. NLP-3 signaling probably acts through the neuropeptide receptor NPR-17, since *nlp-3* overexpression cannot rescue the loss of serotonin stimulated avoidance in *npr-17* mutants (Harris *et al.*, 2010). Mills and colleagues reported that suppression of avoidance to undiluted 1-octanol by octopamine is mediated by several neuropeptides (encoded by *nlp-6, -7, -8* and *-9*) and neuropeptide receptors (encoded by *npr-9*, *npr-15*, *npr-18*, *npr-19*, *npr-20, gnrr-1* and *nmur-1*) (Mills *et al.*, 2012). Tyramine inhibition of 1-octanol avoidance seems to be mediated by neuropeptide signaling as well. NLP-1 and NLP-14 peptides were demonstrated to mediate suppression of avoidance to undiluted 1-octanol by tyramine through the neuropeptide GPCRs NPR-10 and NPR-11, respectively (Hapiak *et al.*, 2013).

This chapter clearly illustrates the power of using *C. elegans* to investigate the molecular and circuit mechanisms underlying complex behavioral states. However, despite the simplicity of the nervous system, the regulation of neural circuits is shown to be complex as well and can be modulated at different levels.

Chapter 3. Identification of novel neuropeptidergic signaling systems in the nematode C. elegans

This chapter has partially been published in:

Frooninckx, L., Van Rompay, L., Temmerman, L., Van Sinay, E., Beets, I., Janssen, T., Husson, S., Schoofs, L. (2012). Neuropeptide GPCRs in *C. elegans*. *Frontiers in Endocrinology, 3*, art.nr. 167, 1-18.

Frooninckx, L., Mirabeau, O., Nelson, M. D., Wouters, A., Temmerman, L., Raizen, D. M., Schoofs, L., Beets, L. Discovery of a wake-promoting neuropeptide pathway in *C. elegans*. Submitted for publication in *eLife*

3.1 Introduction

Several neuropeptide systems present in vertebrates have also been identified in insects and nematodes, indicating that these neuropeptide systems are conserved during the course of evolution and were already established prior to the divergence of protostomes and deuterostomes (Janssen *et al.*, 2010; Mirabeau and Joly, 2013; Jékely, 2013). The availability of the complete *C. elegans* genome sequence allows researchers to browse through it, uncovering putative neuropeptides and their cognate GPCRs. The *C. elegans* genome is predicted to encode approximately 130 neuropeptide GPCRs (Janssen *et al.*, 2010). Only 31 of them have an identified neuropeptide ligand (§1.3.4), leaving many so-called orphan GPCRs. A crucial step in the characterization of an orphan GPCR is the identification of its natural ligand(s). For this purpose, a combined reverse pharmacology approach can be applied (§1.3.3). In this approach the orphan receptor is used as a bait to identify its activating ligands. Therefore the receptor is expressed in an heterologous expression cell system which is challenged with a compound library with putative activating ligands (Beets *et al.*, 2011; Civelli *et al.*, 2013). The major challenges to this approach are the composition of the compound library and the ability to monitor the receptor activation.

Many predicted *C. elegans* orphan neuropeptide GPCRs share a significant degree of homology to known insect and mammalian peptide GPCR families. In line with the receptor-ligand coevolution theory, *in silico* identification of neuropeptide GPCR ligands has become a promising strategy to predict neuropeptide systems (Lindemans *et al.*, 2009b; Lindemans *et al.*, 2009a). However, the conservation between homologous peptide precursor sequences is usually restricted to a few amino acids. Hence it remains challenging to predict the activating ligand of an orphan neuropeptide GPCR. To circumvent this issue, the compound library can be compiled based on bioinformatic predictions and peptidomic analyses of RP-HPLC fractions of a peptide extract (Janssen *et al.*, 2010; Beets *et al.*, 2011; Civelli *et al.*, 2013).

Since the publication of the *C. elegans* genome, many predictions have been made about the number of neuropeptide GPCRs it contains. These predictions are usually based on sequence similarities to vertebrate and insect neuropeptide GPCRs (Bargmann, 1998; Fredriksson and Schiöth, 2005). Compared to other *C. elegans* GPCRs, neuropeptide

GPCRs appear to be less closely related to their vertebrate counterparts. This agrees with the apparently low conservation of the *C. elegans* neuropeptides (Bargmann, 1998). Another way to predict neuropeptide GPCRs is to use all deorphanized neuropeptide GPCRs as a seeding set in a Multiple Expectation Maximization for Motif Elicitation/Motif Alignment and Search Tool (MEME/MAST) analysis. Doing so, a list of 125 potential neuropeptide receptors could already be obtained (Janssen *et al.*, 2010). Since this prediction, the number of deorphanized neuropeptide GPCRs has increased from 6 to 31 (§1.3.4).

In order to obtain an accurate prediction of all neuropeptide GPCRs present in *C. elegans* we enhanced this MEME/MAST analysis by use of an updated seeding set containing all newly deorphanized neuropeptide GPCRs. From the obtained MAST list three groups of orphan receptors related to GnRH/AKH, tachykinin and neuromedin U neuropeptide signalling systems were chosen for ligand identification using a combined *in silico* and library-based reverse pharmacology approach.

3.2 Material and methods

3.2.1 MEME/MAST prediction

In order to identify potential neuropeptide GPCRs in *C. elegans* a MEME/MAST analysis was performed (Bailey *et al.*, 2009). This online application (http://meme.nbcr.net/meme/) allows us to identify motifs representing common features of a dataset of DNA or protein sequences, using the MEME algorithm. This algorithm calculates the maximum likelihood estimates of the parameters of a two-component finite mixture model that could have generated the given dataset of DNA or protein sequences (Bailey and Elkan, 1994). The motif discovered by MEME can subsequently be used to search a database for the occurrence of these motifs using MAST. The MAST application determines the best match in the sequence to each motif. The scores for these best sequence motif matches are combined into a score for the overall match between the complete motif set and the sequence, resulting in an E-value for each sequence. The output from MAST is a list of the sequences for which the E-value is less than a user-specified threshold (Bailey *et al.*, 2009).

In this study MEME motifs were generated by using the protein sequences of all *C. elegans* neuropeptide that were deorphanized at the start of this study (table 3.1). Since the majority

of the GPCRs encoded in the *C. elegans* genome are predicted to be chemoreceptors (Robertson and Thomas, 2006), we used the list of *C. elegans* chemoreceptors as predicted by Thomas and Robertson (Thomas and Robertson, 2008), as a negative sequence dataset. Minimum and maximum length of the motifs was set to 10 and 100 amino acids, respectively. Maximum number of motifs to be identified was set to 20. Distribution of the motifs was set to 'any numbers of repetitions'. Motifs with an E-value smaller then $1e^{-20}$ were used in the MAST application to look for sequences in the *C. elegans* genome (WormBase WS220) that harbor these motifs with an E-value smaller than 0.1 . The obtained list of potential *C. elegans* neuropeptide GPCRs was manually curated and compared to the list of neuropeptide GPCRs published on WormAtlas (Altun, 2011)

Table 3.1. List of deorphanized *C. elegans* neuropeptide GPCRs used as the training set for the MEME analysis

Protein	WormBase ID
NPR-1	WP:CE06941
NPR-3	WP:CE08056
NPR-4	WP:CE37317
NPR-5a	WP:CE33345
NPR-5b	WP:CE36962
NPR-6	WP:CE31509
NPR-10a	WP:CE19767
NPR-10b	WP:CE36989
NPR-11	WP:CE47199
FRPR-3	WP:CE06880
FRPR-18a	WP:CE29348
FRPR-18b	WP:CE29349
NPR-22a	WP:CE31260
CKR-2e	WP:CE48226
CKR-2f	WP:CE48324
GNRR-1a	WP:CE17102
NTR-1	WP:CE13377
NMUR-2	WP:CE38395

Protein	WormBase ID
EGL-6a	WP:CE04219
EGL-6b	WP:CE43400
PDFR-1a	WP:CE30860
PDFR-1b	WP:CE37087
PDFR-1c	WP:CE37088

3.2.2 Phylogenetic analysis

To identify potential tachykinin receptors in *C. elegans*, a protein BLAST search was performed with human substance P (SP), neurokinin A (NKA) and neurokinin B (NKB) receptors (AAA60601.1, NP_001048.2 and NP_001050.1) and the *D. melanogaster* tachykinin (99D) receptor (NP_524556.2) as queries, and using default parameter settings.

For the phylogenetic analysis of the tachykinin receptor family, a protein dataset of tachykinin-related receptors was retrieved, composed of arthropod tachykinin receptors (*D. melanogaster* NP_524556.2; *T. castaneum* XP_970102.2; and *D. pulex* EFX88772.1), arthropod natalisin receptors (*D. pulex* EFX77115.1 and FX77113.1; *T. castaneum* NP_001280511.1; *D. melanogaster* NP_524304.2; and *A. pisum* XP_008185736.1), nematode tachykinin-like receptors (*C. elegans* CAA79546.2, CCD67626.1 and CCD61149.1; *T. spiralis* XP_003381178; and *P. pacificus* JIGTRA00000173002), lophotrochozoan tachykinin receptors (*C. telata* ELT98449.1 and *L. gigantean* XP_009062052.1) and deuterostomian tachykinin receptors (*C. intestinalis* NP_001027809.1; *B. floridae* XP_002604715.1; *T. rubripes* NP_001267026.1, NP_001267036.1, NP_001267041.1 and AAQ02694.1; and *H. sapiens* AAA60601.1, NP_001048.2 and NP_001050.1)

For the phylogenetic analysis of the GnRH/AKH-like receptors, the protein dataset was composed of deuterostomian GnRH receptors (NP_001028994.1, NP_001028997.1, NP_001028996.1, AAW70562.1, XP_002606331.1, XP_002606330.1, NP_000397.1, XP_003965821.1, XP_003977749.1, XP_003967097.1, XP_003969466.1, XP_003969621.1, NP_001116990.1, NP_001116991, NP_001116992.1, AAQ04564.1, ADL14592.1, ABO77118.1, XP_005174743.1, ABQ08716.1, NP_001138451.1 and

NP_001091663.1), bilaterian corazonin (Crz) receptors (XP_006820827, XP_009044166.1, ELT93721.1, XP_002606367.1, ACC68668.1, NP_001137393.1, NP_648571.1, NP_001127719.1 and XP_321555.1), protostomian GnRH/AKH receptors (ACD75498.1, XP_003245942.1, ELU01220.1, ELT92261.1, EOG63VBPF, ELT96363.1, ELU00909.1, NP_477387.1, NP_001076809.1, NP_001035354.1, NP_001037049.1, ABD60146.1, NP_001127745.1, NP_001280549.1, ABX52399.1 and NP_001164571.1) and nematode GnRH/AKH-like receptors (NP_001249720.1, NP_001256583.1, NP_509685.2, NP_001024452.1, NP_504228.2, NP_509865.1, NP_509866.2, NP_502887.1, XP_001898606.1, XP_001898983.1, XP_001897938.1, XP_002639368.1, XP_002637834.1, XP_002643743.1, XP_002644741.1, XP_002647239.1, XP_002644017.1, XP_002644016.1 and CAP32453.2). AVP and NPS receptor sequences were used as outliers (XP_002595923.1, XP_002741531.1, ELU01967.1, AAH30197.1, XP_002600070.1, XP_006815767.1, ELU14444.1, NP_996297.3, ELU12393.1, NP_997055.1, ENSPMAT00000003799, XP_002605430.1, XP_006813812.1, NP_493193.1, NP_510477.1, XP_002586963.1, NP_000045.1, ENSPMAT00000008459, NP_000698.1, CAA46097.1, XP_002735546.2, ELU02228.1 and EFX69326.1).

Sequence alignments were generated using the simultaneous Alignment and Tree Estimation (SATé) software package that uses hill-climbing searches from a collection to retrieve an alignment from which a maximum likelihood (ML) tree can be generated with the optimal ML score (Liu *et al.*, 2009).

For the GnRH/AKH receptors, ML phylogeny was estimated using PhyML. The following parameters were used: LG as the amino-acid replacement matrix (Le and Gascuel, 2008), Subtree Pruning and Regrafting and Nearest Neighbor Interchange for topological moves (Guindon *et al.*, 2010), and a number of discrete gamma rate categories equal to 4. Branch support values were generated using nonparametric bootstrapping (100 bootstraps). Branches with bootstrap values below 50% were collapsed.

3.2.3 Peptide synthesis and purification

The compound library was compiled using a synthetic library of previously predicted and purified *C. elegans* peptides, and newly synthesized peptides corresponding to the *in silico* predicted sequences of *C. elegans* tachykinin peptides. Peptides were custom-synthesized

by GL Biochem Ltd. All peptides were initially tested at a concentration of 10 µM. Receptor activating peptides were purified using reverse-phase HPLC and verified using matrix assisted laser desorption/ionisation time-of-flight analyzer (MALDI-TOF) mass spectrometry. Peptide concentrations were determined with a bicinchoninic acid protein assay (Wiechelman *et al.*, 1988). Peptides were lyophilized and diluted to the desired concentrations.

3.2.4 Receptor cloning

For receptor deorphanization, the open reading frame of each receptor was cloned into a mammalian expression vector. Only receptors with seven alpha-helical transmembrane topology, predicted using TMHMM 2.0 software (http://www.cbs.dtu.dk/services/TMHMM/), were cloned. The open reading frames of the receptors were amplified by Polymerase Chain Reaction (PCR) on cDNA of wild type *C. elegans* (Bristol variety N2). Complementary DNA (cDNA) was obtained through reverse transcriptase PCR (SuperScript III Reverse Transcriptase, Invitrogen) using random primers (Invitrogen) on an mRNA extract from mixed stage wild type *C. elegans* (Rneasy Mini kit, Qiagen). For each receptor, specific forward and reverse primers (Sigma-Aldrich, table 3.2) were designed using NetPrimer (PREMIER Biosoft) based on the predicted cDNA sequence on WormBase (release WS227).

Table 3.2 Gene-specific primer sequences for amplification of receptor cDNAs

receptor	forward primer (5'-3')	reverse primer (5'-3')
gnrr-2a	caccatgtcactaatcttacccaactcaac	ttagttttgcaataacttgcaaatct
gnrr-3	caccatgaacaactcaacatc	tcctcagcatctgccagc
gnrr-5	caccatgagctattccaatgaaaatc	ggaatttatttatgtggcattgaga
gnrr-7	caccatgattgaaacatctac	ctctaaagctagactcgatga
tkr-1	caccatgaatcaagaattcttaattcaact	tcaccgttcatggcaactca
tkr-2	caccatgacaacgtgtcccctacca	tcagaaatccgtatgcgc
nmur-1	caccgatttcagccgagtgaga	acatgatatcgaattagcagga

Pfu polymerase (PfuUltra II Fusion HS DNA Polymerase, Agilent Technologies) was used for PCR amplification. PCR started with initial denaturation for 1 min at 95°C, followed by

30 cycles of [20 s at 95°C, 20 s at 55°C, 1 min at 72°C], followed by final elongation for 3 min at 72°C. The size of the amplicon was checked on a 1% agarose gel and purified with the High Pure PCR Product Purification Kit (Roche). The amplicon was directionally cloned into the pcDNA3.1D/V5-His TOPO expression vector and transformed in One Shot TOP10 chemically competent *E. coli* by means of heat shock (pcDNA3.1 Directional TOPO Expression Kit, Invitrogen). Single colonies were analyzed for the presence of the cloned amplicon by colony PCR using the T7 (5´-TAATACGACTCACTATAGGG-3´) and BGH Reverse (5´-TAGAAGGCACAGTCGAGG-3´) primers. Colonies carrying the expression vector with an insert of the correct size were transferred to 5ml LB medium (25 g/l, Sigma-Aldrich) with ampicillin (50 µg/ml, Invitrogen) and incubated overnight at 37°C in a shaking incubator. Vector DNA was isolated (GenElute Plasmid Miniprep Kit, Sigma-Aldrich) and the insert was sequenced using the ABI PRISM 3130 Genetic Analyzer (Applied Biosystems) according to the ABI PRISM BigDye Terminator Ready Reaction Cycle Sequencing Kit protocol (Applied Biosystems). The receptor sequences were verified to be identical to the predicted cDNA sequence on WormBase. Bacterial cells containing a verified receptor insert were grown at large scale in 200 ml LB medium with ampicillin, and the expression vector was isolated using the EndoFree Plasmid Maxi Kit (QIAgen).

3.2.5 Cell culture and transfection

CHO cells stably expressing apo-aequorin and the promiscuous $G\alpha_{16}$ subunit were used for receptor deorphanization assays. Cells were cultured in Dulbecco's Modified Eagle's Medium Nutrient Mixture Ham F-12 (DMEM/F-12, Invitrogen) to which 1 % penicillin/streptomycin, 2.5 µg/ml amphotericin B and 10% inactivated fetal bovine serum (Sigma-Aldrich) was added. Growth medium was supplemented with 250 µg/ml zeocin or 5 µg/ml puromycin, which serves as a selection reagent for CHO cells with or without the promiscuous $G\alpha_{16}$ subunit, respectively. Cells were grown as a monolayer in a T25 culture flask at 37°C, 5% CO_2 and high humidity, and sub-cultivated twice a week. For transfection, T75 flasks with a confluency of about 60 percent were used. First, 3.75 ml Opti-MEM I (Invitrogen), 7.5 µg pcDNA3.1 construct and 18.75 µl Plus reagent (Invitrogen) were gently mixed in a polystyrene tube. After incubation for 5 minutes at room temperature, 45 µl Lipofectamine LTX (Invitrogen) was added and gently mixed. The transfection reagents were incubated for 30 min at room temperature. Growth medium was removed leaving 3 ml

in the flask and the transfection reagent was added dropwise to the cells. Transfected cells were grown overnight and 20 ml growth medium was added the next day.

To characterize downstream signaling pathways, CHO cells stably expressing apo-aequorin but lacking the promiscuous $G\alpha_{16}$ protein and HEK293T cells were used. HEK293T cells were cotransfected with the receptor construct (5.0 µg) and CRE-luciferase construct (2.5 µg), consisting of the open reading frame of the luciferase gene, downstream of a multimerized cAMP-response-element (CRE6x). For the initial screen, cells were grown for one more day before the assay at 37°C. For dose-response experiments, cells were grown at 28°C 24 hours prior to the screening assay.

3.2.6 Calcium bioluminescence assay

Two days after transfection CHO cells were detached using phosphate buffered saline (PBS) with 0.2% EDTA and collected in 10 ml colorless DMEM/F-12 medium (11039, Gibco). Cell viability was measured using a NucleoCounter NC-100 (Chemometic). Cells were pelleted for 4 min at 800 rpm at room temperature and resuspended to a concentration of 5×10^6 cells/ml in colorless DMEM/F12 with 0.1% bovine serum albumin (BSA). 5 µM coelenterazine H (Invitrogen) was added to the cell suspension. Cells were incubated gently shaking for 4 hours in the dark at room temperature, allowing the aequorin holoenzyme to be reconstituted. After a 10-fold dilution in DMEM/F12 with 0.1% BSA, cells were incubated another 30 min. Peptides were dissolved in DMEM/F12 with 0.1% BSA and 50 µl of the peptide solution was added to the wells of a white flat bottom 96-well plate. Wells containing DMEM/F12 with 0.1% BSA were used as a negative control while wells containing 1 µM ATP were used as a positive control. Incubated cells were added to the wells of the 96-well plate and luminescence was monitored for 30 seconds on a Mithras LB 940 luminometer (Berthold Technologies). After 30 seconds 0.2% Triton X-100 dissolved in DMEM/F12 with 0.1% BSA was added to lyse the cells and light emission was recorded for another 8 seconds. Light emission from each well was calculated relative to the total response (ligand+Triton X-100) using the output file of Mikrowin2000 software (Mikrotek). Half maximal effective concentrations (EC_{50} values) were calculated from dose-response curves that were constructed using a nonlinear regression analysis with a sigmoidal dose-response equation (Graphpad Prism 5).

3.2.7 CRE-luciferase assay

To measure downstream signaling of the receptor through $G\alpha_s$- or $G\alpha_i$-types of G proteins, a CRE-luciferase assay was used to measure an increase or decrease of cAMP in HEK293T cells. Transfected HEK293T cells were detached using PBS with 2% EDTA and collected in 10 ml colorless DMEM/F-12. Viability was quantified and cells were pelleted and resuspended in colorless DMEM/F12, containing 200 µM of 3-isobutyl-1-methylxanthine (IBMX, Sigma-Aldrich), to a concentration of 1 x 10^6 cells/ml. 50 µl of this cell suspension was added to each well of a white flat bottom 96-well plate. Peptides were dissolved in colorless DMEM/F12 with 200 µM IBMX or 200 µM IBMX and 10µM forskolin to test for signaling through $G\alpha_s$ or $G\alpha_i$, respectively. After adding 50 µl of the peptide solution to the wells containing the cell suspension, the 96-well plate was incubated at 37°C and 5% CO_2. After incubation 100 µl SteadyLitePlus (PerkinElmer) was added to each well, and the 96-well plate was incubated for 15 min in the dark. Luminescence was then measured for 5 seconds/well on a Mithras LB 940 luminometer.

3.3 Results

3.3.1 MEME/MAST prediction of C. elegans neuropeptide GPCRs

In order to obtain an accurate list of hypothetical neuropeptide GPCRs encoded in the genome of *C. elegans*, a MEME/MAST analysis was performed. The protein sequences of all *C. elegans* neuropeptide GPCRs that were deorphanized at the beginning of this study were used as a training set to elucidate the common motif sequences present in *C. elegans* neuropeptide GPCRs. MEME analysis revealed 5 motifs in this dataset with an E-value smaller than $1e^{-20}$ (table 3.3).

Table 3.3 *C. elegans* neuropeptide GPCR motif sequences revealed by the MEME analysis

Motif	Width	Best possible match
1	19	HCIAMSSAVWNPIIYAWLN
2	28	QGMSIFVSTWTLVAIALDRWVAICHPLQ
3	11	MVVWFACCWLP
4	26	RSVRNIFLLNLAASDLMMCILSIPIT
5	12	WYFGDVMCHICP

These motifs were used in a MAST analysis to identify additional hypothetical neuropeptide GPCRs in the genome of *C. elegans.* Sequences retrieved from the MAST analysis with an E value smaller than 0.1 were manually revised and compared to the list of neuropeptide GPCRs available on WormAtlas (Altun, 2011). A list of 129 potential *C. elegans* neuropeptide GPCRs was retrieved (table 3.4). The predicted neuropeptide GPCRs were subdivided into the major classes of neuropeptide GPCRs according to the classification adapted by Altun (Altun, 2011).

Table 3.4 List of neuropeptide GPCRs in *C. elegans* ranked according to the GRAFS classification system. Neuropeptide GPCRs were predicted by MAST analysis and manually revised and compared to the list of neuropeptide GPCRs from WormAtlas (Altun, 2011). Receptors marked in dark grey were used as the training set in the MEME analysis.

Receptor group	Gene sequence	Protein	WormBase ID
Rhodopsin family			
Neuropeptide Y /RFamide-like receptors	C39E6.6	NPR-1	WP:CE06941
	T05A1.1a	NPR-2a	WP:CE32924
	T05A1.1b	NPR-2b	WP:CE32925
	C10C6.2	NPR-3	WP:CE08056
	C16D6.2	NPR-4	WP:CE37317
	Y58G8A.4a	NPR-5a	WP:CE33345
	Y58G8A.4b	NPR-5b	WP:CE36962
	F41E7.3	NPR-6	WP:CE31509
	F35G8.1	NPR-7	WP:CE39498
	C56G3.1a	NPR-8a	WP:CE04283
	C56G3.1b	NPR-8b	WP:CE30923
	C53C7.1a	NPR-10a	WP:CE19767
	C53C7.1b	NPR-10b	WP:CE36989
	C25G6.5	NPR-11	WP:CE47199
	T22D1.12	NPR-12	WP:CE17256
	ZC412.1	NPR-13	WP:CE35920
	W05B5.2	NPR-14	WP:CE42751
	T07D4.1	NPR-20	WP:CE46449

Receptor group	Gene sequence	Protein	WormBase ID
	T23C6.5	NPR-21	WP:CE35783
	C02B8.5	FRPR-1	WP:CE47103
	C05E7.4	FRPR-2	WP:CE46227
	C26F1.6	FRPR-3	WP:CE06880
	C54A12.2	FRPR-4	WP:CE36809
	C56A3.3a	FRPR-5a	WP:CE45431
	C56A3.3b	FRPR-5b	WP:CE45452
	F21C10.12	FRPR-6	WP:CE32868
	F53A9.5	FRPR-8	WP:CE43844
	F53B7.2a	FRPR-9a	WP:CE44099
	F53B7.2b	FRPR-9b	WP:CE44063
	K06C4.8	FRPR-11	WP:CE11816
	K06C4.9	FRPR-12	WP:CE29506
	K07E8.5	FRPR-14	WP:CE35992
	K10C8.2	FRPR-15	WP:CE42140
	R12C12.3	FRPR-16	WP:CE02848
	T14C1.1	FRPR-17	WP:CE34212
	T19F4.1a	FRPR-18a	WP:CE29348
	T19F4.1b	FRPR-18b	WP:CE29349
	Y41D4A.8	FRPR-19	WP:CE21846
	C30B5.5	FRPR-20	WP:CE02524
	C09F12.3	C09F12.3	WP:CE33973
	D1014.2	D1014.2	WP:CE44520
Somatostatin and galanin-like receptors	ZK455.3	NPR-9	WP:CE03814
	F56B6.5a	NPR-16a	WP:CE31186
	F56B6.5b	NPR-16b	WP:CE39375
	C06G4.5	NPR-17	WP:CE38997
	C43C3.2a	NPR-18a	WP:CE01524
	C43C3.2b	NPR-18b	WP:CE47537
	C43C3.2c	NPR-18c	WP:CE47497
	C43C3.2d	NPR-18d	WP:CE47523
	C43C3.2e	NPR-18e	WP:CE47594

Receptor group	Gene sequence	Protein	WormBase ID
	C43C3.2f	NPR-18f	WP:CE47636
	C43C3.2g	NPR-18g	WP:CE47570
	R106.2	NPR-24	WP:CE39612
	T02E9.1	NPR-25	WP:CE13062
	T02D1.6	NPR-26	WP:CE30684
	F42C5.2	NPR-27	WP:CE47648
	F55E10.7	NPR-28	WP:CE40072
	ZC84.4	NPR-29	WP:CE24711
	H10E21.2	NPR-30	WP:CE43737
	Y116A8B.5	NPR-32	WP:CE46735
	Y54E2A.1	Y54E2A.1	WP:CE31259
	C17H11.1	C17H11.1	WP:CE29584
	C24B5.1	C24B5.1	WP:CE36981
	F57A8.4	F57A8.4	WP:CE05985
	W10C4.1	W10C4.1	WP:CE39426
Tachykinin-like receptors	C38C10.1	TKR-1	WP:CE44282
	AC7.1a	TKR-3a	WP:CE38261
	AC7.1b	TKR-3b	WP:CE38262
	T27D1.3	NPR-15	WP:CE43181
	Y59H11AL.1a	NPR-22a	WP:CE31260
	Y59H11AL.1b	NPR-22b	WP:CE38456
	C49A9.7	C49A9.7	WP:CE16937
	C50F7.1a	C50F7.1a	WP:CE33574
	C50F7.1b	C50F7.1b	WP:CE04239
	F31B9.1	NPR-33	WP:CE17727
	T11F9.1a	T11F9.1a	WP:CE47396
	T11F9.1b	T11F9.1b	WP:CE47310
CCK/ gastrin-like receptors	T23B3.4	CKR-1	WP:CE45656
	Y39A3B.5e	CKR-2e	WP:CE48226
	Y39A3B.5f	CKR-2f	WP:CE48324
GnRH-, OT/VP-like	F54D7.3a	GNRR-1a	WP:CE17102

Receptor group	Gene sequence	Protein	WormBase ID
receptors	F45D7.3b	GNRR-1b	WP:CE46861
	C15H11.2a	GNRR-2a	WP:CE08179
	C15H11.2b	GNRR-2b	WP:CE45186
	ZC374.1	GNRR-3	WP:CE40886
	C41G11.4a	GNRR-4a	WP:CE29716
	C41G11.4b	GNRR-4b	WP:CE30896
	C41G11.4c	GNRR-4c	WP:CE35428
	H22D07.1	GNRR-5	WP:CE33129
	F13D2.2	GNRR-6	WP:CE03194
	F13D2.3	GNRR-7	WP:CE33996
	Y105C5A.23	GNRR-8	WP:CE24056
	T07D10.2	NTR-1	WP:CE13377
	F14F4.1	NTR-2	WP:CE17670
Neurotensin, neuromedin U, growth hormone secratogogue, thyrotropin releasing hormone-like receptors	C48C5.1	NMUR-1	WP:CE45664
	K10B4.4	NMUR-2	WP:CE38395
	F02E8.2a	NMUR-3a	WP:CE33990
	F02E8.2b	NMUR-3b	WP:CE07017
	C30F12.6	NMUR-4	WP:CE16886
	F57H12.4	FRPR-10	WP:CE43724
	F57B7.1a	DMSR-1a	WP:CE05989
	F57B7.1b	DMSR-1b	WP:CE31009
	C46F4.1a	EGL-6a	WP:CE04219
	C46F4.1b	EGL-6b	WP:CE43400
	B0563.6a	B0563.6a	WP:CE29551
	B0563.6b	B0563.6b	WP:CE33513
	B0563.6c	B0563.6c	WP:CE41751
	R03A10.6	SPRR-1	WP:CE43810
	F42D1.3	SPRR-2	WP:CE31511
	F39B3.2	FRPR-7	WP:CE30978
	K03H6.5	K03H6.5	WP:CE39585
/	C48C5.3	AEXR-3	WP:CE04226
/	T10E10.3	T10E10.3	WP:CE35766

Receptor group	Gene sequence	Protein	WormBase ID
/	T21H3.5	T21H3.5	WP:CE13906
/	Y70D2A.1	Y70D2A.1	WP:CE34231
/	ZK1307.7a	ZK1307.7a	WP:CE37863
/	ZK1307.7b	ZK1307.7b	WP:CE46539
/	B0034.5	B0034.5	WP:CE45030
/	B0334.6	B0334.6	WP:CE30473
Secretin family			
/	C18B12.2	SEB-3	WP:CE23557
	B0457.1a	LAT-1a	WP:CE02945
	B0457.1b	LAT-1b	WP:CE32789
	B0286.2a	LAT-2a	WP:CE36968
	C18B12.2	C18B12.2	WP:CE23557
	ZK643.3a	SECR-1a	WP:CE33750
	ZK643.3b	SECR-1b	WP:CE01112
	C13B9.4a	PDFR-1a	WP:CE30860
	C13B9.4b	PDFR-1b	WP:CE37087
	C13B9.4c	PDFR-1c	WP:CE37088

3.3.2 Identification of a tachykinin-related signaling system in *C. elegans*

To identify tachykinin-related receptors in *C. elegans* a protein BLAST search was performed using human SP, NKA and NKB and *D. melanogaster* tachykinin (99D) receptors as queries. This search revealed the proteins C38C10.1 and C49A9.7, which were annotated as the tachykinin receptors (TKR) TKR-1 and TKR-2 respectively. TKR-1 and TKR-2 share respectively 32% and 37% of sequence identity with the *D. melanogaster* tachykinin (99D) receptor. Besides TKR-1 and TKR-2, AC7.1 was recently annotated as a tachykinin-like receptor (TKR-3) as well. Our BLAST results indicate that this receptor shares 26% sequence identity with the *D. melanogaster* tachykinin (99D) receptor. In order to investigate the evolutionary relationship of *C. elegans* TKRs with known tachykinin receptors, a phylogenetic analysis was performed (figure 3.1). *C. elegans* TKR-1 and TKR-2 cluster together with arthropod and lophotrochozoan tachykinin receptors, while TKR-3

clusters together with the protostomian Luqin receptor outgroup, which were previously demonstrated to be closely related to tachykinin receptors (Mirabeau and Joly, 2013)

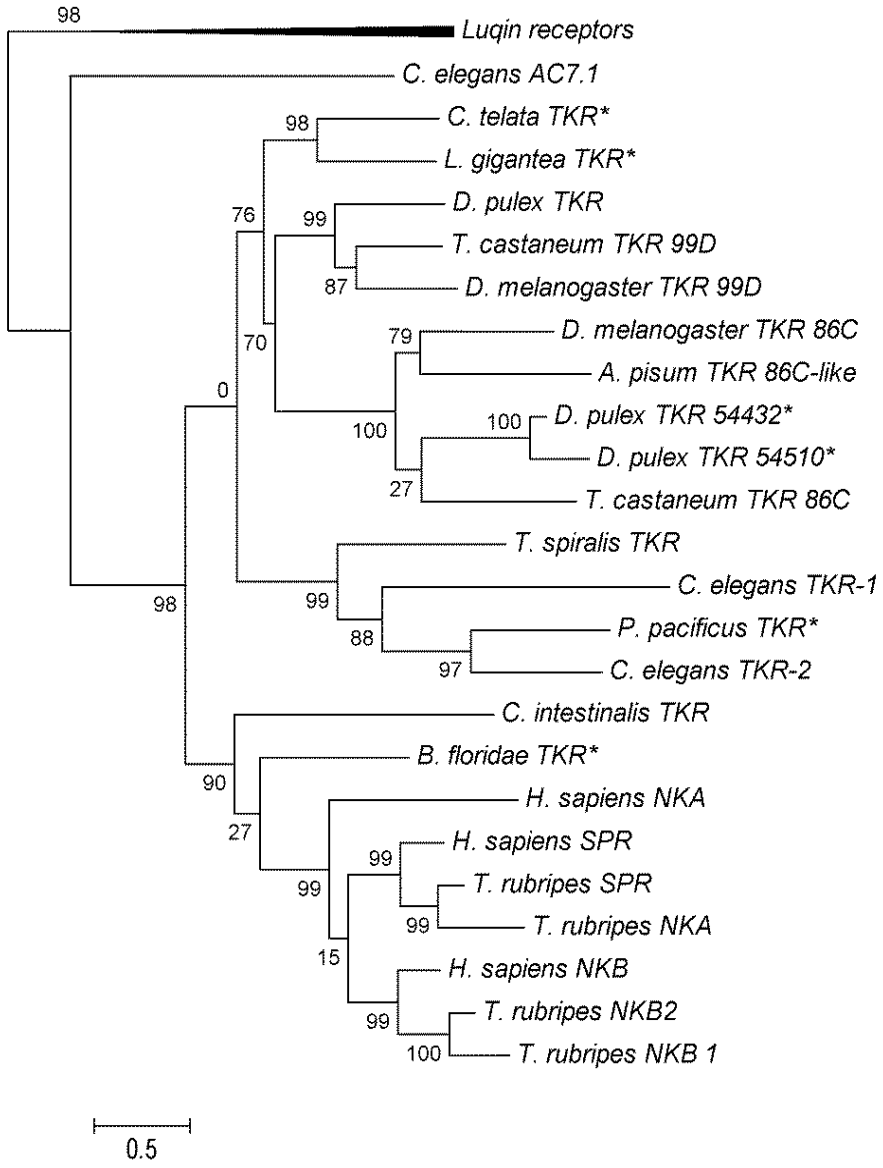

Figure 3.1. Maximum likelihood tree of tachykinin-like receptors. Branch lengths indicate the expected number of substitutions per site. Node numbers are local Shimodaira-Hasegawa test support values (%) derived from 1000 resamples. Abbreviations and accession numbers are provided in the materials and methods. Asterisks indicate sequences first reported in this thesis.

Recently the putative neuropeptide VPMMSLKGLRamide was proposed as a *C. elegans* neuropeptide that is evolutionary related to the tachykinin peptide family (Mirabeau and Joly, 2013). This neuropeptide is encoded by the T07C12.15 gene, which encodes a protein with the typical features of a neuropeptide preproprotein. Manual inspection of the T07C12.15 protein reveals that this precursor may encode for three peptides, which we annotated as tachykinin 1 (TK-1, SGPSSASEGEAYAFPGLRGLRamide), tachykinin 2a (TK-2a, VPMMSLKGLRamide) and tachykinin 2b (TK-2b, DPTYHKRVPMMSLKGLRamide), in which TK-2b is the longer variant of TK-2a (figure 3.2a). Alignment of these peptides with known vertebrate and invertebrate tachykinins indicates that these peptides share the C-terminal FXGL(R/M)G consensus sequence that is typical of the tachykinin peptide family (figure 3.2b).

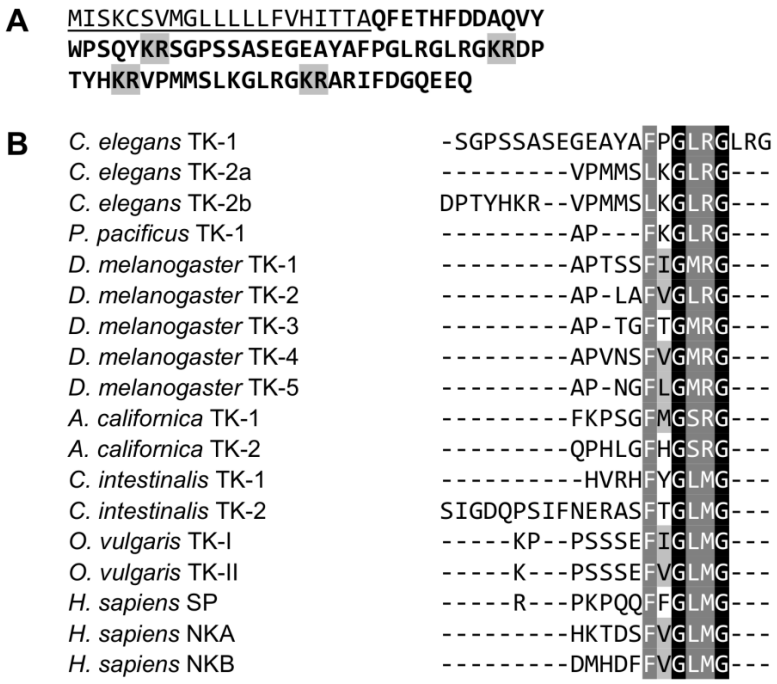

Figure 3.2 T07C12.15 encoded peptides resemble tachykinin peptides. (A) The T07C12.15 protein has the typical architecture of a neuropeptide precursor. The signal peptide is underlined and dibasic cleavage sites are indicated in grey. (B) Amino acid sequence alignment of vertebrate and invertebrate tachykinin peptides, generated using the MUSCLE alignment software (http://www.ebi.ac.uk/Tools/msa/muscle/). *In vivo* the C-terminal glycine is converted into a C-terminal amidation. Identical residues are highlighted in black, conserved residues in dark grey, similar residues in light grey.

In order to identify the cognate ligand(s) of the *C. elegans* receptors TKR-1, TKR-2 and AC7.1, a reverse pharmacology approach was used. For that, the cDNA of each receptor was cloned and expressed in CHO cells stably expressing apo-aequorin and the promiscuous $G\alpha_{16}$ subunit. These cells were challenged with a library of 265 synthetic identified and predicted *C. elegans* peptides, which included the three peptides encoded by the T07C12.15 protein (TK-1, TK-2a, and TK-2b). Several FLP peptides and the T07C12.15 peptides were able to activate both TKR-1 and TKR-2 in an initial screen. Cells transfected with the AC7.1 receptor did not respond to any of the peptides. After HPLC purification of the TKR-1 and TKR-2 activating peptides, only the T07C12.15 peptides TK-1, TK-2a and TK-2b remained capable to activate TKR-1 and TKR-2 dose-dependently with EC_{50} values in the nanomolar range (figure 3.3).

To characterize the intracellular signaling properties of TKR-2, we tested whether the receptor is capable to elicit a calcium response in CHO cells without the promiscuous $G\alpha_{16}$ subunit. A dose-dependent increase in aequorin bioluminescence was seen upon activation of the receptor by TK-1, TK-2a and TK-2b, indicating that the endogenous $G\alpha_q$ in these cells can couple this receptor to a Ca^{2+} response (figure 3.4).

To study whether TKR-2 signals through cAMP, the receptor was expressed in HEK293T cells that were co-transfected with a CRE-luciferase reporter construct. Addition of TK-1 or TK-2a at a concentration of 10 µM elicits a strong cAMP response, suggesting that the receptor can couple to $G\alpha_s$ (figure 3.5).

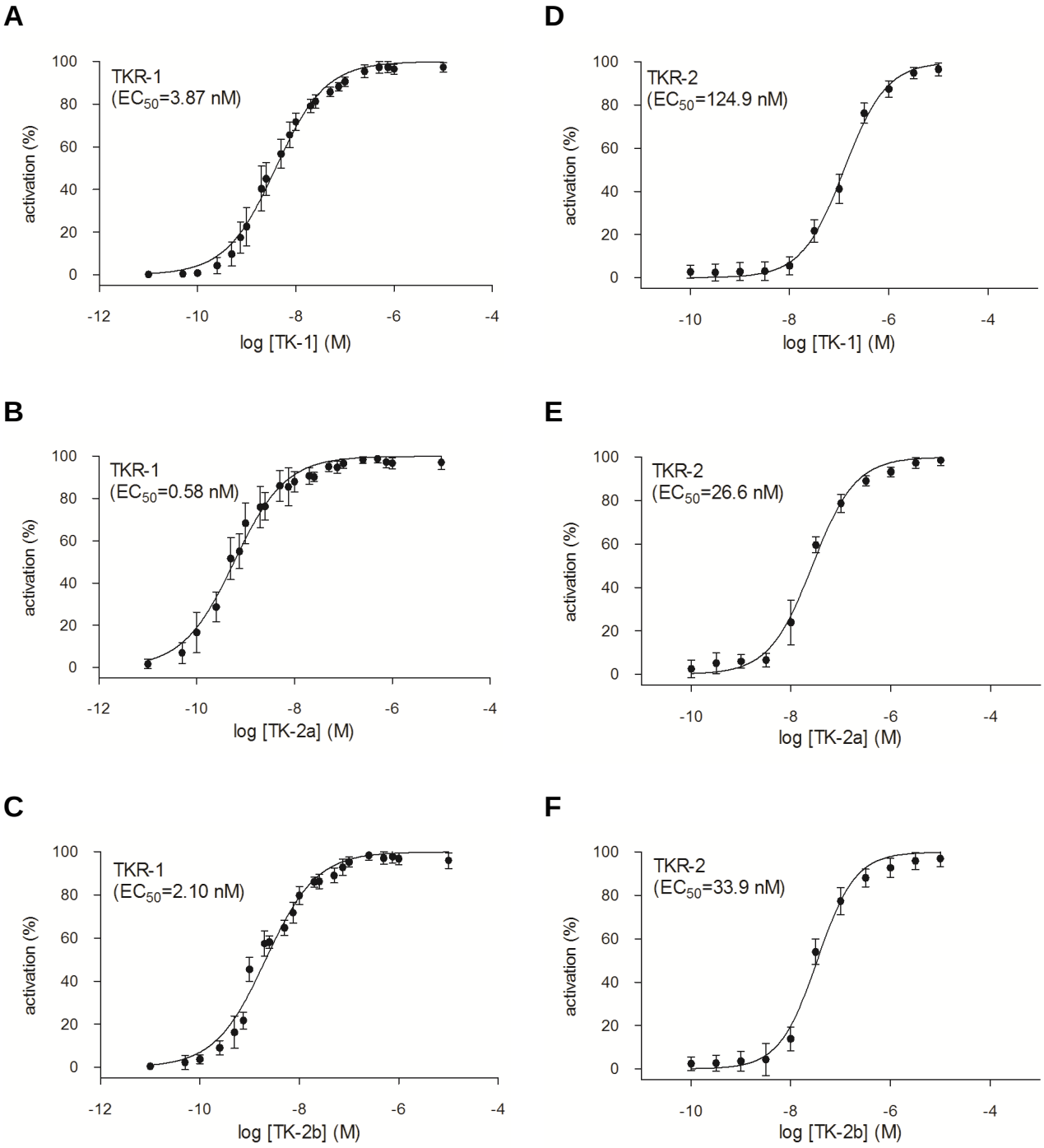

Figure 3.3 Dose-dependent calcium responses to TK-1, TK-2a and TK-2b of CHO cells expressing TKR-1 (A, B and C) or TKR-2 (D, E and F). Dose-response data are shown as relative (%) to the highest value (100% activation). Each data point represents the mean ± SEM of at least two independent experiments carried out in triplicate. EC_{50} values for each receptor-ligand couple are indicated in the top left corner. For TKR-1 Log (EC50) ± 95% CI of TK-1, TK-2a and TK-2b are -8.41 ± 0.03, -9.24 ± 0.04 and -8.68 ± 0.03, respectively. For TKR-2 Log (EC50) ± 95% CI of TK-1, TK-2a and TK-2b are -6.90 ± 0.04, -7.57 ± 0.05 and -7.47 ± 0.05, respectively.

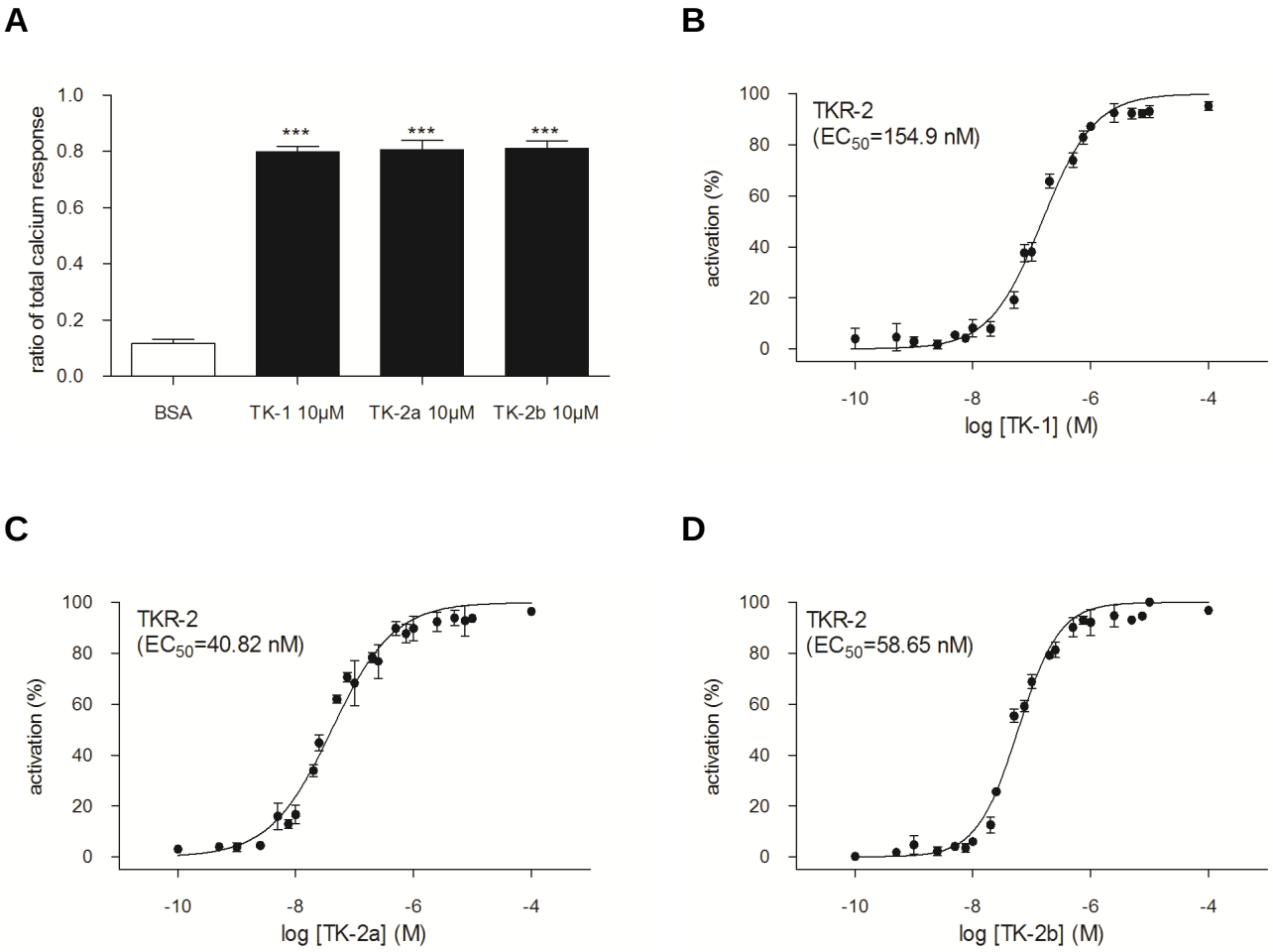

Figure 3.4 TKR-2 signaling is mediated by calcium. (A) Ratio of total calcium response and (B, C and D) dose-dependent calcium responses to TK-1, TK-2a and TK-2b of TKR-2 expressing CHO cells lacking the promiscuous $G\alpha_{16}$ Dose-response data are shown as relative (%) to the highest value (100% activation). Log (EC50) ± 95% CI of TK-1, TK-2a and TK-2b are -6.83 ± 0.05, -7.40 ± 0.07 and -7.23 ± 0.04, respectively. Each data point represents the mean ± SEM of at least two independent experiments carried out in triplicate. Statistical significance was determined using one-way ANOVA and Tukey post-hoc comparison. *** P<0.001.

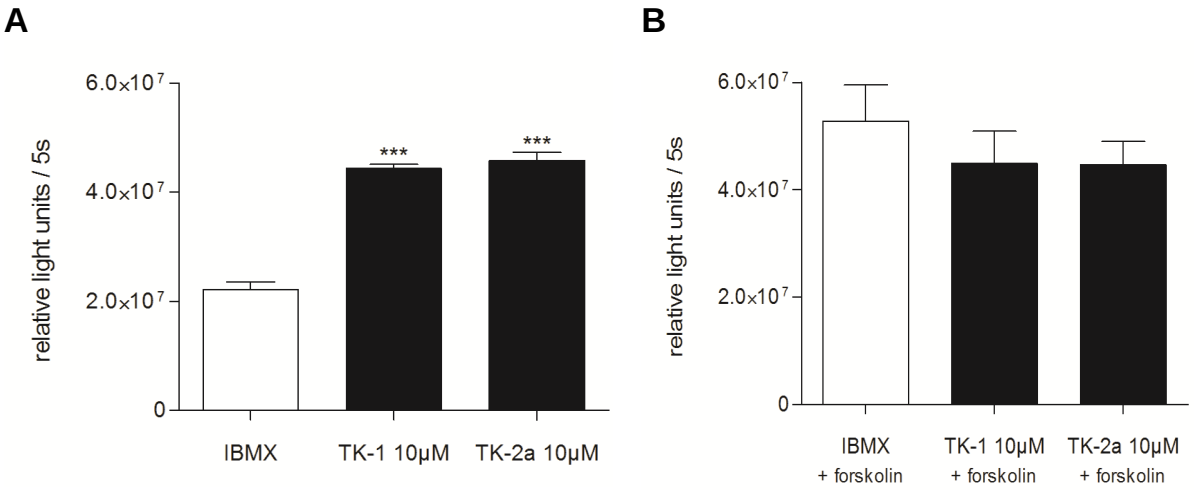

Figure 3.5 TKR-2 signaling is mediated by cAMP. CRE-luciferase reporter activity measured in TKR-2 expressing HEK293T cells when challenged with 10 µM TK-1 or TK-2a in the absence (A) or presence (B) of forskolin. Statistical significance was determined using one-way ANOVA and Tukey post-hoc comparison. *** $P<0.001$. Error bars depict SEM ($n \geq 3$).

3.3.3 Activation of the gonadotropin-releasing hormone/adipokinetic hormone like receptor GNRR-3 by RPamides

Eight GnRH/AKH-like receptors (GNRR-1 to GNRR-8) have been annotated in the genome of *C. elegans.* Phylogenetic analysis of these receptors shows that they are indeed related to the GnRH/AKH receptor family as the nematode GnRH/AKH-like receptors cluster together with other ecdysozoan GnRH/AKH receptors (figure 3.6). The nematode clade can be subdivided in two groups consisting of GNRR-1, which is located more basal to the clade node, and the other GnRH/AKH-like receptors, which appear to have diverged significantly. The more basal receptor GNRR-1, which has already been identified as a GnRH/AKH-like receptor, is the only receptor for which an activing neuropeptide ligand was identified at the start of this study (Vadakkadath Meethal *et al.*, 2006; Lindemans *et al.*, 2009b).

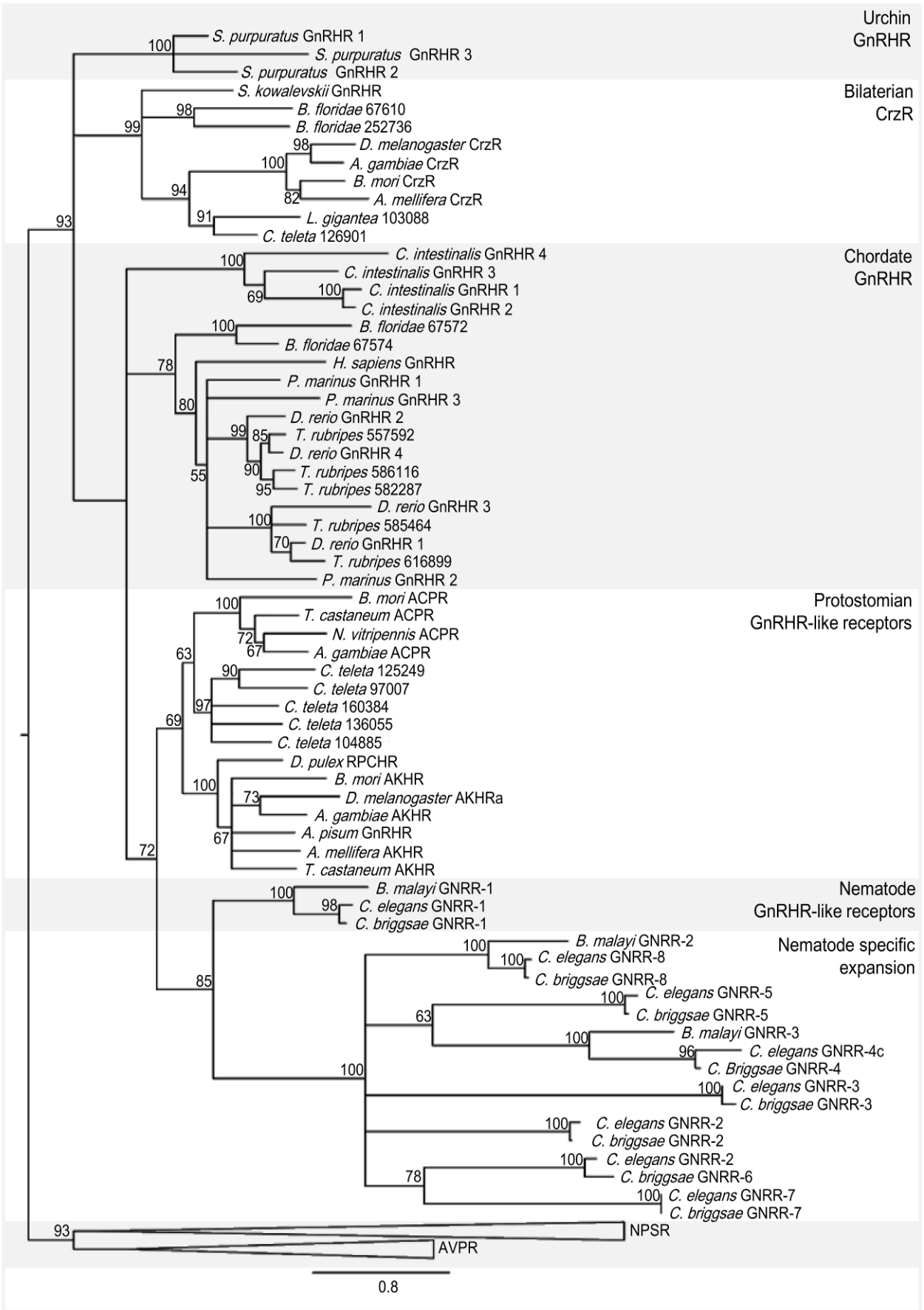
Urchin GnRHR
S. purpuratus GnRHR 1
S. purpuratus GnRHR 3
S. purpuratus GnRHR 2
Bilaterian CrzR
S. kowalevskii GnRHR
B. floridae 67610
B. floridae 252736
D. melanogaster CrzR
A. gambiae CrzR
B. mori CrzR
A. mellifera CrzR
L. gigantea 103088
C. teleta 126901
Chordate GnRHR
C. intestinalis GnRHR 4
C. intestinalis GnRHR 3
C. intestinalis GnRHR 1
C. intestinalis GnRHR 2
B. floridae 67572
B. floridae 67574
H. sapiens GnRHR
P. marinus GnRHR 1
P. marinus GnRHR 3
D. rerio GnRHR 2
T. rubripes 557592
D. rerio GnRHR 4
T. rubripes 586116
T. rubripes 582287
D. rerio GnRHR 3
T. rubripes 585464
D. rerio GnRHR 1
T. rubripes 616899
P. marinus GnRHR 2
Protostomian GnRHR-like receptors
B. mori ACPR
T. castaneum ACPR
N. vitripennis ACPR
A. gambiae ACPR
C. teleta 125249
C. teleta 97007
C. teleta 160384
C. teleta 136055
C. teleta 104885
D. pulex RPCHR
B. mori AKHR
D. melanogaster AKHRa
A. gambiae AKHR
A. pisum GnRHR
A. mellifera AKHR
T. castaneum AKHR
Nematode GnRHR-like receptors
B. malayi GNRR-1
C. elegans GNRR-1
C. briggsae GNRR-1
Nematode specific expansion
B. malayi GNRR-2
C. elegans GNRR-8
C. briggsae GNRR-8
C. elegans GNRR-5
C. briggsae GNRR-5
B. malayi GNRR-3
C. elegans GNRR-4c
C. Briggsae GNRR-4
C. elegans GNRR-3
C. briggsae GNRR-3
C. elegans GNRR-2
C. briggsae GNRR-2
C. elegans GNRR-2
C. briggsae GNRR-6
C. elegans GNRR-7
C. briggsae GNRR-7
NPSR
AVPR
0.8

◄Figure 3.6 Maximum likelihood tree of vertebrate and invertebrate GnRH/AKH receptors. Branch lengths indicate the expected number of substitutions per site. Node numbers are probabilities (%) derived from 100 non-parametric bootstraps. Abbreviations and accession numbers are provided in the materials and methods.

GNRR-1 was shown to bind the neuropeptide NLP-47, which was predicted as an GnRH/AKH-like peptide using an *in silico* motif-based approach (Lindemans *et al.*, 2009b). The more diverged GnRH/AKH-like receptors GNRR-2 to GNRR-8 are all orphan receptors. Predictions of their transmembrane topology reveal that only GNRR-2a, GNRR-3, GNRR-5, and GNRR-7 have a seven alpha-helical transmembrane topology. In order to identify their cognate ligands, the open reading frame of each receptor was cloned into the pcDNA3.1 expression vector and expressed in CHO cells stably expressing apo-aequorin and the promiscuous $G\alpha_{16}$ subunit. These cells were challenged with a *C. elegans* peptide library. Of all the tested GNRRs, only one receptor, GNRR-3, showed activity in this assay. Only the RPamides NLP-2-1 (SIALGRSGFRPamide), NLP-2-2 (SMAMGRLGLRPamide), NLP-2-3 (SMAYGRQGFRPamide), NLP-22 (SIAIGRAGFRPamide) and NLP-23-2 (SMAIGRAGMRPamide) could activate the receptor in a dose dependent manner (figure 3.7).

To characterize the intracellular signaling properties of GNRR-3, we tested whether the receptor is capable to elicit a calcium response in CHO cells without the promiscuous $G\alpha_{16}$ subunit. Addition of NLP-2-1, NLP-2-2, NLP-2-3, NLP-22 or NLP-23-2 at a concentration of 10 µM elicited a strong aequorin bioluminescence response, suggesting that the receptor can couple to $G\alpha_q$-type proteins (figure 3.7).

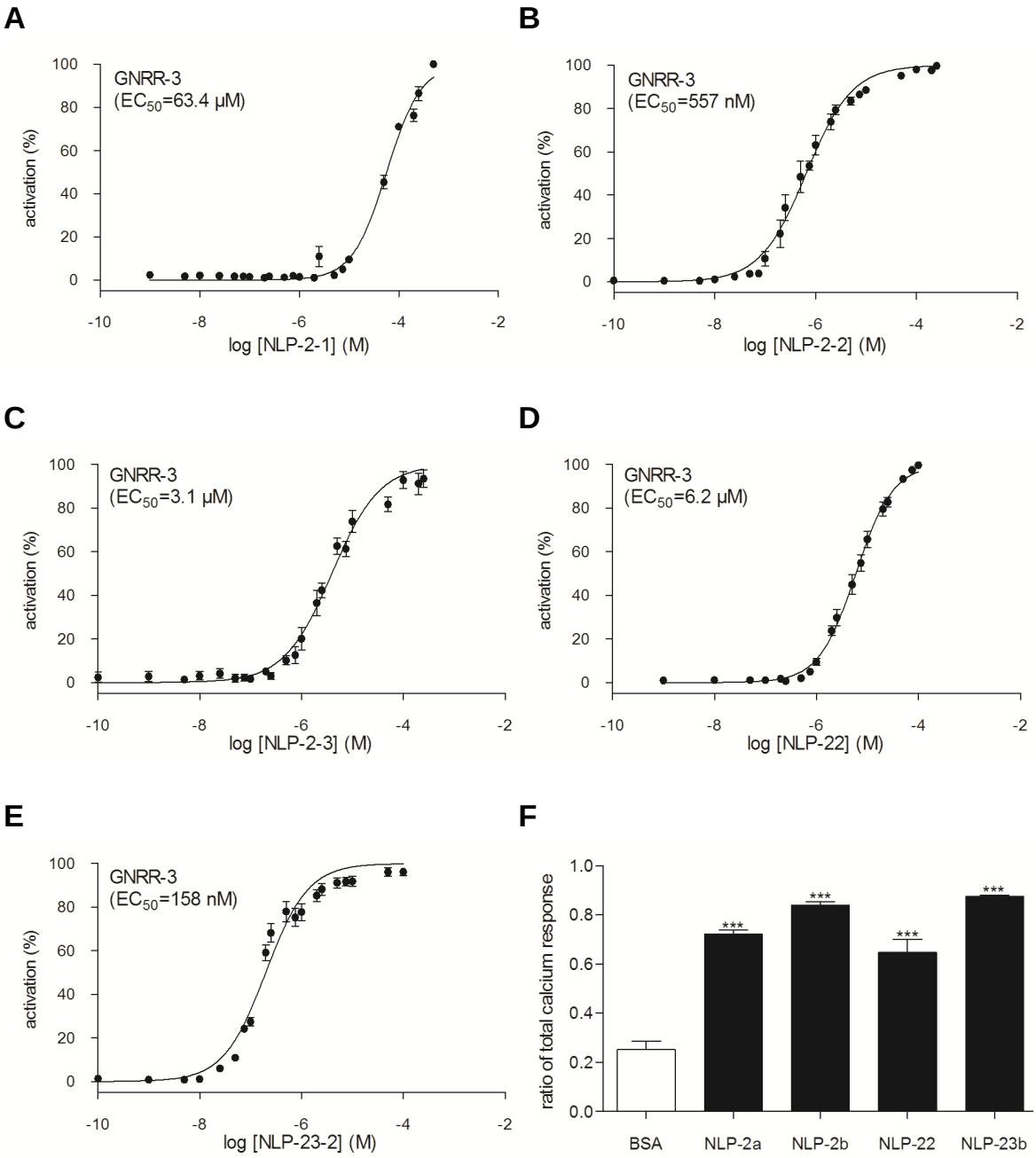

Figure 3.7 Calcium responses to NLP-2-1, NLP-2-2, NLP-2-3, NLP-22 and NLP-23-2 CHO cells expressing GNRR-3. (A-E) Dose-response data are shown as relative (%) to the highest value (100% activation). EC_{50} values for each receptor-ligand couple are indicated in the top left corner. Log (EC50) ± 95% CI of NLP-2-1, NLP-2-2, NLP-2-3, NLP-22 and NLP-23-2 are -4.25 ± 0.03, -6.19 ± 0.04, -5.40 ± 0.06, -5.23 ± 0.03 and -6.70 ± 0.05, respectively. (F) Ratio of total calcium response of CHO cells lacking the promiscuous $G\alpha_{16}$. Each data point represents the mean ± SEM of at least two independent experiments carried out in triplicate. Statistical significance was determined using one-way ANOVA and Tukey post-hoc comparison. *** P<0.001.

To study whether GNRR-3 signals through cAMP, the receptor was expressed in HEK293T cells that were co-transfected with a CRE-luciferase reporter construct. Activation of the receptor by 10 µM of NLP-2-1, NLP-2-2, NLP-22 and NLP-23-2 resulted in a cAMP response, suggesting that this receptor can couple to the endogenous $G\alpha_s$ in these cells (figure 3.8).

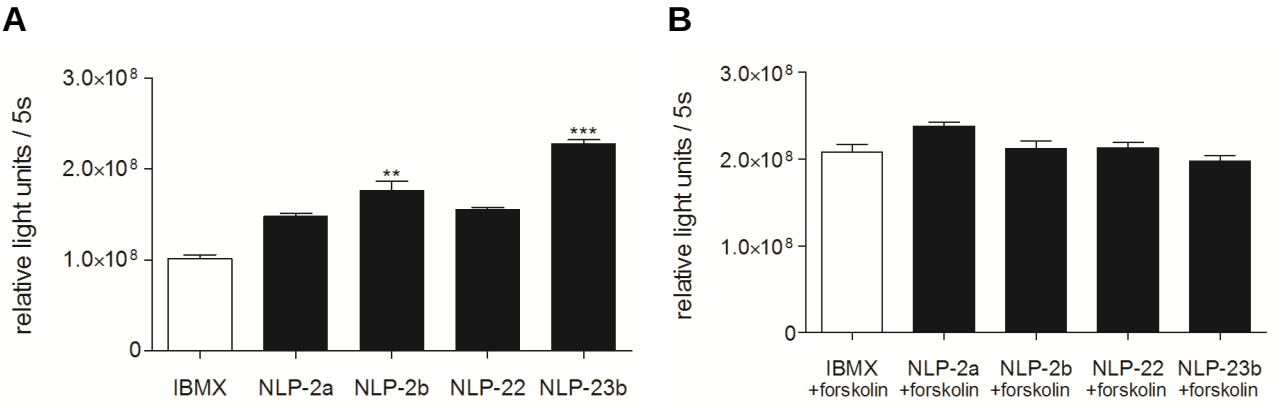

Figure 3.8 GNRR-3 signaling is mediated by cAMP. CRE-luciferase reporter activity measured in GNRR-3 expressing HEK293T cells when challenged with 10 µM NLP-2-1, NLP-2-2, NLP-22, NLP-23-2 in the absence (A) or presence (B) of forskolin. Statistical significance was determined using one-way ANOVA and Tukey post-hoc comparison. **P<0.01, *** P<0.001. Error bars depict SEM ($n \geq 3$).

To elucidate whether the GNRR-3 ligands are conserved in nematodes, a protein BLAST search was performed using NLP-2-1, NLP-2-2, NLP-2-3, NLP-22 and NLP-23-2 as query sequences. This search revealed that the neuropeptide NLP-46 is also part of this peptide family and that these neuropeptides are well conserved in nematodes (figure 3.9). This neuropeptide family is characterized by its C-terminal RPG motif in which the C-terminal glycine is most likely converted into a C-terminal amidation *in vivo*. Therefore, we classified it as the RPamide peptide family. In addition to the conserved C-terminus, the nematode RPamides have a conserved alanine at position three and a conserved glycine and arginine at position five and six, respectively.

Our phylogenetic analysis showed that GNRR-3 is related to GnRH/AKH receptors. Since neuropeptide sequences of orthologous receptors have been shown to share sequence similarities, we investigated whether these RPamides could be related to the GnRH/AKH peptide family (Janssen *et al.*, 2010; Mirabeau and Joly, 2013; Jékely, 2013). Alignment of

these RPamides and GnRH/AKH peptides reveals that nematode RPamides share the C-terminal amidation and have a conserved glycine and proline in common with several GnRH peptides (figure 3.10).

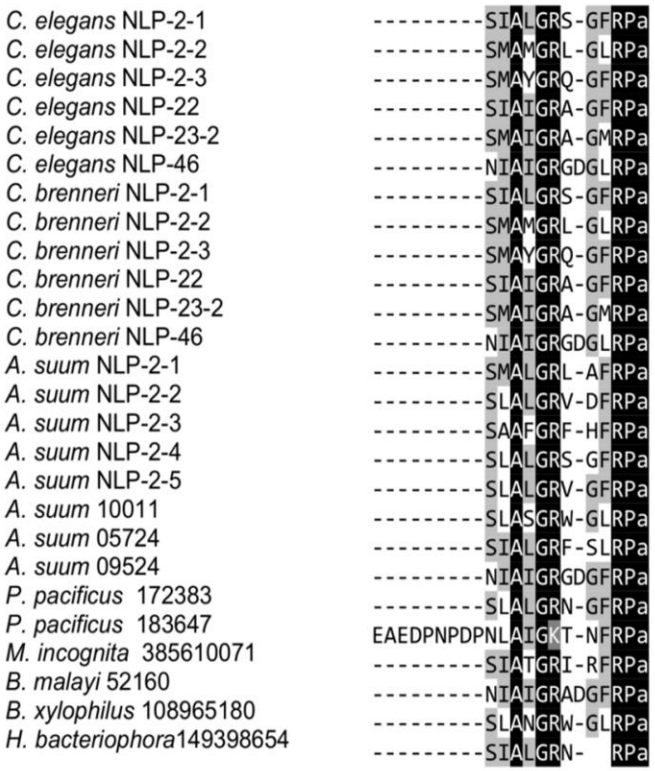

Figure 3.9 Amino acid sequence alignment of nematode RPamides. Neuropeptide sequences were retrieved through a protein BLAST search restricted to nematodes using *C. elegans* NLP-2-1, NLP-2-2, NLP-2-3, NLP-22 and NLP-23-2 as a query. Sequence alignment was generated using the MUSCLE algorithm. Identical residues are depicted in black, highly conserved residues are depicted in grey.

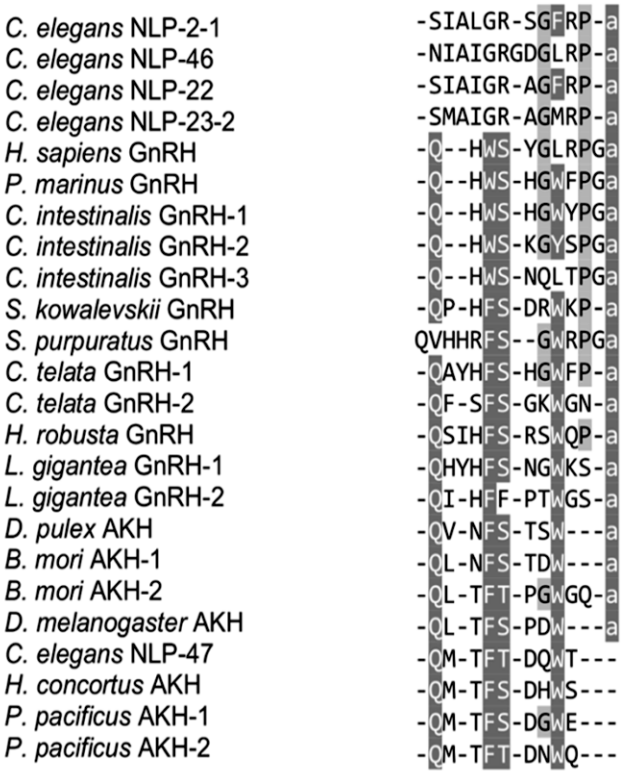

Figure 3.10 Amino acid sequence alignment of RPamides and GnRH/AKH peptides. Neuropeptide sequences were collected from literature (Lindemans *et al.*, 2011; Roch *et al.*, 2011; Mirabeau and Joly, 2013). Sequence alignment was generated using the MUSCLE algorithm. Identical residues are depicted in black, highly conserved residues are depicted in grey.

3.3.4 Deorphanization of the neuromedin U-like receptor NMUR-1

In 1985, Minamino and colleagues purified two neuropeptides, NMU-8 (YFLFRPRNamide) and NMU-25 (FKVDEEFQGPIVSQNRRYFLFRPRNamide), from porcine spinal cord which exerted potent contractile activity on the uterus (Minamino *et al.*, 1985). Subsequently several peptides sharing a conserved C-teminal FRPRNamide were isolated from several other vertebrate species which were all designated as NMU peptides (Brighton *et al.*, 2004; Malendowicz *et al.*, 2012). NMU peptides are involved in a broad range of functions such as the regulation of smooth muscle contraction, feeding and energy homeostasis, ion transport and stress response (Brighton *et al.*, 2004; Malendowicz *et al.*, 2012).

Insect pyrokinins (PK) share sequence resemblance in their C-terminal pentapeptide to these vertebrate NMU peptides (figure 3.11b). Insect PK peptides are encoded by the *capability (capa)* and *hugin* genes. CAPA encodes three peptides: CAPA-periviscerokinin (PVK)-1, CAPA-PVK-2 and CAPA-PK. HUGIN encodes two peptides hugin-PK and hugin-gamma. CAPA-PVK peptides share a C-terminal LXXFPRVamide motif, while the PK peptides share a C-terminal FXPRLamide motif (Predel and Wegener, 2006; Altstein *et al.*, 2013). Insect pyrokinins seem to be mainly involved in the hormonal regulation of diuresis and the modulation of muscle contractions (Predel and Wegener, 2006).

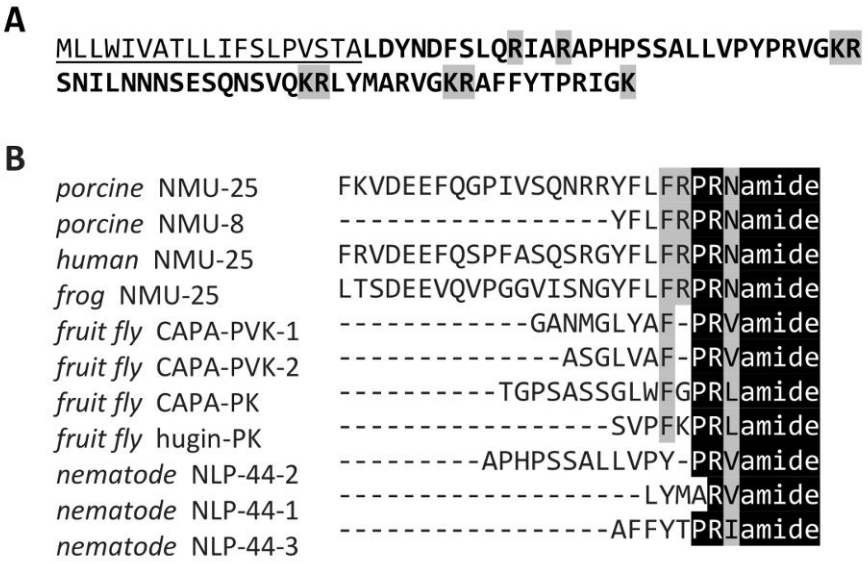

Figure 3.11 NLP-44 encoded peptides resemble tachykinin peptides. (A) The NLP-44 protein has the typical architecture of a neuropeptide precursor. The signal peptide is underlined and dibasic cleavage sites are indicated in grey. (B) Alignment of vertebrate NMU and invertebrate PK peptides. Alignment was generated using the MUSCLE alignment software (http://www.ebi.ac.uk/Tools/msa/muscle/). Sequences are aligned for Porcine (*Sus scrofa)* (Minamino *et al.*, 1985), Human (*Homo* sapiens) (Austin *et al.*, 1995),Frog (*Rana temporaria)* (Domin *et al.*, 1989), fruit fly (*Drosophila melanogaster)* (Kean *et al.*, 2002; Meng *et al.*, 2002) and nematode (*Caenorhabditis elegans*) (Lindemans *et al.*, 2009a) NMU/PK peptides. Identical residues are highlighted in black, conserved residues in dark grey, similar residues in light grey.

Interestingly, insect PK receptors share high similarity with mammalian NMU receptors, indicating that these neuropeptide systems could have a common ancestral origin (Park *et*

al., 2002). This hypothesis was further substantiated by the discovery of a NMU/PK-like system in *C. elegans* (Lindemans *et al.*, 2009a). Four NMUR homologs are annotated in the *C. elegans* genome. Lindemans and colleagues were able to deorphanize one of these receptor, NMUR-2, based on an *in silico* search for *C. elegans* homologs of the *Drosophila* pyrokinin peptides. This revealed three putative PRXamide peptides, NLP-44-1 (APHPSSALLVPYPRVamide), NLP-44-2 (LYMARVamide) and NLP-44-3 (AFFYTPRIamide), all encoded by the same peptide precursor gene *nlp-44* (figure 3.11a). Only one of these peptides, NLP-44-3, could activate NMUR-2 (Lindemans *et al.*, 2009a). However, the protein sequence resemblance of *nlp-44* to insect CAPA precursors was striking. NLP-44-1 and NLP-44-2 display a clear sequence similarity with insect CAPA-PVKs, whereas NLP-44-3 is similar to CAPA-PK (Lindemans *et al.*, 2009a).

Using a library-based reverse pharmacology approach, we aimed to identify the activating ligands of another *C. elegans* NMU-like receptor, NMUR-1. The open reading frame of NMUR-1 was cloned into the mammalian expression vector pcDNA3.1. The receptor construct was expressed in CHO cells stably expressing apo-aequorin and the promiscuous $G\alpha_{16}$ subunit and these cells were challenged with a *C. elegans* peptide library. NLP-44-1 and NLP-44-3 were able to activate the receptor dose-dependently with an EC_{50} value in the nanomolar range (figure 2.11). When the receptor construct was expressed in CHO cells lacking the promiscuous $G\alpha_{16}$, a similar response was measured, indicating that NMUR-1 can signal through the release of calcium (figure 2.12).

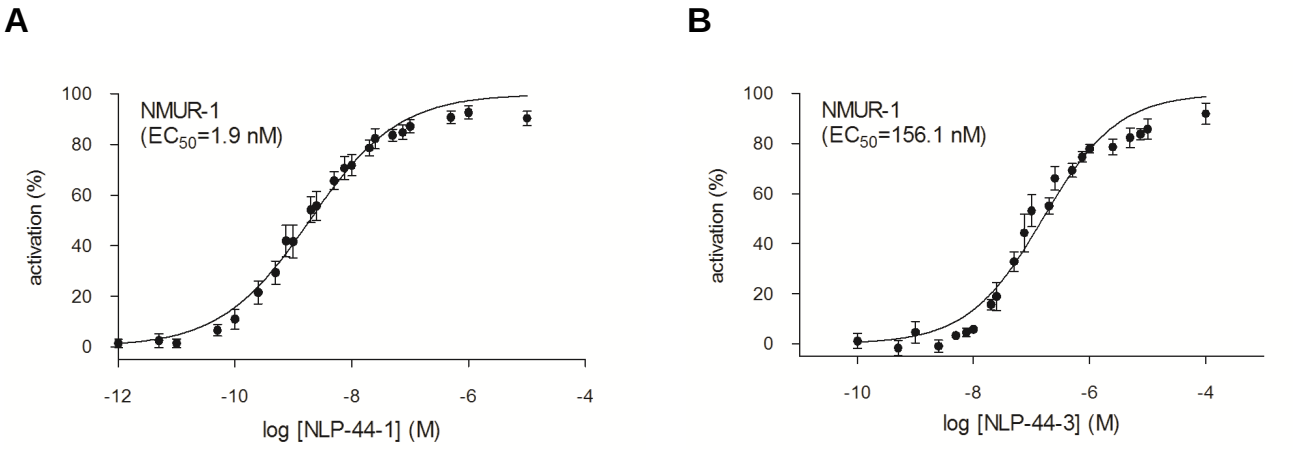

Figure 2.11 Dose-dependent calcium responses to NLP-44-1 and NLP-44-3 of CHO cells expressing NMUR-1. Dose-response data are shown as relative (%) to the highest value (100% activation). Each data point represents the mean ± SEM of at least two independent experiments carried out in triplicate. EC_{50} values for each receptor-ligand couple are indicated in the top left corner. Log (EC50) ± 95% CI of NLP-44-1 and NLP-44-3 are -8.72 ± 0.08 and -6.81 ± 0.07, respectively.

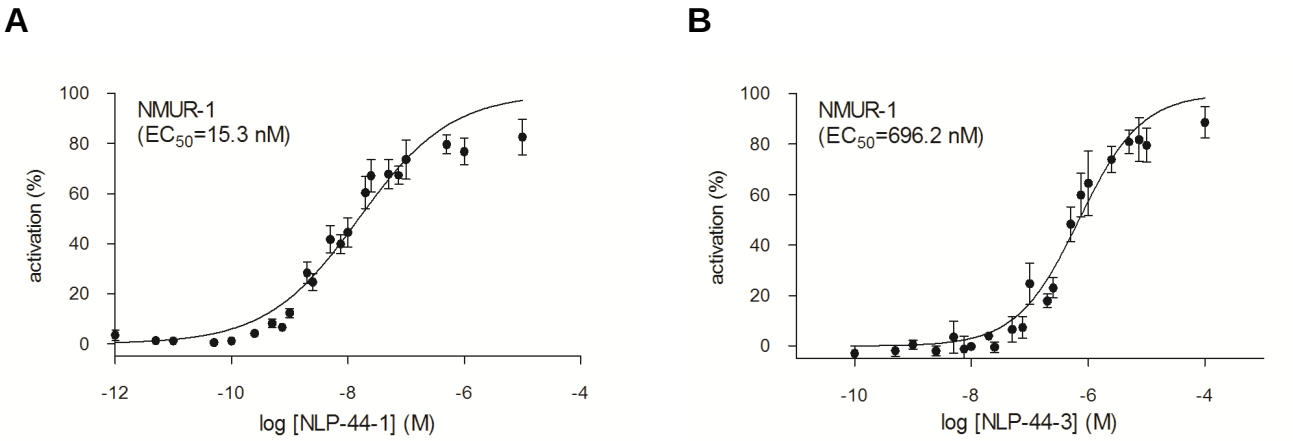

Figure 2.12 NMUR-1 signaling is mediated by calcium. Dose-dependent calcium responses to (A) NLP-44-1 and (B) NLP-44-3 of NMUR-1 expressing CHO cells lacking the promiscuous $G\alpha_{16}$. Dose-response data are shown as relative (%) to the highest value (100% activation). Each data point represents the mean ± SEM of at least two independent experiments carried out in triplicate. Log (EC50) ± 95% CI of NLP-44-1 and NLP-44-3 are -7.813 ± 0.10 and -6.16 ± 0.10, respectively.

3.4 Discussion and conclusion

3.4.1 MEME/MAST prediction of *C. elegans* neuropeptide GPCRs

In the past several predictions have been made about the amount of neuropeptide GPCRs encoded in the genome of *C. elegans.* Along with the publication of the *C. elegans* genome initially 54 neuropeptide GPCRs were predicted based on sequence similarities to vertebrate neuropeptide GPCRs (Bargmann, 1998). Subsequent estimates predicted 38 (Keating *et al.*, 2003) to 129 (Fredriksson and Schiöth, 2005) *C. elegans* neuropeptide GPCRs using a phylogenetic strategy. Recently, Janssen and colleagues applied the MEME/MAST tool to predict *C. elegans* neuropeptide GPCR using deorphanized *C. elegans* GPCRs as a template (Janssen *et al.*, 2010). Doing so, 125 neuropeptide GPCRs were predicted, of which several have since then been deorphanized (Janssen *et al.*, 2008a; Janssen *et al.*, 2008b; Lindemans *et al.*, 2009b; Lindemans *et al.*, 2009a; Beets *et al.*, 2012). In order to obtain an accurate overview of the *C. elegans* neuropeptide GPCRs, we decided to repeat the MEME/MAST analysis using an updated training set, containing all 23 neuropeptide GPCRs that were deorphanized at the start of this project.

After manual curation and comparison to previous predictions we obtained a list of 129 potential *C. elegans* neuropeptide GPCRs. All predicted neuropeptide GPCRs could be grouped in the rhodopsin and secretin families according to the GRAFS classification system (Schiöth and Fredriksson, 2005). Rhodopsin GPCRs were subdivided based on their resemblance to insect and mammalian neuropeptide GPCRs according to the classification adapted by Altun (Altun, 2011). The neuropeptide Y (NPY)/RFamide-like receptor family, containing 41 receptors, represents the best characterized group. Twelve of its representatives have been deorphanized and all are activated by FMRFamide like peptides (NPR-1, NPR-3, NPR-4, NPR-5a/b, NPR-6, NPR-10a/b, NPR-11, FRPR-3, and FRPR-18a/b). Their corresponding signaling pathways are involved in a multitude of functions such as locomotion, feeding, energy metabolism, and reproduction (de Bono and Bargmann, 1998; Keating *et al.*, 2003; Lowery *et al.*, 2003; Kubiak *et al.*, 2003a; Rogers *et al.*, 2003; Mertens *et al.*, 2004a; Kubiak *et al.*, 2008; Cohen *et al.*, 2009; Chalasani *et al.*, 2010). So far, none of the 24 receptors belonging to the somatostatin and galanin-like receptor group have been deorphanized. Only NPR-9 has shown to be involved in local search behavior and

fat accumulation (Bendena *et al.*, 2008). For the remaining receptors only RNAi phenotypes with respect to locomotion and fat metabolism have been observed for this poorly studied group (Keating *et al.*, 2003; Ashrafi *et al.*, 2003). The tachykinin (neurokinin)-like receptor group contains 12 receptors. Mertens *et al*. (2006) deorphanized one of these receptors, namely NPR-22a. This GPCR was activated by a handful of FaRPs. The cholecystokinin (CCK)/gastrin-like receptor and gonadotropin releasing hormone (GnRH), oxytocin (OT), vasopressin (VP)-like receptor groups contain 3 and 14 receptors, respectively. Deorphanization of CKR-2e/f GNRR-1a and NTR-1 supports the theory of receptor-ligand coevolution (Janssen *et al.*, 2010). Although no clear CCK or sulfakinin orthologs could be identified through *in silico* searches, library-based screening led to the identification of NLP-12a and NLP-12b as the endogenous ligands of CKR-2e/f. Alignment of these peptides to vertebrate CCK/gastrin hormones and arthropod sulfakinins revealed their similarity. The endogenous ligand of GNRR-1a was found using an *in silico* approach. GNRR-1a and its ligand, NLP-47, are both involved in reproduction as shown by RNAi experiments (Lindemans et al., 2009a). The VP/OT-like receptor NTR-1 has only recently been identified and deorphanized. The VP/OT-related signaling system is involved in gustatory associative learning and male reproduction (Beets et al., 2012; Garrison et al., 2012). The group of neurotensin, NMU, growth hormone secretagogue, and thyrotropin releasing hormone (TRH)-like receptors contains 17 receptors, of which three have been deorphanized: NMUR-2 and EGL-6a/b. Only the EGL-6a/b receptors are functionally characterized and they proved to be involved in the regulation of egg-laying (Ringstad and Horvitz, 2008). The secretin family of GPCRs contains nine receptors. Of these, the three pigment dispersing factor (PDF) GPCRs are deorphanized and play a role in locomotion, sleep, egg-laying and male mating (Janssen *et al.*, 2008a; Meelkop *et al.*, 2012; Barrios *et al.*, 2013; Choi *et al.*, 2013; Flavell *et al.*, 2013).

3.4.2 Identification of a tachykinin-related signaling system in *C. elegans*

The first tachykinin peptide was discovered by Von Euler and Gaddum in 1931 (Von Euler and Gaddum, 1931). They identified a substance in horse brain and intestine extracts that induced contraction of isolated rabbit jejunum and a fall in blood pressure of anesthetized rabbits. Forty years later, Chang and colleagues identified the amino acid sequence of this peptide called substance P (Von Euler and Gaddum, 1931; Chang *et al.*, 1971). Since the

discovery of substance P, several other peptides have been identified in vertebrates that share sequence similarities to substance P and this group of structurally related peptides is called the tachykinin peptide family. Vertebrate tachykinins all share the C-terminal FXGLMamide in which X represents a variable hydrophobic amino acid (Steinhoff *et al.*, 2014). The first invertebrate tachykinin peptides were identified by Schoofs and colleagues from brain extracts from the migratory locust, *Locusta migratoria*. These peptides were myostimulating. They designated these peptides as locustatachykinins because of their sequence resemblance to vertebrate tachykinins and suggested they could be evolutionary related (Schoofs *et al.*, 1990b; Schoofs *et al.*, 1990a). The identification of several invertebrate tachykinin peptides including in other insects, mollusks and annelids, substantiated this hypothesis. Today the conservation of tachykinin peptides in vertebrates and invertebrates seems to be generally accepted. However, in nematodes, no tachykinin system was identified at the start of this study.

Conserved neuropeptides and receptors can be identified based on sequence similarities and several receptor-ligand couples have successfully been identified in *C. elegans* using this phylogenetic approach (Lindemans *et al.*, 2009b; Lindemans *et al.*, 2009a; Janssen *et al.*, 2010; Beets *et al.*, 2012; Mirabeau and Joly, 2013; Jékely, 2013). A protein BLAST search and phylogenetic analysis indicated that the *C. elegans* genome encodes two tachykinin receptors, TKR-1 and TKR-2. Using a reverse pharmacology strategy, we showed that the *in silico* predicted *C. elegans* tachykinins, encoded by T07C12.15, are able to activate both TKR-1 and TKR-2 dose-dependently with EC_{50} values in the nanomolar range. Besides TKR-1 and TKR-2, a third receptor, AC7.1, was recently annotated as TKR-3. Therefore we tested this receptor in the reverse pharmacology assay as well. No activation was seen upon challenging of AC7.1 transfected cells with the compound library. These results were in line with our phylogenetic analysis, which indicates that AC7.1 does not belong to the TKR family. Characterization of the downstream signaling pathway indicates that TKR-2 can signal through both calcium and cAMP messengers. The identification of this tachykinin signaling system indicates the conservation of this system in the entire ecdysozoan clade. These results provide the possibility to investigate the fundamental molecular pathways of this complex neuropeptide system in *C. elegans*.

3.4.3 Activation of the gonadotropin-releasing hormone/adipokinetic hormone like receptor GNRR-3 by RPamides

The *C. elegans* genome encodes eight GnRH/AKH-like receptors. Using a reverse pharmacology approach we showed that one of these receptors, GNRR-3, is activated dose-dependently by the RPamides NLP-2-1, NLP-2-2, NLP-2-3, NLP-22 and NLP-23-2. Characterization of the downstream signaling pathway indicates that GNRR-3 can signal through both calcium and cAMP. The neuropeptides encoded by *nlp-2*, *nlp-22* and *nlp-23* have been identified based on structural and sequence resemblance of their precursor with known peptide genes (Nathoo *et al.*, 2001). Previous studies also suggested homology of *C. elegans* RPamides with molluscan myomodulins. Both peptide families have N-terminal sequences in common (Nathoo *et al.*, 2001), but myomodulins lack the conserved C-terminal motif thought to be important for the functional activity of nematode RPamides (Nelson *et al.*, 2013). The *nlp-2*, *nlp-22* and *nlp-23* genes are clustered in close apposition on the X chromosome, suggesting that they arose from tandem gene duplications. Based on sequence similarities, we found that these peptides belong to a peptide family which is highly conserved in nematodes, which we annotated the RPamides.

Phylogenetic analysis of the *C. elegans* GnRH/AKH-like receptors indicates that these receptors arose from nematode-specific duplications, and shows high divergence of these receptors compared to other GnRH/AKH receptors. Gene duplication is a common feature in *C. elegans* and in line with the receptor-ligand coevolution theory one would expect that their corresponding ligands have diverged as well (Woollard, 2005; Mirabeau and Joly, 2013). Corroborating this, GNRR-8 is suggested to act as a promiscuous dimerization partner for GPCRs binding a diverse family of small molecule ascarosides (Park *et al.*, 2012). The high divergence of GNRR-3 may explain the low degree of sequence similarity between nematode RPamides and GnRH/AKH peptide sequences, which is restricted to the C-terminal amidation and a conserved glycine and proline, as a consequence of neuropeptide-receptor co-evolution. Alternatively we cannot exclude that the RPamide peptide family is nematode specific and that sequence resemblance is due to convergent evolution, giving these peptides the potency to activate GnRH/AKH-like receptors.

3.4.4 Deorphanization of the neuromedin U-like receptor NMUR-1

We identified NMUR-1 as a novel NMUR-like receptor, which is activated by the *C. elegans* CAPA peptides NLP-44-1 and NLP-44-3. So far, NMUR-1 is the only *C. elegans* NMUR-like receptor with a characterized function. Maier and colleagues showed that NMUR-1 affects food type dependent ageing (Maier *et al.*, 2010). Wild-type *C. elegans* have altered lifespan on different *E. coli* strains, living longer on *E. coli* HT115 than on *E. coli* OP50. In order to identify the pathway underlying this phenotype, Maier and colleagues screened all available chemoreceptor, neuropeptide and neuropeptide GPCR mutants on their influence of this food type dependent lifespan. The *nmur-1 (ok1387)* deletion mutant did no longer showed food type dependent lifespan. Rescue of *nmur-1 (ok1387)* by expression of the wild-type *nmur-1* allele indicates that this phenotype is due to the *nmur-1* deletion and not caused by background mutations (Maier *et al.*, 2010). In contrast to NMUR-1, NMUR-2, which is activated by NLP-44-3, does not affect food type dependent ageing (Maier *et al.*, 2010). Therefore it would be interesting to investigate if NLP-44-1 and/or NLP-44-3 peptide signaling is involved in this process.

The identification of the *Drosophila* and *C. elegans* PK peptides which activate NMUR-like receptors, suggests that vertebrate NMU and ecdysozoan PK systems share a common origin (Melcher and Pankratz, 2005b; Lindemans *et al.*, 2009a; Mirabeau and Joly, 2013). Both insect and vertebrate NMUR signaling pathways are implicated in food-related functions (Brighton *et al.*, 2004; Predel and Wegener, 2006). However, at present, it is unknown whether insect or vertebrate NMUR signaling pathways are involved in the regulation of lifespan. This would be an interesting research question to investigate in the future.

3.4.5 Conclusion

In this chapter four orphan receptors related to tachykinin, GnRH/AKH and NMU peptide systems were deorphanized using a combined reverse pharmacology approach.

The identification of a tachykinin signaling system in *C. elegans* further supports the theory that tachykinin systems are evolutionary conserved and were already established prior to the divergence of protostomes and deuterostomes. This emphasizes the importance of these

systems in both vertebrates and invertebrates. The identification of NLP-44-1 and NLP-44-3 as ligands of NMUR-1 also represents a fine example of receptor-ligand coevolution.

Furthermore, we identified five RPamides as activating ligands of the GnRH/AKH-like receptor GNRR-3. Our results suggest that the *C. elegans* GnRH/AKH receptor family arose from nematode-specific duplications and that this receptor clade has diverged substantially. In line with this, we showed that the sequence resemblance of their putative cognate ligands with the GnRH/AKH peptide family is limited.

The identification of these receptor-ligand couples is an important step in the elucidation of the function of these neuropeptide systems. In this thesis, we focused on the functional characterization of the GNRR-3 (chapter 4) and TKR-1/2 (chapter 5) neuropeptide systems, for which at the start of this project no phenotype had yet been investigated in *C. elegans*.

Chapter 4. NLP-2/GNRR-3 signaling promotes arousal during lethargus in *C. elegans*

This chapter has partially been published in:

Frooninckx, L., Mirabeau, O., Nelson, M. D., Wouters, A., Temmerman, L., Raizen, D. M., Schoofs, L., Beets, L. Discovery of a wake-promoting neuropeptide pathway in *C. elegans*. Submitted for publication in *eLife*

4.1 Introduction

Mammalian GnRH (GnRH1) is one of the most important hormones involved in the signal transduction pathway that regulates reproduction. The hypothalamus secretes GnRH1 that activates the GnRH1 receptor in the pituitary gland. This receptor then activates a signaling pathway that causes the release of the gonadotropins, namely follicle stimulating hormone (FSH) and luteinizing hormone (LH). These gonadotropins in turn act on the gonads leading to their development and the production of sex steroids (Kah *et al.*, 2007). Besides GnRH1, most mammals also posses a second GnRH peptide termed GnRH2. Some teleost fish poses a third form of GnRH, which is referred to as GnRH3 (figure 4.1). Phylogenetic analysis of the peptide precursors of all 3 forms indicate that they arose early in the vertebrate lineage before the divergence of teleosts and tetrapods, where some forms subsequently got lost throughout evolution: in most mammalian species both the GnRH2 and GnRH3 gene has been deleted or silenced, while some teleosts seem to have lost the GnRH1 or GnRH3 gene (Okubo and Nagahama, 2008). The duplicated GnRH genes have undergone subfunctionalization during the evolution of vertebrates. GnRH1 has become the major stimulator of gonadotropins, whereas GnRH2 and GnRH3 seem to function as neuromodulators in most species.

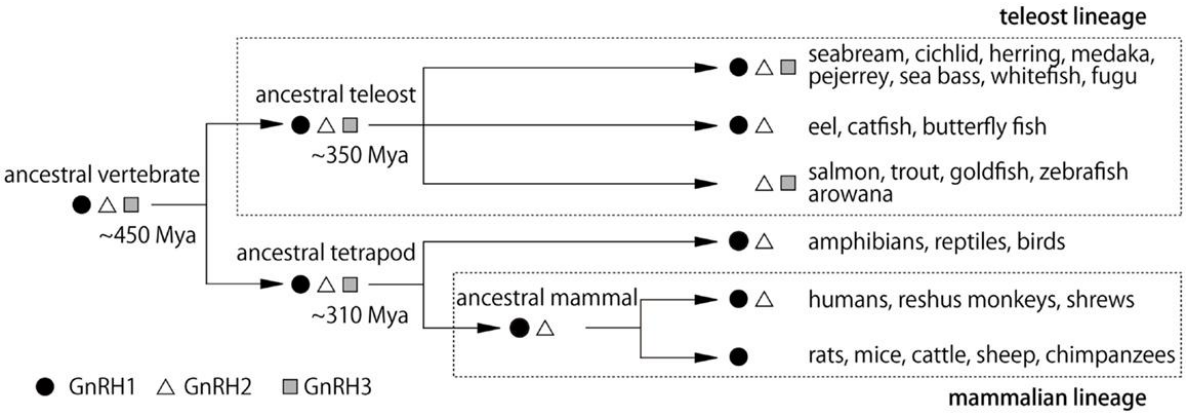

Figure 4.1 Hypothetical scheme for GnRH evolution in vertebrates (adapted from Okubo and Nagahama, 2008).

It is interesting to note that in non-mammalian vertebrates, the amino acid sequence of GnRH1 is greatly diversified among species, whereas that of GnRH2 and GnRH3 is completely unchanged (Okubo and Nagahama, 2008). Besides vertebrates, GnRH-like

peptides and peptide precursors have been identified in other deuterostomes (tunicates and echinoderms) as well (Adams *et al.*, 2003; Roch *et al.*, 2011).

In protostomes, GnRH-like peptides and peptide precursors were initially only identified in Lophotrochozoa (Iwakoshi *et al.*, 2002; Zhang *et al.*, 2008; Tsai and Zhang, 2008; Roch *et al.*, 2011). Because insect GnRH-like receptors were shown to be activated by peptides of the AKH-like family, which do not show obvious sequence similarity to the known deuterostomian GnRHs, Tsai and Zhang proposed that deuterostomian and protostomian GnRHs likely share a common ancestor, but that they were lost in Ecdysozoa and were preserved in Lophotrochozoa. According to their view, GnRH-like receptors had been retained in Ecdysozoa but had recruited other ligands to bind. A major breakthrough into the common evolution of AKH and GnRH peptides came with the identification of the AKH/GnRH-like neuropeptide NLP-47 in *C. elegans*, which resembles both insect AKHs and chordate GnRHs, and was shown to activate the *C. elegans* GnRH/AKH-like receptor GNRR-1 (Lindemans *et al.*, 2009b). Today, phylogenetic analysis of vertebrate GnRH and invertebrate AKH peptides and their receptors substantiate the theory that these signaling systems evolved from the same ancestral neuropeptide system (Lindemans *et al.*, 2011; Roch *et al.*, 2011; Mirabeau and Joly, 2013).

In contrast to the pronounced role for chordate GnRH signaling in reproduction, insect AKH signaling seems to be primarily involved in the regulation of energy metabolism, more particularly in the mobilization of energy during flight and locomotion (Gäde, 2009). However, Lindemans and colleagues showed that in *C. elegans*, RNAi knockdown of GNRR-1 and NLP-47 resulted in a delay in egg laying and a decrease in total brood size. This suggests that the NLP-47/GNRR-1 system could play a conserved role in reproduction in *C. elegans* (Lindemans *et al.*, 2009b).

According to our MEME/MAST prediction and phylogenetic analysis, the *C. elegans* genome encodes eight GNRH/AKH-like receptors (GNRR-1 to GNRR-8). Using a combined reverse pharmacology assay we were able to identify five RPamides (NLP-2a, NLP-2b, NLP-22 and NLP-23b) as peptide ligands of GNRR-3 (§ chapter 3).

One of the identified ligands, NLP-22, was recently reported to regulate lethargus, a sleep-like state in *C. elegans* (§ 2.1). Nelson and colleagues showed that mRNA levels of the neuropeptide NLP-22 has a cyclical expression in synchrony with lethargus and is regulated by the PERIOD homolog LIN-42. Overexpression of *nlp-22* induced quiescence that resembles all behavioral aspects of lethargus quiescence, indicating that NLP-22 plays a profound role in lethargus (Nelson *et al.*, 2013).

As the GnRH/AKH system is evolutionary well conserved, it is conceivable that some of the functions described in other animals could be retained in *C. elegans* as well. Therefore, we first investigated if the identified GnRH/AKH receptors are involved in hermaphrodite reproduction or lipid storage, by assessing these processes in *gnrr* deletion mutants. Next, we investigated a role for the GNRR-3 receptor and its RPamide ligands in lethargus, based on the somnogenic function of the GNRR-3 ligand NLP-22.

4.2 Material and methods

4.2.1 Strains and cultivation

Strains were cultured at 20°C under standard conditions on NGM agar plates seeded with *E. coli* OP50 (Brenner, 1974). Worms were cultivated twice a week and always grown in the presence of abundant food. As our wild type strain, we used N2 Bristol.

The following mutant strains were used (x times crossed to N2): RB509 *[gnrr-1 (ok238) I]*, LSC504 *[gnrr-2 (ok3618) V]*, LSC503 *[gnrr-2 (tm4867) V]*, FX04152 *[gnrr-3 (tm4152) X]*, LSC505 *[gnrr-3 (tm4152) X]* (x2), LSC714 *[gnrr-3 (tm4152) X]* (x8), LSC506 *[gnrr-4 (tm4218) X] (x2),* FX04160 *[gnrr-5 (tm4160) V]*, LSC509 *[gnrr-6 (ok3465) X] (x2),* LSC508 *[gnrr-6 (tm4944) X] (x2),* LSC511 *[gnrr-8 (tm1450) IV]*, FX01908 *[nlp-2 (tm1908) X]*, NQ596 *[nlp-22 (gk509904) X]* (x2) and NQ638 *[nlp-23 (tm5531) X]* (x2). A schematic overview of the *nlp-2*, *nlp-22*, *nlp-23* and *gnrr-3* intron-exon structures and mutant alleles is provides in figure 4.2. Transgenic strains used in this study are listed in table 4.1.

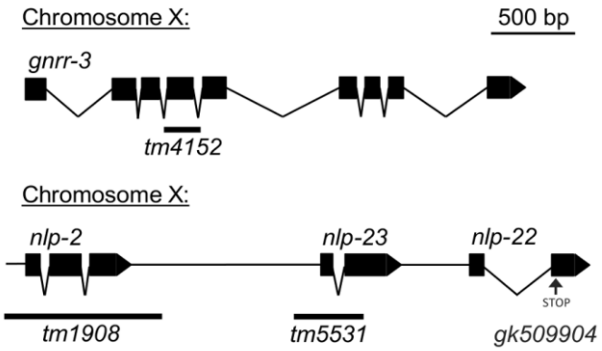

Figure 4.2 *nlp-2, nlp-22, nlp-23* and *gnrr-3* intron-exon structures and mutations. Coding sequences are depicted as solid boxes. Sequences deleted in alleles *tm4152, tm1908 and tm5531* are indicates as bars. The arrowhead indicates the position of the *gk509904* mutation, which encodes a point mutation (GGA=>TGA) introducing a premature stop codon.

Table 4.1. Transgenic strains used in this study

Strain name	Genotype	Description
NQ251	*qnIs142 [Phsp16.2::nlp-22; Phsp16.2::gfp; Pmyo-2::mCherry; unc-119(+)]*	*Heat-shock inducible nlp-22 expression*
LSC559	*gnrr-3 (tm4152); qnIs142 [Phsp16.2:nlp-22; Phsp16.2::gfp; Pmyo-2::mCherry; unc-119(+)]*	*Heat-shock inducible nlp-22 expression in gnrr-3 (-) background*
NQ644	*qnEx343 [Pgnrr-3::gnrr-3; Pmyo-2::mCherry]*	*gnrr-3 (OE)*
NQ692	*qnEx363 [Pnlp-2::nlp-2; Pmyo-2::mCherry]*	*nlp-2 (OE)*
NQ776	*gnrr-3 (tm4152) X; qnEx363 [Pnlp-2::nlp-2; Pmyo-2::mCherry]*	*nlp-2 (OE) ; gnrr-3 (-)*
NQ774	*qnEx423[Pnlp-2:gfp; Pglr-3:mCherry; rol-6(d)]*	*nlp-2 reporter strain*

4.2.2 Fat staining

Oil-Red-O staining was performed as described previously (Pino *et al.*, 2013). Briefly, 200-300 day-1 adult worms were washed from their cultivation plates and collected in an eppendorf tube. Worms were washed three times with 1xPBS buffer (137 mM NaCl, 2.7 mM KCl, 10 mM Na_2HPO_4 and 1.8 mM KH_2PO_4) and resuspended in 120 µl PBS. An

equal volume of 2x MRWB-PFA (160 mM KCl, 40 mM NaCl, 14 mM Na_2EGTA, 1 mM spermidine-HCl, 0.4 mM spermine, 30 mM Na-PIPES pH 7.4, 0.2% ß-mercaptoethanol and 2% paraformaldehyde) was added to the tube to permeablilize the worms. After shaking on room temperature for one hour worms were washed three times with PBS buffer and resuspended in 1 mL of 60% isopropanol (v/v in water) to dehydrate. After incubation for 15 minutes, worms were allowed to settle and the supernatant was removed. Subsequently, 1 mL of 60% Oil-Red-O stain (Sigma-Aldrich) was added to the tubes and incubated overnight at room temperature while gently shaking. The next day, worms were gently washed twice with 1x PBS with 0.01% Triton.

Oil-Red-O was prepared as follows: 0.5 g of Oil-Red-O powder was dissolved in 100 ml isopropanol and stored as a stock solution. The solution was then freshly diluted with 40% water to get a 60% working solution and allowed to sit 10 minutes at room temperature and filtered using 0.2 to 0.4 mm filters.

Bright field images of the worms were acquired using a Zeiss Axio Imager Z1 microscope. Images were inverted to give a dark background and the blue plane of each RGB image was top-hat filtered to compensate for non-uniform background, then auto-thresholded to identify regions corresponding to worms. Within these regions, the level of Oil-Red-O was quantified from the original images by determining the excess intensity in the red channel in comparison to the blue and green channels, with regions with less red than blue or green ignored. These red-excess regions were auto-thresholded to separate background redness from Oil-Red-O stained areas, with mean fatness per image estimated as the total intensity within stained regions normalized by the area of the worm regions. Statistical significance of the results was determined using one-way ANOVA and the Tukey post-hoc test, with the GraphPad software package.

4.2.3 Egg-laying

Total brood size and egg-laying progression were determined for 30 synchronized, well-fed hermaphrodites per strain. Late L4 nematodes were placed on a single NGM plate with *E. coli* OP50. For approximately five days, worms were transferred to a fresh, seeded NGM plate every twelve hours. The number of offspring on each plate was determined when in L3/L4 stage. Incomplete offspring counts due to escape or death of the hermaphrodite

mother were removed from the data set. Statistical significance of the total brood size was determined using one-way ANOVA and the Tukey post-hoc test, with the GraphPad software package.

4.2.4 Locomotion activity

Locomotion activity was measured with microtracker one (Phylumtech). Fifty day one adult worms were picked into a well of a 96-well plate (U bottom) containing 200 µl of S Medium (Stiernagle, 2006) with 50 µM 5-fluoro-2'-deoxyuridine (FUdR) to prevent the worms from reproducing, 50 Units/ml nystatin, and 20 µl *E. coli* OP50 ($OD_{600\ nm}$ = 1). Activity of the worms was measured for eight hours using the 'threshold binary' algorithm (Simonetta and Golombek, 2007). Statistical significance of activity differences was determined using one-way ANOVA and Tukey post-hoc for multiple comparisons with the GraphPad Prism software package. Experiments were performed on at least two independent days.

4.2.5 Quiescence assays

To measure feeding and locomotion after heat-shock induced expression of NLP-22, day one adult worms were placed on a 55 mm diameter NGM agar plate seeded with *E. coli* OP50. Plates were double wrapped with parafilm and incubated in a water bath at 33°C for 30 min. After heat-shock, worms were recovered at 20°C for 2-3 hours. Quiescence was analyzed by measuring feeding and locomotion activity. Pharyngeal pumping was counted for 20 seconds. To measure the duration of L4 lethargus feeding quiescence, late L4 worms were individually transferred to freshly seeded NGM agar plates. Pharyngeal pumping was observed by stereomicroscopy every 10 minutes. Quiescence duration was measured as the time between the offset and onset of pharyngeal pumping.

Arousal threshold was analyzed by measuring the response latency of individual worms to blue light during lethargus. A response to blue light was defined as a backward movement equal to one-half of the worm's length.

For automated measurements of total quiescence and quiescence duration, late L4 worms were monitored for 9 hours in 2 concave wells (3 mm diameter, 2.5 mm depth) of a polydimethylsiloxane (PDMS) chip filled with 15 µl NGM agar and seeded with *E. coli*

OP50. For each measurement, one control and one experimental animal were manually placed in adjacent wells. The PDMS chip was placed on a microscope base (Diagnostics Instruments) with a fiber optic cable DCR III light source (Schott) for bright-field illumination. Worms were monitored by a camera (659 x 494 pixels, scA640-70fm, Basler Vision Technologies), which was mounted on a stereomicroscope (Zeiss Stemi 2000). 8-bit grayscale images with a spatial resolution of 12.5 µm per pixel were captured every 10 seconds. Quiescence was quantified using a machine vision frame subtraction method (Raizen *et al.*, 2008).

Statistical significance was determined using one-way ANOVA and Tukey post-hoc for multiple comparisons with the GraphPad Prism software package. Experiments were performed on at least two independent days.

4.2.6 Developmental time course of mRNA expression

Developmental mRNA expression was analyzed using qRT-PCR as described (Temmerman *et al.*, 2012). Wild type *C. elegans* were synchronized as L1 diapause larvae and cultured in S-medium (Stiernagle, 2006) with E. *coli* K12 as food source, while gently shaking at 20°C. Worms were sampled every hour. mRNA was isolated (Rneasy Mini kit, Qiagen) and reverse transcribed to cDNA (SuperScript® III Reverse Transcriptase, Invitrogen) using random primers (Invitrogen). Primer pairs for *nlp-2* and *nlp-23* were designed with Primer Express (Applied Biosystems) and VectorNTI (Invitrogen). The specific primers used for the qPCR were: forward 5'-CTGAAGGAGCAATGGGCAAA -3' and reverse 5'-ATGATGAGATCACTAACATCCACAG -3' for *nlp-2*; forward 5'-CGTCATTTGGATGGCACTTCT -3' and reverse 5'-AGACGTTGGATGTTCCGAGTAAA -3' for *nlp-23*. The transcript profile of *lin-42b/c* was used as a marker for developmental timing, using *lin-42 fwd* TGTGCCCAACGCCAATC and *lin-42 rev* CACCTTCCTCACGCATTGC as primers. A melt curve analysis confirmed the absence of primer dimers and other non-specific products. Fast SYBR Green Master Mix (Applied Biosystems) was used for qRT-PCR and performed using the StepOnePlus Real-Time PCR system (Applied Biosystems). Cycling parameters were 600 seconds at 95°C, followed by 40 cycles of 3 seconds at 95°C and 30 seconds at 60°C. Each sample was analyzed in triplicate to assess technical variation. A no template

control consisting of milli-Q water instead of cDNA was added as a negative control. The normalized relative quantity of cDNA was calculated using the geometric mean of three reference genes (*cdc-42, tba-1* and *pmp-3* as the three best performing out of *cdc-42, tba-1, pmp-3, rpb-12, gpd-2* and *Y45F10D.4* using geNorm (Vandesompele *et al.*, 2002).

4.2.7 Molecular cloning

Overexpression constructs were generated by amplifying genomic DNA including the promoter, the unspliced coding sequence, and the 3'-untranslated region by PCR using Herculase Enhanced DNA polymerase (Agilent Technologies) and wild type *C. elegans* genomic DNA as template. The primers used for the PCR amplification were: *gnrr-3* forward 5'-AGGATAAGTGTCACTCTTCGGAC-3' and *gnrr-3* reverse 5'-TCATTTCCTAAACAACCCAGAC-3' ; *nlp-23* forward 5'-AATCGTGTTCTGTTTTTTAGAGTTTT-3' and *nlp-23* reverse 5'-CAATGATTTGTTCTCTGGAAACG-3'; *nlp-2* forward 5'-ATGACACGTACTATATTGTTCAAAGATG-3' and *nlp-2* reverse 5'-ATATAGAATTTATTCAATTGTATGGAGA-3' . PCR started with initial denaturation for 1 min at 95°C, followed by 30 cycles of [20 sec at 95°C, 20 sec at 55°C, 1 min 30 sec at 72°C], followed by final elongation for 3 min at 72°C. The size of the PCR product was checked by electrophoretic separation in a 1% agarose gel.

GFP reporter constructs were created using overlap-extension PCR as described previously (Boulin *et al.*, 2006; Nelson and Fitch, 2011). Each DNA fragment was amplified individually using Herculase Enhanced DNA polymerase with the same conditions as described above. Promoter fragments were amplified (with primers A and B) from genomic DNA of wild-type *C. elegans* and *gfp* was amplified (with primers B and C) from the vector pPD95.75 (Addgene). The sequence of the primers used for the PCR amplification are listed in table 4.2.

Table 4.2 Gene-specific primer sequences for fluorescent reporter constructs

Primer name	Sequence (5'-3')
Pgnrr-3 A	AGGATAAGTGTCACTCTTCGGAC
Pgnrr-3 A'	GATTAGATGATTCGCTTATCTCCGAAG
Pgnrr-3::gfp B	TCCTGAAAATGTTCTATGTTATGTTTCTGAAAAG TTTCACAATTG
Pgnrr-3::gfp C	CAATTGTGAAACTTTTCAGAAACATAACATAGA ACATTTTCAGGA
Pnlp-2 A	ATGACACGTACTATATTGTTCAAAGATG
Pnlp-2 A'	GACAACGTGATTTTGAACAAAAAC
Pnlp-2::gfp B	AAAAGTTCTTCTCCTTTACTCATTGCTCGCATTTC TCGCGTTGT
Pnlp-2::gfp C	TCCCAACAACGCGAGAAATGCGAGCAATGAGTA AAGGAGAAGAACTTTT
gfp D'	GAGAAGTTTTTTGATAATAACAAAAATAGG
gfp D	AAAAGAAGCTAAAAAACAAAGAAATTA

4.2.8 Transgenesis

Transgenic worms were obtained through microinjection of the distal core cytoplasm of the gonads using a Leica DMIRB inverted DIC microscope equipped with an Eppendorf Femtojet microinjection system (Evans, 2006). Each construct was injected at a concentration of 50 ng/µl in combination with 5 ng/µl pCFJ90 (*Pmyo-2::mCherry*) or with 5 ng/µl (*Prol-6::rol-6*) and P*glr-3::gfp* as co-injection marker, and 1kb DNA ladder as carrier DNA.

4.2.9 Expression pattern analysis

Animals were mounted on 2 % agarose pads and immobilized with 5 mM sodium azide. Expression patterns of fluorescent reporters were observed on an Olympus Fluoview FV1000 (IX81) confocal microscope. Confocal Z-stack images were processed using Imaris

7.2 (Olympus). To identify expression in amphid sensory neurons, *nlp-2::gfp* transgenic animals were stained with the lipophilic dye 1,1′-Dioctadecyl-3,3,3′,3′-tetramethylindocarbocyanine perchlorate (DiI) (Hedgecock *et al.*, 1985).

4.3 Results

4.3.1 Lipid storage

Mobilization of sugars and lipids during energy-demanding processes is a classical regulatory role for AKH in insects. The AKH peptides activate their receptor on the fat body, which initiates the conversion of stored triacylglyceroles or glycogen to diacylglycerol or trehalose, respectively, or initiates the synthesis of the amino acid proline from alanine and fatty acids. Diacylglycerols, trehalose, or proline are subsequently released from the fat body and their concentrations become elevated in the haemolymph (Gäde and Marco, 2013). As a consequence, RNAi knockdown of the AKH(/GnRH) receptor was shown to increase body fat up to 65-127% in the fruit fly *D. melanogaster* (Grönke *et al.*, 2007). To investigate if the identified *C. elegans* GnRH/AKH receptors could be mediating in the regulation of energy metabolism as well, fat stores in the worms were measured using Oil-Red-O staining. The lipophilic dye Oil-Red-O stains the major fat stores in *C. elegans* which is shown to correlate with biochemically measured triglyceride mass (Pino *et al.*, 2013). Of all *gnrr* mutants tested, none showed increased Oil-Red-O staining compared to wild-type worms. However, both *gnrr-6* mutants, showed a small, yet significant, decrease in staining intensity.

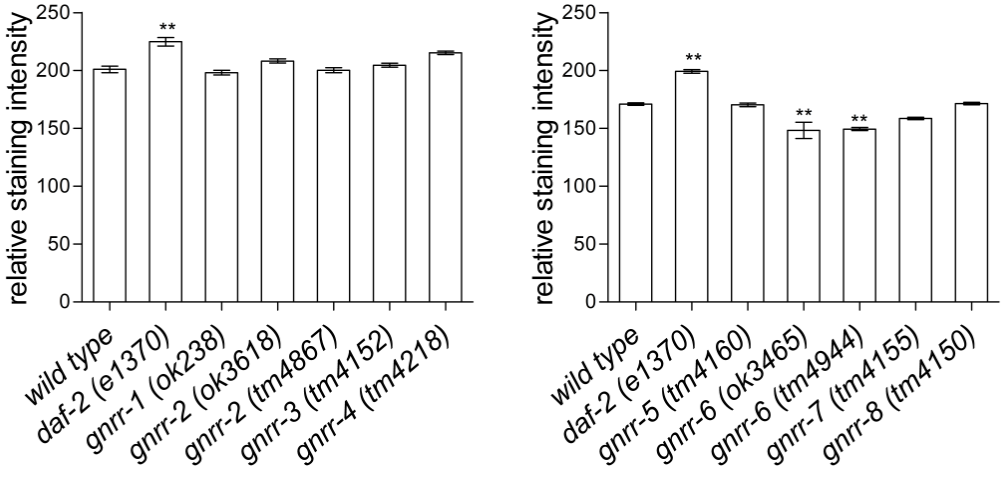

Figure 4.3 *gnrr* mutants do not increase lipid accumulation. Shown is the quantification of the Oil-Red-O staining intensity of young adult hermaphrodite wild-type worms, *daf-2 (e1370)* mutants that serve as a positive control and the *gnrr* mutants. (One-way ANOVA and Tukey post-hoc comparison; $^{**}P < 0.01$; $N \geq 10$; error bars represent s.e.m).

4.3.2 Hermaphrodite reproduction

In deuterostomes the regulatory role of GnRH signaling in reproduction is shown to be well conserved (Kah *et al.*, 2007). In some protostomes GnRH peptides and their receptors seem to be regulating reproduction as well. Treatment with synthetic octopus GnRH results in steroidogenesis in octopus ovary and testis after treatment with synthetic octopus GnRH (Kanda *et al.*, 2006). In *C. elegans* RNAi knockdown of both *gnrr-1* and the peptide precursor *nlp-47* resulted in delayed egg-laying and a decreased amount of progeny suggesting that they are involved in hermaphrodite reproduction (Lindemans *et al.*, 2009b). These results indicated that the GnRH system in invertebrates shares some functional characteristics with that of the vertebrates, in addition to other potential roles. To address whether the identified *C. elegans* GnRH/AKH receptors could be involved in hermaphrodite reproduction, we analyzed total brood size and progression of egg-laying for the *gnrr* mutants. *C. elegans* hermaphrodites are self fertile and produce about 300 progeny during their reproductive stage of approximately four days (Hart, 2006). In our experiments wild type animals generated an average of 250 progeny, which was not significantly different for the *gnrr* mutants (figure 4.4 and 4.5).

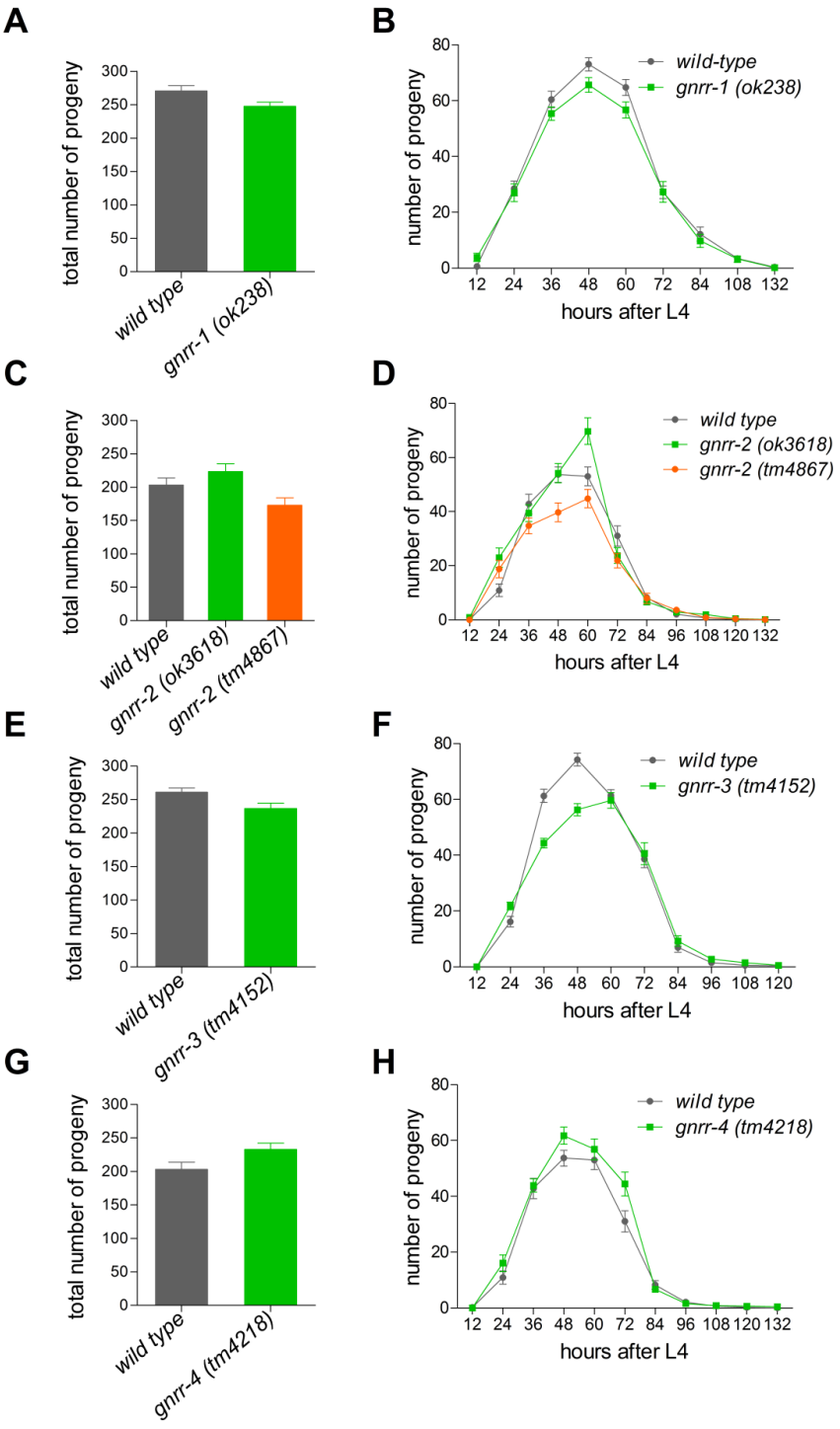

Figure 4.4 Total brood size and progression of egg-laying of *C. elegans* hermaphrodites. The total amount of progeny produced during the hermaphrodite reproductive stage (A, C, E and G) and time course representing the amount of progeny at different worm ages (B, D, F and H) of *gnrr-1*, *gnrr-2*, *gnrr-3* and *gnrr-4* mutants were compared to wild types (One-way ANOVA and Tukey post-hoc comparison; $N \geq 30$; error bars represent s.e.m)

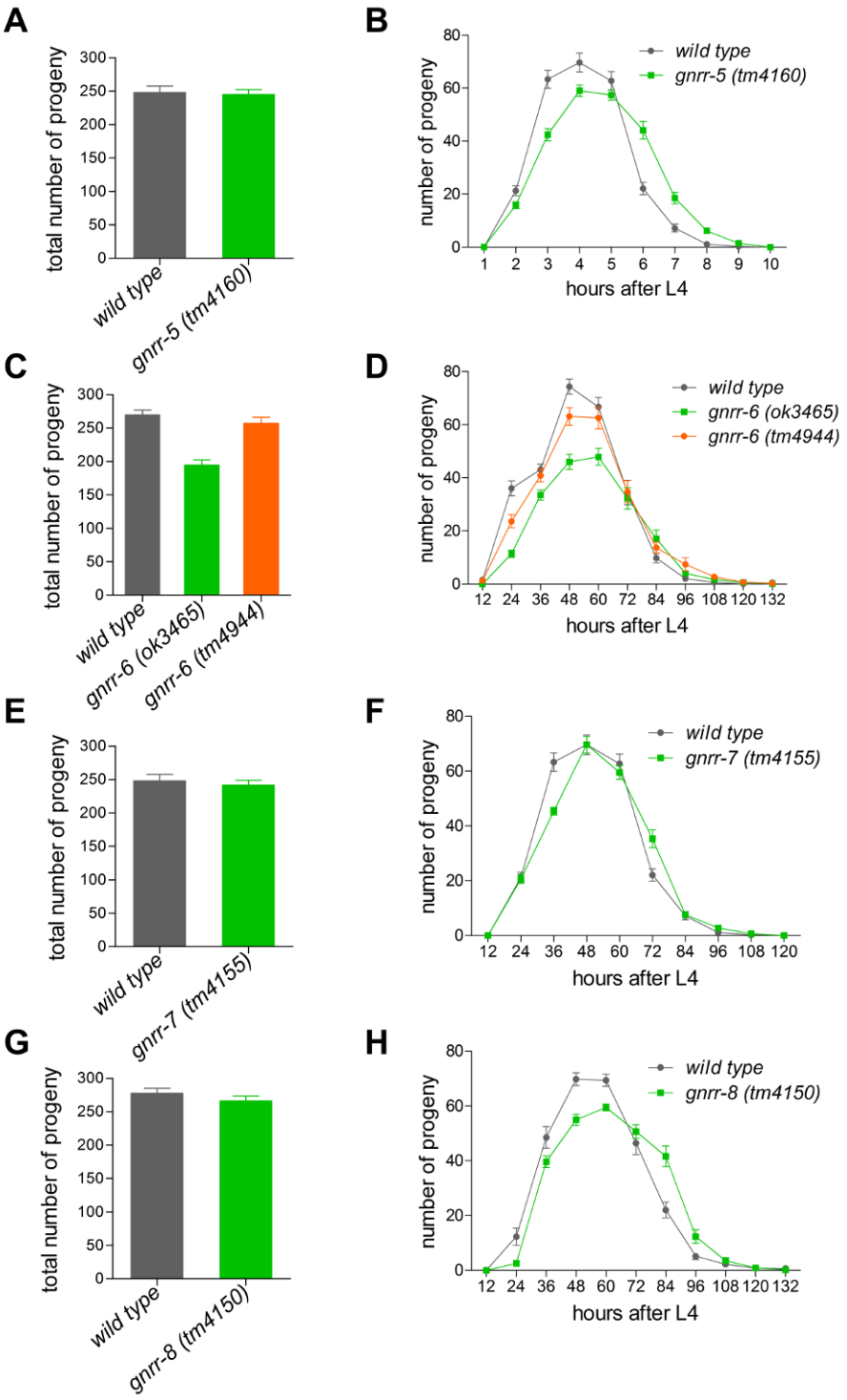

Figure 4.5 Total brood size and progression of egg-laying of *C. elegans* hermaphrodites. The total amount of progeny produced during the hermaphrodite reproductive stage (A, C, E and G) and time course representing the amount of progeny at different worm ages (B, D, F and H) of *gnrr-5*, *gnrr-6*, *gnrr-7* and *gnrr-8* mutants were compared to wild types (One-way ANOVA and Tukey post-hoc comparison; $N \geq 30$; error bars represent s.e.m)**.**

4.3.3 Locomotion activity

Using a reverse pharmacology assay we were able to identify the RPamides NLP-2a, NLP-2b, NLP-2c, NLP-22 and NLP-23b as activating ligands of one of the predicted *C. elegans* GnRH/AKH-like receptors GNRR-3 (§ 3.4.3). The RPamide peptide NLP-22 has previously been identified as a somnogenic neuropeptide in *C. elegans* (Nelson *et al.*, 2013). Overexpression of *nlp-22* induces sleep-like properties in adult worms and *nlp-22* mutant animals display reduced quiescence during lethargus. Since NLP-22 was one of the ligands identified for GNRR-3, we hypothesized that GNRR-3 signaling could also be involved in the regulation of sleep. Because most assays to characterize sleep measure differences in locomotion behavior, we decided to first characterize locomotion activity in adult worms with altered GNRR-3 signaling (figure 4.6). Both deletion and overexpression of *gnrr-3* did not alter activity compared to wild-type worms. Besides NLP-22, GNRR-3 was also activated by NLP-2 and NLP-23 peptides in our *in vitro* assay and we tested activity for both deletion and overexpression strains of their peptide precursors. Our results indicate that deletion of *nlp-2* results in a minor, yet significant, reduction of locomotion activity.

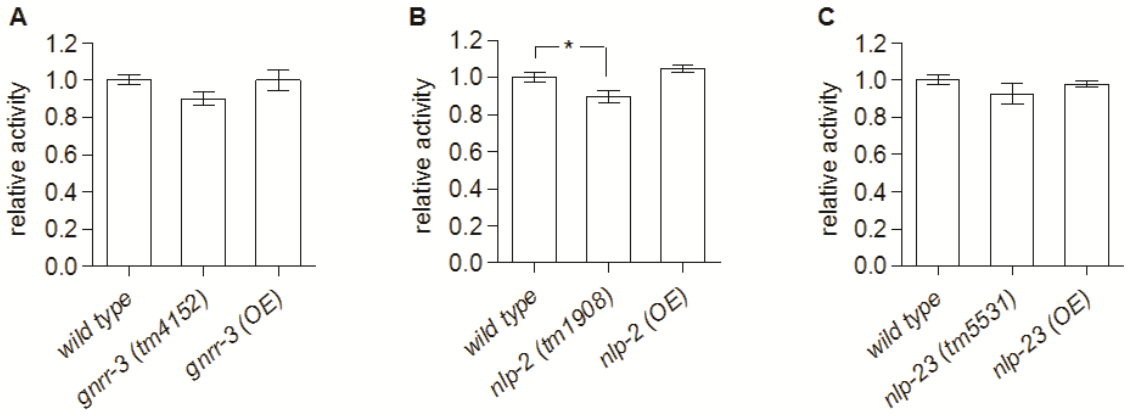

Figure 4.6 Average relative locomotion activity (A) of *gnrr-3 (tm4152)* deletion mutants, *gnrr-3* overexpression *(qnEx343)* animals, (B) *nlp-2 (tm1908)* mutants, *nlp-2 (qnEx362)* overexpression animals, (C) *nlp-23 (tm5531)* mutants and *nlp-23 (qnEX365)* overexpression animals (One-way ANOVA and Tukey post-hoc comparison; N > 20; error bars indicate s.e.m.).

4.3.4 NLP-22 does not induce L4 lethargus quiescence through GNRR-3

If the RPamide receptor GNRR-3 were activated by NLP-22 *in vivo,* then its role in sleep regulation should resemble that of NLP-22. This implies that *gnrr-3* knockout mutants would be expected to show reduced quiescence properties during lethargus, while overexpression of *gnrr-3* would increase quiescence. We measured locomotion quiescence during L4 lethargus for both *gnrr-3 (tm4152)* deletion mutants (figure S1) and *gnrr-3*-overexpressing *(qnEx343)* animals. Total quiescence (figure 4.7a) and quiescence duration (figure 4.7c) were slightly increased though not significantly different in *gnrr-3 (tm4152)* mutants in comparison to wild type animals. On the other hand, overexpression of *gnrr-3* significantly decreased both total quiescence (figure 4.7b) and quiescence duration (figure 4.7d) during L4 lethargus. This modulation of locomotion was restricted to lethargus as adult worms lacking or overexpressing *gnrr-3* did not show altered activity (figure 4.6).

If GNRR-3 represents the sole receptor for NLP-22 *in vivo*, elimination of *gnrr-3* function should abrogate the somnogenic effects of *nlp-22* overexpression. In contrast to this prediction, we found that *nlp-22* overexpression induced behavioral quiescence equally well in wild type and *gnrr-3* mutant backgrounds (figure 4.7e, f). Taken together, our results suggest that GNRR-3 is not a prime receptor for NLP-22 in sleep regulation and more interestingly, that GNRR-3 promotes wakefulness.

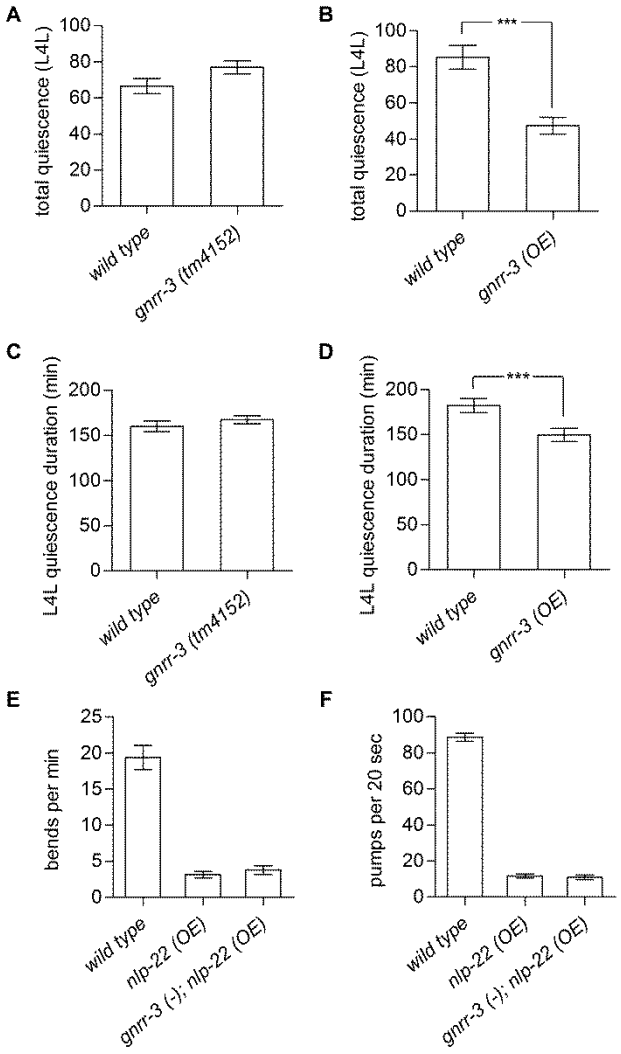

Figure 4.7 GNRR-3 promotes wakefulness during lethargus and is not required for NLP-22 induced quiescence. Average total quiescence during L4 lethargus (L4L) of (A) *gnrr-3 (tm4152)* deletion mutants and (B) *gnrr-3*-overexpressing *(qnEx343)* strains (Paired student's two-tailed t-test; ***$P < 0.001$; N > 10; error bars represent s.e.m.). Average quiescence duration during L4L of (C) *gnrr-3 (tm4152)* deletion mutants and (D) *gnrr-3*-overexpressing *(qnEx343)* strains (Paired student's two-tailed t-test; ***$P < 0.001$; N > 10; error bars represent s.e.m.). Forced overexpression of *nlp-22* in *gnrr-3 (tm4152)* deletion mutants induces (E) locomotion and (F) feeding quiescence in the same manner as it does in a wild type genetic background (N > 10 animals, error bars represent s.e.m).

4.3.5 NLP-2 peptides inhibit locomotion quiescence during L4 lethargus through GNRR-3

Since our *in vivo* experiments suggested that NLP-22 does not activate GNRR-3 in lethargus quiescence and since NLP-2 and NLP-23 peptides also activated GNRR-3 *in vitro*, we hypothesized that instead, NLP-2 or NLP-23 peptides may activate GNRR-3 in lethargus quiescence. Hence, we would expect that genetically manipulating their levels would have similar effects to those observed when genetically manipulating GNRR-3. We first measured total quiescence and quiescence duration during L4 lethargus for *nlp-2 (tm1908)* and *nlp-23 (tm5531)* mutants (figure 4.8a-d, figure S1). While *nlp-23* mutant animals displayed no difference in L4 lethargus quiescence or quiescence duration in comparison to wild type worms, *nlp-2* mutants showed significantly increased quiescence. Similar to *gnrr-3*, overexpression of *nlp-2* resulted in increased activity during lethargus (figure 4.8e) and a decrease in total quiescence and in quiescence duration (figure 4.8f), while adult worms did not show altered activity (figure 4.6). Thus, *nlp-2* and *gnrr-3* overexpression result in similar phenotypic consequences. If GNRR-3 is a prime *in vivo* receptor for NLP-2 peptides in sleep regulation, then removal of *gnrr-3* should abrogate the wake-promoting effects of *nlp-2* overexpression. Corroborating this, we found that mutation of *gnrr-3* eliminated the reduced quiescence effect in animals overexpressing *nlp-2* (figure 4.8g,h). These results, together with our *in vitro* data suggest a model in which NLP-2 peptides activate GNRR-3 to promote locomotion activity during lethargus.

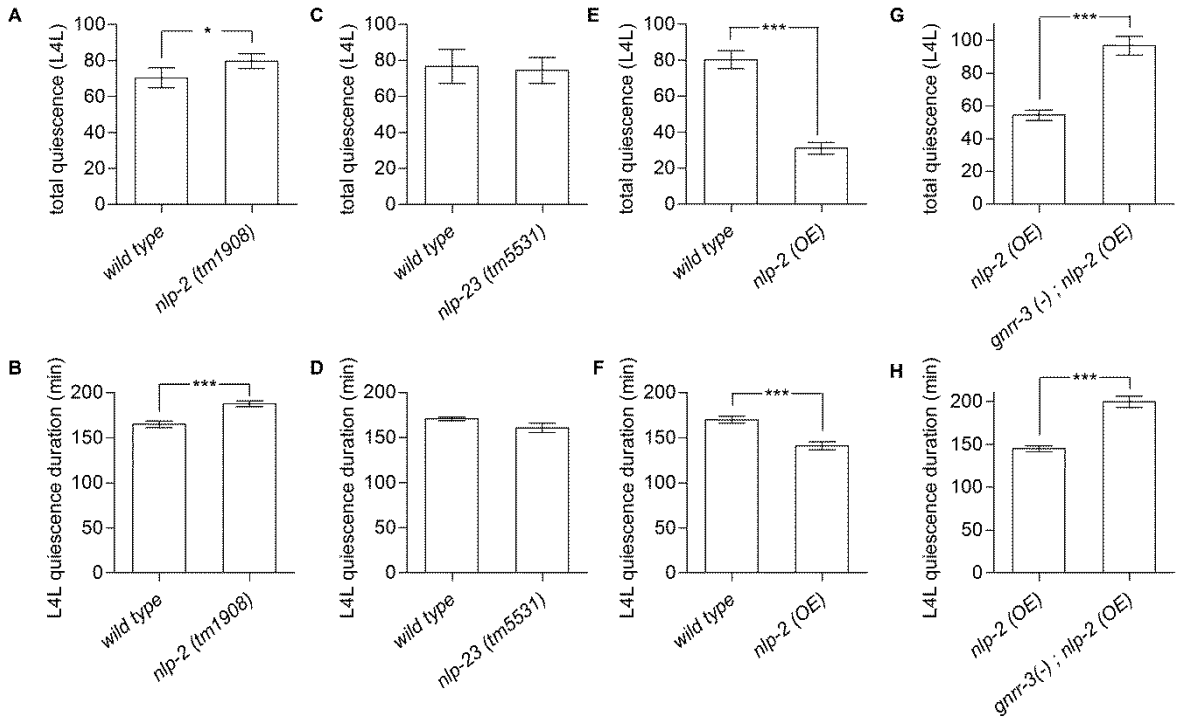

Figure 4.8 NLP-2 peptides inhibit L4 lethargus quiescence through GNRR-3 Average total quiescence during L4 lethargus (L4L) and average quiescence duration of L4L of (A, B) *nlp-2 (tm1908)* mutants (N = 8), (C, D) *nlp-23 (tm5531)* mutants (N = 6), (E, F) *nlp-2 (qnEx362)* overexpression animals (N = 10), and (E,F) *nlp-2* overexpression in a *gnrr-3* mutant (NQ776) (Paired student's two-tailed t-test; **P* < 0.001; ****P* < 0.001; error bars represent s.e.m.).

4.3.6 GNRR-3 and NLP-2 peptides do not modulate arousal threshold and duration of feeding quiescence during L4 lethargus

In *C. elegans*, sleep behavior during L4 lethargus is characterized by cessation of locomotion and feeding, reduced responsiveness to external stimuli, and homeostasis (Raizen *et al.*, 2008; Nelson and Raizen, 2013). To determine whether inhibition of locomotion quiescence by the NLP-2/GNRR-3 neuropeptide system extends to feeding quiescence, we analyzed the duration of feeding quiescence during L4 lethargus for *gnrr-3* and *nlp-2* mutants and for overexpression animals. There was no difference in the duration of feeding quiescence during L4 lethargus, indicating that NLP-2/GNRR-3 signaling controls locomotion quiescence but not feeding quiescence (figure 4.9a).

Other mutants with reduced quiescence during lethargus, such as *egl-4* and *npr-1* loss-of-function mutants, have been shown to display an increased responsiveness to sensory stimuli during lethargus (Raizen *et al.*, 2008; Choi *et al.*, 2013), possibly explaining their reduced quiescence phenotype. To test whether the observed reduction of locomotion quiescence can be explained by an increased sensitivity to arousing stimuli, we measured the time required for animals to be aroused by blue light during lethargus (Driver *et al.*, 2013). There was no significant difference in response latency between wild-type worms and *nlp-2*/*gnrr-3* mutant or overexpression animals (figure 4.9b). Therefore, the reduced quiescence phenotype of *gnrr-3*- and *nlp-2*-overexpressing animals is unlikely to be explained by a general increased sensitivity to sensory stimuli. However, increased sensitivity to particular sensory cues cannot be excluded.

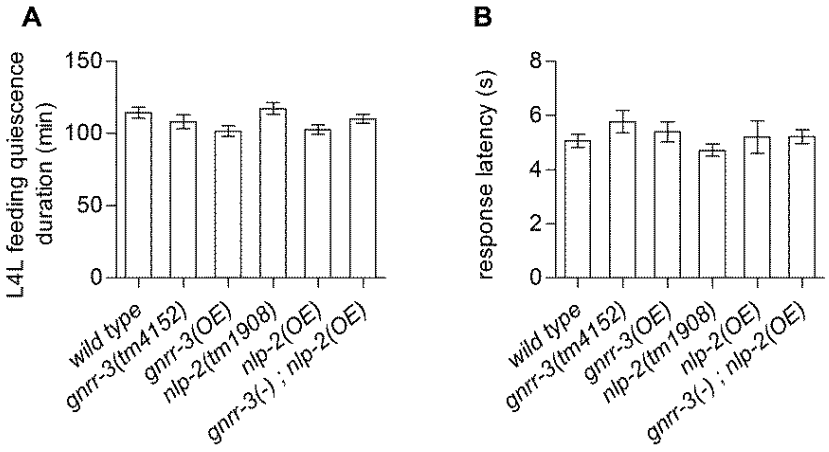

Figure 4.9 GNRR-3 and NLP-2 peptides do not modulate the duration of feeding quiescence or blue light responsiveness during L4 lethargus. (A) Average feeding quiescence duration and (B) response latency to blue light during L4 lethargus (L4L) of *gnrr-3 (tm4152)* deletion mutants, *gnrr-3* overexpression *(qnEx343)* animals, *nlp-2 (tm1908)* mutants, *nlp-2 (qnEx362)* overexpression animals, and *nlp-2* overexpression in a *gnrr-3* mutant (NQ776). (One-way ANOVA and Tukey post-hoc comparison; N > 20; error bars represent s.e.m.).

4.3.7 *nlp-2* expression cycles with a developmental clock

The somnogenic RPamide NLP-22 has a cyclical mRNA expression pattern (Nelson *et al.*, 2013). Therefore, we investigated whether the expression pattern of *nlp-2* mRNA cycles throughout development. We used quantitative reverse-transcription PCR (qRT-PCR) to analyze *nlp-2* mRNA expression over a 30h time frame, which covered both L3 and L4

lethargus periods. Developmental progression in *C. elegans* is timed by *lin-42* transcript profiles, which cycle with the larval stages, being lowest during each molt (Jeon *et al.*, 1999). We found that *nlp-2* expression cycles with a constant phase to *lin-42* during larval development (figure 4.10a). *nlp-2* mRNA expression peaks in preparation of the L3 and L4 molts, when *lin-42* levels are low.

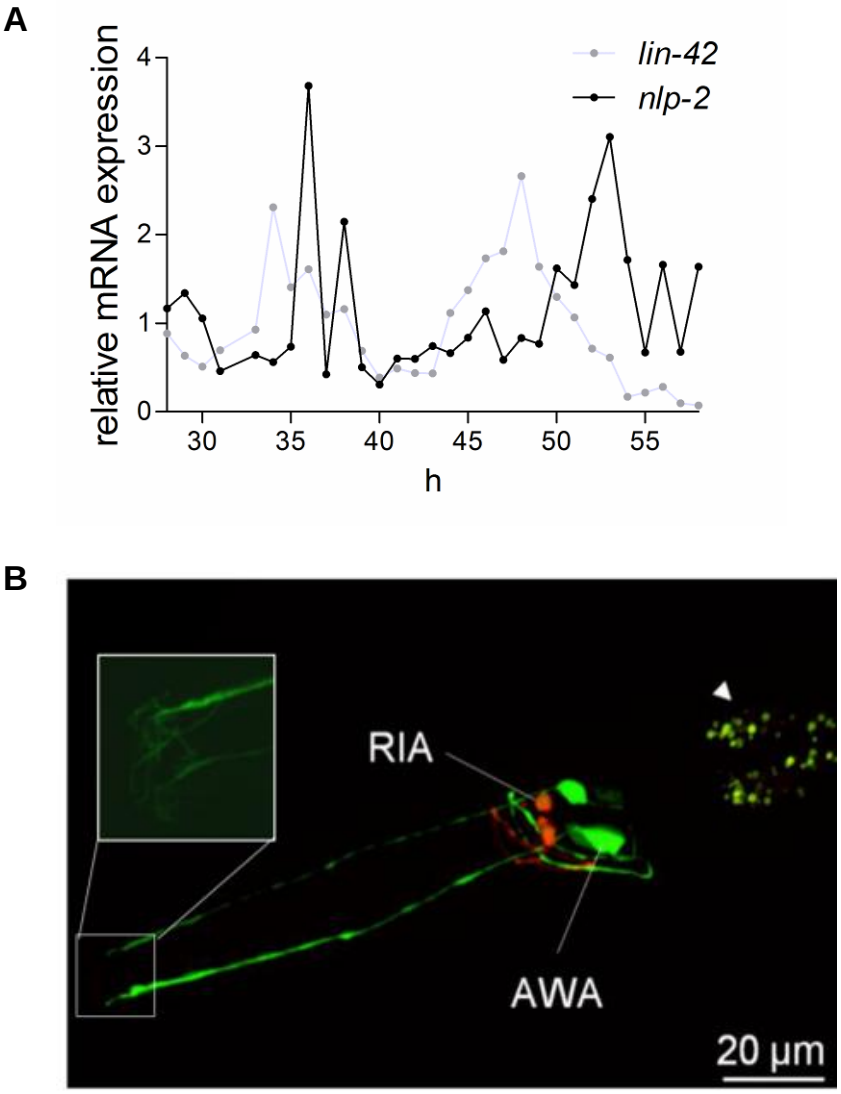

Figure 4.10 Expression analysis of *nlp-2*. (A) Relative qRT PCR expression of *nlp-2* during larval development. The *nlp-2* and *lin-42* expression levels are plotted during one-hour time intervals of postembryonic development at 20°C after L1 larval arrest. (B) Confocal Z-stack projections of the head region of an adult *nlp-2::gfp* transgenic animal. Expression of the *nlp-2* reporter is represented in green and *glr-3* co-injection marker, which marks the RIA neurons, in red. The white arrow indicates auto-fluorescence of the intestine.

To identify the cells that express *nlp-2*, we generated a transcriptional green fluorescent protein (GFP) reporter construct, which expresses *gfp* driven from *nlp-2* regulatory DNA. Expression of the *nlp-2* reporter was restricted to one pair of head neurons and four uterus cells (figure 4.10b and supplementary figure 1). Based on morphology and localization compared to DiI stained sensory neurons, the head neurons represent most likely the AWA neurons, olfactory sensory cells that have elaborate sensory cilia. The uterus cells were identified as the neurosecretory uv1 cells based on their location and morphology.

4.4 Discussion and conclusion

4.4.1 Investigating a conserved role for the *C. elegans* GnRH/AKH receptors

Based on the well-conserved function of GnRH signaling in vertebrate reproduction and AKH signaling in insect energy metabolism, we hypothesized that the identified *C. elegans* GNRRs may play a role in reproduction or energy metabolism. Therefore we tested this hypothesis by investigating whether *gnrr* mutants showed altered hermaphrodite reproduction or fat storage.

In order to test if the *C. elegans* GnRH/AKH receptors may regulate energy metabolism, we investigated whether fat storage of *gnrr* mutants differs from wild type animals using Oil-Red-O staining. Quantification of Oil-Red-O staining showed no difference between most *gnrr* deletion mutants and wild type worms. However, both *gnrr-6* deletion mutants showed decreased staining, indicating that these mutants store less fat.

To investigate whether the *C. elegans* GnRH/AKH receptors may regulate reproduction, we compared hermaphrodite egg-laying profiles of *gnrr* mutants to that of wild type animals. The total amount of progeny in *gnrr* deletion mutants was similar to wild type indicating that the *C. elegans* AKH/GnRH receptors do not affect this aspect of reproduction.

For its reproduction, like many other species, *C. elegans* relies on the formation of egg-yolk to enable embryogenesis. Recently, Van Rompay showed that RNAi knockdown of *gnrr-6* results in decreased yolk production in *C. elegans* (Van Rompay, 2014). In vertebrates GnRH signaling regulates reproduction through the release of the gonadotropins (FSH and LH), which in turn act on the gonads leading to their development and the stimulation of steroidogenesis, the release of estrogen, androgen and progestogen, the stimulation of

gametogenesis and gamete release (Kah *et al.* 2007). One downstream process regulated by this axis in ovuliparous and oviparous vertebrate females is the synthesis of egg-yolk proteins, which are required for oogenesis (Awruch, 2013). The results of Van Rompay and colleagues suggest that GNRR-6 could induce a similar pathway to regulate egg-yolk production in *C. elegans.*

4.4.2 nlp-2/gnrr-3 signaling promotes arousal during lethargus in *C. elegans*

For the remainder of the functional studies we focused on the deorphanized GnRH/AKH-like receptor GNRR-3. Based on the fact that one of its ligands, NLP-22, regulates lethargus in *C. elegans* (Nelson et al., 2013), we hypothesized a role for the GNRR-3 receptor and its ligands in sleep behaviour.

To test this hypothesis, we analysed overexpression strains and deletion mutants in a locomotion quiescence assay during lethargus. This analysis revealed that GNRR-3 and NLP-2 peptides seem to inhibit this sleep-like state. Moreover, we show that inhibition of quiescence by NLP-2 peptides requires GNRR-3 *in vivo*. Together with our *in vitro* assay, these results suggest that NLP-2 peptides inhibit quiescence through the activation of GNRR-3. The role of the NLP-2/GNRR-3 system in lethargus quiescence seems to be restricted to locomotion, as the duration of pharyngeal pumping quiescence is not altered in *nlp-2/gnrr-3* mutants or in animals overexpressing these genes. While this phenotype is superficially similar to the lethargus phenotypes of loss-of-function mutants of the neuropeptide receptor NPR-1 and its ligands FLP-18 and FLP-21, there are also differences. Whereas the hypersensitivity to sensory stimulation during lethargus may explain the reduced quiescence of *npr-1* mutants (Nagy *et al.*, 2014), the arousal threshold measured by blue light stimulation remained unaffected in the case of *nlp-2* and *gnrr-3* overexpression.

The activity of the quiescence-inhibiting NLP-2 signaling pathway is at least partially regulated at the level of *nlp-2* mRNA transcripts, which cycle relative to a LIN-42/PER-based larval clock that controls the synchronization of lethargus quiescence. Peak expression of *nlp-2* is delayed compared to expression of the *lin-42/per* gene that sets the timing for sleep-like behavior, which is in line with our evidence for the wake-promoting effects of NLP-2 signaling. The up-regulation of *nlp-2* transcripts when *lin-42/per* expression is high suggests that *nlp-2* expression can be a clock output signal, regulated by

the activity of the PER-related protein LIN-42. Interestingly, a similar mechanism has been described for regulating the expression of the sleep-inducing RPamide gene *nlp-22*, which oscillates in response to the LIN-42/PER-based larval clock (Nelson *et al.*, 2013). The *nlp-2* and *nlp-22* genes are clustered on the X chromosome (Nathoo *et al.*, 2001), providing a way to possibly co-regulate wake- and sleep-promoting signals. Similar to the actions of the *Drosophila* PERIOD protein, *C. elegans* LIN-42 may regulate *nlp-2* and *nlp-22* expression through cell-autonomous interactions with transcriptional regulators of these genes. Alternatively, *nlp-2* expression could be regulated by non-cell autonomous actions of LIN-42, or provide an independent input signal to the timing of lethargus behavior.

Expression of an *nlp-2* reporter was restricted to a pair of head neurons and the connecting uv1 cells of the adult uterus and vulva, consistent with previously reported expression patterns for *nlp-2* (Li *et al.*, 1999; Nathoo *et al.*, 2001). Our expression analysis suggests that NLP-2 peptides may be released from AWA chemosensory neurons to mediate arousal from lethargus. During lethargus stimulus-evoked neural activities are shown to be reduced in the sensory nociceptive ASH, mechanosensory ALM, and salt sensing ASE neurons (Schwarz *et al.*, 2011; Cho and Sternberg, 2014). However, the reduced responsiveness of a sensory modality can be rapidly reversed by another stimulus causing arousal from the sleep-like state. Environmental signals are thought to mediate this arousal by restoring synchronous activity in downstream interneurons of the motor circuit (Cho and Sternberg, 2014), allowing to rapidly wake up from a sleep-like state. As sleep comes with certain advantages but also trade-offs, including reduced opportunities to forage or mate, sleep-like states need to be properly aligned with competing or complementary behaviors (Roth *et al.*, 2010; Griffith, 2014). The release of NLP-2 from sensory neurons, most likely in response to environmental and/or internal stimuli, may therefore represent an important switch between sleep-wake states. The *nlp-2*-expressing AWA neurons have ciliated sensory endings and are known to mediate chemotaxis toward attractive chemicals signaling the presence of food (Nickell *et al.*, 2002; Bargmann, 2006). AWA neurons have previously been shown to promote diacetyl-induced entry into L1 quiescence via the odorant receptor ODR-10 (Hoffmann *et al.*, 2010). Odorants sensed by the olfactory AWA neurons might be important for the regulation of NLP-2 synthesis and release to evoke arousal (or ’reward/fear’-related) responses. The identification of NLP-2 target cells expressing its

receptor should provide further insight into the arousal-promoting NLP-2 circuit, but we were unable to obtain an unambiguous reporter strain to identify the expression pattern of *gnrr-3*. Preliminary results indicate that this receptor is expressed in neurons of the motor circuit, which may provide a direct link to the observed role of the NLP-2/GNRR-3 neuropeptide system in locomotion quiescence.

Remarkably, NLP-2 and NLP-22 RPamides belonging to the same peptide family have opposite effects on locomotion quiescence. Whereas overexpression of *nlp-2* increases locomotion during lethargus, *nlp-22* overexpression induces quiescence of both locomotion and feeding (Nelson *et al.*, 2013). Our *in vivo* data suggest that these effects result from the activation of different receptors by NLP-2 or NLP-22 peptides. As the sleep-inducing effects of *nlp-22* persisted in the absence of GNRR-3, this GPCR does not seem to act as a prime endogenous receptor for NLP-22 in the regulation of lethargus quiescence. Corroborating this, *in vitro*, GNRR-3 is a low affinity receptor for NLP-22 with a micromolar EC_{50} value, whereas most neuropeptide receptors have high affinities for their ligand consistent with EC_{50} values in the nanomolar range. Although the potency of a ligand to activate its receptor could be influenced by several factors in *in vitro* assays (Mertens *et al.*, 2004b), the high concentration needed to activate the receptor is not in support for GNRR-3 being a prime endogenous receptor for NLP-22. Structural similarities have been suggested for NLP-22 and mammalian neuromedin S, but none of the *C. elegans* neuromedin-like receptors seem to be involved in NLP-22-induced quiescence (Nelson *et al.*, 2013). GNRR-3 is thus the only known RPamide receptor so far. On the other hand, we cannot exclude the possibility that NLP-22 acts through GNRR-3 in another functional paradigm aside from lethargus quiescence. Additional functions for GNRR-3 are also suggested by the high affinity response of this receptor for NLP-23 peptides, for which we did not find evidence suggesting a role in L4 lethargus behavior.

To date, no direct role has been described for GnRH/AKH systems in the regulation of sleep-like behaviors. *Drosophila* mutants with reduced insulin/insulin-like growth factor signaling (IIS) have improved sleep quality at night and higher activity levels during the day (Metaxakis *et al.*, 2014). This increased activity during the day depends on AKH signaling. Although AKH receptor mutants show no difference in day activity or sleep, the increase in

daytime activity in IIS mutants was eliminated by an AKH receptor mutation (Metaxakis *et al.*, 2014). Moreover, AKH signaling seems to depend on the transcription factor dFOXO and promotes increased day activity through the regulation of octopamine. In humans, GnRH pulse frequency is down-regulated during sleep (Shaw *et al.*, 2011), although this seems to be an output of the diurnal cycle rather than having a regulatory role in sleep-wake behavior.

4.4.3 Conclusion

Regardless of their evolutionary relationship, our results suggest a model where RPamide neuropeptides encoded by *nlp-2* signal through GNRR-3 *in vivo* to regulate quiescence during sleep-like behavior. We show that NLP-2 mRNA transcript levels are cyclic and in phase with the LIN-42/PER-based larval clock that controls the synchronization of lethargus quiescence. Expression of the *nlp-2* gene in AWA chemosensory neurons suggests that the release NLP-2 from sensory neurons, most likely in response to environmental and/or internal stimuli, may represent an important switch between sleep-wake states.

Chapter 5. Tachykinin signaling in *C. elegans*: *In vivo* localization and functional study

5.1 Introduction

The first tachykinin peptide to be discovered was substance P. This ‘substance’ was extracted from horse brain and intestine tissue and shown to stimulate the contraction of isolated intestine tissue and vasodilatation upon intravenous injection (Von Euler and Gaddum, 1931). Tachykinin signaling has been studied intensively in mammals and shown to be involved in a plethora of physiological processes in the nervous, immune, gastrointestinal, respiratory, and dermal systems, including inflammation, nociception, and smooth muscle contractility and proliferation (reviewed in (Steinhoff *et al.*, 2014).

In invertebrates most phenotypic assays have focused on the myostimulatory effect of tachykinins on several muscle tissues. Using *in vitro* assays it was shown that insect tachykinins stimulate muscle contractions of insect oviduct, gut tissues, visceral and skeletal muscle (Schoofs *et al.*, 1990b; Schoofs *et al.*, 1990a; Nässel, 1999). Several neuromodulatory functions have been described for invertebrate tachykinin signaling systems as well, especially in *Drosophila* where tachykinin signaling was shown to be involved in the regulation of insulin signaling and olfactory perception.

In *Drosophila* the tachykinin receptor (DTKR) is expressed in the brain and insulin producing cells (IPCs) of renal tubules. Based on this colocalization, a role for tachykinin signaling in the regulation of insulin signaling was investigated (Söderberg *et al.*, 2011; Birse *et al.*, 2011). RNAi knockdown of DTKR (*dtkr*-RNAi) in the brain IPCs was shown to increase the expression of the *Drosophila* insulin-like peptide genes, *dilp2* and *dilp3*, while *dilp5* levels were shown to be increased upon *dtkr*-RNAi in the renal tubules. Reduced insulin signaling is shown to increase stress resistance and survival upon starvation (Broughton *et al.*, 2005). In line with the upregulation of *dilp* levels upon *dtkr*-RNAi, survival during starvation was shown to decrease upon *dtkr*-RNAi (Söderberg *et al.*, 2011; Birse *et al.*, 2011).

So far the best characterized function of *Drosophila* tachykinin signaling is its role in modulation olfactory perception. Based on the predominant expression of tachykinins in the local interneurons (LN) of the antennal lob, Winther and colleagues investigated a role for tachykinin signaling in olfactory processing and found that pan-neuronal RNAi knockdown of the drosophila tachykinin gene (*dtk*-RNAi) suppressed avoidance behavior of adult flies

towards high concentration of benzaldehyde, butanol and especially isoamyl acetate (Winther *et al.*, 2006). On the other hand, in larvae, which are attracted to these odors, *dtk*-RNAi resulted in indifference toward undiluted benzaldehyde or isoamyl acetate, whereas control animals were attracted. The reduced responsiveness to odors in *dtk*-RNAi animals was not due to impaired locomotor activity as *dtk*-RNAi animals were shown to be more active than control animals (Winther *et al.*, 2006; Kahsai *et al.*, 2010). These results indicated that in the fruit fly tachykinins regulate the sensitivity of specific odorants and concentrations. Since the tachykinin expressing LNs regulate the transformation of olfactory information through synaptic interactions with the olfactory receptor neurons (ORNs) and projection neurons (PNs), expression of the tachykinin receptor DTKR in these neurons was investigated. Indeed, using immunocytochemistry, expression of DTKR was shown to be localized in the cell bodies of the ORNs (Ignell *et al.*, 2009). Ignell and colleagues showed that calcium flux elicited by electrical stimulation of the ORNs is reduced upon the administration of DTKs. This reduction is abolished in flies with *dtkr* knockdown in the ORNs (Ignell *et al.*, 2009). In line with this, activation of the ORNs by methyl hexanoate and ethyl-3-hydroxybutyrate is reduced upon DTK administration, which is abolished by ORN specific *dtkr*-RNAi. Moreover, this modulation of ORNs by tachykinin signaling is translated into odor-guided behavior. Normally, flies are attracted to low concentrations of methyl hexanoate and ethyl-3-hydroxybutyrate, whereas they avoid high concentration of these odors. ORN specific *dtkr*-RNAi results in flies that remain attracted to high concentrations of methyl hexanoate and ethyl-3-hydroxybutyrate, while flies overexpressing this receptor are more sensitive to these odors (Ignell *et al.*, 2009). These results indicate that the ORNs are modulated presynaptically by tachykinin signaling, which behaviorally results in the modulation of the dynamic range in sensitivity to relevant odors. Recently, it was shown that besides the ORNs, DTKRs are also expressed in the tachykinin expressing LNs (Winther and Ignell, 2010). LN-specific *dtkr*-RNAi results in avoidance towards low concentrations of methyl hexanoate and ethyl-3-hydroxybutyrate, while control animals are attracted to these low concentrations (Winther and Ignell, 2010). Remarkably this is the opposite effect of ORN-specific *dtkr*-RNAi. These results suggest that in *Drosophila* tachykinin signaling acts in a disinhibitory network to modulate olfactory perception. According to this model, at low concentrations of the investigated odors, DTK from one

population of LNs inhibits the peptidergic release of LNs that send projections to the ORNs. Whereas at high concentrations this inhibition is relieved and the LNs will release DTK that inhibit the ORNs presynaptically (figure 5.1). However, so far the absence of connectivity of the DTK and DTKR expressing neurons in the antennal lobe remains uncharacterized making it impossible to elucidate the exact circuit in which tachykinin signaling regulates olfactory perception.

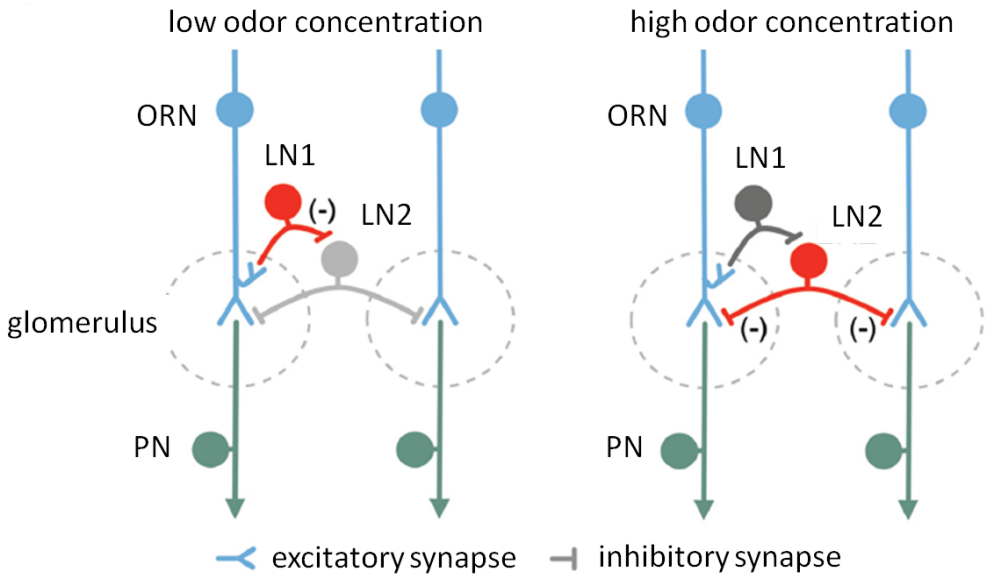

Figure 5.1 Hypothetical model of modulation of the olfactory circuit by tachykinin signaling in *Drosophila*. Two glomerular channels in the antennal lobe are depicted, symbolized by grey circles. Each channel consists of a synaptic connection between an ORN and a PN (blue and green respectively). Two populations of inhibitory LNs are represented: one that expresses the peptide DTK (LN1) and one that express DTK and the receptor DTKR (LN2). Active inhibitory LNs are colored red. At low odor concentrations LN1 suppresses the activity of a tonically active LN2 (depicted by -). Odor-evoked activity depresses LN1 and in the absence of inhibition LN2 suppresses ORNs presynaptically (depicted by -) (adapted from (Winther and Ignell, 2010).

In this chapter we aimed to explore the functions of tachykinin signaling in *C. elegans.* In order to gain more information about the identified tachykinin systems in *C. elegans* we first determined the expression pattern of both *C. elegans* tachykinin receptor genes, *tkr-1* and *tkr-2*, and of the T07C12.15 neuropeptide precursor gene. Based on the identified expression pattern and function of tachykinin systems in other organisms we investigated locomotion, learning and avoidance behavior in worms with impaired tachykinin signaling.

Because of the intriguing expression pattern of TKR-2 we focused on phenotypic characterization of *tkr-2* mutants.

5.2 Material and methods

5.2.1 Strains and cultivation

Strains were cultured at 20°C under standard conditions on NGM agar plates seeded with *E. coli* OP50. Worms were cultivated twice a week. As wild type strain N2 Bristol was used. Mutants were obtained from the *Caenorhabditis* Genetics Center and outcrossed to wild type N2. Mutant strains (x times crossed to N2) used in this chapter are listed in table 5.1.

Table 5.1 mutant strains used for phenotypic assays.

Strain name	Genotype (x times crossed to N2)
LSC711	*tkr-2(ok1620) (6x)*
LSC782	*tkr-1(ok2886) (4x)*
MT6308	*eat-4(ky-5)*
CX10	*osm-9(ky-10)*
VC1262	*osm-9(ok1677)*
MT150	*egl-3 (nt150)*

5.1.1 Linear reporter constructs

GFP and dsRed linear reporter constructs were generated by fusion PCR as described previously (Nelson and Fitch, 2011). Briefly, each fragment was amplified using PfuUltra II Fusion HS DNA Polymerase (Agilent Technologies). Promoter and gene fragments were amplified (with primers A and B) from genomic DNA of wild type *C. elegans.* The *gfp* or *dsRed* fragment together with a 3'UTR from *unc-54* were amplified (with primers C and D) from the pPD95.75 vector (Addgene) or pHC183 (Clontech), respectively. The specific primers used for the PCR amplification are listed in table 5.2.

Table 5.2 Gene specific primer sequences for generating linear reporter constructs

Primer	Sequence (5'-3')
pT07C12.15 A	ggaatgtattagacaacagt
*pT07C12.15 A**	tagacaacagttgctgtgt
pT07C12.15::GFP B	tcctgaaaatgttctatgttatgagccccgcccactttctg
pT07C12.15::GFP C	cagaaagtgggcggggctcataacatagaacattttcagga
pT07C12.15::dsRed B	gttctcggaggaggccatttgttcctcttgtccatcaaag
pT07C12.15::dsRed C	ctttgatggacaagaggaacaaatggcctcctccgagaac
GFP D	ggagctgcatgtgtcagaggtt
ptkr-2 A	cgaaattgtttcataggttccatg
*ptkr-2 A**	ttgccgaatattcccattg
ptkr-2::dsRed B	gttctcggaggaggccatcgattggaatgtacagttgatcag
ptkr-2::dsRed C	ctgatcaactgtacattccaatcgatggcctcctccgagaac
*dsRED D**	cggtcataaactgaaacgtaac
dsRED D	gcatgatttgacgtcatgagag

A T07C12.15 transcriptional reporter was generated by fusing a 1.6 kb sequence upstream of the T07C12.15 start codon with the full length T07C12.15 gene to the ORF of the *gfp* reporter gene. A T07C12.15 translational fusion construct was created by fusing the 2 kb promoter fragment and the full length T07C12.15 gene with the *dsRed* fragment. The *tkr-2* linear reporter construct was generated from a fusion of the *dsRed* reporter sequence and a 4.2 kb genomic fragment including a 3 kb sequence upstream from the *tkr-2* start codon as a promoter region and a genomic DNA fragment encoding the first exon and intron of *tkr-2*.

5.1.2 Reporter constructs using pSM vector

A vector based translational reporter construct was generated for the T07C12.15 gene and both *tkr-1* and *tkr-2* genes. For the receptors, a promoter region consisting of a 3.5 kb sequence upstream of the receptor start codons and the ORF each were cloned into the multiple cloning site of the pJG7-pSM-SL2-GFP vector (kindly provided by Cori Bargmann, Rockefeller University, New York, USA). Receptor promoter fragments were cloned between the NheI and KpnI restriction sites of the pJG7-pSM-SL2-GFP vector, whereas the ORF of the receptors were cloned between the BamHI and NheI restriction sites. Therefore, promoter- and gene-specific primers were designed with a 5' extension consisting of the restriction enzyme splice and docking (5'act3') sites (table 5.3). For the

putative promoter sequence of T07C12.15, a 1.6 kb fragment was amplified and cloned between the NheI and KpnI restriction sites of the pJG7-pSM-SL2-GFP vector, whereas the ORF of T07C12.15 was cloned between the BamHI and XbaI restriction sites.

Table 5.3 Primer sequences for amplification of gene fragments cloned into the pJG7-pSM-SL2-GFP vector.

Primer	Sequence (5'-3')
ctkr-1 Fw NheI	actgctagcatgaatcaagaattcttaattcaact
ctkr-1 Rev KpnI	actggtacctcaccgttcatggcaactca
Ptkr-1 Fw NotI	actgcggccgccattgggtttgtaatcaaaatg
Ptkr-1 Rev BamHI	actggatcctgcgtctgaaattatttatatactat
ctrk-2 Fw NheI	actgctagcatgacaacgtgtcccctacca
ctkr-2 Rev KpnI	actggtacctcagaaatccgtatgcgc
Ptkr-2 Fw NotI	actgcggccgcttgccgaatattcccattgatt
Ptkr-2 Rev BamHI	actggatcctctgaaacttgtagaatatttgaaacag
cT07C12.15 Fw NheI	actgctagcatgatctccaaatgttctgtgatg
cT07C12.15 Rev KpnI	actggtaccttattgttcctcttgtccatcaaag
PT07C12.15 Fw NotI	actgcggccgccacactgaacattacggctcata
PT07C12.15 Rev XbaI	acttctagaagccccgcccactttctg

5.1.3 Transgenesis

Transgenic strains were generated using standard injection techniques as described previously (Evans, 2006). Reporter constructs were purified by LiCl cleanup, and injected into the germline syncytium of young adult hermaphrodites using L4440 vector DNA as carrier DNA and a *Pelt-2::gfp* or *Pelt-2::mCherry* reporter construct as a coinjection marker. Final concentration of the injected DNA was 100 ng/µl. Strains generated for this project are listed in table 5.4.

Table 5.4 transgenic strains generated for this project.

Strain	Description
LSC635, LSC636, LSC637	*[PT07C12.15::gfp; Pelt-2::mCherry]*
LSC710	*[Ptkr-2::gfp; Pelt-2::gfp]*
LSC761	*[PT07C12.15::T07C12.15::SL2::gfp; Pelt-2::mCherry]*
LSC762, LSC763	*[Ptkr-1::tkr-1::SL2::gfp; Pelt-2::mCherry]*
LSC764, LSC765, LSC766	*[Ptkr-2::tkr-2::SL2::gfp; Pelt-2::mCherry]*

5.1.4 Expression pattern analysis

Animals were mounted on 2% agarose pads and immobilized with 5mM sodium azide. Expression patterns of fluorescent reporters were observed on an Olympus Fluoview FV1000 (IX81) confocal microscope. Confocal Z-stack images were processed using Imaris 7.2 (Olympus). Expression patterns were first analyzed by staining transgenes with the lyophilic dye DiI that stains the ASK, ADL, ASI, AWB, ASH and ASJ amphid neurons and PVQ phasmid neurons. By crossing transgenes with marker strains, the expression patterns were further determined based on colocalization with or relative position to cells expressing the fluorescent reporters in these marker strains. Marker strains used in this project are listed in table 5.5.

Table 5.5 Marker strains used in this project.

Strain	Reporter	Expression pattern	Obtained from
RJP601	*Pegl-13::gfp* and *Pegl-13::mCherry*	URXL/R and BAGL/R	Roger Pocock, University of Copenhagen, Copenhagen, Denmark
CX3465	*Psra-6::gfp*	ASHL/R, ASIL/R and PVQL/R	CGC
VM4264	*Pnmr-1::gfp*	AVAL/R, AVDL/R	Andres Villu Maricq, University of Utah, Salt Lake City, USA
OH3191	*Pgcy-7::gfp*	ASEL	CGC
	pgcy-8::mCherry	AFD	Miriam Goodman, Stanford University, Stanford, USA
GR1366	*Ptph-1::gfp*	ADF	CGC

5.1.5 Salt chemotaxis

Chemotaxis toward NaCl was tested using the quadrant plate assay (Jansen *et al.*, 2002). In this assay pairs of opposite quadrants of four-quadrant petri plates (Falcon X plate, Becton Dickinson Labware, Franklin Lakes, New Jersey, USA) were filled with buffered agar (1.7% agar, 5 mM KH2PO4/K2HPO4 pH 6.6, 1 mM CaCl2 and 1 mM MgSO4) supplemented with NaCl in one of both quadrant pairs. Salt chemotaxis was tested for 0.1, 100, 200, 300 or 400 mM NaCl. Assay plates were prepared fresh and left open to dry for 1 hour. Plates were closed to store for use on the same day. Right before the start of the assay, adjacent quadrants were connected with a thin layer of molten agar (without NaCl). Well-fed, young adult worms were washed off plates with CTX buffer (5 mM 6 KH2PO4/ K2HPO4 pH 6.6, 1 mM CaCl2 and 1 mM MgSO4), and washed three times with CTX over a period of 15 minutes. 100-200 worms were placed at the intersection of the assay plate and the distribution of animals over the quadrants was determined at 10 minutes. The chemotaxis index was calculated as (A-C)/(A+C), where A is the number of worms within the quadrants containing NaCl and C is the number of worms within the control quadrants (no NaCl). Salt chemotaxis assays were performed on three separate days. Results were determined using one-way ANOVA and Tukey post-hoc test, with the GraphPad software package.

5.1.6 Locomotion behavior

5.1.6.1 Velocity

Locomotion velocity was measured with the Parallel Worm Tracker. Young adult worms were transferred from the culture plate to an assay plate 20 minutes before measurements. Assay plates consisted of standard NGM agar, which was poured in 55 mm petri dishes one day before the assay. For on food velocity analysis plates were seeded with 50 µl of an overnight *E. coli* OP50 culture, which was allowed to dry for a few hours on room temperature. Worms were filmed individually for 20 seconds using a video recording system consisting of a Stingray F145B digital camera (ALLIED Vision Technologies) mounted on a stereomicroscope (Leica M165 FC, Leica Microsystems). The Matlab Image Acquisition Tool was used to control the camera and acquire AVI files for analysis by the Parallel Worm Tracker (Ramot *et al.*, 2008). The Parallel Worm Tracker identifies worms

according to predefined parameters such as contrast and amount of pixels. After positive identification of a worm, its centre was determined and centroid velocity was calculated. Statistical significance of the results was determined using one-way ANOVA and the Tukey post-hoc test, with the GraphPad software package.

5.1.1.1 Local search behavior

Local search behavior was analyzed using well-fed young adult worms. Worms were transferred from the culture plate to an unseeded intermediate plate and allowed to crawl away from the transferred bacteria before being transferred to the assay plate. Assay plates consisted of standard NGM agar, which was poured one day before the assay and allowed to dry on room temperature. Worms were filmed individually for 40 minutes using a video recording system consisting of a Stingray F145B digital camera (ALLIED Vision Technologies) mounted on a stereomicroscope (Leica M165 FC, Leica Microsystems). The Matlab Image Acquisition Tool™ was used to control the camera and acquire AVI files for analysis. Short reversals, long reversals and omega turns were scored manually as defined previously (Gray *et al.*, 2005). Statistical significance of the results was determined using a student t-test with the GraphPad software package.

5.1.2 Avoidance behavior

5.1.2.1 Drop-test

Avoidance for high osmotic strength or heavy metals was tested using a drop test with glycerol or $CuCl_2$ respectively (Hilliard *et al.*, 2002). In this assay, a small drop of repellent is delivered near the tail of a forward moving animal. Once in contact with the tail, the drop surrounds the entire animal by capillary action reaching the anterior sensory organs, which provokes an avoidance response. Repellents are dissolved in M13 buffer (30 mM Tris-HCl pH 7.0, 100 mM NaCl, 10 mM KCl) and delivered as a small drop (approximately 5 nl) using a 10 µl glass capillary pulled by hand on a flame to reduce the diameter of the tip. The avoidance index is calculated as the number of positive responses divided by the total number of trials. An avoidance response is defined as positive when the animal stops moving forward and reverses within 4 seconds. Assays were performed both on and off food. Assay plates consisted of standard NGM agar, which was poured freshly into 55 mm

petri dishes and allowed to dry with the lid open on room temperature. For on food assays, plates were seeded with 50 µl of an overnight *E. coli* OP50 culture and allowed to dry for one hour on room temperature with the lid open. For on food assays a single worm assay was performed. In this assay each animal was transferred to an individual assay plate 20 minutes before the experiments started and repeated drops were delivered to the same animal with an inter stimuli interval of at least two minutes between successive drops to the same animal. Each animal was tested with no more than 20 successive drops. For the off food drop test a population assay was used in order to be able to test the animals within 15 minutes, to prevent starvation. Prior to this assay, young adult animals were transferred to an unseeded plate and allowed to crawl away from the bacteria that were carried over. 10 animals per assay plate are transferred 10 minutes before the experiments started and each animal was tested only once. Assays were performed on at least 3 separate days. Statistical significance was determined using one-way ANOVA and the Tukey post-hoc test, with the GraphPad software package.

5.1.1.1 Smell-on-a-stick

To test avoidance for the volatile 1-octanol a smell-on-a-stick assay was performed (Chao *et al.*, 2004). In this assay young adult worms were transferred to an assay plate 20 minutes before the experiment started. Experiments were performed at 23°C. Assay plates consisted of standard NGM agar which was poured fresh and allowed to dry with the lid open for one hour on room temperature. For the assays with serotonin, serotonin (Sigma) was mixed into melted NGM agar at a final concentration of 4 mM. The blunt end of a hair from a Loew-Cornell (Teaneck, NJ) 9000 Kolinsky 7 paintbrush, taped to a Pasteur pipette, was dipped in 1-octanol and placed in front of the nose of a forward-moving animal. 1-octanol avoidance was analyzed by measuring the amount of time it took for an animal to initiate a reversal. 1-octanol was diluted fresh each day in ethanol. Experiments were performed on three separate days. Statistical significance was determined using one-way ANOVA and the Tukey post-hoc test, with the GraphPad software package.

5.1.2 Tap habitutation

For the tap habituation assay the Multi Worm Tracker was used, allowing the recording and analysis of *C. elegans* locomotion for up to 120 worms at the same time (Swierczek *et al.*,

2011). Approximately 100 young adult worms were collected in M9 buffer and transferred to a standard seeded NGM agar plate. The habituation protocol was then performed, with 30 taps with an inter stimulus interval of 10 seconds. Taps were administered to the side of the petri plate by a computer controlled mechanical solenoid, meaning that each tap is of the same magnitude (1-2 Newton) and duration. A software program named 'Beethoven' was used to analyze the habituation data for proportion of worms reversing, mean reversal duration, and speed. Tap habituation assays were performed on two separate days. Statistical significance was determined using one-way ANOVA and Tukey post-hoc test, with the GraphPad software package.

5.2 Results

5.2.1 *In vivo* localization of TKR-1, TKR-2 and T07C12.15

The transparency of *C. elegans* allows us to investigate gene expression patterns in whole animals using fluorescent reporter constructs. The well-defined anatomy of its nervous system makes it possible to analyze these expression patterns with single-cell resolution, providing valuable information to direct functional characterization of these genes (Chalfie, 1995; Boulin *et al.*, 2006; Bargmann, 2012). To determine the expression pattern for *tkr-2* both a transcriptional and translational reporter were used. Expression of the *Ptkr-2::dsRed* transcriptional reporter construct was only observed in the nervous system. Most fluorescent cell bodies were located in the head. Four pairs of neurons could be identified by overlap with GFP reporters with an identified expression pattern. Expression of the *Ptkr-2::dsRed* reporter construct in the AVA and AVD interneurons was identified based on the overlap with the *Pnmr-1::gfp* reporter (figure 5.2). Another pair of *Ptkr-2::dsRed* expressing head neurons could be identified as the sensory ASH neurons based on their overlap with a *Psra-6::gfp* reporter. The same reporter was used to determine the expression of *Ptkr-2::dsRed* in the sensory PVQ neurons in the tail (figure 5.2).

To verify this expression pattern a translational reporter construct for *tkr-2* was generated by cloning the promoter fragment and the *tkr-2* cDNA into the pJG7-psm-SL2-GFP vector. The expression pattern obtained using the vector based reporter construct mainly overlapped with the linear transcriptional *tkr-2* reporter construct. Using DiI staining, expression in the ASH, AVA and PVQ neurons could be validated and expression in the ADL, ASK and AIB

neurons could be determined based on overlap with and position relative to DiI labeled neurons (figure 5.3 and supplementary figure 2b).

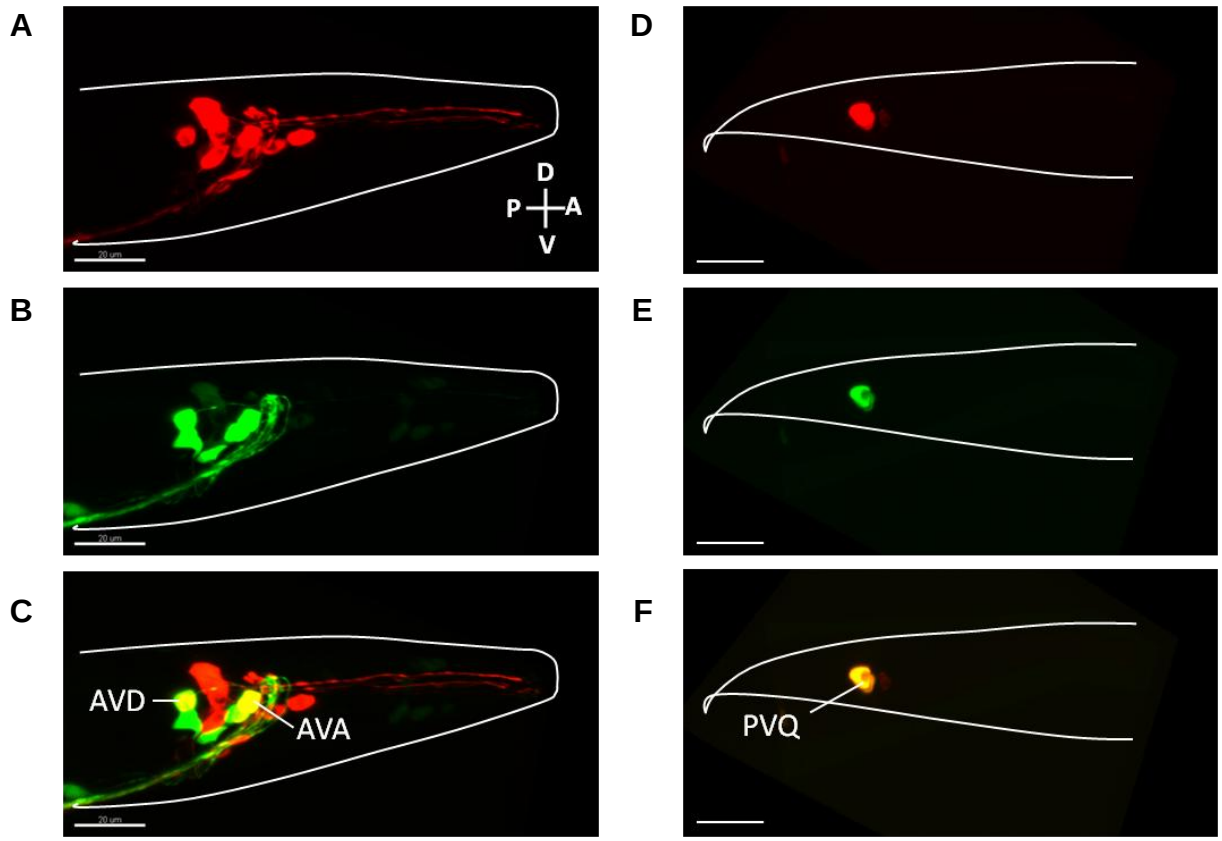

Figure 5.2 Identification of *Ptkr-2::dsRed* expression pattern by overlap with GFP reporter constructs. Confocal Z-stack projections of (A, B and C) the head and (D, E and F) tail region of an adult *Ptkr-2::dsRed* transgene. Expression pattern of (A) *Ptkr-2::dsRed,* (B) *Pnmr-1::gfp* and (C) overlap thereof. Expression pattern of (A) *Ptkr-2::dsRed,* (B) *Psra-6::gfp* and (C) overlap thereof. Scale bar represents 20 µm.

Expression of the *tkr-1* gene was investigated using a translational reporter construct which was generated by cloning a 3.2 kb fragment upstream of the *tkr-1* start codon as promoter region together with the *tkr-1* cDNA into the pJG7-pSM-SL2-GFP vector. Expression was only seen consistently in one pair of sensory neurons in the head, which were identified as the ASG neurons based on morphology and position relative to DiI labeled neurons (figure 5.3 and supplementary figure 2b).

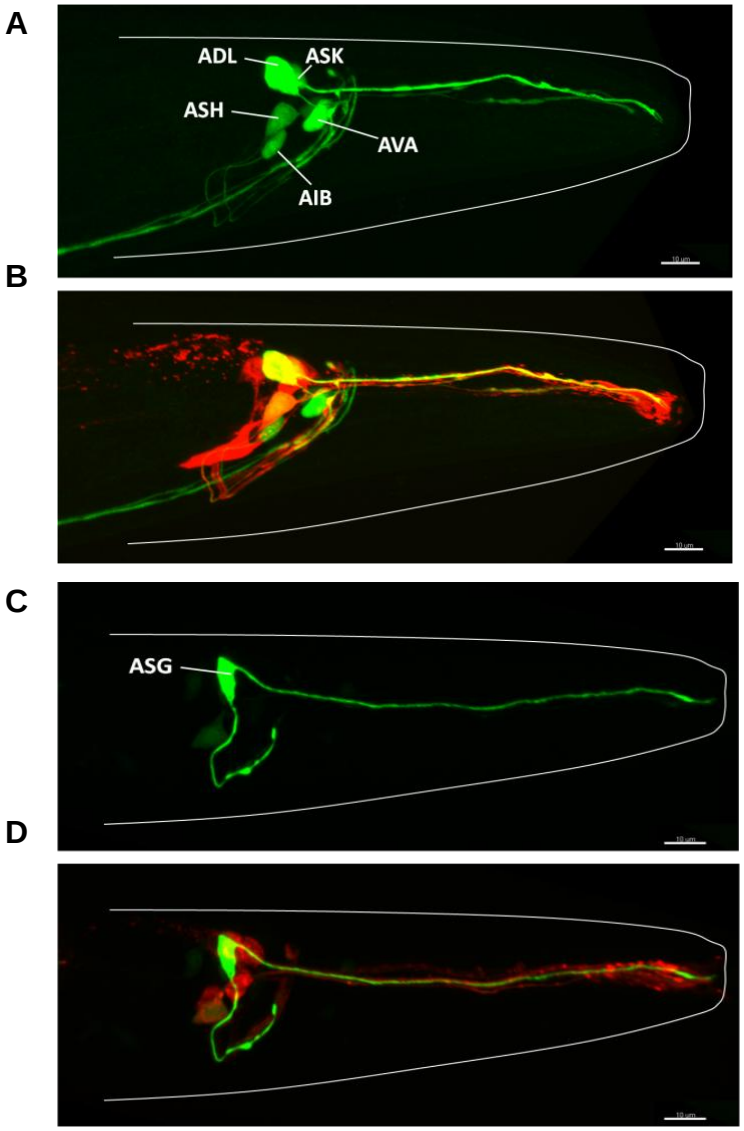

Figure 5.3 Identification of *Ptkr-2::tkr-2::SL2::gfp* and *Ptkr-1::tkr-1::SL2::gfp* expression pattern using DiI staining. Confocal Z-stack projections of head region of an adult (A,B) *Ptkr-2::tkr-2::SL2::gfp* and (C,D) *Ptkr-1::tkr-1::SL2::gfp* transgene. Expression of reporter is represented in green and DII staining in red. Scale bar represents 10 µm.

To determine the expression of the *T07C12.15* gene, both a transcriptional and translational fusion reporter construct were generated. No expression was observed in transgenes carrying the translational reporter. Expression of the T07C12.15 transcriptional reporter was observed in several neurons in the head, and often in the dorsal en ventral muscles in the head. No overlap was seen when *PT07C12.15::gfp* transgenic animals were stained with DiI, excluding the ASK, ADL, ASI, AWB, ASH and ASJ amphid neurons as the

PT07C12.15::gfp expressing neurons. Expression of *PT07C12.15::gfp* in the BAG neurons could be verified by overlap with *Pegl-13::mCherry* (figure 5.4). No overlap was seen when the *PT07C12.15::gfp* transgene was crossed with marker trains expressing a fluorescent reporter in AFD, ADF, ASE or URX.

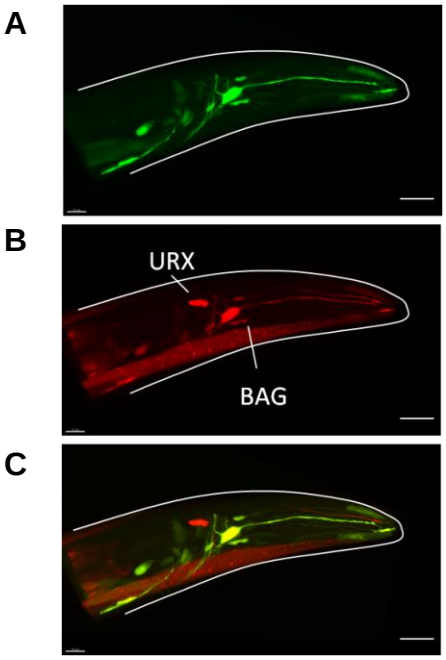

Figure 5.4 Identification of *PT07C12.15::gfp* expression pattern by overlap with mCherry reporter construct. Confocal Z-stack projections of the head region of an adult *PT07C12.15-2::gfp* transgene. Expression pattern of (A) *PT07C12.15::gfp,* (B) *Pegl-13::mCherry* and (C) overlap thereof. Scale bar represents 20 µm.

5.1.1 Salt chemotaxis

The sensory neurons expressing *tkr-1* and *tkr-2* have shown to mediate chemotaxis responses of *C. elegans* toward NaCl (Bargmann, 2006). *C. elegans* is attracted to low concentrations of salt, typically below 200 nM NaCl, but avoids high salt concentrations. To investigate whether *tkr-1* or *tkr-2* signaling is involved in chemotaxis toward NaCl, the quadrant plate assay was used (Jansen *et al.*, 2002). Worms were placed in the middle of the intersection of four quadrants and given the choice between opposite pairs of quadrants that were filed with control agar (without NaCl) or with NaCl-containing agar. NaCl chemotaxis of *tkr-1*, *tkr-2* and wild types worms was assayed for 0.1, 100, 200, 300 and 400 mM NaCl. The distribution of the worms over the four quadrants was determined after 10 min and represented by the chemotaxis index. For all NaCl concentrations tested no significant

difference in salt chemotaxis was determined between *tkr-1*, *tkr-2* and wild types worms (figure 5.5).

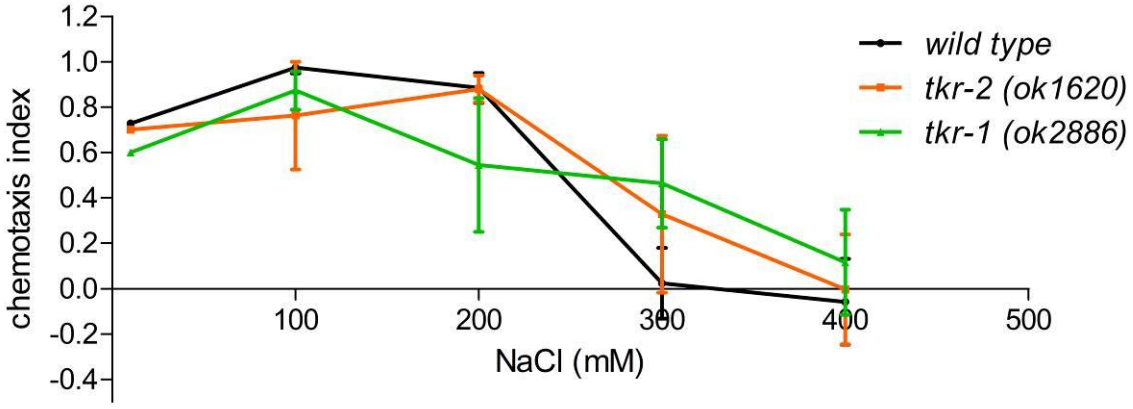

Figure 5.5 Salt chemotaxis of *tkr-1* and *tkr-2* mutants. Data represents mean chemotaxis index of wild type and mutant animals to increasing concentrations of NaCl, analyzed using the four quadrant chemotaxis assay (n = 3 assays, error bars represent standard error of mean).

5.1.2 Locomotion behavior

C. elegans explores its environment by interrupting its forward movement with occasional turns and reversals. Reversals are defined as backward movement, which are usually followed by a turn, which results in a change in direction. When the head of the worm touches the tail during turning, this is defined as an omega turn. The AVA and AIB neurons which were identified to express *tkr-2* are the main interneurons that regulate the execution of turning and reversals (Gray *et al.*, 2005; Piggott *et al.*, 2011; Pokala *et al.*, 2014). Inactivation of the AVA neurons results in worms which perform less reversals, whereas inactivation of the AIB neurons results in worms which execute less omega turns (Gray *et al.*, 2005). Moreover inactivation of AVA or AIB neurons reduces forward locomotion velocity with 50% or 25%, respectively (Pokala *et al.*, 2014). To address whether tachykinin signaling through *tkr-2* is involved in the regulation of forward locomotion, forward locomotion velocity of *tkr-2 (ok1620)* deletion mutant animals was analyzed and compared to that of wild type worms. Forward locomotion speed was analyzed on standard NGM agar plates both on food and off food. No difference was seen between the *tkr-2* mutants and wild type worms (figure 5.6). For both strains, the average velocity was approximately 0.1 mm/s on food and 0.2 mm/s off food.

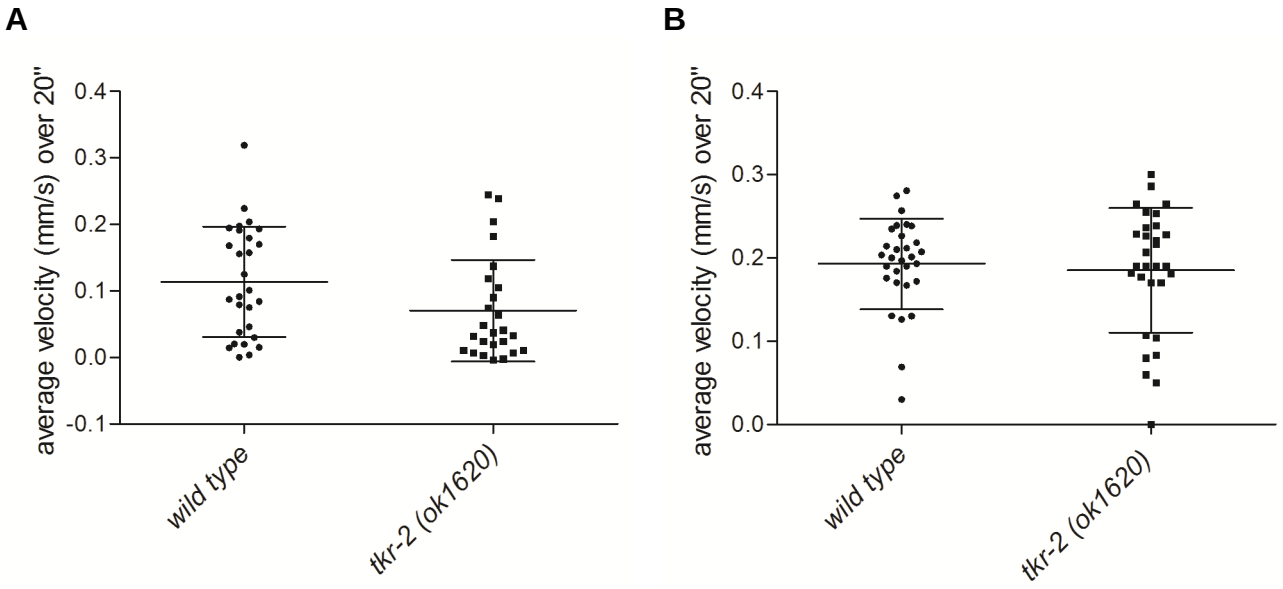

Figure 5.6 Average velocities of *tkr-2* mutants and wild type worms. Average velocity of forward moving worms was measured (A) on food and (B) off food ($n \geq 20$, error bars represent standard error of mean).

In order to investigate if TKR-2 signaling plays a role in the execution of turning and reversals we decided to analyze the local search behavior of *tkr-2* mutant animals (§ 2.2). Both the *tkr-2* expressing AVA and AIB interneurons play an important role in this behavior. Moreover, the olfactory AWC and *tkr-2* expressing gustatory ASK neurons were shown to be the main trigger of this local search behavior (Gray *et al.*, 2005). To investigate the involvement of *tkr-2* signaling in local search behavior, the frequency of short reversals, long reversals and omega turns were analyzed in the presence of food and when worms were removed from their food source. No significant differences in turning and reversal executions and frequencies could be determined between *tkr-2* mutants and wild type worms (figure 5.7). As described in literature, only short reversals were observed in the presence of food, whereas long turns and omega turns appeared upon removal from the food source.

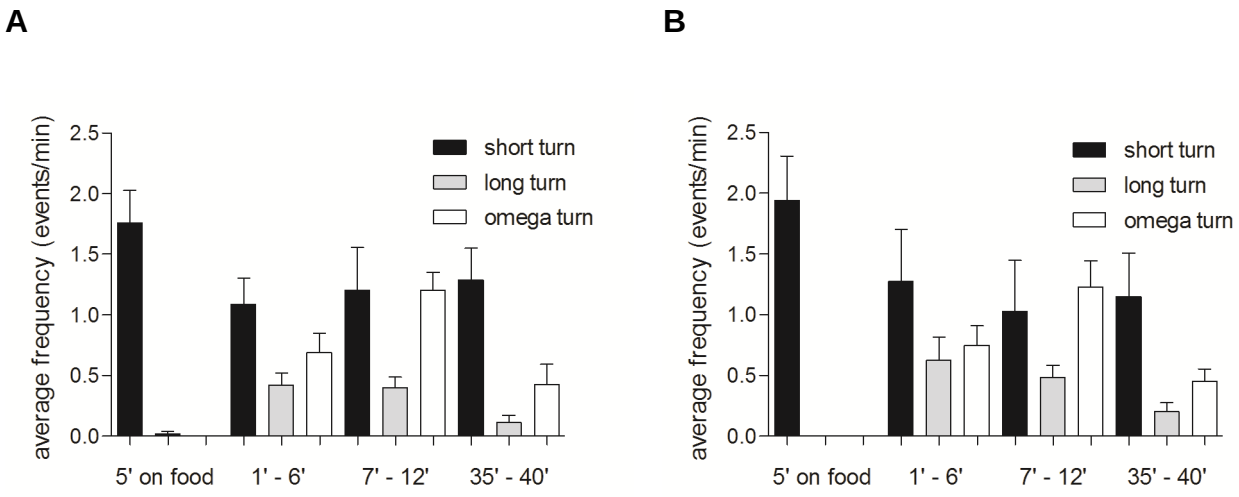

Figure 5.7 Local search behavior upon removal of food. Average frequency of short turns, long turns and omega turns was calculated for 5 minutes on food and off food during 3 time frames from 1 to 6 minutes, 7 to 12 minutes and from 35 to 40 minutes after removal of food for (A) wild type worms and (B) *tkr-2 (ok1620)* deletion mutants (error bars represent standard error of mean, $n \geq 9$).

5.1.3 Avoidance behavior

The sensory neurons ASH, ADL and ASK that were identified to express *tkr-2* are shown to be involved in sensing repellents and mediate avoidance behavior. The ASH neurons are the main nociceptor neurons which are shown to mediate avoidance from high osmotic strength, nose touch, volatile repellents, heavy metals, detergents, protons, high salt and alkaloids. ADL neurons regulate avoidance behavior from heavy metals, volatile repellents, high osmotic strength and detergents, whereas ASK neurons are involved in avoidance behavior from detergents, alkaloids and protons (Troemel *et al.*, 1997; Sambongi *et al.*, 2000; Hilliard *et al.*, 2002). Downstream to these nociceptors, the *tkr-2* expressing AIB and AVA interneurons regulate the executions of turning and reversal behavior in the avoidance response (§ 2.2). This intriguing expression pattern of *tkr-2* suggests a role for tachykinin signaling in avoidance behavior.

Involvement of *tkr-2* signaling in avoidance to hyperosmolarity, heavy metals and volatile repellents was tested using the drop-test (Hilliard *et al.*, 2002) and smell-on-a-stick assay (Chao *et al.*, 2004).

5.1.3.1 Drop-test

To test for impairments in avoidance from high osmotic strength or heavy metals, wild type worms and *tkr-2* mutants were challenged with a drop containing glycerol (0.5 and 1 M) or $CuCl_2$ (0.1 and 1 mM), respectively. Besides wild type worms and *tkr-2* deletion mutants, *eat-4 (ky5)* and *osm-9 (ok1677* or *ky10)* mutants were used as a positive control. *eat-4* encodes a glutamate transporter and *osm-9* a TRPV channel, which are both necessary for a proper avoidance response to glycerol and $CuCl_2$ (Colbert *et al.*, 1997; Berger *et al.*, 1998). To assess the avoidance response in the presence of food a single worm assay was used, which is in agreement to most drop-test assays in literature. No significant difference was noticed between the avoidance of *tkr-2* mutants and wild type worms when challenged with 0.5 and 1 M glycerol or with 1 and 10 mM $CuCl_2$ (figure 5.8). To assess avoidance behavior off food a population drop-test assay was performed, allowing to test sufficient worms within 15 minutes before starvation sets in. No significant difference was noticed between the avoidance of *tkr-2* mutants and wild type worms when challenged with any of the stimuli in the absence of food (figure 5.9).

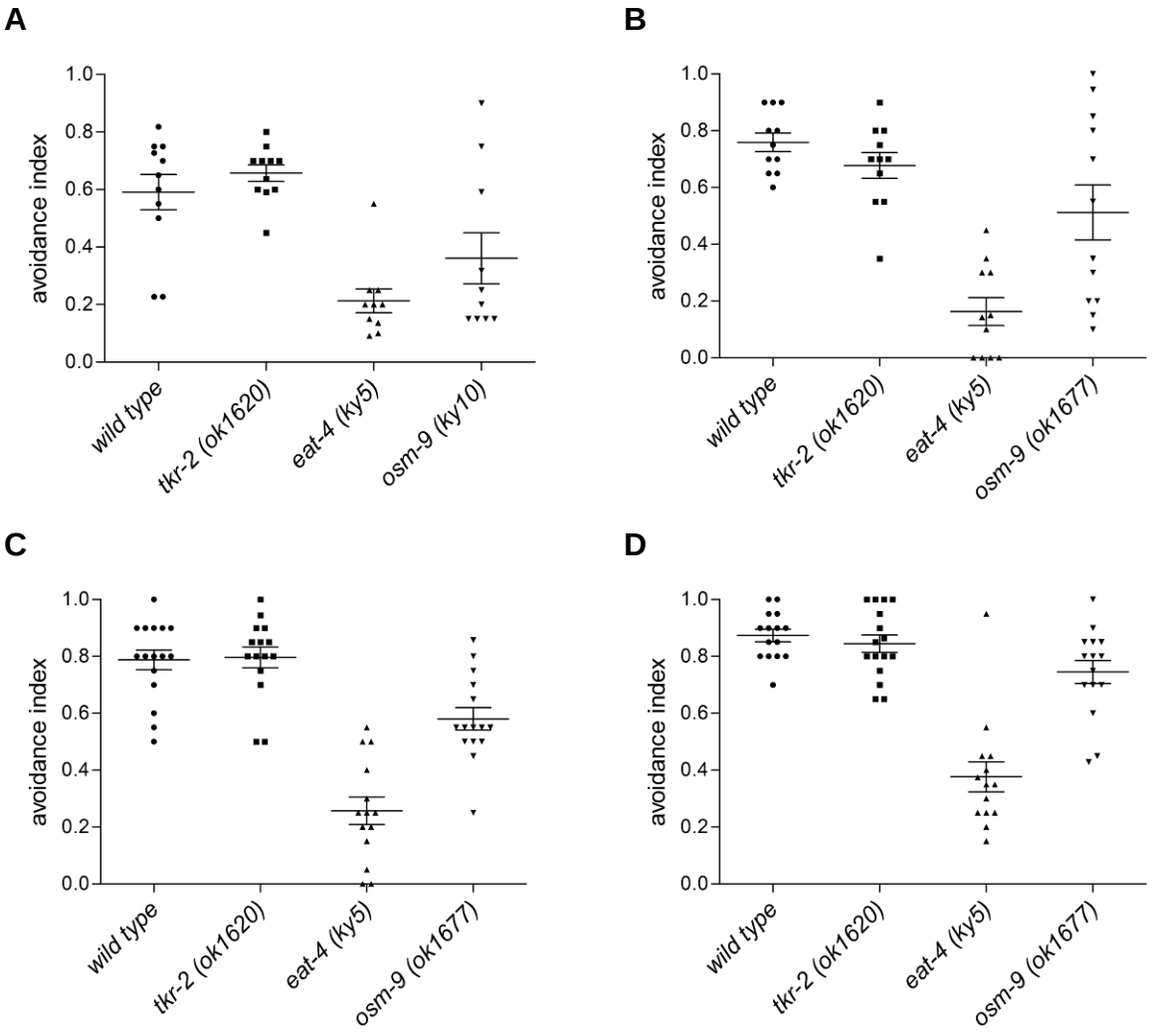

Figure 5.8 On food drop test. Each data point represents the avoidance index of an individual worm that was challenged with 10 successive drops with (A) 0,5 M glycerol, (B) 1M glycerol, (C) 1mM $CuCl_2$, (D) 10 mM $CuCl_2$ (data was collected on at least two different days, $n \geq 10$, error bars represent standard error of mean).

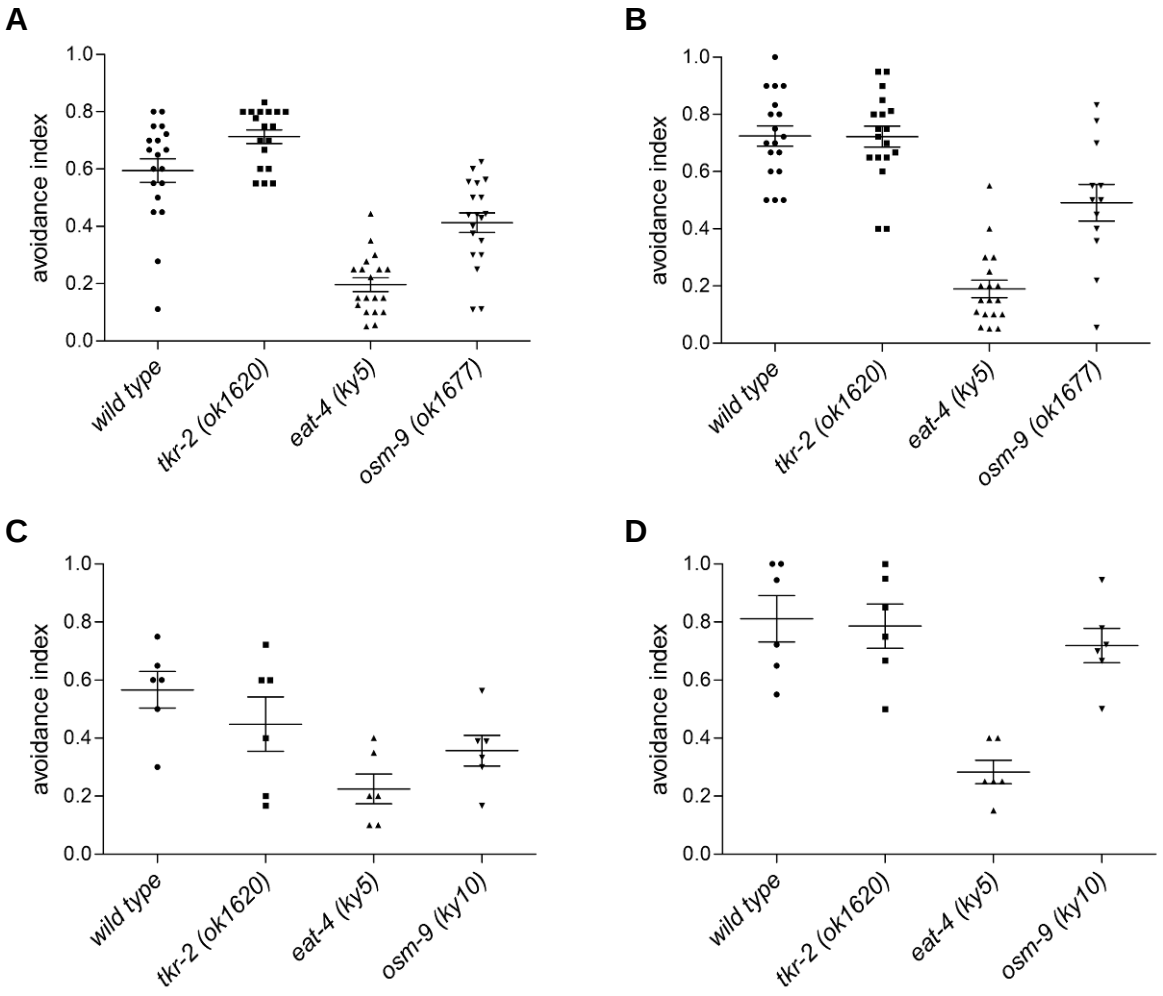

Figure 5.9 Off food drop test population assay. Each data point represents the avoidance index of a population of 10 worms when challenged with (A) 0,5 M glycerol, (B) 1M glycerol, (C) 1mM $CuCl_2$, (D) 10 mM $CuCl_2$ (Glycerol assays were performed on three different days, $n \geq 20$. $CuCl_2$ assay was only performed once, $n = 6$. Error bars represent standard error of mean).

5.1.3.2 Smell-on-a-stick

To assess avoidance to the volatile repellent 1-octanol a smell-on-a-stick assay was performed on standard NGM agar plates and plates supplemented with serotonin. The effect of food on several behaviors such as pharyngeal pumping, egg laying and locomotion can largely be recapitulated by the presence of exogenous serotonin (Chao *et al.,* 2004). Avoidance behavior to diluted (30%) 1-octanol is stimulated in the presence of food or serotonin, whereas the avoidance response to undiluted 1-octonal is similar off food as on

food/serotonin. However, off food only ASH seems to mediate the response to undiluted 1-octanol, whereas on food or serotonin ADL is engaged in this response as well.

Besides wild type worms and *tkr-2* deletion mutants *eat-4 (ky5), osm-9 (ok1677* or *ky10)* and the proprotein convertase *egl-3 (nt150)* mutants were used as a positive control. Off food *egl-3* mutants exhibit wild type avoidance to diluted 1-octanol. However, in the presence of 5-HT, *egl-3* mutants do not increase aversive responses to dilute 1-octanol (Harris *et al.*, 2010). No significant difference was noticed between the avoidance of *tkr-2* mutants and wild type worms when challenged with 30% or 100% 1-octanol both on standard NGM agar plates and plates supplemented with serotonin (figure 5.10).

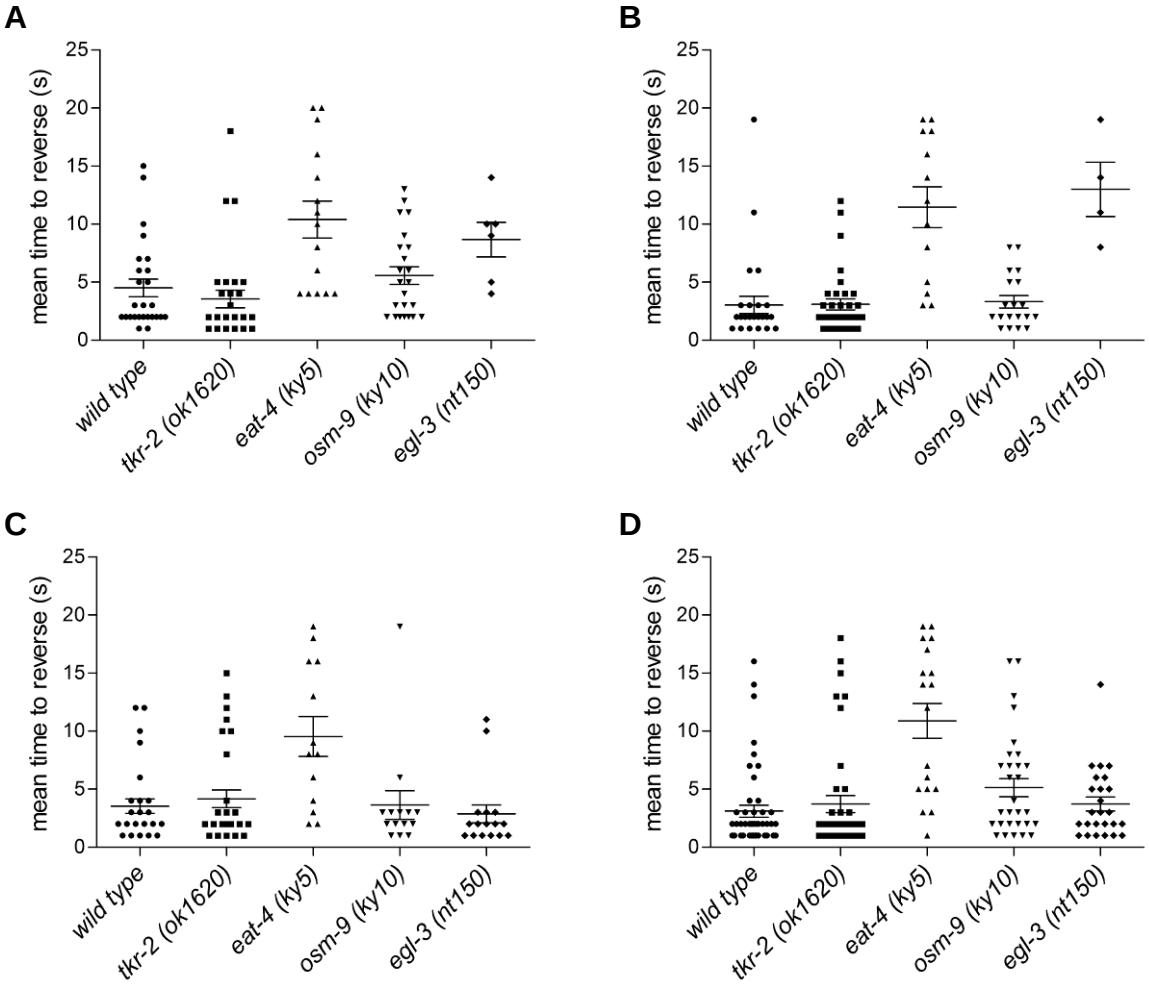

Figure 5.10 Avoidance from 1-octanol using the smell-on-a-stick assay. Data points represent the time to reverse for individual worms when challenged with (A) 30% 1-octanol and 4 mM serotonin, (B) 100% 1-octanol and 4 mM serotonin, (C) 30% 1-octanol and (D) 100% 1-octanol. (data was collected on at least two different days, n ≥ 10, error bars represent standard error of mean).

5.1.4 Tap habitutation

As no obvious role for *tkr-2* signaling in locomotion or avoidance could be determined in the previous assays, we wanted to investigate if *tkr-2* signaling could be involved in the modulation of behaviors dependent on the internal state of the animals, or context and previous experience of the stimulatory cue (Bargmann, 2012). One of the most robust and high throughput assays to test plasticity in *C. elegans* is the repeated tap withdrawal response (Swierczek *et al.*, 2011). Tapping the side of a culture dish causes a non-localized mechanical stimulus to which worms respond by a reversal response. However, after repeated tapping, the amplitude and frequency of the backward movement declines and worms habituate to the stimulus (Rankin *et al.*, 1990). The neuronal circuit underlying the tap withdrawal response has been identified 10 years ago. Wicks and Rankin showed that a non localized mechanical stimulus from a tap activates both the anterior and posterior mechanosensory neurons (ALM, AVM, PLM, and PVD), which activate the interneurons (AVD, AVA, AVB, PVC, and DVA) mediating the tap withdrawal response (Wicks and Rankin, 1995). In 2003, Suzuki and colleagues demonstrated that repeated activation could alter the response properties of the mechanosensory neurons, indicating that habituation happened at the level of the sensory neurons (Suzuki *et al.*, 2003). Rankin and Wicks found that disrupting glutamate transmission alters habituation to tap. *eat-4* mutants, which are deficient in glutamergic transmission have wild type tap withdrawal behavior, but habituate to tap more quickly and fail to dishabituate following a brief electric shock (Rankin and Wicks, 2000). This suggests that modulation of glutamate release is an important component of mechanosensory habituation, perhaps downstream from cell excitability or as part of a parallel pathway. Recently, Cai and colleagues showed that the activity reduction after repeated stimulation was mediated by phosphorylation and subsequent inhibition of potassium channels in the mechanosensory cells, which dampens cells excitability (Cai *et al.*, 2009).

The involvement of *tkr-2* signaling in tap habituation was investigated by Evan Ardiel at the lab of Catharine Rankin (University of British Columbia, Vancouver, Canada). To investigate if *tkr-2* singaling modulates tap habituation, the proportion reversing, reversal duration and reversal speed were analyzed when petri dishes harbouring the worms were tapped with an interstimulus interval of 10 seconds for 5 minutes. No significant differences

in initial tap response or habituation could be determined between *tkr-2* mutants and wild type worms (figure 5.11). As described in literature, when taps were applied, initially nearly all worms responded with large reversals, but with repeated taps the proportion of worms responding and size of responses decreased.

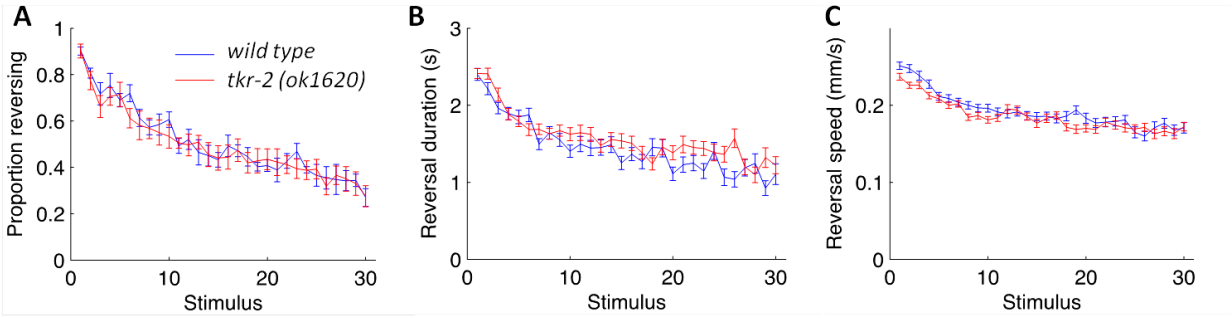

Figure 5.11 Foraging behavior during tap habituation for wild type worms and *tkr-2* mutants. Taps were given every 10 seconds for 5 minutes. Three different tap response metrics were analyzed: (A) proportion of the population reversing, (B) average reversal duration, and (C) average reversal speed (error bars represent standard error of mean, n > 60).

5.2 Discussion and conclusion

5.2.1 *In vivo* localization

In order to gain more insight into the functions of the *C. elegans* tachykinin system, we aimed to identify the cellular expression pattern of the T07C12.15 neuropeptide precursor gene and both *tkr-1* and *tkr-2* genes. To investigate the expression pattern of the tachykinin precursor, both transcriptional (*PT07C12.15::gfp*) and translational (*PT07C12.15::T07C12.15::dsRed* and *PT07C12.15::T07C12.15::SL2::gfp*) reporter constructs were generated of the T07C12.15 peptide precursor. Only the transgenes carrying the transcriptional reporter construct had a clear expression of the fluorescent reporter. Up till now only one pair of neurons, the BAG neurons, could be identified. In line with this, Hallem and coworkers showed an enrichment with a 3.75 fold change of the T07C12.15 transcript in embryonic BAG neurons compared to other embryonic neurons (Hallem *et al.*, 2011). The sensory BAG neurons were demonstrated to be involved in reproduction, lifespan, oxygen sensing and carbon dioxide sensing. BAG neurons have shown to inhibit egg-laying through the release of *flp-17* encoded peptides, which act on the EGL-6 receptors

that localize in the HSN neurons. Activation of EGL-6 is suggested to inhibit HSN and thereby egg-laying (Ringstad and Horvitz, 2008).

In vivo calcium imaging shows that BAG neurons are activated by elevated carbon dioxide levels, and upon the decrease of oxygen concentration (Zimmer *et al.*, 2009; Bretscher *et al.*, 2011). Activation of the BAG neurons by elevated levels of carbon dioxide depends on the cGMP-gated channel units TAX-2/TAX-4 and the guanlylate cyclase GCY-9 (Hallem *et al.*, 2011). On the other hand, activation of BAG neurons by an oxygen downshift seems to depend on the expression of the guanylate cyclases GCY-31 and GCY-33 (Zimmer *et al.*, 2009). Recently it was demonstrated that elevated levels of carbon dioxide (5%) and moderately low oxygen (4-12%) levels extends lifespan in *C. elegans* (Sharabi *et al.*, 2009; Liu and Cai, 2013). In line with this, ablation of the carbon dioxide sensing BAG neurons extend lifespan as well (Liu and Cai, 2013)

Expression of *tkr-1* was investigated using a vector-based translational reporter (*Ptkr-1::ctrk-1::SL2::GFP),* which was expressed in the sensory ASG neurons. ASG neurons are involved in chemotaxis to NaCl, a behavior that is enhanced under hypoxia (Bargmann, 2006; Pocock and Hobert, 2010). Pockock and Hobert showed that the hypoxia-enhanced chemotaxis to NaCl is due to enhanced gustatory sensory perception of the ASG sensory neurons. More specifically, this seems to be mediated by the upregulation of serotonin synthesis in the ASG neurons. Furthermore, the ASG neurons modulate lifespan and entry into the dauer stage (Bargmann and Horvitz, 1991; Schackwitz *et al.*, 1996; Alcedo and Kenyon, 2004)

Using a linear transcriptional (*Ptkr-2::dsRed*) and a vector-based translational (*Ptkr-2::tkr-2::SL2::gfp*) reporter construct, expression of *tkr-2* was identified in the ASH, ADL, ASK and PVQ sensory neurons and in the AVA and AIB interneurons. Remarkably, the expression pattern of *tkr-2* overlaps with the main neurons involved in the neuronal circuit that guides avoidance behavior in *C. elegans.* The sensory TKR-2 expressing ASH neurons are polymodal nociceptor neurons, involved in sensing high osmotic strength, nose touch, volatile repellents, heavy metals, detergents, protons, high salt and alkaloids. The sensory ADL neurons which were also shown to express *tkr-2* mediate avoidance behavior from heavy metals, volatile repellents, high osmotic strength and SDS (Troemel *et al.*, 1997;

Hilliard *et al.*, 2002). ASK neurons mediate avoidance behavior from detergents, alkaloids and protons (Troemel *et al.*, 1997; Sambongi *et al.*, 2000; Hilliard *et al.*, 2002).When encountering a noxious stimulus, *C. elegans* exerts an avoidance response by stopping locomotion, reversing away from the noxious stimulus and turning to move away from the stimulus. This avoidance response is shown to be mediated by interaction of the AVA, AVB, AVD, PVC, AIB and RIM interneurons, that activate and inhibit the appropriate motor neurons to guide escape behavior (§4 2.2) (Piggott *et al.*, 2011; Donnelly *et al.*, 2013; Pokala *et al.*, 2014).

5.1.1 Functional characterization

Since sensory neurons shown to express *tkr-1* and *tkr-2* are reported to be involved in the chemotaxis response of *C. elegans* toward NaCl (Bargmann, 2006), chemotaxis to different concentrations of NaCl was investigated. Neither *tkr-2*, nor *tkr-1* mutants showed a different chemotaxis behavior compared to wild type worm indicating that impaired tachykinin signaling does not interfere with sensing of NaCl and the subsequent attraction or avoidance response.

Based on the identified expression pattern of *tkr-2* we primarily investigated a putative role for *tkr-2* signaling in the regulation of locomotion and avoidance behavior in *C. elegans.* By investigating local search behavior, we showed that impaired *tkr-2* signaling had no effect on the execution of reversals and turns and the initiation of local search behavior upon the removal of food. Measurement of locomotion velocity showed that *tkr-2* signaling does not influence velocity of spontaneously forward moving worms, neither on food nor off food. Involvement of *tkr-2* signaling in avoidance to hyperosmolarity or heavy metals was tested for glycerol (0.5 and 1 M) or $CuCl_2$ (0.1 and 1 mM) using the drop-test assay, whereas avoidance to volatile repellents was tested for 1-octanol using the smell-on-a-stick assay. No difference was determined between wild type worms and *tkr-2* mutants indicating that *tkr-2* signaling does not compromise the detection of these repellent and the subsequent aversive response. Besides directed stimuli that cause avoidance, analysis of the tap withdrawal response or habituation to tapping was tested as well. *tkr-2* mutants were shown to respond normal to tapping and tap habituation.

Localization of *tkr-2* suggests that *tkr-2* signaling is involved in the regulation of nociception in *C. elegans.* We showed that *tkr-2* signaling is not required to sense tapping, hyperosmolarity, heavy metals or volatile odors and the subsequent aversive responses to these cues. However, expression in both sensory and interneurons of the neuronal avoidance circuit pattern suggest a neuromodulatory role for *tkr-2* signaling in avoidance behavior. In line with this hypothesis, members of our lab recently demonstrated that the avoidance response upon optogenetic activation of the polymodal nociceptor ASH is increased in *tkr-2* deletion mutants, indicating that *tkr-2* signaling suppresses ASH mediated avoidance (Watteyne J., personal communication).

Neuromodulators shape neuronal circuits by transforming the intrinsic firing properties of circuit neurons and alter effective synaptic strength (Bargmann, 2012; Civelli *et al.*, 2013). Based on the expression of the tachykinin precursor in the low oxygen and high carbon dioxide sensing neurons, it would be interesting to test if avoidance behavior is modulated by these environmental cues and if *tkr-2* signaling is involved in this modulation.

5.1.2 Conclusion

Using fluorescent reporters we were able to identify the cellular expression pattern of both *tkr-1* and *tkr-2. tkr-1* was identified to be expressed in the ASG sensory neurons, involved in the enhancement of salt chemotaxis under hypoxic stress. Expression of *tkr-2* was determined in the sensory ASH, ASK, ADL and PVQ neurons, and the AVA and AIB interneurons, indicating the potential involvement of *tkr-2* signaling in nociception. So far involvement of tachykinin signaling could not be found in salt chemotaxis, or avoidance to tapping, hyperosmolarity, heavy metals or volatile odors.

Chapter 6. General discussion and conclusion

The nematode *C. elegans* was introduced almost half a century ago as a model organism to investigate how genes encode for complex structures such as the nervous system. Today this tiny animal required the status of super model as it is being investigated in several scientific disciplines ranging from systems biology to genetics. Several genetic pathways identified in *C. elegans* have contributed to a better understanding of various fundamental biological processes. For instance, the genes that control programmed cell death were first identified in *C. elegans* and subsequently shown to be conserved throughout the entire animal kingdom (Ellis and Horvitz, 1986; Yuan *et al.*, 1993). These findings had important implications for understanding normal development as well as human diseases such as cancer, autoimmune and neurodegenerative diseases. The power of using *C. elegans* as a model organism to investigate biological processes is especially appreciable in the field of neuroscience. For example, several key proteins required for synaptic functioning have first been discovered in nematodes (Maruyama and Brenner, 1991; Hosono *et al.*, 1992; Alfonso *et al.*, 1993; Lesa *et al.*, 2003; Richmond *et al.*, 2008).

The functional properties of the nervous system are largely determined by the structure and connectivity between neurons, however unraveling this connectivity map is usually hampered by the complexity of the neural network in most organisms. Compared to the human brain, which is estimated to contain 86 billion neurons and 100 trillion synapses (Azevedo *et al.*, 2009), the anatomy of the nervous system of *C. elegans* is relatively simple. The connectome of its somatic nervous system consist of 282 neurons and approximately 6000 chemical synapses (White *et al.*, 1986; Varshney *et al.*, 2011). This neuronal wiring diagram allows researchers to dissect the neural circuits underlying behavioral and physiological processes, and investigate the molecular pathways that mediate them. Completion of the *C. elegans* genome sequence in 1998 demonstrated that almost all gene families involved in neuronal functioning in vertebrates are present in this roundworm as well, indicating that this genetic model may help us to elucidate the cellular and molecular pathways they mediate in (Bargmann, 1998).

Neuropeptides play an important role in several physiological and behavioral processes such as nociception, sleep, learning and aging. As a consequence of this diverse range of functions, they also contribute to multiple pathological processes. Since neuropeptide

GPCRs have ligand-binding and allosteric modulatory sites located on the outer cell surface membrane that are easily accessible to pharmacological agents, neuropeptide systems are highly investigated by the pharmaceutical industry as potent drug targets. However, incomplete understanding of the pathways they mediate, has hampered the successful identification of potent drugs, as most of them cause many side effects (Rask-Andersen *et al.*, 2013). Although many advantages have been made in the field of neuroscience using vertebrate models, elucidating neuropeptide functioning at the cellular and systems level is usually hampered by the complexity of the anatomy of the organism and the multiple functions they mediate. However, the evolutionary conservation of neuropeptide systems allows us to elucidate their fundamental features in less complex organisms such as *C. elegans* and help us to speed up neuropeptide research in vertebrates.

6.1 Neuropeptidergic signaling in C. elegans

In this thesis, the first aim was to elucidate novel neuropeptide systems in *C. elegans* (**chapter 3**). First, we revised the current estimation of the repertoire of neuropeptide GPCRs encoded in the genome of *C. elegans.* In order to obtain an accurate overview of *C. elegans* neuropeptide GPCRs, we repeated the MEME/MAST analysis performed by Janssen and colleagues using an updated training set, containing all 23 neuropeptide GPCRs that had been deorphanized at the start of this project. This prediction allowed us to identify 129 potential neuropeptide GPCRs, which matched largely with the current list available on WormAtlas (**chapter 3**). In line with other metazoan neuropeptide GPCRs, all 129 predicted neuropeptide GPCRs could be classified to the Rhodopsin or Secretin GPCR family (Schiöth and Fredriksson, 2005). Based on sequence similarities to known neuropeptide GPCRs, we were able to subdivide these receptors to NPY/RFamide-; somatostatin- and galanin-; tachykinin-; CCK-, GnRH- and OT/VP-; neurotensin, NMU, growth hormone secretagogue, and TRH-like receptors according to the classification adapted by Altun (Altun, 2011).

Even though our MEME/MAST analysis did only identify a handful of GPCRs that had not been annotated before as hypothetical neuropeptide receptors, we believe that novel predictions could ameliorate the current list and eliminate false positive predicted or predict novel neuropeptide GPCRs. For example, AEX-2 which was recently shown to be activated

by NLP-40 peptides, was not annotated as a neuropeptide GPCR in our list (Wang *et al.*, 2013). The performed MEME/MAST prediction has the advantage that it is relatively simple to perform and may identify specific features, such as G protein-binding sites, of *C. elegans* neuropeptide GPCRs. However, one major drawback is that the prediction is biased towards the characterized *C. elegans* receptors. Most neuropeptide GPCR predictions use a phylogenetic strategy. Here, common motifs of neuropeptide GPCRs identified in other species are used to scan genome databases to identify sequences harboring these motifs. This strategy has the advantage that it can help to recognize the evolutionary relationship between sequences, but possibly is not able to identify neuropeptide GPCRs which have diverged significantly or do not exist in these species (Strotmann *et al.*, 2011).

From the revised *C. elegans* neuropeptide GPCR list we choose three groups of receptors, related to GnRH/AKH, tachykinin and Neuromedin U receptors, for further characterization. Using a reverse pharmacology strategy, we were able to identify activating ligands for four receptors, more particularly: (1) the GnRH/AKH-like receptor GNRR-3 responds to the RPamides NLP-2a, NLP-2b, NLP-2c, NLP-22 and NLP-23b, (2 and 3) the *in silico* predicted *C. elegans* tachykinins, encoded by T07C12.15, are able to activate the tachykinin-like receptors TKR-1 and TKR-2 dose-dependently with EC_{50} values in the nanomolar range and (4) the NMUR-like receptor NMUR-1 is activated by the *C. elegans* CAPA peptides NLP-44-1 and NLP-44-3. These deorphanizations bring the number of characterized *C. elegans* neuropeptide GPCRs to 31.

The identified tachykinin- and NMU-like peptide systems support the theory of receptor-ligand coevolution. According to this theory receptor-ligand pairs have an ancient origin and coevolved in order to maintain optimal receptor-ligand binding and activation (Janssen *et al.*, 2010; Mirabeau and Joly, 2013; Jékely, 2013). The idea that neuropeptide systems could be conserved throughout the entire animal kingdom was introduced in the early nineties, when several invertebrate peptides were isolated that shared sequence similarities with known vertebrate neuropeptides (De Loof and Schoofs, 1990). The identification of neuropeptide GPCRs and analysis of their sequences substantiated this hypothesis (Hoyle, 1998; Darlison and Richter, 1999). With the publication of the *D. melanogaster* and *C. elegans* genomes, it became possible to browse through it and identify their entire neuropeptide and

neuropeptide GPCR repertoire (Bargmann, 1998; Vanden Broeck, 2001; Hewes and Taghert, 2001). However, although several predicted invertebrate GPCRs seemed to be related to vertebrate neuropeptide receptors, their corresponding neuropeptides could often not be identified. This was initially attributed to an apparent lack of ligand coevolution and it was proposed that these receptors could have acquired novel ligands. Nevertheless, using a reverse pharmacology assay, in which these orphan GPCRs are used as a hook to fish out their cognate ligands from a compound library, several invertebrate neuropeptide systems could be identified. (Mertens *et al.*, 2004b; Janssen *et al.*, 2010; Caers *et al.*, 2012; Frooninckx *et al.*, 2012). Moreover, detailed sequence analysis of the peptide ligands suggested that they do show sequence similarities with vertebrate peptides that bind related neuropeptide GPCRs, supporting the idea that they have a common origin (Janssen *et al.*, 2010). Phylogenetic reconstruction of bilaterian neuropeptide and neuropeptide GPCR families further substantiated the theory of receptor-ligand coevolution (Mirabeau and Joly, 2013; Jékely, 2013).

In line with the theory of receptor-ligand coevolution, Lindemans and colleagues showed that the neuropeptide NLP-47, which is able to activate the *C. elegans* AKH/GnRH-like receptor GNRR-1, resembles both GnRH and AKH peptides (Lindemans *et al.*, 2009b). Remarkably, phylogenetic analysis shows that the genome of *C. elegans* encodes eight GnRH/AKH-like receptors (GNRR-1 to GNRR-8). According to our phylogenetic reconstruction, GNRR-2 to GNRR-8 seem to be evolved from nematode-specific duplications of the bona fide GnRH/AKH-like receptor GNRR-1. In order to shed light on their relationship, we cloned all GNRRs predicted to have a 7TM topology and used a reverse pharmacology approach to identify peptides that could activate these receptors. Only one receptor, GNRR-3, responded when challenged with our peptide library. GNRR-3 was activated by 5 neuropeptides (NLP-2a, NLP-2b, NLP-2c, NLP-22, NLP-23b), which all have a common C-terminal RPamide and seem to be highly conserved among nematodes. However, the RPamides do not resemble the previously identified GnRH/AKH-like NLP-47 and sequence resemblance of these neuropeptides to other GnRH/AKH-like peptides is restricted to the C-terminal amidation and a conserved glycine and proline. Based on the principle of receptor-ligand coevolution, one could expect that together with the highly diverged GnRH/AKH-like receptor, cognate ligands may have diverged equally, rendering

it almost impossible to elucidate their evolutionary relationship (Strotmann *et al.*, 2011). On the other hand one cannot exclude the possibility that the RPamides are not related to the GnRH/AKH peptide family, but instead acquired the capacity to bind the nematode specific GnRH/AKH-like receptor by convergent evolution. Identification of the ligands of the remaining orphan GNRRs will help us to elucidate their relationship to other neuropeptide systems.

6.2 The science of sleep

Sleep is an intriguing behavior that has fascinated scientists for centuries. Although we all seem to know the general consequences of reduced sleep, we still don't fully understand why we sleep and how it is regulated. Living in a world with increasing economic and social demands, we are rapidly evolving into a 24-h society. Frequently disrupted and restricted sleep is a common problem for many people in our modern around-the-clock society. Sleep deprivation studies demonstrate the profound negative impact of sleep loss on mood, cognitive performance, motor function, metabolism and immune system (Knutson *et al.*, 2007; Spiegel *et al.*, 2009; Palma *et al.*, 2013). As a consequence, the appreciation for understanding the molecular regulation of sleep is rising. In contrast to initial assumptions, sleep is not simply the passive absence of wakefulness, but it is an actively regulated process that requires the coordinated activity of neuronal circuits.

In mammals, sleep and wakefulness are regulated by specific sleep- and wake-promoting neurons in the brains. Sleep is promoted by the core neurons of the ventrolateral preoptic nucleus (VLPO), while neurons from the ascending reticular activating system mediate arousal. These sleep and wake promoting neurons are mutually disinhibitory and suggested to act as an electrical flip-flop switch. In this model disinhibitory neurons turn each other off when they obtain a small advantage over the others, thereby assuring a rapid and complete transition of sleep-wake states (Saper *et al.*, 2010). The coordination of these neuronal circuits requires multiple neurochemical systems, including classical neurotransmitters and neuropeptides. The core neurons of the sleep-promoting VLPO project heavily to wake promoting GABAergic/histaminergic neurons of the tuberomammillary nucleus (TMN), serotonergic neurons of the dorsal raphe nucleus (DR), and norepinephrine neurons of the locus coeruleus (LC). The VLPO neurons are active during sleep and shown to inhibit

TMN, DR and LC neurons through the release of GABA and galanin, whereas serotonin and norepinephrine inhibit most VLPO neurons (Brown *et al.*, 2013). Similarly, histamine excites a subpopulation of inhibitory interneurons in the VLPO and thereby causes an indirect inhibition of the VLPO projection neurons. In addition, histamine neurons utilize GABA as a co-transmitter. Wake promoting neurons are stabilized by lateral hypothalamic (LH) excitatory orexinergic neurons, which in turn are inhibited by release of GABA and galanin from the VLPO neurons (Fuller *et al.*, 2006; Saper *et al.*, 2010; Brown *et al.*, 2013). Several processes act on these sleep and wake promoting brain areas in order to obtain consolidated bouts of sleep and wakefulness. Sleep timing, length and depth are regulated by circadian and homeostatic processes, and depend on the internal physiological state and environmental stimuli. Neuropeptides play an important role in the coordination of the global nature of sleep and wake states. They integrate physiological subsystems such as circadian time, energy homeostasis, and stress to generate appropriate sleep-wake behaviors. However, the multifunctionality of neuropeptides and complexity of brain structures, hampers progress in elucidating how they regulate the neural circuits underlying sleep and wake behavior.

Sleep is mainly investigated in mammals, however the appreciation that sleep could be conserved throughout the animal kingdom, allows scientists to investigate the molecular mechanisms underlying the regulation of sleep using model organisms with a simple and well defined anatomy and a powerful genetic toolbox (Zimmerman *et al.*, 2008). Beside *C. elegans* (discussed in **chapter 2**), the presence of a sleep-like state has been described in other non-mammalian model organisms as well. The zebra fish *Danio rerio* shows a sleep-like state that is characterized by reversible periods of quiescence that cycle with a circadian rhythm, being active during the day and resting at night (Yokogawa *et al.*, 2007). In the fruit fly *Drosophila melanogaster* rest meets the behavioral criteria of sleep (Hendricks *et al.*, 2000a). Several neuropeptides have been found to have somnogenic or arousing effects in these organisms, suggesting that the balanced action of sleep- and wake-promoting neuropeptides could be a conserved mechanism for regulating sleep/wake cycles.

Only a few neuropeptides have been found to control sleep-like behaviors in *C. elegans* so far (§ 2.1). Recently, FMRFamide-like FLP-13 neuropeptides were shown to facilitate adult

sleep-like states induced by cellular stress (Hill *et al.*, 2014; Nelson *et al.*, 2014). The neuropeptide receptor NPR-1 and its ligands FLP-18 and FLP-21 are somnogenic as well, and regulate the cessation of locomotion and reduced responsiveness during lethargus (Choi *et al.*, 2013). This seems to be mediated through the lethargus-specific inhibition of secretion of PDF-1, a conserved arousal-promoting peptide that reduces quiescence in *npr-1* mutants. Finally, sleep-like behavior during lethargus is induced by the RPamide NLP-22 whose expression cycles in phase with the expression of LIN-42, the *C. elegans* homolog of the circadian protein PERIOD (Nelson *et al.*, 2013).

Based on the somnogenic function of the RPamide NLP-22, one of the ligands of GNRR-3, we investigated a role for GNRR-3 signaling in sleep-like behavior during lethargus. Our results indicate that NLP-2 signaling through GNRR-3 inhibits locomotion quiescence during lethargus. Expression of *nlp-2* in the sensory AWA neurons suggests that the NLP-2/GNRR-3 signaling system could regulate sleep/wake transitions in response to sensory stimuli.

The study of sleep and wake behaviors in *C. elegans* is still in its infancy. Only a few of the signaling pathways and relevant cells regulating lethargus behavior have been identified so far, and unraveling the full circuit of neurons regulating sleep/wake-like behavioral states will be a challenging task. The present and recent findings that neuropeptides balance sleep and wake behaviors in *C. elegans* is a major step forward in our understanding of this fundamental biological process, common to most animals. Taking advantage of the conservation of sleep-like behaviors and molecular pathways, invertebrate models should allow to rapidly further delineate sleep-regulatory networks and how these are shaped by environmental and intrinsic factors. Further progress will also require technical advances. Most automated quantitative methods to measure behavioral quiescence during lethargus only focus on locomotion quiescence and posture dynamics (Nagy *et al.*, 2014). However, in addition to locomotion quiescence, animals are also quiescent for feeding and are less responsive to stimuli during lethargus. Moreover, like sleep in mammals, quiescent behavior during lethargus is under homeostatic regulation (Raizen *et al.*, 2008). The development of quantitative methods to study these other behaviors is an important but ongoing endeavor (Nagy *et al.*, 2014).

6.3 Functional conservation of tachykinin signaling?

In order to investigate the functional role of the identified tachykinin signaling systems in *C. elegans* we investigated the *in vivo* expression pattern of both receptors, *tkr-1* and *tkr-2*, and the *T07C12.15* neuropeptide precursor.

tkr-2 is expressed in both sensory and interneurons, which is complementary to the expression of *dtkr* in the fruit fly *D. melanogaster*. In *Drosophila*, signaling is proposed to act in a disinhibitory circuit that modulates the dynamic range in sensitivity to odors. Expression of *tkr-2* indicates that this signaling system is involved in the regulation of avoidance behavior in *C. elegans.* In line with this expression pattern, members of our lab recently demonstrated that the avoidance response upon optogenetic activation of the polymodal nociceptor ASH is increased in *tkr-2* deletion mutants, indicating that *tkr-2* signaling dampens ASH mediated avoidance (Watteyne J., personal communication). However, so far we did not identify how TKR-2 signaling affects avoidance. In mammals, tachykinin signaling is implicated in several aspects of nociception. Tachykinin-containing sensory neurons are shown to mediate nociceptive responses to physical (thermal, mechanical) and chemical stimuli (Steinhoff *et al.*, 2014). In mice, deletion of the preprotachykinin A gene attenuates moderate to intense pain (Cao *et al.*, 1998). In line with this, deletion of the SP receptor is shown to suppress stress-induced pain (Cloning *et al.*, 1998).

Expression of *tkr-2* in both sensory neurons and interneurons mediating avoidance behavior suggests that TKR-2 signaling could be involved in the modulation of avoidance responses. Avoidance behavior is modulated by several stimuli (§ 2.2.2). An important step to identify the function of tachykinin signaling in *C. elegans* could be elucidated by the expression profile of the T07C12.15 precursor gene. So far we have only been able to identify expression of the T07C12.15 precursor in the BAG neurons. These sensory neurons have recently gained interest for their role in avoidance of hypoxia or high concentrations of carbon dioxide. Interestingly, the ASG neurons, in which we showed expression of *tkr-1*, mediate NaCl chemotaxis induced by hypoxia (Pocock and Hobert, 2010). We tested NaCl chemotaxis for both *tkr-1* and *tkr-2* mutants and observed no involvement of these receptors

in NaCl chemotaxis. However, it could be interesting to investigate NaCl chemotaxis under hypoxic conditions.

6.4 Conclusion and future prospects

Neuropeptidergic signaling clearly plays a profound role in guiding *C. elegans* behavior. However, compared to other model organisms such as *D. melanogaster*, relatively little is known about the repertoire of neuropeptides and their receptors. In this work we predict that the genome of *C. elegans* encodes 129 neuropeptide GPCRs and deorphanized four (GNRR-3, TKR-1, TKR-2 and NMUR-1) of them using a reverse pharmacology assay. So far only 31 (24%) *C. elegans* neuropeptide GPCRs have been matched to their cognate neuropeptides leaving 76% so-called orphan GPCRs. Because matching neuropeptides to their receptor is an important step forward to improve our knowledge on how neuropeptides exert their effect, our lab aims at deorphanizing all *C. elegans* neuropeptide GPCRs (Beets *et al.*, 2014).

TKR-1, TKR-2 and NMUR-1 neuropeptidergic signaling systems that have been identified in this work share homology to vertebrate and protostomian systems. Although we were unable to identify the function of the tachykinin signaling system, the expression patterns suggest a conserved role for this neuropeptide system in the modulation of sensory perception such as nociceptive cues. In order to guide future phenotyping assays, it is of primary importance to further identify the expression pattern of the *C. elegans* tachykinin precursor. Because we already established that the T07C12.15 precursor is expressed in the BAG neurons, both oxygen and carbon dioxide could be interesting stimuli to investigate.

Although several peptidergic signaling systems that have been identified in *C. elegans* seem to have coevolved, we were unable to verify that the RPamides binding to the GnRH/AKH-like receptor GNRR-3 are related to the GnRH/AKH peptide family. Deorphanization of the remaining orphan GNRRs could shed light on the relationship of the RPamides and AKH/GnRH peptides. Regardless of the phylogenetic relationship with vertebrate GnRH systems, our results indicate that NLP-2/GNRR-3 signaling mediates sleep-like behavior in *C. elegans.* Expression analysis of *gnrr-3* can help us to elucidate how NLP-2/GNRR-3 signaling inhibits quiescence during lethargus. Expression of the *nlp-2* precursor in the sensory AWA neurons suggests that peptidergic signaling mediates arousal upon external

stimuli sensed by AWA. In order to find out if the effect of NLP-2/GNRR-3 is ‘sleep’-specific, it would be interesting to test how NLP-2/GNRR-3 signaling influences heat or satiety-induced quiescence.

References

Abrahante JE, Miller EA, Rougvie AE (1998). Identification of heterochronic mutants in *Caenorhabditis elegans* : temporal misexpression of a collagen :: green fluorescent protein fusion gene. *Genetics* 28: 1335–1351.

Adams B a, Tello J a, Erchegyi J, Warby C, Hong DJ, Akinsanya KO, Mackie GO, Vale W, Rivier JE, Sherwood NM (2003). Six novel gonadotropin-releasing hormones are encoded as triplets on each of two genes in the protochordate, *Ciona intestinalis*. *Endocrinology* 144: 1907–19.

Alcedo J, Kenyon C (2004). Regulation of *C. elegans* longevity by specific gustatory and olfactory neurons. *Neuron* 41: 45–55.

Alfonso A, Grundahl K, Duerr JS, Han HP, Rand JB (1993). The *Caenorhabditis elegans unc-17* gene: a putative vesicular acetylcholine transporter. *Science* 261: 617–619.

Alivisatos AP, Chun M, Church GM, Greenspan RJ, Roukes ML, Yuste R (2012). The brain activity map project and the challenge of functional connectomics. *Neuron* 74: 970–974.

Alkema MJ, Hunter-Ensor M, Ringstad N, Horvitz HR (2005). Tyramine functions independently of octopamine in the *Caenorhabditis elegans* nervous system. *Neuron* 46: 247–260.

Altstein M, Hariton A, Nachman RJ (2013). The FXPRLamide (pyrokinin/PBAN) family. In: Kastin AJ (ed) *Handbook of Biologically Active Peptides*, Elsevier Press: San Diego, CA, pp 255–266.

Altun ZF (2011). Neurotransmitter and neuropeptide receptors in *C. elegans*. In: *WormAtlas*,

Altun ZF, Hall DH (2009). Introduction. In: *WormAtlas*, doi:10.3908/wormatlas.1.1.

Altun ZF, Hall DH (2011). Nervous system, general description. In: *WormAtlas*, doi:10.3908/wormatlas.1.18.

Arora S, Anubhuti (2006). Role of neuropeptides in appetite regulation and obesity-a review. *Neuropeptides* 40: 375–401.

Ben Arous J, Laffont S, Chatenay D (2009). Molecular and sensory basis of a food related two-state behavior in *C. elegans*. *PloS one* 4: e7584.

Ben Arous J, Tanizawa Y, Rabinowitch I, Chatenay D, Schafer WR (2010). Automated imaging of neuronal activity in freely behaving *Caenorhabditis elegans*. *Journal of neuroscience methods* 187: 229–234.

Ashrafi K, Chang FY, Watts JL, Fraser AG, Kamath RS, Ahringer J, Ruvkun G (2003). Genome-wide RNAi analysis of *Caenorhabditis elegans* fat regulatory genes. *Nature* 421: 268–272.

Austin C, Lo G, Nandha KA, Meleagros L, Bloom SR (1995). Cloning and characterization of the cDNA encoding the human neuromedin U (NmU) precursor: NmU expression in the human gastrointestinal tract. *Journal of Molecular Endocrinology* 14: 157–169.

Awruch C a (2013). Reproductive endocrinology in chondrichthyans: the present and the future. *General and comparative endocrinology* 192: 60–70.

Azevedo F a C, Carvalho LRB, Grinberg LT, Farfel JM, Ferretti REL, Leite REP, Jacob Filho W, Lent R, Herculano-Houzel S (2009). Equal numbers of neuronal and nonneuronal cells make the human brain an isometrically scaled-up primate brain. *The Journal of comparative neurology* 513: 532–541.

Baidya M, Genovez M, Torres M, Chao MY (2014). Dopamine modulation of avoidance behavior in *Caenorhabditis elegans* requires the NMDA receptor NMR-1. *PloS one* 9: e102958.

Bailey TL, Boden M, Buske F a, Frith M, Grant CE, Clementi L, Ren J, Li WW, Noble WS (2009). MEME SUITE: tools for motif discovery and searching. *Nucleic acids research* 37: W202–W208.

Bailey TL, Elkan C (1994). Fitting a mixture model by expectation maximization to discover motifs in biopolymers. In: *Proceedings of the Second International Conference on Intelligent Systems for Molecular Biology*, AAAI Press: Menlo Park, California, pp 28–36.

Banerjee D, Kwok A, Lin S-Y, Slack FJ (2005). Developmental timing in *C. elegans* is regulated by *kin-20* and *tim-1*, homologs of core circadian clock genes. *Developmental cell* 8: 287–295.

Bargmann CI (1998). Neurobiology of the *Caenorhabditis elegans* Genome. *Science* 282: 2028–2033.

Bargmann CI (2006). Chemosensation in *C. elegans*. In: The *C. elegans* Research Community (ed) *WormBook*, doi:10.1895/wormbook.1.123.1, pp 1–29.

Bargmann CI (2012). Beyond the connectome: How neuromodulators shape neural circuits. *BioEssays : news and reviews in molecular, cellular and developmental biology* 34: 458–65.

Bargmann CI, Horvitz HR (1991). Control of larval development by chemosensory neurons in *Caenorhabditis elegans*. *Science* 251: 1243–1246.

Bargmann CI, Kaplan JM (1998). Signal transduction in the *Caenorhabditis elegans* nervous system. *Annual Review of Neuroscience* 21: 279–308.

Bargmann CI, Thomas J, Horvitz H (1990). Chemosensory cell function in the behavior and development of *Caenorhabditis elegans*. *Cold Spring Harbor Symposia on Quantitative Biology* 55: 529–538.

Barrios A, Ghosh R, Fang C, Emmons SW (2013). PDF-1 neuropeptide signaling modulates a neural circuit for mate-searching behavior in *C. elegans*. *Nature neuroscience* 15: 1675–1682.

Bastiani CA, Gharib S, Simon MI, Sternberg PW (2003). *Caenorhabditis elegans* Gαq regulates egg-laying behavior via a PLCβ-independent and serotonin-dependent signaling pathway and likely functions both in the nervous system and in muscle. *Genetics* 165: 1805–1822.

Bastiani C, Mendel J (2006). Heterotrimeric G proteins in *C. elegans*. In: The *C. elegans* Research Community (ed) *WormBook*, doi:10.1895/wormbook.1.75.1.

Baumeister R, Wittenburg N (1999). Thermal avoidance in *Caenorhabditis elegans* : An approach to the study of nociception. *Proceedings of the National Academy of Sciences* 96: 10477–10482.

Baylis HA, Vázquez-Manrique RP (2012). Genetic analysis of IP(3) and calcium signalling pathways in *C. elegans*. *Biochimica et Biophysica Acta* 1820: 1253–1268.

Beets I (2013). Molecular and functional study of vasopressin/oxytocin-mediated neuroplasticity in *Caenorhabditis elegans*. KU Leuven.

Beets I, Janssen T, Meelkop E, Temmerman L, Suetens N, Rademakers S, Jansen G, Schoofs L (2012). Vasopressin/oxytocin-related signaling regulates gustatory associative learning in *C. elegans*. *Science* 338: 543–545.

Beets I, Lindemans M, Janssen T, Verleyen P (2011). Deorphanizing G protein-coupled receptors by a calcium mobilization assay (A Merighi, Ed.). *Neuropeptides* 789: 377–391.

Beets I, Peymen K, Temmerman L, Schoofs L (2014). The Peptide-GPCR Project: matching *C. elegans* neuropeptides to their cognate receptors. *The worm breeder's gazette* 20: 12–13.

Bendena WG, Boudreau JR, Papanicolaou T, Maltby M, Tobe SS, Chin-Sang ID (2008). A *Caenorhabditis elegans* allatostatin/galanin-like receptor NPR-9 inhibits local search behavior in response to feeding cues. *Proceedings of the National Academy of Sciences of the United States of America* 105: 1339–1342.

Berger AJ, Hart AC, Kaplan JM (1998). Gαs-induced neurodegeneration in *Caenorhabditis elegans*. *The Journal of neuroscience : the official journal of the Society for Neuroscience* 18: 2871–80.

Bhattacharya R, Touroutine D, Barbagallo B, Climer J, Lambert CM, Clark CM, Alkema MJ, Francis MM (2014). A conserved dopamine-cholecystokinin signaling pathway shapes context-dependent *Caenorhabditis elegans* behavior. *PLoS genetics* 10: e1004584.

Birse RT, Söderberg J a E, Luo J, Winther AME, Nässel DR (2011). Regulation of insulin-producing cells in the adult *Drosophila* brain via the tachykinin peptide receptor DTKR. *The Journal of experimental biology* 214: 4201–4208.

De Bono M, Bargmann CI (1998). Natural variation in a neuropeptide Y receptor homolog modifies social behavior and food response in *C. elegans*. *Cell* 94: 679–689.

De Bono M, Maricq AV (2005). Neuronal substrates of complex behaviors in *C. elegans*. *Annual review of neuroscience* 28: 451–501.

Boulin T, Etchberger JF, Hobert O (2006). Reporter gene fusions. In: The *C. elegans* Research Community (ed) *WormBook*, doi: 10.1895/wormbook.1.106.1, pp 1–23.

Brenner S (1974). The genetics of *Caenorhabditis elegans*. *Genetics* 77: 71–94.

Bretscher AJ, Kodama-Namba E, Busch KE, Murphy RJ, Soltesz Z, Laurent P, de Bono M (2011). Temperature, oxygen, and salt-sensing neurons in *C. elegans* are carbon dioxide sensors that control avoidance behavior. *Neuron* 69: 1099–1113.

Brighton PJ, Szekeres PG, Willars GB (2004). Neuromedin U and its receptors : structure, function, and physiological roles. *Pharmacological Reviews* 56: 231–248.

Vanden Broeck J (2001). Neuropeptides and their precursors in the fruitfly, *Drosophila melanogaster*. *Peptides* 22: 241–254.

Broughton SJ, Piper MDW, Ikeya T, Bass TM, Jacobson J, Driege Y, Martinez P, Hafen E, Withers DJ, Leevers SJ, *et al.* (2005). Longer lifespan, altered metabolism, and stress resistance in *Drosophila* from ablation of cells making insulin-like ligands. *Proceedings of the National Academy of Sciences of the United States of America* 102: 3105–3110.

Brown RE, Basheer R, Mckenna JT, Strecker RE, Robert W (2013). Control of sleep and wakefulness. *Physiological Reviews* 92: 1087–1187.

Van Buskirk C, Sternberg PW (2007). Epidermal growth factor signaling induces behavioral quiescence in *Caenorhabditis elegans*. *Nature neuroscience* 10: 1300–1307.

Byerly L, Cassada RC, Russell RL (1976). The life cycle of the nematode *Caenorhabditis elegans*. *Developmental Biology* 51: 23–33.

Caers J, Verlinden H, Zels S, Vandersmissen HP, Vuerinckx K, Schoofs L (2012). More than two decades of research on insect neuropeptide GPCRs: an overview. *Frontiers in endocrinology* 3: 151.

Cai S-Q, Wang Y, Park KH, Tong X, Pan Z, Sesti F (2009). Auto-phosphorylation of a voltage-gated K+ channel controls non-associative learning. *The EMBO journal* 28: 1601–1611.

Campbell SS, Tobler I (1984). Animal sleep: a review of sleep duration across phylogeny. *Neuroscience and biobehavioral reviews* 8: 269–300.

Cao YQ, Mantyh PW, Carlson EJ, Gillespie A, Epstein CJ, Basbaum AI (1998). Primary afferent tachykinins are required to experience moderate to intense pain. *Nature* 392: 390–394.

Cassada RC, Russell RL (1975). The dauerlarva, a post-embryonic developmental variant of the nematode *Caenorhabditis elegans*. *Developmental biology* 46: 326–342.

Chalasani SH, Kato S, Albrecht DR, Nakagawa T, Abbott LF, Bargmann CI (2010). Neuropeptide feedback modifies odor-evoked dynamics in *Caenorhabditis elegans* olfactory neurons. *Nature neuroscience* 13: 615–21.

Chalfie M (1995). Green fluorsecent protein. *Photochemistry and Photobiology* 62: 651–656.

Chalfie M, Sulston J (1981). Developmental genetics of the mechanosensory neurons of *Caenorhabditis elegans*. 370: 358–370.

Chalfie M, Sulston J, White JG, Southgate E, Thomson JN, Brenner S (1985). The neural circuit for touch sensitivity in *Caenorhabditis elegans*. *The Journal of neuroscience : the official journal of the Society for Neuroscience* 5: 956–964.

Chalfie M, Thomson JN (1979). Organization of neuronal microtubules in the nematode *Caenorhabditis elegans*. *Journal of cell biology* 82: 278–289.

Chang AJ, Chronis N, Karow DS, Marletta MA, Bargmann CI (2006). A distributed chemosensory circuit for oxygen preference in *C. elegans*. *PLoS biology* 4: 1588–1602.

Chang MM, Leeman SE, Niall HD (1971). Amino-acid Sequence of Substance P. *Nature* 232: 86–87.

Chao MY, Komatsu H, Fukuto HS, Dionne HM, Hart A (2004). Feeding status and serotonin rapidly and reversibly modulate a *Caenorhabditis elegans* chemosensory circuit. *Proceedings of the National Academy of Sciences of the United States of America* 101: 15512–15517.

Chase DL, Koelle MR (2007). Biogenic amine neurotransmitters in *C. elegans*. In: the *C. elegans* Research Community (ed) *WormBook,* doi: 10.1895/wormbook.1.132.1, pp 1–15.

Chatzigeorgiou M, Schafer WR (2011). Lateral facilitation between primary mechanosensory neurons controls nose touch perception in *C. elegans*. *Neuron* 70: 299–309.

Chatzigeorgiou M, Yoo S, Watson JD, Lee W, Clay W, Kindt KS, Hwang SW, Iii DMM, Treinin M (2011). Specific roles for DEG / ENaC and TRP channels in touch and thermosensation in *C . elegans* nociceptors. *Nature neuroscience* 13: 861–868.

Cheung BHH, Cohen M, Rogers C, Albayram O, de Bono M (2005). Experience-dependent modulation of *C. elegans* behavior by ambient oxygen. *Current biology : CB* 15: 905–917.

Cho JY, Sternberg PW (2014). Multilevel modulation of a sensory motor circuit during *C. elegans* sleep and arousal. *Cell* 156: 249–260.

Choi S, Chatzigeorgiou M, Taylor KP, Schafer WR, Kaplan JM (2013). Analysis of NPR-1 reveals a circuit mechanism for behavioral quiescence in *C. elegans*. *Neuron* 78: 869–880.

Cirelli C, Tononi G (2008). Is sleep essential? *PLoS biology* 6: e216.

Civelli O, Reinscheid RK, Zhang Y, Wang Z, Fredriksson R, Schiöth HB (2013). G protein-coupled receptor deorphanizations. *Annual review of pharmacology and toxicology* 53: 127–146.

Cloning K, Julius D, Levine J, Lisberger S, Malmberg A, Martin W (1998). Altered nociception, analgesia and aggression in mice lacking the receptor for substance P. *Nature* 8060: 394–397.

Cohen M, Reale V, Olofsson B, Knights A, Evans P, de Bono M (2009). Coordinated regulation of foraging and metabolism in *C. elegans* by RFamide neuropeptide signaling. *Cell metabolism* 9: 375–385.

Colbert HA, Smith TL, Bargmann C (1997). OSM-9, a novel protein with structural similarity to channels, is required for olfaction, mechanosensation, and olfactory adaptation in *Caenorhabditis elegans*. *The Journal of neuroscience* 17: 8259–8269.

Collins PY, Patel V, Joestl SS, March D, Insel TR, Daar AS, Walport M (2011). Grand challenges in global mental health. *Nature* 475: 27–30.

Couto A, Oda S, Nikolaev VO, Soltesz Z, de Bono M (2013). *In vivo* genetic dissection of O2-evoked cGMP dynamics in a *Caenorhabditis elegans* gas sensor. *Proceedings of the National Academy of Sciences of the United States of America* 110: E3301–10.

Coward P, Chan SDH, Wada HG, Humphries GM, Conklin BR (1999). Chimeric G proteins allow a high-throughput signaling assay of Gi -coupled receptors. *Analytical Biochemistry* 248: 242–248.

Culotti JG, Russell RL (1978). Osmotic avoidance defective mutants of the nematode *Caenorhabditis elegans*. *Genetics* 90: 243–256.

Darlison MG, Richter D (1999). Multiple genes for neuropeptides and their receptors: co-evolution and physiology. *Trends in Neurosciences* 22: 81–88.

Davies AG, Bettinger JC, Thiele TR, Judy ME, McIntire SL (2004). Natural variation in the *npr-1* gene modifies ethanol responses of wild strains of *C. elegans*. *Neuron* 42: 731–43.

Domin J, Yiangous Y, Spokes RA, Aitkenll A, Parmar KB, Chrysanthous BJ, Bloom SR (1989). The distribution, purification, and pharmacological action of an amphibian neuromedin U. *The Journal of Biological Chemistry* 264: 20881–20885.

Donlea J, Leahy A, Thimgan MS, Suzuki Y, Hughson BN, Sokolowski MB, Shaw PJ (2012). Foraging alters resilience/vulnerability to sleep disruption and starvation in *Drosophila*. *Proceedings of the National Academy of Sciences of the United States of America* 109: 2613–2618.

Donnelly JL, Clark CM, Leifer AM, Pirri JK, Haburcak M, Francis MM, Samuel ADT, Alkema MJ (2013). Monoaminergic orchestration of motor programs in a complex *C. elegans* behavior. *PLoS biology* 11: e1001529.

Driver RJ, Lamb AL, Wyner AJ, Raizen DM (2013). DAF-16/FOXO regulates homeostasis of essential sleep-like behavior during larval transitions in *C. elegans*. *Current Biology* 23: 501–506.

Dusenbery D (1974). Analysis of chemotaxis in the nematode *Caenorhabditis elegans* by countercurrent separation. *Journal of Experimental Biology* 188: 41–48.

Ellis HM, Horvitz HR (1986). Genetic control of programmed cell death in the nematode *C . elegans*. *Cell* 44: 817–829.

Von Euler US, Gaddum JH (1931). An unidentified depressor substance in certain tissue extracts. *The Journal of Physiology* 72: 74–87.

Evans T (2006). Transformation and microinjection. In: The *C. elegans* Research Community (ed) *WormBook*, doi:10.1895/wormbook.1.108.1, pp 1–15.

Ezcurra M, Tanizawa Y, Swoboda P, Schafer WR (2011). Food sensitizes *C. elegans* avoidance behaviours through acute dopamine signalling. *The EMBO journal* 30: 1110–22.

Félix M-A, Braendle C (2010). The natural history of *Caenorhabditis elegans*. *Current Biology* 20: 965–969.

Feng G, Reale V, Chatwin H, Kennedy K, Venard R, Ericsson C, Yu K, Evans PD, Hall LM (2003). Functional characterization of a neuropeptide F-like receptor from *Drosophila melanogaster*. *European Journal of Neuroscience* 18: 227–238.

Fire A, Xu S, Montgomery MK, Kostas SA, Driver SE, Mello CC (1998). Potent and specific genetic interference by double-stranded RNA in *Caenorhabditis elegans*. *Nature* 391: 806–811.

Flavell SW, Pokala N, Macosko EZ, Albrecht DR, Larsch J, Bargmann CI (2013). Serotonin and the neuropeptide PDF initiate and extend opposing behavioral states in *C. elegans*. *Cell* 154: 1023–35.

Foltenyi K, Greenspan RJ, Newport JW (2007). Activation of EGFR and ERK by rhomboid signaling regulates the consolidation and maintenance of sleep in *Drosophila*. *Nature neuroscience* 10: 1160–1167.

Fredriksson R, Schiöth HB (2005). The Repertoire of G Protein-Coupled Receptors in Fully Sequenced Genomes. *Molecular Pharmacology* 67: 1414–1425.

Friedland AE, Tzur YB, Esvelt KM, Colaiácovo MP, Church GM, Calarco JA (2013). Heritable genome editing in *C. elegans* via a CRISPR-Cas9 system. *Nature methods* 10: 741–3.

Frooninckx L, Rompay L Van, Temmerman L, Sinay E Van, Beets I, Janssen T, Husson SJ, Schoofs L (2012). Neuropeptide GPCRs in *C. elegans*. *Frontiers in endocrinology* 3: Article 167.

Fujiwara M, Sengupta P, McIntire SL (2002). Regulation of body size and behavioral state of *C. elegans* by sensory perception and the EGL-4 cGMP-dependent protein kinase. *Neuron* 36: 1091–1102.

Fuller PM, Gooley JJ, Saper CB (2006). Neurobiology of the sleep-wake cycle: sleep architecture, circadian regulation, and regulatory feedback. *Journal of biological rhythms* 21: 482–493.

Gäde G (2009). Peptides of the adipokinetic hormone/red pigment-concentrating hormone family: a new take on biodiversity. *Annals of the New York Academy of Sciences* 1163: 125–36.

Gäde G, Marco HG (2013). AKH/RPCH Peptides. In: Kastin AJ (ed) *Handbook of Biologically Active Peptides*, Elsevier: San Diego, CA, p 1942.

Garrison JL, Macosko EZ, Bernstein S, Pokala N, Albrecht DR, Bargmann C (2012). Oxytocin/vasopressin-related peptides have an ancient role in reproductive behavior. *Science* 338: 540–543.

Geffeney SL, Cueva JG, Glauser DA, Doll JC, Hau- T, Lee C, Montoya M, Karania S, Garakani AM, Pruitt BL, *et al.* (2011). DEG/ENaC but not TRP channels are the major mechanoelectrical transduction channels in a C. elegans nociceptor. *Neuron* 71: 845–857.

Glauser DA, Chen WC, Agin R, Macinnis BL, Hellman AB, Garrity PA, Tan M-W, Goodman MB (2011). Heat avoidance is regulated by transient receptor potential (TRP) channels and a neuropeptide signaling pathway in *Caenorhabditis elegans*. *Genetics* 188: 91–103.

Graves L a, Hellman K, Veasey S, Blendy J a, Pack AI, Abel T (2003). Genetic evidence for a role of CREB in sustained cortical arousal. *Journal of Neurophysiology* 90: 1152–1159.

Gray JM, Hill JJ, Bargmann CI (2005). A circuit for navigation in *Caenorhabditis elegans*. *Proceedings of the National Academy of Sciences of the United States of America* 102: 3184–3191.

Gray JM, Karow DS, Lu H, Chang AJ, Chang JS, Ellis RE, Marletta M a, Bargmann CI (2004). Oxygen sensation and social feeding mediated by a *C. elegans* guanylate cyclase homologue. *Nature* 430: 317–22.

Griffith LC (2014). Neuromodulatory control of sleep in *Drosophila melanogaster*: Integration of competing and complementary behaviors. *Current opinion in neurobiology* 23: 819–823.

Grönke S, Müller G, Hirsch J, Fellert S, Andreou A, Haase T, Jäckle H, Kühnlein RP (2007). Dual lipolytic control of body fat storage and mobilization in *Drosophila*. *PLoS biology* 5: e137.

Guindon S, Dufayard J-F, Lefort V, Anisimova M, Hordijk W, Gascuel O (2010). New algorithms and methods to estimate maximum-likelihood phylogenies: assessing the performance of PhyML 3.0. *Systematic biology* 59: 307–321.

Hallem EA, Spencer WC, McWhirter RD, Zeller G, Henz SR, Rätsch G, Miller DM, Horvitz HR, Sternberg PW, Ringstad N (2011). Receptor-type guanylate cyclase is required for carbon dioxide sensation by *Caenorhabditis elegans*. *Proceedings of the National Academy of Sciences of the United States of America* 108: 254–259.

Hallem EA, Sternberg PW (2008). Acute carbon dioxide avoidance in *Caenorhabditis elegans*. *Proceedings of the National Academy of Sciences of the United States of America* 105: 8038–8043.

Hamanaka Y, Yasuyama K, Numata H, Shiga S (2005). Synaptic connections between pigment-dispersing factor-immunoreactive neurons and neurons in the pars lateralis of the blow fly *Protophormia terraenovae*. *The Journal of comparative neurology* 491: 390–399.

Hapiak V, Summers P, Ortega A, Law WJ, Stein A, Komuniecki R (2013). Neuropeptides amplify and focus the monoaminergic inhibition of nociception in *Caenorhabditis elegans*. *The Journal of neuroscience* 33: 14107–14116.

Harris TW, Antoshechkin I, Bieri T, Blasiar D, Chan J, Chen WJ, De La Cruz N, Davis P, Duesbury M, Fang R, *et al.* (2009a). WormBase: a comprehensive resource for nematode research. *Nucleic Acids Research* 38: 463–467.

Harris G, Hapiak VM, Wragg RT, Miller SB, Hughes LJ, Hobson RJ, Steven R, Bamber B, Komuniecki RW (2009b). Three distinct amine receptors operating at different levels within the locomotory circuit are each essential for the serotonergic modulation of chemosensation in *Caenorhabditis elegans*. *The Journal of neuroscience : the official journal of the Society for Neuroscience* 29: 1446–56.

Harris G, Mills H, Wragg R, Hapiak V, Castelletto M, Komuniecki R (2010). The monoaminergic modulation of sensory-mediated aversive responses in *Caenorhabditis elegans* requires glutamatergic/peptidergic cotransmission. *Journal of Neuroscience* 30: 7889–7899.

Hart A (2006). Behavior. In: The *C. elegans*Research Community (ed) *WormBook*, doi: 10.1895/wormbook.1.87.1, pp 1–67.

Hart A, Sims S, Kaplan JM (1995). Synaptic code for sensory modalities revealed by *C. elegans* GLR-1 glutamate receptor. *Nature* 378: 82–5.

Hedgecock EM, Culotti JG, Thomson JN, Perkins L a. (1985). Axonal guidance mutants of *Caenorhabditis elegans* identified by filling sensory neurons with fluorescein dyes. *Developmental Biology* 111: 158–170.

Heilig M (2004). The NPY system in stress, anxiety and depression. *Neuropeptides* 38: 213–224.

Hendricks JC, Finn SM, Panckeri KA, Chavkin J, Williams JA, Sehgal A, Pack AI (2000a). Rest in *Drosophila* is a sleep-like state. *Neuron* 25: 129–138.

Hendricks JC, Sehgal A, Pack a I (2000b). The need for a simple animal model to understand sleep. *Progress in neurobiology* 61: 339–351.

Hendricks JC, Williams J a, Panckeri K, Kirk D, Tello M, Yin JC, Sehgal A (2001). A non-circadian role for cAMP signaling and CREB activity in *Drosophila* rest homeostasis. *Nature Neuroscience* 4: 1108–1115.

Hendriks G-J, Gaidatzis D, Aeschimann F, Großhans H (2014). Extensive oscillatory gene expression during *C. elegans* larval development. *Molecular cell* 53: 380–392.

Hewes RS, Taghert PH (2001). Neuropeptides and neuropeptide receptors in the *Drosophila melanogaster* genome. *Genome research* 11: 1126–1142.

Hill AJ, Mansfield R, Lopez JMNG, Raizen DM, Van Buskirk C (2014). Cellular stress induces a protective sleep-like state in *C. elegans*. *Current Biology* 24: 2399–2405.

Hilliard M, Apicella AJ, Kerr R, Suzuki H, Bazzicalupo P, Schafer WR (2005). *In vivo* imaging of *C. elegans* ASH neurons: cellular response and adaptation to chemical repellents. *The EMBO journal* 24: 63–72.

Hilliard M a, Bargmann CI, Bazzicalupo P (2002). *C. elegans* responds to chemical repellents by integrating sensory inputs from the head and the tail. *Current Biology* 12: 730–734.

Hilliard M, Bergamasco C, Arbucci S, Plasterk RH, Bazzicalupo P (2004). Worms taste bitter: ASH neurons, QUI-1, GPA-3 and ODR-3 mediate quinine avoidance in *Caenorhabditis elegans*. *The EMBO journal* 23: 1101–1011.

Hoffmann MC, Sellings LHL, van der Kooy D (2010). A diacetyl-induced quiescence in young *Caenorhabditis elegans*. *Behavioural brain research* 214: 12–17.

Hosono R, Hekimi S, Kamiya Y, Sassa T, Murakami S, Nishiwaki K, Miwa J, Taketo A, Kodaira KI (1992). The *unc-18* gene encodes a novel protein affecting the kinetics of acetylcholine metabolism in the nematode *Caenorhabditis elegans*. *Journal of neurochemistry* 58: 1517–1525.

Hoyle CH. (1998). Neuropeptide families: evolutionary perspectives. *Regulatory Peptides* 73: 1–33.

Hu Z, Pym ECG, Babu K, Murray ABV, Kaplan JM (2011). A neuropeptide-mediated stretch response links muscle contraction to changes in neurotransmitter release. *Neuron* 71: 92–102.

Hu XZ, Vashlishan-murray AB, Kaplan JM (2015). NLP-12 engages different UNC-13 proteins to potentiate tonic and evoked release. 35: 1038–1042.

Hukema RK, Rademakers S, Jansen G (2008). Gustatory plasticity in *C. elegans* involves integration of negative cues and NaCl taste mediated by serotonin, dopamine, and glutamate. *Learning & memory* 15: 829–836.

Husson SJ, Clynen E, Baggerman G, Janssen T, Schoofs L (2006). Defective processing of neuropeptide precursors in *Caenorhabditis elegans* lacking proprotein convertase 2 (KPC-2/EGL-3): mutant analysis by mass spectrometry. *Journal of Neurochemistry* 98: 1999–2012.

Husson SJ, Clynen E, Baggerman G, De Loof A, Schoofs L (2005). Discovering neuropeptides in *Caenorhabditis elegans* by two dimensional liquid chromatography and mass spectrometry. *Biochemical and biophysical research communications* 335: 76–86.

Husson SJ, Janssen T, Baggerman G, Bogert B, Kahn-Kirby AH, Ashrafi K, Schoofs L (2007a). Impaired processing of FLP and NLP peptides in carboxypeptidase E (EGL-21)-deficient *Caenorhabditis elegans* as analyzed by mass spectrometry. *Journal of neurochemistry* 102: 246–260.

Husson SJ, Mertens I, Janssen T, Lindemans M, Schoofs L (2007b). Neuropeptidergic signaling in the nematode *Caenorhabditis elegans*. *Progress in neurobiology* 82: 33–55.

Husson SJ, Reumer A, Temmerman L, De Haes W, Schoofs L, Mertens I, Baggerman G (2014). Worm peptidomics. *EuPA Open Proteomics* 3: 280–290.

Ignell R, Root CM, Birse RT, Wang JW, Nässel DR, Winther AME (2009). Presynaptic peptidergic modulation of olfactory receptor neurons in *Drosophila*. *Proceedings of the National Academy of Sciences of the United States of America* 106: 13070–5.

Iwakoshi E, Takuwa-Kuroda K, Fujisawa Y, Hisada M, Ukena K, Tsutsui K, Minakata H (2002). Isolation and characterization of a GnRH-like peptide from *Octopus vulgaris*. *Biochemical and biophysical research communications* 291: 1187–93.

Iwanir S, Tramm N, Nagy S, Wright C, Ish D, Biron D (2013). The microarchitecture of *C. elegans* behavior during lethargus: homeostatic bout dynamics, a typical body posture, and regulation by a central neuron. *Sleep* 36: 385–395.

Jang H, Kim K, Neal SJ, Macosko E, Kim D, Butcher RA, Zeiger DM, Bargmann CI, Sengupta P (2012). Neuromodulatory state and sex specify alternative behaviors through antagonistic synaptic pathways in *C. elegans*. *Neuron* 75: 585–592.

Jansen G, Thijssen KL, Werner P, Horst M Van Der, Hazendonk E, Plasterk RHA (1999). The complete family of genes encoding G proteins of *Caenorhabditis elegans* . *Nature Genetics* 21: 414–419.

Jansen G, Weinkove D, Plasterk RHA (2002). The G-protein g subunit *gpc-1* of the nematode *C* . *elegans* is involved in taste adaptation. *The EMBO journal* 21: 986–994.

Janssen T, Husson SJ, Lindemans M, Mertens I, Rademakers S, Ver Donck K, Geysen J, Jansen G, Schoofs L (2008a). Functional characterization of three G protein-coupled receptors for pigment dispersing factors in *Caenorhabditis elegans*. *The Journal of biological chemistry* 283: 15241–15249.

Janssen T, Husson SJ, Meelkop E, Temmerman L, Lindemans M, Verstraelen K, Rademakers S, Mertens I, Nitabach M, Jansen G, *et al.* (2009a). Discovery and characterization of a conserved pigment dispersing factor-like neuropeptide pathway in *Caenorhabditis elegans*. *Journal of neurochemistry* 111: 228–241.

Janssen T, Lindemans M, Meelkop E, Temmerman L, Schoofs L (2010). Coevolution of neuropeptidergic signaling systems: from worm to man. *Annals of the New York Academy of Sciences* 1200: 1–14.

Janssen T, Meelkop E, Lindemans M, Verstraelen K, Husson SJ, Temmerman L, Nachman RJ, Schoofs L (2008b). Discovery of a cholecystokinin-gastrin-like signaling system in nematodes. *Endocrinology* 149: 2826–2839.

Janssen T, Meelkop E, Nachman RJ, Schoofs L (2009b). Evolutionary conservation of the cholecystokinin/gastrin signaling system in nematodes. *Annals of the New York Academy of Sciences* 1163: 428–32.

Jarrell TA, Wang Y, Bloniarz AE, Brittin CA, Xu M, Thomson JN, Albertson DG, Hall DH, Emmons SW (2012). The connectome of a decision-making neural network. *Science* 337: 437–444.

Jékely G (2013). Global view of the evolution and diversity of metazoan neuropeptide signaling. *Proceedings of the National Academy of Sciences* 110 : 8702–8707.

Jeon M, Gardner EA, Miller EA, Deshler J, E. RA (1999). Similarity of the *C. elegans* developmental timing protein LIN-42 to circadian rhythm proteins. *Science* 286: 1141–1146.

Jones D, Candido EPM (1999). Feeding is inhibited by sublethal concentrations of toxicants and by heat stress in the nematode *Caenorhabditis elegans* : relationship to the cellular stress response. *Journal of Experimental Biology* 157: 147–157.

Kah O, Lethimonier C, Somoza G, Guilgur LG, Vaillant C, Lareyre JJ (2007). GnRH and GnRH receptors in metazoa: a historical, comparative, and evolutive perspective. *General and comparative endocrinology* 153: 346–64.

Kahsai L, Martin J-R, Winther AME (2010). Neuropeptides in the *Drosophila* central complex in modulation of locomotor behavior. *The Journal of experimental biology* 213: 2256–2265.

Kamath R, Ahringer J (2003). Genome-wide RNAi screening in *Caenorhabditis elegans*. *Methods* 30: 313–321.

Kanda A, Takahashi T, Satake H, Minakata H (2006). Molecular and functional characterization of a novel gonadotropin-releasing-hormone receptor isolated from the common octopus (*Octopus vulgaris*). *The Biochemical journal* 395: 125–135.

Kang C, Avery L (2009). Systemic regulation of starvation response in *Caenorhabditis elegans*. *Genes & Development* 23: 12–17.

Kaplan JM, Driscoll M (1997). Mechanotransduction. In: Riddle DL, Blumenthal T, Meyer BJ, Priess JR (eds) *C. elegans II 2nd edition*, Cold Spring Harbor Laboratory Press: New York.

Kaplan JM, Horvitz HR (1993). A dual mechanosensory and chemosensory neuron in *Caenorhabditis elegans*. *Proceedings of the National Academy of Sciences of the United States of America* 90: 2227–31.

Kean L, Cazenave W, Costes L, Broderick KE, Graham S, Pollock VP, Davies SA, Veenstra JANA, Dow JAT, Insectes N, *et al.* (2002). Two nitridergic peptides are encoded by the gene *capability* in <I>Drosophila melanogaster</i>. *American Journal of Physiology - Regulatory, Integrative and Comparative Physiology* 282: 1297–1307.

Keating CD, Kriek N, Daniels M, Ashcroft NR, Hopper NA, Siney EJ, Holden-dye L, Burke JF (2003). Whole-Genome Analysis of 60 G Protein-Coupled Receptors in *Caenorhabditis elegans* by Gene Knockout with RNAi. *Current biology* 13: 1715–1720.

Knutson KL, Spiegel K, Penev P, Van Cauter E (2007). The metabolic consequences of sleep deprivation. *Sleep medicine reviews* 11: 163–178.

Korswagen HC, Park JH, Ohshima Y, Plasterk RH (1997). An activating mutation in a *Caenorhabditis elegans* Gs protein induces neural degeneration. *Genes & Development* 11: 1493–1503.

Kostenis E (2001). Is Gα16 the optimal Is Gα tool for fishing ligands of orphan receptors? *Trends in pharmacological sciences* 22: 560–564.

Kramer A, Yang FC, Snodgrass P, Li X, Scammell TE, Davis FC, Weitz CJ (2001). Regulation of daily locomotor activity and sleep by hypothalamic EGF receptor signaling. *Science* 294: 2511–2515.

Kubiak TM, Larsen MJ, Bowman JW, Geary TG, Lowery DE (2008). FMRFamide-like peptides encoded on the *flp-18* precursor gene activate two isoforms of the orphan *Caenorhabditis elegans* G-protein-coupled receptor Y58G8A.4 heterologously expressed in mammalian cells. *Biopolymers* 90: 339–348.

Kubiak TM, Larsen MJ, Nulf SC, Zantello MR, Burton KJ, Bowman JW, Modric T, Lowery DE (2003a). Differential activation of "social" and "solitary" variants of the *Caenorhabditis elegans* G protein-coupled receptor NPR-1 by its cognate ligand AF9. *The Journal of Biological Chemistry* 278: 33724–33729.

Kubiak TM, Larsen MJ, Zantello MR, Bowman JW, Nulf SC, Lowery DE (2003b). Functional annotation of the putative orphan *Caenorhabditis elegans* G-protein-coupled receptor C10C6.2 as a FLP15 peptide receptor. *The Journal of biological chemistry* 278: 42115–20.

Kutscher LM, Shaham S (2014). Forward and reverse mutagenesis in *C . elegans*. In: The C. elegans Research Community (ed) *WormBook*, doi:10.1895/wormbook.1..167.1.

Lackner MR, Nurrish SJ, Kaplan JM (1999). Facilitation of synaptic transmission by EGL-30 Gqα and EGL-8 PLCβ: DAG binding to UNC-13 is required to stimulate acetylcholine release. *Neuron* 24: 335–346.

Langmesser S, Franken P, Feil S, Emmenegger Y, Albrecht U, Feil R (2009). cGMP-dependent protein kinase type I is implicated in the regulation of the timing and quality of sleep and wakefulness. *PloS one* 4: e4238.

Le SQ, Gascuel O (2008). An improved general amino acid replacement matrix. *Molecular biology and evolution* 25: 1307–1320.

Lesa GM, Palfreyman M, Hall DH, Clandinin MT, Rudolph C, Jorgensen EM, Schiavo G (2003). Long chain polyunsaturated fatty acids are required for efficient neurotransmission in *C. elegans*. *Journal of cell science* 116: 4965–4975.

Li W, Kang L, Piggott B, Feng Z, Shawn Xu XZ (2011). The neural circuits and sensory channels mediating harsh touch sensation in *C. elegans*. *Nature communications* 2: 315.

Li C, Kim K (2008). Neuropeptides. In: The *C. elegans* Research Community (ed) *WormBook*, doi/10.1895/wormbook.1.142.1.

Li C, Nelson LS, Kim K, Nathoo A (1999). Neuropeptide gene families in the nematode *Caenorhabditis elegans*. *Annals of the New York Academy of Sciences* 897: 239–252.

Lindemans M, Janssen T, Beets I, Temmerman L, Meelkop E, Schoofs L (2011). Gonadotropin-releasing hormone and adipokinetic hormone signaling systems share a common evolutionary origin. *Frontiers in endocrinology* 2: 16.

Lindemans M, Janssen T, Husson SJ, Meelkop E, Temmerman L, Clynen E, Mertens I, Schoofs L (2009a). A neuromedin-pyrokinin-like neuropeptide signaling system in *Caenorhabditis elegans*. *Biochemical and biophysical research communications* 379: 760–764.

Lindemans M, Liu F, Janssen T, Husson SJ, Mertens I, Gäde G, Schoofs L (2009b). Adipokinetic hormone signaling through the gonadotropin-releasing hormone receptor modulates egg-laying in *Caenorhabditis elegans*. *Proceedings of the National Academy of Sciences of the United States of America* 106: 1642–1647.

Liu T, Cai D (2013). Counterbalance between BAG and URX neurons via guanylate cyclases controls lifespan homeostasis in *C. elegans*. *The EMBO journal* 32: 1529–1542.

Liu K, Raghavan S, Nelesen S, Linder CR, Warnow T (2009). Rapid and accurate large-scale coestimation of sequence alignments and phylogenetic trees. *Science* 324: 1561–1564.

Liu S, Schulze E, Baumeister R (2012). Temperature- and touch-sensitive neurons couple CNG and TRPV channel activities to control heat avoidance in *Caenorhabditis elegans*. *PloS one* 7: e32360.

De Loof A, Schoofs L (1990). Homologies between the amino acid sequences of some vertebrate peptide hormones and peptides isolated from invertebrate sources. *Comparative Biochemistry and Physiology Part B: Comparative Biochemistry* 95: 459–468.

Los FCO, Ha C, Aroian R V (2013). Neuronal Goα and CAPS regulate behavioral and immune responses to bacterial pore-forming toxins. *PloS one* 8: e54528.

Lowery DE, Geary TG, Kubiak TM, Larsen MJ (2003). G protein-coupled receptor-like receptors and modulators thereof. : United States, Patent 6,632,621.

Luo J, Phan TX, Yang Y, Garelick MG, Storm DR (2013). Increases in cAMP, MAPK Activity and CREB Phosphorylation during REM Sleep: Implications for REM Sleep and Memory Consolidation. *Journal of Neuroscience* 33: 6460–6468.

Macosko EZ, Pokala N, Feinberg EH, Chalasani SH, Butcher R a, Clardy J, Bargmann CI (2009). A hub-and-spoke circuit drives pheromone attraction and social behaviour in *C. elegans*. *Nature* 458: 1171–1175.

Maier W, Adilov B, Regenass M, Alcedo J (2010). A neuromedin U receptor acts with the sensory system to modulate food type-dependent effects on *C. elegans* lifespan. *PLoS biology* 8: e1000376.

Malendowicz LK, Ziolkowska A, Rucinski M (2012). Neuromedins U and S involvement in the regulation of the hypothalamo-pituitary-adrenal axis. *Frontiers in endocrinology* 3: 156.

Marder E (2012). Neuromodulation of neuronal circuits: Back to the future. *Neuron* 76: 1–11.

Maricq A V., Peckol E, Driscoll M, Bargmann CI (1995). Mechanosensory signalling in *C. elegans* mediated by the GLR-1 glutamate receptor. *Nature* 378: 78–81.

Maruyama IN, Brenner S (1991). phorbol ester/diacylglycerol-binding protein encoded by the *unc-13* gene of *Caenorhabditis elegans*. *Proceedings of the National Academy of Sciences* 88: 5729–5733.

Meelkop E, Temmerman L, Janssen T, Suetens N, Beets I, Van Rompay L, Shanmugam N, Husson SJ, Schoofs L (2012). PDF receptor signaling in *Caenorhabditis elegans* modulates locomotion and egg-laying. *Molecular and cellular endocrinology* 361: 232–240.

Meelkop E, Temmerman L, Schoofs L, Janssen T (2011). Signalling through pigment dispersing hormone-like peptides in invertebrates. *Progress in neurobiology* 93: 125–147.

Melcher C, Pankratz MJ (2005a). Candidate gustatory interneurons modulating feeding behavior in the *Drosophila* brain. *PLoS biology* 3: e305.

Melcher C, Pankratz MJ (2005b). Neuromedin U and its putative *Drosophila* homolog *hugin*. *PLoS biology* 3: e305.

Mellem JE, Brockie PJ, Zheng Y, Madsen DM, Maricq A V (2002). Decoding of polymodal sensory stimuli by postsynaptic glutamate receptors in *C. elegans*. *Neuron* 36: 933–44.

Meng X, Wahlström G, Immonen T, Kolmer M, Tirronen M, Predel R, Kalkkinen N, Heino T, Sariola H, Roos C (2002). The *Drosophila hugin* gene codes for myostimulatory and ecdysis-modifying neuropeptides. *Mechanisms of development* 117: 5–13.

Mertens I, Clinckspoor I, Janssen T, Nachman R, Schoofs L (2006). FMRFamide related peptide ligands activate the *Caenorhabditis elegans* orphan GPCR Y59H11AL.1. *Peptides* 27: 1291–6.

Mertens I, Meeusen T, Janssen T, Nachman R, Schoofs L (2005). Molecular characterization of two G protein-coupled receptor splice variants as FLP2 receptors in *Caenorhabditis elegans*. *Biochemical and biophysical research communications* 330: 967–74.

Mertens I, Vandingenen A, Meeusen T, Janssen T, Luyten W, Nachman RJ, De Loof A, Schoofs L (2004a). Functional characterization of the putative orphan neuropeptide G-protein coupled receptor C26F1.6 in *Caenorhabditis elegans*. *FEBS letters* 573: 55–60.

Mertens I, Vandingenen A, Meeuwen T, De Loof A, Schoofs L, Meeusen T (2004b). Postgenomic characterization of G-protein-coupled receptors. *Future Medicine* 5: 657–672.

Metaxakis A, Tain LS, Grönke S, Hendrich O, Hinze Y, Birras U, Partridge L (2014). Lowered insulin signalling ameliorates age-related sleep fragmentation in *Drosophila*. *PLoS biology* 12: e1001824.

Mills H, Wragg R, Hapiak V, Castelletto M, Zahratka J, Harris G, Summers P, Korchnak A, Law W, Bamber B, *et al.* (2012). Monoamines and neuropeptides interact to inhibit aversive behaviour in *Caenorhabditis elegans*. *The EMBO journal* 31: 667–678.

Milward K, Emanuel K, Joseph R, Bono M De, Olofsson B (2011). Neuronal and molecular substrates for optimal foraging in *Caenorhabditis elegans*. *Proceedings of the National Academy of Sciences*.

Minamino N, Kangawa K, Matsuo H (1985). Neuromedin U-8 and U-25 : novel uterus stimulating and hypertensive peptides identified in porcine spinal cord. *Biochemical and biophysical research communications* 130: 1078–1085.

Mirabeau O, Joly J (2013). Molecular evolution of peptidergic signaling systems in bilaterians. *Proceedings of the National Academy of Sciences* 110: 2028–2037.

Mohri A, Kodama E, Kimura KD, Koike M, Mizuno T, Mori I (2005). Genetic control of temperature preference in the nematode *Caenorhabditis elegans*. *Genetics* 169: 1437–50.

Monsalve GC, Van Buskirk C, Frand AR (2011). LIN-42/PERIOD controls cyclical and developmental progression of *C. elegans* molts. *Current Biology* 21: 2033–2045.

Nagy S, Raizen DM, Biron D (2014). Measurements of behavioral quiescence in *Caenorhabditis elegans*. *Methods* 68: 500–507.

Nässel DR (1999). Tachykinin-related peptides in invertebrates: a review. *Peptides* 20: 141–158.

Nathoo AN, Moeller RA, Westlund BA, Hart AC (2001). Identification of neuropeptide-like protein gene families in *Caenorhabditis elegans* and other species. *Proceedings of the National Academy of Sciences of the United States of America* 98: 14000–14005.

Nelson MD, Fitch DHA (2011). Overlap Extension PCR : An Efficient Method. *Methods in Molecular Biology* 772: 459–470.

Nelson LS, Kim K, Memmott JE, Li C (1998). FMRFamide-related gene family in the nematode *Caenorhabditis elegans*. *Brain research* 58: 103–111.

Nelson MD, Lee KH, Churgin MA, Hill AJ, Van Buskirk C, Fang-Yen C, Raizen DM (2014). FMRFamide-like FLP-13 neuropeptides promote quiescence following heat stress in *Caenorhabditis elegans*. *Current Biology* 24: 2406–2410.

Nelson MD, Raizen DM (2013). A sleep state during *C. elegans* development. *Current opinion in neurobiology* 23: 824–830.

Nelson MD, Trojanowski NF, George-Raizen JB, Smith CJ, Yu C-C, Fang-Yen C, Raizen DM (2013). The neuropeptide NLP-22 regulates a sleep-like state in *Caenorhabditis elegans*. *Nature communications* 4: 2846.

Nickell WT, Pun RYK, Bargmann CI, Kleene SJ (2002). Single ionic channels of two *Caenorhabditis elegans* chemosensory neurons in native membrane. *The Journal of membrane biology* 189: 55–66.

Okubo K, Nagahama Y (2008). Structural and functional evolution of gonadotropin-releasing hormone in vertebrates. *Acta physiologica (Oxford, England)* 193: 3–15.

Ozkaya O, Rosato E (2012). The circadian clock of the fly: a neurogenetics journey through time. *Advances in genetics* 77: 79–123.

Palma J-A, Urrestarazu E, Iriarte J (2013). Sleep loss as risk factor for neurologic disorders: a review. *Sleep medicine* 14: 229–236.

Park Y, Kim Y-J, Adams ME (2002). Identification of G protein-coupled receptors for *Drosophila* PRXamide peptides, CCAP, corazonin, and AKH supports a theory of ligand-receptor coevolution. *Proceedings of the National Academy of Sciences of the United States of America* 99: 11423–11428.

Park D, O'Doherty I, Somvanshi RK, Bethke A, Schroeder FC, Kumar U, Riddle DL (2012). Interaction of structure-specific and promiscuous G-protein-coupled receptors mediates small-molecule signaling in *Caenorhabditis elegans*. *Proceedings of the National Academy of Sciences of the United States of America* 109: 9917–9922.

Peymen K, Watteyne J, Frooninckx L, Schoofs L, Beets I (2014). The FMRFamide-Like Peptide Family in Nematodes. *Frontiers in endocrinology* 5: Article 90.

Pierce SB, Costa M, Wisotzkey R, Devadhar S, Homburger SA, Buchman AR, Ferguson KC, Heller J, Platt DM, Pasquinelli A a, *et al.* (2001). Regulation of DAF-2 receptor signaling by human insulin and ins-1 , a member of the unusually large and diverse *C . elegans* insulin gene family. *Genes & development* 15: 672–686.

Pierce KL, Premont RT, Lefkowitz RJ (2002). Seven-transmembrane receptors. *Nature reviews Molecular cell biology* 3: 639–650.

Piéron H (1913). *Le problème physiologique du Sommeil.* Masson: Paris.

Piggott BJ, Liu J, Feng Z, Wescott S a, Xu XZS (2011). The neural circuits and synaptic mechanisms underlying motor initiation in *C. elegans*. *Cell* 147: 922–933.

Pino EC, Webster CM, Carr CE, Soukas A a (2013). Biochemical and high throughput microscopic assessment of fat mass in *Caenorhabditis elegans*. *Journal of visualized experiments : JoVE*: 1–11.

Pocock R, Hobert O (2010). Hypoxia activates a latent circuit for processing gustatory information in *C. elegans*. *Nature neuroscience* 13: 610–614.

Pokala N, Liu Q, Gordus A, Bargmann CI (2014). Inducible and titratable silencing of *Caenorhabditis elegans* neurons *in vivo* with histamine-gated chloride channels. *Proceedings of the National Academy of Sciences of the United States of America* 111: 2770–2775.

Predel R, Wegener C (2006). Biology of the CAPA peptides in insects. *Cellular and molecular life sciences* 63: 2477–2490.

Raizen D, Song B, Trojanowski N, You Y (2012). Methods for measuring pharyngeal behaviors. In: The C. elegans Research Community (ed) *WormBook*, doi: 10.1895/wormbook.1.15.

Raizen DM, Zimmerman JE, Maycock MH, Ta UD, You Y, Sundaram M V, Pack AI (2008). Lethargus is a *Caenorhabditis elegans* sleep-like state. *Nature* 451: 569–572.

Ramot D, Johnson BE, Berry TL, Carnell L, Goodman MB (2008). The Parallel Worm Tracker: a platform for measuring average speed and drug-induced paralysis in nematodes. *PloS one* 3: e2208.

Rankin CH, Beck CD, Chiba CM (1990). *Caenorhabditis elegans*: a new model system for the study of learning and memory. *Behavioural brain research* 37: 89–92.

Rankin CH, Wicks SR (2000). Mutations of the *Caenorhabditis elegans* brain-specific inorganic phosphate transporter *eat-4* affect habituation of the tap – withdrawal response without affecting the response itself. *The Journal of Neuroscience* 20: 4337–4344.

Rask-Andersen M, Masuram S, Schiöth HB (2013). The druggable genome: evaluation of drug targets in clinical trials suggests major shifts in molecular class and indication. *Annual review of pharmacology and toxicology*.

Rechtschaffen A, Bergmann B, Everson C, Kushida C, Gilliland M (1989). Sleep deprivation in the rat: X. Integration and discussion of the findings. *Sleep* 25: 68–87.

Reddy KC, Andersen EC, Kruglyak L, Kim DH (2009). A polymorphism in *npr-1* is a behavioral determinant of pathogen susceptibility in *C. elegans*. *Science (New York, NY)* 323: 382–4.

Richmond JE, Davis WS, Jorgensen EM (2008). UNC-13 is required for synaptic vesicle fusion in *C. elegans*. *Nature neuroscience* 2: 959–964.

Richter C, Woods IG, Schier AF (2014). Neuropeptidergic control of sleep and wakefulness. *Annual review of neuroscience* 37: 503–531.

Ringstad N, Horvitz HR (2008). FMRFamide neuropeptides and acetylcholine synergistically inhibit egg-laying by *C. elegans*. *Nature neuroscience* 11: 1168–1176.

Ritter SL, Hall R a (2009). Fine-tuning of GPCR activity by receptor-interacting proteins. *Nature reviews Molecular cell biology* 10: 819–830.

Robertson HM, Thomas JH (2006). The putative chemoreceptor families of *C. elegans*. In: The *C. elegan* Research Community (ed) *WormBook*, doi:10.1895/wormbook.1.66.1, pp 1–12.

Roch GJ, Busby ER, Sherwood NM (2011). Evolution of GnRH: diving deeper. *General and comparative endocrinology* 171: 1–16.

Rogers C, Persson A, Cheung B, de Bono M (2006). Behavioral motifs and neural pathways coordinating O2 responses and aggregation in *C. elegans*. *Current Biology* 16: 649–659.

Rogers C, Reale V, Kim K, Chatwin H, Li C, Evans P, de Bono M (2003). Inhibition of *Caenorhabditis elegans* social feeding by FMRFamide-related peptide activation of NPR-1. *Nature neuroscience* 6: 1178–85.

Romanowski A, Garavaglia MJ, Goya ME, Ghiringhelli PD, Golombek DA (2014). Potential conservation of circadian clock proteins in the phylum nematoda as revealed by bioinformatic searches. *PloS one* 9: e112871.

Van Rompay L (2014). Genetic regulators of yolk protein production in the nematode <i>Caenorhabditis elegans<i>.

Roth TC, Rattenborg NC, Pravosudov V V (2010). The ecological relevance of sleep: the trade-off between sleep, memory and energy conservation. *Philosophical transactions of the Royal Society of London Series B, Biological sciences* 365: 945–959.

Saeki S, Yamamoto M, Iino Y (2001). Plasticity of chemotaxis revealed by paired presentation of a chemoattractant and starvation in the nematode *Caenorhabditis elegans*. *The Journal of experimental biology* 204: 1757–64.

Sambongi Y, Nagae T, Liu Y, Yoshimizu T, Takeda K, Wada Y, Futai M (1999). Sensing of cadmium and copper ions by externally exposed ADL , ASE , and ASH neurons elicits avoidance response in *Caenorhabditis elegans*. *Neuroreport* 10: 665–893.

Sambongi Y, Takeda K, Wakabayashi T, Ueda I, Wada Y (2000). *Caenorhabditis elegans* senses protons through amphid chemosensory neurons : proton signals elicit avoidance behavior. *Neuroreport* 11: 2229–2232.

Sanders J, Nagy S, Fetterman G, Wright C, Treinin M, Biron D (2013). The *Caenorhabditis elegans* interneuron ALA is (also) a high-threshold mechanosensor. *BMC neuroscience* 14: Article 156.

Saper CB, Fuller PM, Pedersen NP, Lu J, Scammell TE (2010). Sleep state switching. *Neuron* 68: 1023–42.

Schackwitz WS, Inoue T, Thomas JH (1996). Chemosensory Neurons Function in Parallel to Mediate a Pheromone Response in *C. elegans*. *Neuron* 17: 719–728.

Schild LC, Glauser D a (2013). Dynamic switching between escape and avoidance regimes reduces *Caenorhabditis elegans* exposure to noxious heat. *Nature communications* 4: 2198.

Schiöth HB, Fredriksson R (2005). The GRAFS classification system of G-protein coupled receptors in comparative perspective. *General and comparative endocrinology* 142: 94–101.

Schoofs L, Holman GM, Hayes TK, Kochansky JP, Nachman RJ, De Loof A (1990a). Locustatachykinin III and IV: two additional insect neuropeptides with homology to peptides of the vertebrate tachykinin family. *Regulatory peptides* 31: 199–212.

Schoofs L, Holman GM, Hayes TK, Nachman RJ, De Loof A (1990b). Locustatachykinin I and II, two novel insect neuropeptides with homology to peptides of the vertebrate tachykinin family. *FEBS letters* 261: 397–401.

Schwarz J, Lewandrowski I, Bringmann H (2011). Reduced activity of a sensory neuron during a sleep-like state in *Caenorhabditis elegans*. *Current Biology* 21: 983–984.

Schwarz J, Spies J, Bringmann H (2012). Reduced muscle contraction and a relaxed posture during sleep-like lethargus. *Worm* 1: 12–14.

Seugnet L, Suzuki Y, Merlin G, Gottschalk L, Duntley SP, Shaw PJ (2011). Notch signaling modulates sleep homeostasis and learning after sleep deprivation in *Drosophila*. *Current Biology* 21: 835–840.

Sharabi K, Hurwitz A, Simon AJ, Beitel GJ, Morimoto RI, Rechavi G, Sznajder JI, Gruenbaum Y (2009). Elevated CO2 levels affect development, motility, and fertility and extend life span in *Caenorhabditis elegans*. *Proceedings of the National Academy of Sciences of the United States of America* 106: 4024–4029.

Shaw ND, Gill S, Lavoie HB, Marsh EE, Hall JE (2011). Persistence of sleep-associated decrease in GnRH pulse frequency in the absence of gonadal steroids. *The Journal of clinical endocrinology and metabolism* 96: 2590–2595.

Shaw PJ, Tononi G, Greenspan RJ, Robinson DF (2002). Stress response genes protect against lethal effects of sleep deprivation in *Drosophila*. *Nature* 417: 287–291.

Shingai R (2000). Durations and frequencies of free locomotion in wild type and GABAergic mutants of *Caenorhabditis elegans*. *Neuroscience Research* 38: 71–84.

Simonetta SH, Golombek D a (2007). An automated tracking system for *Caenorhabditis elegans* locomotor behavior and circadian studies application. *Journal of neuroscience methods* 161: 273–280.

Sing RN, Sulston JE (1978). Some observations on moulting in *Caenorhabditis elegans*. *Nematologica* 24: 63–71.

Singh K, Chao MY, Somers G a, Komatsu H, Corkins ME, Larkins-Ford J, Tucey T, Dionne HM, Walsh MB, Beaumont EK, *et al.* (2011). *C. elegans* Notch signaling regulates adult chemosensory response and larval molting quiescence. *Current biology : CB* 21: 825–34.

Singh K, Ju JY, Walsh MB, DiIorio M a, Hart AC (2014). Deep conservation of genes required for both *Drosphila melanogaster* and *Caenorhabditis elegans* sleep includes a role for dopaminergic signaling. *Sleep* 37: 1439–1451.

Söderberg J a E, Birse RT, Nässel DR (2011). Insulin production and signaling in renal tubules of *Drosophila* is under control of tachykinin-related peptide and regulates stress resistance. *PloS one* 6: e19866.

Spiegel K, Tasali E, Leproult R, Van Cauter E (2009). Effects of poor and short sleep on glucose metabolism and obesity risk. *Nature reviews Endocrinology* 5: 253–61.

Sporns O (2014). Contributions and challenges for network models in cognitive neuroscience. *Nature neuroscience* 17: 652–660.

Steinhoff MS, von Mentzer B, Geppetti P, Pothoulakis C, Bunnett NW (2014). Tachykinins and their receptors: contributions to physiological control and the mechanisms of disease. *Physiological reviews* 94: 265–301.

Stiernagle T (2006). Maintenance of *C. elegans*. In: The *C. elegans* Research Community (ed) *WormBook*, doi:10.1895/wormbook.1.101.1, pp 1–11.

Strotmann R, Schröck K, Böselt I, Stäubert C, Russ A, Schöneberg T (2011). Evolution of GPCR: change and continuity. *Molecular and cellular endocrinology* 331: 170–8.

Styer KL, Singh V, Macosko E, Steele SE, Bargmann CI, Aballay A (2008). Innate immunity in *Caenorhabditis elegans* is regulated by neurons expressing NPR-1/GPCR. *Science* 322: 460–464.

Sulston JE, Schierenberg E, White JG, Thomson JN (1983). The embryonic cell lineage of the nematode *Caenorhabditis elegans*. *Developmental biology* 100: 64–119.

Suzuki H, Kerr R, Bianchi L, Frøkjær-Jensen C, Slone D, Xue J, Gerstbrein B, Driscoll M, Schafer WR (2003). *In Vivo* imaging of *C. elegans* mechanosensory neurons demonstrates a specific role for the MEC-4 channel in the process of gentle touch sensation. *Neuron* 39: 1005–1017.

Swierczek N a, Giles AC, Rankin CH, Kerr R a (2011). High-throughput behavioral analysis in *C. elegans*. *Nature methods* 8: 592–598.

Temmerman L, Bogaerts a, Meelkop E, Cardoen D, Boerjan B, Janssen T, Schoofs L (2012). A proteomic approach to neuropeptide function elucidation. *Peptides* 34: 3–9.

Tensen CP, Cox KJ, Burke JF, Leurs R, van der Schors RC, Geraerts WP, Vreugdenhil E, Heerikhuizen H (1998). Molecular cloning and characterization of an invertebrate homologue of a neuropeptide Y receptor. *The European journal of neuroscience* 10: 3409–3416.

The *C. elegans* Sequencing Consortium (1998). Genome Sequence of the Nematode *C. elegans*: A Platform for Investigating Biology. *Science* 282: 2012–2018.

Thomas JH, Robertson HM (2008). The *Caenorhabditis* chemoreceptor gene families. *BMC biology* 6.

Troemel ER, Chou JH, Dwyer ND, Colbert H a., Bargmann CI (1995). Divergent seven transmembrane receptors are candidate chemosensory receptors in *C. elegans*. *Cell* 83: 207–218.

Troemel ER, Kimmel BE, Bargmann CI (1997). Reprogramming chemotaxis responses: sensory neurons define olfactory preferences in *C. elegans*. *Cell* 91: 161–169.

Tsai P-S, Zhang L (2008). The emergence and loss of gonadotropin-releasing hormone in protostomes: orthology, phylogeny, structure, and function. *Biology of reproduction* 79: 798–805.

Turek M, Bringmann H (2014). Gene expression changes of *Caenorhabditis elegans* larvae during molting and sleep-like lethargus. *PloS one* 9: e113269.

Turek M, Lewandrowski I, Bringmann H (2013). An AP2 transcription factor is required for a sleep-active neuron to induce sleep-like quiescence in *C. elegans*. *Current Biology* 23: 2215–2223.

Ueno T, Tomita J, Tanimoto H, Endo K, Ito K, Kume S, Kume K (2012). Identification of a dopamine pathway that regulates sleep and arousal in *Drosophila*. *Nature neuroscience* 15: 1516–1523.

Vadakkadath Meethal S, Gallego MJ, Haasl RJ, Petras SJ, Sgro J-Y, Atwood CS (2006). Identification of a gonadotropin-releasing hormone receptor orthologue in *Caenorhabditis elegans*. *BMC evolutionary biology* 6: 103.

Vandesompele J, Preter K De, Poppe B, Roy N Van, Paepe A De (2002). Accurate normalization of real-time quantitative RT -PCR data by geometric averaging of multiple internal control genes. *Genome Biology* 3: research0034.

Varshney LR, Chen BL, Paniagua E, Hall DH, Chklovskii DB (2011). Structural properties of the *Caenorhabditis elegans* neuronal network. *PLoS computational biology* 7: e1001066.

Wakabayashi T, Kitagawa I, Shingai R (2004). Neurons regulating the duration of forward locomotion in *Caenorhabditis elegans*. *Neuroscience research* 50: 103–11.

Wang H, Girskis K, Janssen T, Chan JP, Dasgupta K, Knowles J a, Schoofs L, Sieburth D (2013). Neuropeptide secreted from a pacemaker activates neurons to control a rhythmic behavior. *Current B* 23: 746–754.

Ward S (1973). Chemotaxis by the nematode *Caenorhabditis elegans*: identification of attractants and analysis of the response by use of mutants. *Proceedings of the National Academy of Sciences of the United States of America* 70: 817–21.

Ward S, Carrel JS (1979). Fertilization and sperm competition in the nematode *Caenorhabditis elegans*. *Developmental Biology* 73: 304–321.

Ward A, Liu J, Feng Z, Xu XZS (2008). Light-sensitive neurons and channels mediate phototaxis in *C. elegans*. *Nature neuroscience* 11: 916–922.

Way JC, Chalfie M (1989). The *mec-3* gnen of *Caenorhadbitis elegans* requires its own product for maintained expression and is expressed in three neuronal cell types. *Genes & Development* 3: 1823–1833.

White JG, Southgate E, Thomson JN, Brenner S (1986). The structure of the nervous system of the nematode *Caenorhabditis elegans*. *Philosophical Transactions of the Royal Society of London* 314: 1–340.

Wicks SR, Rankin CH (1995). Integration of mechanosensory stimuli in *Caenorhabditis elegans*. *The Journal of Neuroscience* 15: 2434–2444.

Wiechelman KJ, Braun RD, Fitzpatrick JD (1988). Investigation of the bicinchoninic acid protein assay: Identification of the groups responsible for color formation. *Analytical Biochemistry* 175: 231–237.

Winther AME, Acebes A, Ferrús A (2006). Tachykinin-related peptides modulate odor perception and locomotor activity in *Drosophila*. *Molecular and cellular neurosciences* 31: 399–406.

Winther AME, Ignell R (2010). Local peptidergic signaling in the antennal lobe shapes olfactory behavior. *Fly* 4: 167–171.

Woollard A (2005). Gene duplications and genetic redundancy in *C. elegans*. In: The *C. elegans* Research Community (ed) *WormBook*, doi:10.1895/wormbook.1.2.1, pp 1–6.

Wragg RT, Hapiak V, Miller SB, Harris GP, Gray J, Komuniecki PR, Komuniecki RW (2007). Tyramine and octopamine independently inhibit serotonin-stimulated aversive behaviors in *Caenorhabditis elegans* through two novel amine receptors. *The Journal of neuroscience : the official journal of the Society for Neuroscience* 27: 13402–12.

Yemini E, Jucikas T, Grundy LJ, Brown AEX, Schafer WR (2013). A database of *Caenorhabditis elegans* behavioral phenotypes. *Nature methods* 10: 877–879.

Yokogawa T, Marin W, Faraco J, Pézeron G, Appelbaum L, Zhang J, Rosa F, Mourrain P, Mignot E (2007). Characterization of sleep in zebrafish and insomnia in hypocretin receptor mutants. *PLoS biology* 5: 2379–2397.

You Y, Kim J, Raizen DM, Avery L (2008). Insulin, cGMP, and TGF-β signals regulate food intake and quiescence in *C. elegans*: A model for satiety. *Cell metabolism* 7: 249–257.

Yu W, Hardin PE (2006). Circadian oscillators of *Drosophila* and mammals. *Journal of cell science* 119: 4793–4795.

Yuan Q, Joiner WJ, Sehgal A (2006). A sleep-promoting role for the *Drosophila* serotonin receptor 1A. *Current Biology* 16: 1051–1062.

Yuan J, Ledoux S, Ellis SHM, Horvitzt HR (1993). The *C . elegans* cell death gene *ced-3* encodes a protein similar to mammalian interleukin-1 p-converting enzyme. *Cell* 75: 641–652.

Zhang L, Tello J a, Zhang W, Tsai P-S (2008). Molecular cloning, expression pattern, and immunocytochemical localization of a gonadotropin-releasing hormone-like molecule in the gastropod mollusk, *Aplysia californica*. *General and comparative endocrinology* 156: 201–9.

Zheng Y, Brockie PJ, Mellem JE, Madsen DM, Maricq A V (1999). Neuronal Control of Locomotion in *C . elegans* Is Modified by a Dominant Mutation in the GLR-1 Ionotropic Glutamate Receptor. *Neuron* 24: 347–361.

Zimmer M, Gray JM, Pokala N, Chang AJ, Karow DS, Marletta M a, Hudson ML, Morton DB, Chronis N, Bargmann CI (2009). Neurons detect increases and decreases in oxygen levels using distinct guanylate cyclases. *Neuron* 61: 865–879.

Zimmerman JE, Naidoo N, Raizen DM, Pack AI (2008). Conservation of sleep: insights from non-mammalian model systems. *Trends in neurosciences* 31: 371–376.

List of publications

Research papers

Peymen, K., Watteyne, J., Frooninckx, L., Schoofs, L., Beets, I. (2014). The FMRFamide-like peptide family in Nematodes. *Frontiers in Endocrinology, 5*, art.nr. 90, 1-21.

De Haes, W., Frooninckx, L., Van Assche, R., Smolders, A., Depuydt, G., Billen, J., Braeckman, B., Schoofs, L., Temmerman, L. (2014). Metformin promotes lifespan through mitohormesis via the peroxiredoxin PRDX-2. *Proceedings of the National Academy of Sciences of the United States of America, 111* (24), art.nr. Doi: 10.1073/pnas.1321776111, E2501-E2509.

Frooninckx, L., Van Rompay, L., Temmerman, L., Van Sinay, E., Beets, I., Janssen, T., Husson, S., Schoofs, L. (2012). Neuropeptide GPCRs in *C. elegans*. *Frontiers in Endocrinology, 3*, art.nr. 167, 1-18.

Meeting lectures and posters

Frooninckx, L., Watteyne, J., Van Sinay, E., Van der Auwera, P., Janssen, T., Mirabeau, O., Schoofs, L., Beets, I. (2014). Pharmacological and functional characterization of a conserved tachykinin signaling system in *C. elegans*. Congress of the European Comparative Endocrinologists (CECE). Rennes, France, 25-29 August 2014.

Beets, I., Janssen, T., Temmerman, L., Frooninckx, L., Schoofs, L. (2014). Oxytocin/vasopressin signaling as ancient modulator of associative learning in *C. elegans*. Physiological Society Meeting 2014. London, U.K., 30 June - 2 July 2014, Abstract No. Invited lecture.

Watteyne, J., Frooninckx, L., Van der Auwera, P., Beets, I., Temmerman, L., Husson, S., Schoofs, L. (2014). Optogenetic analysis of the nociceptor ASH in Caenorhabditis elegans. FENS Forum of Neuroscience. Milan,Italy, 5-9 July 2014.

De Haes, W., Frooninckx, L., Van Assche, R., Smolders, A., Depuydt, G., Billen, J., Braeckman, B., Schoofs, L., Temmerman, L. (2014). Metformin promotes lifespan through mitohormesis. Berlin *C. elegans* Meeting 2014. Berlin, Germany, 15-17 May 2014, Abstract No. Oral presentation by Temmerman L.

Temmerman, L., Van Assche, R., Braeckman, B., Roessner, U., Watteyne, J., Van Sinay, E., Frooninckx, L., Beets, I., Schoofs, L. (2014). Metabolic fingerprinting of Alzheimer's disease in *C. elegans* and its relevance to neuropeptidergic research.Invertebrate Neuropeptide Conference (INC 2014). El Calafate, Argentina, 16-20 February 2014, Abstract No. Invited speaker.

Beets, I., Frooninckx, L., Watteyne, J., Van Sinay, E., Mirabeau, O., Schoofs, L. (2014). Matching of neuropeptide-receptor couples reveals ancient behavioral modulation by tachykinin

signaling. *C. elegans* topic meeting: neuronal development, synaptic function & behavior (CeNeuro 2014). Madison, U.S.A., 7-10 July 2014.

Beets, I., Watteyne, J., Frooninckx, L., Peeters, L., Van Calster, K., Van Sinay, E., Schoofs, L. (2014). Evolutionary conserved neuropeptide signalling and behavioural modulation in *C. elegans*. Congress of the European Comparative Endocrinologists (CECE). Rennes, France, 25-29 August 2014, Abstract No. State-of-the-Art Lecture.

Van Calster, K., Borghgraef, C., Beets, I., Janssen, T., Frooninckx, L., Temmerman, L., Schoofs, L. (2014). Cholecystokinin-like signaling in *C. elegans*. Congress of the European Comparative Endocrinologists (CECE). Rennes, France, 25-29 August 2014.

Van Rompay, L., Frooninckx, L., Beets, I., Temmerman, L., Janssen, T., Schoofs, L. (2013). Molecular genetic deciphering of the reproductive pathway in *Caenorhabditis elegans*. International *C. elegans* Meeting. Los Angeles, USA, 26-30 June 2013.

Frooninckx, L., Janssen, T., Van Sinay, E., Van Calster, K., Watteyne, J., Mirabeau, O., Schoofs, L. (2013). Identification of a tachykinin-like signaling system in the nematode *C. elegans*. International Congress of Comparative Endocrinology. Barcelona, Spain, 15-19 July 2013.

De Haes, W., Frooninckx, L., Van Rompay, L., Temmerman, L., Schoofs, L. (2013). Disrupting GnRH/AKH signaling in *C. elegans* promotes longevity. International Congress of Comparative Endocrinology. Barcelona, Spain, 15-19 July 2013.

Beets, I., Temmerman, L., Janssen, T., Meelkop, E., Frooninckx, L., Jansen, G., Schoofs, L. (2013). Conserved neuropeptidergic regulation of associative learning by vasopressin/oxytocin-related peptides. International *C. elegans* Meeting. Los Angeles, USA, 26-30 June 2013.

Frooninckx, L., Van Rompay, L., Beets, I., Janssen, T., Schoofs, L. (2012). GnRHR-related receptors in *C. elegans*. EMBO Conference Series: *C. elegans* Neurobiology. EMBL Heidelberg, Germany, 14-17 June 2012.

Van Rompay, L., Frooninckx, L., Meelkop, E., Temmerman, L., Janssen, T., Husson, S., Schoofs, L. (2012). A forward mutagenesis approach to study the control of reproduction in *C. elegans*. EMBO Conference Series: *C. elegans* Neurobiology.EMBL Heidelberg, Germany, 14-17 June 2012.

Appendix

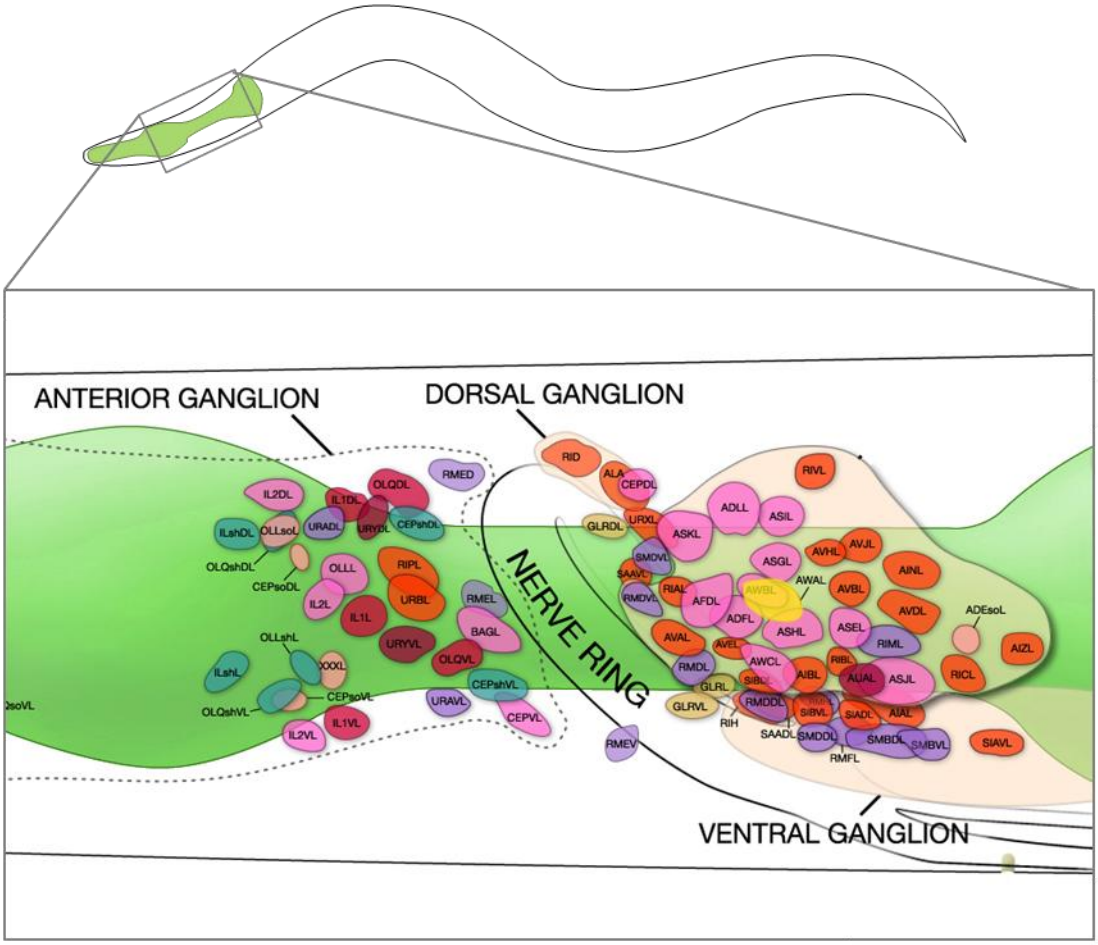

Supplementary figure 1 Schematic representation of *nlp-2 in vivo* expression pattern. The locations of the cell bodies of neurons in the anterior and dorsal ganglia of the head are shown in left-hand view. The left AWA neuron identified to express the *nlp-2* reporter construct is indicated in yellow. (Adapted frow WormAtlas)

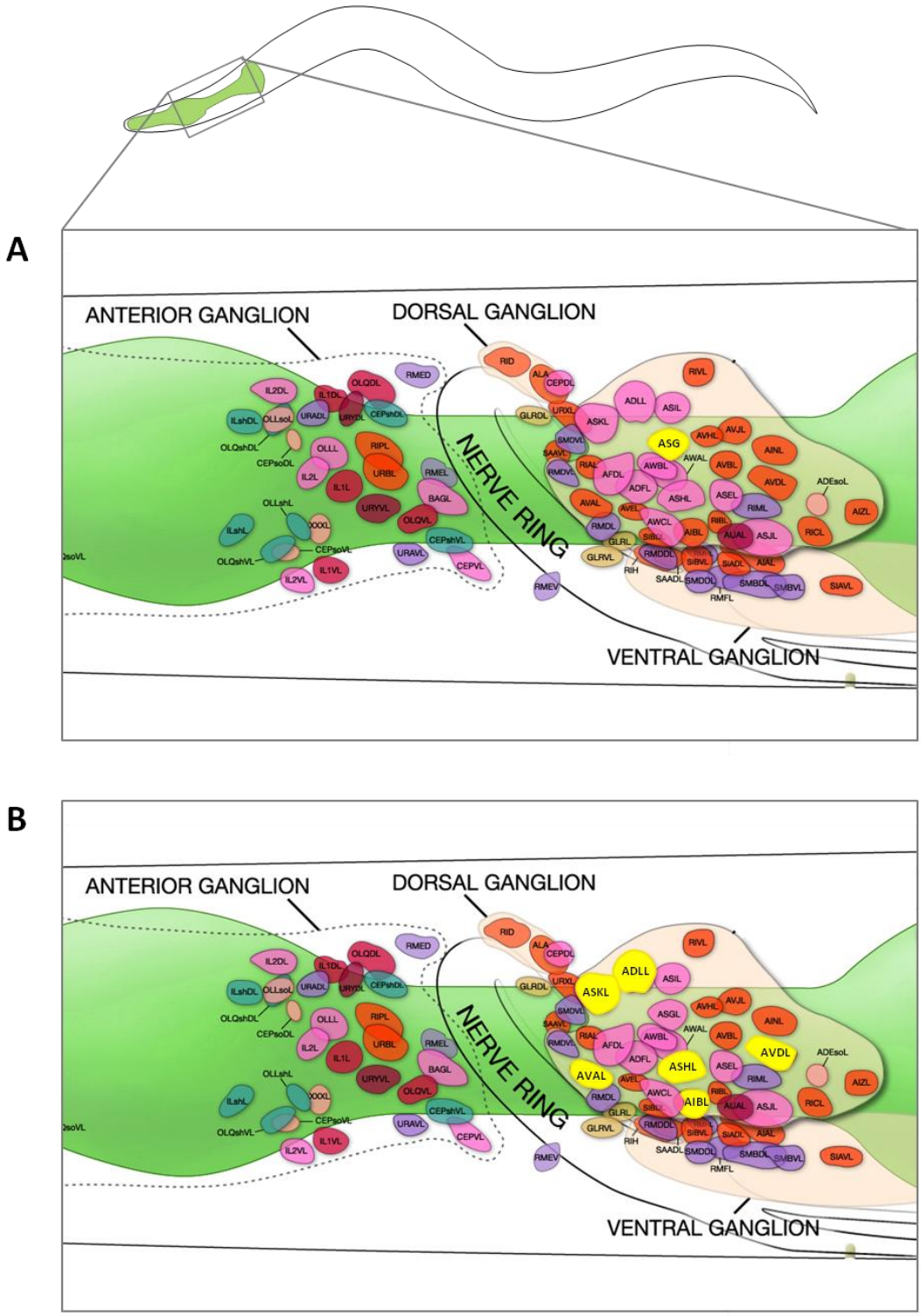

Supplementary figure 2 Schematic representation of *tkr-1* and *tkr-2 in vivo* expression patterns. The locations of the cell bodies of the neurons in the anterior and dorsal ganglia of the head are shown in left-hand view. Cells identified to express the *tkr-1* (A) or *tkr-2* (B) reporter constructs are indicated in yellow. (Adapted frow WormAtlas)